The delta inverter.

Dodson, R. C.

Award date:
1984

Awarding institution:
University of Bath

THE DELTA INVERTER

Submitted by

R.C. Dodson, B.Sc.

for the degree of

Doctor of Philosophy

of the University of Bath

1984

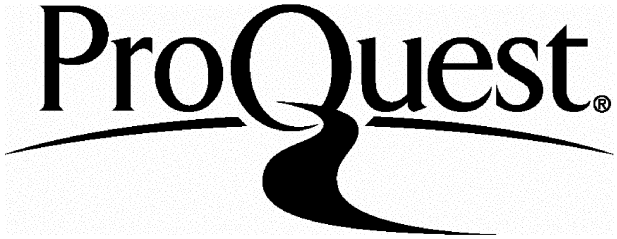

CONTENTS

ABSTRACT

The research outlined in this thesis is involved with some aspects of power electronics. In particular, within the area of machine drives, a new type of inverter is investigated. This inverter, referred to as the delta inverter, is principally intended for incorporation into an ac drive system. The inverter appears to offer some advantage in circuit design over conventional inverters and this is discussed in the context of the inverters overall performance and characteristics.

Chapter 1 presents a review of machine drives, both ac and dc systems, and, in accepting the relative merits of the ac squirrel cage induction machine, outlines the penalties generally paid in conventional ac inverter complexity. The delta inverter configuration, which appears to offer a reduction in circuit complexity, is then introduced.

Chapter 2 investigates the general behaviour of the delta inverter, specifically with passive loads, and outlines a suitable control strategy for the inverter.

Chapter 3 deals with the subject of harmonic improvement of inverter waveforms. Two methods which appear particularly attractive, selective harmonic reduction (SHR) and sinusoidal pulse-width modulation (PWM), are presented. Using the strategy suggested in Chapter 2, the implementation of methods of sinusoidal pulse-width modulation applicable to the delta inverter are derived in this chapter and a theoretical comparison is made with the conventional bridge inverter.

Chapter 4 presents both experimental and computed results for a delta inverter ac drive system using the previously derived switching techniques. The results are compared with the bridge inverter performance and with a mains quality sinusoidal supply. This chapter concludes with some discussion of the delta inverter ac drive system and some general points are made.

Chapter 5 summarises the main conclusions that have been established, in the course of the present research, concerning the delta inverter system and its feasibility as an alternative ac drive circuit.

ACKNOWLEDGEMENTS

The author would like to express his gratitude to Professor J.F. Eastham of the School of Electrical Engineering, University of Bath, for his helpful guidance.

A similar expression of thanks is due to Dr. P.D. Evans for his daily supervision and kind encouragement.

My thanks are due to KGEL for financial support for one year and to the University of Bath for a two year studentship from the University Research Fund.

Thanks are also given to other members of the School of Electrical Engineering, including Mr. R.J. Hill-Cottingham, for their assistance.

Finally, to Mrs. Agnes Balchin a grateful thanks for typing the manuscript.

LIST OF PRINCIPAL SYMBOLS

A_n	-	Amplitude of n^{th} harmonic, using exponential form of Fourier series assuming half period even symmetry
C_n	-	Amplitude of n^{th} harmonic, using exponential form of Fourier series, general case
D_1, D_2, D_3	-	Diodes
i_B, i_C, i_E, I_E	-	Transistor base/collector/emitter current
I_a, I_b, I_c	-	Load currents
I_{harm}	-	Total rms harmonic current
I_n	-	n^{th} harmonic current
I_R, I_Y, I_B	-	Line currents
j	-	$\sqrt{-1}$
k	-	Pulse number
L_a, L_b, L_c	-	Load inductance
n	-	Harmonic number
p	-	Number of pulses per cycle
R_a, R_b, R_c	-	Load resistance
R_s, R_r	-	Stator and rotor resistance
S	-	Slip
t	-	Time
T	-	Period
T_1, T_2, T_3	-	Transistors
v_{BE}, v_{CE}, V_{CE}	-	Transistor voltages (base-emitter/collector-emitter)
V_a, V_b, V_c	-	Load voltages
V_B	-	dc supply voltage, bridge inverter

V_D	-	dc supply voltage, delta inverter
V_n	-	n^{th} harmonic voltage
V_{RG}, V_{YG}, V_{BG}	-	Phase voltages to a notional reference potential
V_{RN}, V_{YN}, V_{BN}	-	Phase voltages
V_{RY}, V_{YB}, V_{BR}	-	Line voltages
X_s, X_r, X_m	-	Stator leakage, rotor leakage, magnetising reactance
α_k	-	k^{th} pulse position angle
δ_k	-	k^{th} modulating angle
Δ	-	pulse period/section width
θ	-	conduction angle
σ	-	weighted harmonic voltage distortion
τ	-	time constant
ω	-	angular frequency
ω_s	-	stator frequency
ω_r	-	rotor speed

CHAPTER 1

INTRODUCTION: ELECTRIC DRIVES

1.1 Introduction

Over the last 20 years new solid state devices have provided an unprecedented ability to control and utilise power, with one important application being in the field of electrical machine drives. Such solid state drive systems can exhibit a variety of advantages over conventional methods requiring auxiliary rotating machines, from reduced initial capital costs and long term running and maintenance costs, to improved reliability and efficiency.

Traditionally the induction machine has provided fixed speed drives simply and economically. Where variable speed drives were essential the dc motor was generally used (incorporated with two additional rotating machines into a Ward-Leonard set) except, perhaps, where compactness of the motor was critical - for example in multi-motor mill drives[1,2].

At present, with the advantages of the squirrel cage induction machine being its low cost per kW and high reliability it accounts for around 90% of all electric drives used in industry[3]. Comparing total demand for dc drives to ac inverter/induction motor drives, forecasted EEC demand shows the ac system rising by 1990, from approximately one sixth in 1983/84, to around one quarter the dc system demand[4]. This comparison shows two factors: the predominance at the present time of the dc drive system and the expected large percentage increase in popularity of the ac variable speed drive system (forecast as approximately doubling over the next six years).

Factors affecting the relative popularities of the two systems can be clearly differentiated. Whilst the dc machine suffers from such problems as brush life and motor commutation its speed is easily controlled by varying the average applied voltage and this leads to relatively simple, cheap and reliable electronic controllers. In comparison, while the squirrel cage induction machine is virtually maintenance free and, in general, has improved motor performance, speed control tends to be more complicated and expensive. Although limited speed adjustment can be obtained by variable voltage control (for example, small fans up to 1 or 2 kW, both single-phase and three-phase, which are extensively used in agriculture and industry)[5], for most applications variable frequency control of the induction motor is necessary - together with voltage control, to maintain correct flux loading of the machine. However, whilst hitherto induction machines have been considered essentially constant speed motors, two major factors are altering this view[3]:

a) Static frequency inverters and converters using thyristors, transistors and newer devices such as GTOs (gate assisted turn-off thyristors) are becoming available at high powers and reducing costs.

b) Greater awareness is being shown by industry of the economic benefits accruing from the use of variable speed drives for optimising duty cycles and for potential energy savings.

In order to assess the potential for a new type of inverter for an ac drive system (but which has been conceived to apply some of the advantages associated with the simplified electronics of the dc variable speed drive system), the conventional static converter systems for both dc and ac drives are discussed in the next two sections, respectively.

Having briefly reviewed the variety of basic solid state drive configurations that are available, Section 1.3.3 then introduces some possible alternative arrangements for ac inverter drives and derives the circuit configuration for this new type of three-phase inverter.

1.2 DC Machine Drives

Industrial applications of variable speed electric motor drives have traditionally been met by dc machines. This is primarily because the speed of a dc machine changes in response to the average terminal voltage applied to it. This can be shown in the following standard manner:

$$V = I_a R_a + E \tag{1.1}$$

$$E = K\omega\phi \tag{1.2}$$

$$\therefore \quad \omega = \frac{V - I_a R_a}{K\phi} \tag{1.3}$$

and if R_a is negligibly small,

$$\omega = \frac{V}{K\phi} \tag{1.4}$$

where

V is the applied voltage

I_a and R_a refer to the armature current and resistance

E is the induced back emf

ω is the angular speed

ϕ is the pole flux

K is a constant

Thus, for a constant pole flux, speed and applied voltage are proportional. Sufficient current is drawn into the machine to provide the torque to achieve the speed. The dc machine can, therefore, provide continuous

control of speed in a convenient manner and can exhibit both long term stability and good transient performance. The shunt-wound dc motor controlled by a naturally commutated, phase controlled thyristor converter represents a most common form of variable speed package[6].

The dc machine itself has a number of disadvantages. Concerning the necessity for a mechanical commutator: construction of this can increase costs; necessitate regular maintenance (typically[4] at least 5000 hours or approximately 2 years service life); can limit the armature voltage, the current and rate of change of current and can limit maximum motor speed. The dc machine also tends to have approximately half the power to weight ratio of a squirrel cage induction machine - but with a dramatic increase in performance over the last decade. From the early nineteen hundreds, with the advent of interpoles to improve commutation performance, outputs of 36 W/kg were possible from the dc motor. By 1970 a range of class F polyester based enamels enabled specific output in excess of 50 W/kg to be obtained, but by 1978 the laminated square framed motor had a power to weight ratio of 120 W/kg and 180 W/kg, subsequently, by 1980[7].

Traditional methods of voltage control used Ward-Leonard type systems; where a constant speed ac motor drives a dc generator which in turn feeds the dc machine. Only simple field control of the dc generator is then required. By this method the subsequent variable armature voltage controls the motor speed leaving the field flux of the machine constant, avoiding poor motor commutation. However, by 1970 the motor-generator set was virtually obsolete for new applications (apart from drives requiring high peak supply fluctuations[8], where in terms of technical justification the m.g. set still remains supreme). In general terms the thyristor drive can be said to have the following advantages[9] over the Ward-Leonard system: faster time response, minimal maintenance, high efficiency

(above 95%), smaller size, smaller weight and lower initial and running costs. Similarly, however, disadvantages include[9,10] motor heating and commutation problems due to converter output ripple[11], a lower overload capability and poorer power factor performance.

Speed control both above and below base speed can be obtained with a dc converter (usually by field weakening and armature voltage control, repectively). Three basic speed control methods are possible - phase control, integral cycle control and chopper control. Phase control and integral cycle methods are similar, converting from ac to dc by rectification. Integral cycle control has not been found satisfactory for speed control[9] and will not be discussed further. Phase controlled thyristor converters are self commutating, so can be relatively simple and inexpensive. They offer voltage control over a wide range, although power factor may be poor (i.e. at low output voltages). In comparison, chopper type circuits tend to have both a better transient response and improved power factor performance. Versions of each type can provide both motoring and regenerative operation. Phase controlled circuits are discussed in Section 1.2.1 and choppers in Section 1.2.2.

1.2.1 Phase controlled converters

These types of converter have an ac input and are naturally line commutating. Using rectifier grade thyristors a simple and reliable converter can be produced to provide from one up to full four quadrant control. Various texts describe these circuits in detail[9,12,13,14].

Numerous circuit configurations of this converter type are available for both single-phase and three-phase operation in full- and half-bridge versions. The three-phase circuit shown in Fig.1.1 allows bidirectional power flow, both motoring and regenerating modes but with unidirectional

current, i.e. a two quadrant controller. A "dual converter", consisting of two bridges, can provide four quadrant control - both motoring and regenerating in both directions of rotation.

The output current waveforms can be considered as consisting of an average value and superimposed ripple. The time average value of current produces the main torque and there is an additional pulsating torque which must be considered. The rms value of current, the heat producing component, exceeds the time average value increasing specific heat loss, which may imply additional cooling or machine derating. Similarly, commutation processes in the dc machine can be adversely affected - in which case the peak value of the current may be considered[10]. Commutation problems have been largely alleviated by the use of laminated motor bodies and some additional design changes[11].

The advent of the microprocessor appears to offer the possibility of increased flexibility and complexity for control strategies. In this context Lukas[15] utilises a programmable neutral full-wave bridge and multiple bridges to improve power factor. Recent microprocessor schemes that have been produced give separate algorithms for continuous and discontinuous modes of conduction, which can compensate for the non-linearities introduced when the converter operates in the discontinuous mode[16,17,18]. Improvements brought about in transient response of the circuit can, however, increase stresses within the drive machine, which may have to be considered[11].

1.2.2 Chopper type circuits

Choppers require a dc source. Either a battery stack, such as with industrial fork-lift trucks and electric vehicles, or a rectified ac mains supply can be used. Particular chopper configurations are capable

of regeneration (provided the dc supply is suitable). Again these circuits are well represented in standard texts[9,13].

The simplest type of chopper, a step-down chopper, is shown in Fig.1.2. Referring to this diagram, under continuous current conditions the average potential at point X, V_X, is given by

$$V_X = \alpha V_S \qquad (1.5)$$

and with zero average voltage across L,

$$E = \alpha V_S \qquad (1.6)$$

where α is the mark-period ratio of the switching waveform of the power switch. The switch is a semiconductor device, such as a thyristor (with its associated commutation circuit, as forced commutation is necessary - which is not shown in Fig. 1.2) or a power transistor. As its name suggests, the voltage applied to the load cannot be greater than the supply voltage, as can be seen from (1.5) and (1.6). This simple circuit, with a device which carries unidirectional current, is a single quadrant controller.

In comparison to the step-down circuit, Fig. 1.3 shows a step-up chopper. With this arrangement energy can be returned to the supply. From Fig. 1.3, when S is closed, energy is stored in L as current builds up in the 'short circuited' machine. When S is open, this current fly-wheels into the supply via the diode. In this case V_S must be greater than E,

$$V_S = \frac{E}{(1 - \alpha)} \qquad (1.7)$$

As before, this is a single quadrant controller.

To achieve two quadrant control from a dc supply, i.e. motoring and regenerating with one direction of rotation, a composite circuit block consisting of a combined step-up and step-down chopper can be used. This is known as a regenerative chopper and shown in Fig. 1.4. In this case the voltage of point X can be clamped at the positive or negative supply rail by either transistor and current can flow in both directions for each polarity.

Developing these circuits further, four quadrant control can be achieved with two regenerative choppers, Fig.1.5. At this point, it may be noted that this circuit is capable of providing both positive and negative current and voltage and it therefore appears able to operate as an ac controller - in fact this is a single-phase inverter.

Early chopper circuits (i.e. from the 1960's onwards)[19-26] generally used thyristors as the main switching element and, as the chopper is not self commutating, considerable design effort was applied to produce efficient commutation procedures. Power transistors are also now extensively used as the switching elements[27,28,29] as they can simplify chopper design and also allow higher switching speeds, reducing ripple currents. At lower power ratings (less than 5 kW) power field effect transistors (FETs) have some desirable characteristics and, again, GTOs show potential[30].

Considerable emphasis in recent literature has again been put on the use of microprocessors, on both two quadrant[31] and four quadrant choppers[32]. The possibility of more complex control strategies can facilitate reduced input ripple current and output ripple voltage, as well as possible lower commutation per chopper cycle (for thyristor choppers) and better utilisation factors for the switching elements[32].

In particular, in a double conversion system where the chopper is supplied by a rectified supply, it is important that the chopper operation mode is correctly chosen as otherwise subharmonics, for instance, may be introduced[33].

1.3 AC Machine Drives

The ac machine can possess certain advantages over the dc machine. In particular, the squirrel cage induction motor is a brushless electric machine which has, therefore, a potentially much higher maximum speed than the dc machine. As only the stator winding need be carefully insulated the squirrel cage induction motor can also be constructed, without difficulty, to operate over approximately twice the temperature range of the dc machine[34]. As discussed earlier (Section 1.1), therefore, the lack of commutator and simplified rotor construction can reduce initial cost, make the induction machine virtually maintenance free and significantly improve motor performance. One possible basic disadvantage of the ac system can be a relatively poor response at very low speed - the dc machine can conveniently operate at very small fractions of a Hertz.

As already stated (Section 1.1) for accurate control of an induction machine over a wide speed range, both the stator frequency and voltage must be varied. As the frequency reduces, the applied voltage must reduce to prevent excessive losses due to saturation and, similarly, an increase in frequency requires an increase in voltage to maintain the flux density. A constant Volts/Hz ratio is normally maintained over the speed range except at low frequency where voltage boosting is used to overcome resistive voltage drops in the machine.

As with the dc machine, conventional control methods used multiple machine sets to derive a variable frequency supply. Driving a synchronous alternator at variable speed, maintaining constant field current, produces a constant Volts/Hz source, as both synchronous generator output voltage and frequency are proportional to speed. In some circumstances, to obtain high speed accuracy with a rotating converter may not be straightforward[35].

Clearly, as with the dc drive, potential has existed for a static frequency converter ac drive. Early attempts to use the recently introduced grid-controlled mercury-arc rectifiers found application in only a few isolated cases[36]. World-wide investigation and rapid development followed the introduction of the high power thyristor[34,37-40] and latterly the arrival of the high power switching transistors. Also the newer power devices, GTOs and FETs have a place in this development.

Conventional variable speed static frequency converters fall into two main types, cycloconverters and dc link inverters, described in Sections 1.3.1 and 1.3.2, respectively. Voltage source inverters are treated within the present research but Section 1.3.2 also briefly discusses the current source inverter.

Consideration is mainly given, here, to open loop voltage control methods, where the speed demand sets the Volts per Hertz ratio. A number of other control methods exist. One method, commonly referred to as the controlled slip drive[35,41,42], controls the stator current and rotor slip frequency and requires therefore two feedback signals. This method might have advantages over the open loop control method in terms of system transient performance. It is important, for instance,

to ensure with the open loop method that the supply frequency variation should not exceed the rotor breakdown frequency. Other control methods adjust for optimum machine efficiency - in one method, voltage and frequency are adjusted for the required steady state torque at the specified speed, with minimum losses in the machine[43]. Constant horse-power ac drives may also be achieved[35,44].

1.3.1 Cycloconventers

The cycloconverter is a direct frequency changer and consists of a number of phase-controlled rectifier circuits connected to an ac supply. Originally patented in 1923[45] (with practical circuits appearing in the early 1930's, following the introduction of mercury-arc rectifiers), major development followed the advent of the silicon controlled rectifier, around the 1960's[2,46-48] (McMurray[49] gives an extensive reference list).

With the use of thyristors, line commutation is obtained - eliminating the need for forced commutation components. To restrict harmonic losses to manageable levels, the cycloconverter operates with an output frequency substantially below the supply frequency. It is, however, possible to produce circuits with a higher frequency output than the supply frequency - these are commonly used for induction heating purposes and are termed cycloinverters[50].

The basic circuit of a three-phase to three-phase cycloconverter is shown in Fig. 1.6. Each line has a positive group and a negative group of thyristors, in order to control the current in both directions - thus, both rectifying and inverting modes are implemented and the circuit is capable of regeneration. This simple arrangement uses three-phase half-

wave circuits and requires 18 thyristors. Replacement of each thyristor group by a full three-phase bridge would require 36 thyristors. Harmonic improvement is further possible using, say, a six-phase circuit - although, again, this requires a corresponding increase in the number of thyristors.

Although the mean output voltage of the positive and negative thyristor groups can be maintained equal, the sum of the instantaneous voltages are not equal, resulting in ripple voltages driving circulating currents. The effect can be reduced by fitting current limiting reactors, as shown in Fig. 1.6, or, more commonly these days, by blanking the gate pulses to the inactive groups. Both these techniques can have disadvantages - one alternative cycloconverter was proposed by Jenkins[51], utilising split motor windings, but this initial design suffered from poor efficiency.

More recent work has been aimed at introducing the microprocessor to provide control functions. Chen[52] directly translates the analogue cosine timing wave approach using a numerical approximation, whilst Singh and Hoft[53], basically, use a square-wave timing reference which simplifies computation but produces an output voltage of the cycloconverter which no longer approximates to a sinusoid. Further improvements in control methods are possible using microprocessors[54]. The cycloconverter is a relatively complex drive circuit and this type of control will obviously benefit from improvements in the real time capabilities of microprocessor systems. Some simplification of converter operation is also suggested by the use of triacs as the main switching device[55] and a microprocessor system which provides timing computations, converter selection, blanking control and variable frequency and amplitude control has recently been reported[56].

1.3.2 Conventional inverters

An inverter takes a dc supply - either a battery supply or rectified ac - and converts it to an ac output. Both frequency and amplitude control of the output may be provided by an inverter.

It was shown in Section 1.2.2 that the four quadrant dc controller, consisting of two regenerative choppers, Fig. 1.5, was equivalent to a single-phase bridge inverter. Three such single-phase circuits can be used to produce a three-phase inverter[57] but this arrangement requires twelve antiparallel transistor-diode pairs. Half this component count is achieved by the conventional three-phase bridge inverter.

The dc link converter[35] consists, in general, of a rectifier, which provides the dc supply, and an inverter. Two main types of inverter are distinguishable, the voltage source inverter and the current source inverter. The use of a large inductor in the dc link (i.e. after the rectifier) produces an almost constant dc current which is switched through the phases of the load, in turn, by the current source inverter[58,59].

The current source inverter can use low cost rectifier-grade thyristors, as switching times are not critical. This circuit also has two special advantages[30]. First, the absence of flywheel diodes in the inverter allows the dc link voltage to be reversed by, in this case, the phase controlled rectifier, which permits regenerative operation of of the system without reversal of current direction. Secondly, the inductance in the dc link controls inverter currents under many of the fault conditions that occur, thus enabling satisfactory protection of the inverter to be provided. A drawback of the circuit may, however, be torque pulsations or instability at low speeds, due to the non-sinusoidal nature of the motor currents. This problem is absent in voltage source

inverters with sinusoidal pulse-width modulation - investigation has been restricted, within the present work, to voltage source inverters.

A conventional dc link converter using a three-phase voltage source bridge inverter is shown in Fig. 1.7. The bridge rectifier and filter provide the dc voltage, and variable frequency operation may then be obtained by controlling the switching rate of the inverter. A number of alternatives are available for obtaining variable voltage operation (and hence constant Volts/Hz). Either the dc link voltage may be varied, or the inverter switching can be modulated to perform this function. The former alternative may be provided in a number of ways, usually either by using a phase controlled rectifier (in place of the diode bridge shown in Fig. 1.7) or by incorporating a dc chopper into the dc link[60]. Both these circuit configurations are well accepted and can produce straightforward and reliable systems.

The output voltage waveform of the converter with voltage control of the dc link is usually, but not exclusively, the so called quasi-square voltage shown in Fig. 1.7. This is the simplest waveform normally used with the bridge inverter. The alternative voltage control method, modulating the inverter switching, produces more complex output waveforms.

Behaviour of the ac machine on non-ideal supplies is quite good and, in general, machine design changes are unnecessary for successful operation with inverters. Typically, less than 10% extra heat loss is generated using the quasi-square voltage waveform. However, some benefits in efficiency can be gained by improving the harmonic content of the inverter waveforms[61]. More seriously, the interaction of harmonic fluxes and currents can, especially at low speeds, produce pulsating torques. Forms of sinusoidal modulation therefore have definite advantages,

albeit at the expense of increased device switching within the inverter. Sinusoidal pulse-width modulation techniques are popular and effective - these (together with other forms of harmonic improvement) are discussed in Chapter 3.

Suitable forms of all three voltage control methods mentioned above are capable of providing regenerative operation. The dc supply, itself, must be capable of accepting regenerative power - otherwise some form of "dumping" can be provided. Dumping generally involves monitoring the dc link capacitor voltage and then switching in a dissipation resistance.

The transistorised bridge inverter is now a well established piece of equipment[57,62,63]. Recent work has, to a large extent, concentrated on producing the more complex switching waveforms and control strategies and in this context the microprocessor has been utilised. The use of microprocessors to perform these functions is discussed in Chapter 4 (Section 4.8.3).

1.3.3 Alternative inverter configurations

The requirement for a relatively complex power converter for the ac drive system appears to be a major disadvantage. This section discusses alternative approaches which produce ac controllers with reduced component counts.

As a first alternative, one arrangement[64] uses only two legs of a conventional bridge inverter. This circuit thus uses only four main switching transistors but requires a centre tapped supply. Two of the three phase currents of a three-phase set are controlled and the third current must be the resultant sum of the other two load currents.

The conventional bridge inverter can be considered as built up by combining a number of regenerative choppers which can themselves be considered as made up of the combination of step-up and step-down choppers (Sections 1.2.2 and 1.3.2). In order to consider somewhat more radical departures from the bridge inverter arrangement, it is useful to derive similar "building blocks" for these alternative inverters.

From the circuit shown in Fig. 1.8a, it can be seen that, with this configuration, energy is transferred from the battery source to the load when the power switch is On and flywheels into a separate battery when the switch is Off. This circuit can be further developed by using coupled windings to produce a modified arrangement which requires only one battery source, Fig. 1.8b. These two circuits form the building blocks for two alternative inverter configurations.

From Fig. 1.8b, a three-phase inverter may be produced which only requires three main switches and one dc supply[65], but which also requires a special wound motor with centre tapped windings. Using the alternative building block shown in Fig. 1.8a, the mutual arrangement of three such circuits, shown in Fig. 1.8c, enables bidirectional current to be controlled through a standard three-phase load. Although this latter arrangement requires three isolated dc supplies it appears capable of directly driving a conventional three-phase motor. This particular inverter configuration has been termed the delta inverter[66].

1.4 Conclusions

This chapter has briefly summarised the variety of both ac and dc drive circuits available. Whilst the ac motor appears to have definite advantages over the dc motor as a drive machine, in general, the resulting power electronics to produce a variable speed ac drive system

seem more complex. Some alternative inverter arrangements which produce simplified drive circuits were, therefore, considered. One particular new inverter type, the delta inverter, has been introduced. This inverter forms the subject of the research program outlined in the present work.

1.5 References

1. Stokes, R.W.: "Inverter-fed induction motors", Conf. Proc. 'Drives/Motors/Controls 83', Harrogate, October 1983, pp.182-183.

2. Hamilton, R.A. and Lezan, G.R.: "Thyristor adjustable frequency power supplies for hot strip mill run-out tables", IEEE Trans., IGA-3, No.2, Mar/Apr 1967, pp.168-175.

3. Williams, I.J.: "Induction motors for inverter drives", Conf. Proc. 'Drives/Motors/Control 83", Harrogate, October 1983, pp.81-88.

4. Briggs, K.L.: "DC drives v 'The Rest'", Conf. Proc. 'Drives/Motors/Controls 83', Harrogate, October 1983, pp.179-181.

5. Binks, N.: "Induction motor development", Electronics and Power, Vol.25, No.10, October 1979, pp.699-702.

6. Russell, C.P.: "A transistor pulse-width modulated controller and Permanent-magnet motor", Electronics and Power, Vol.25, No.10, October 1979, pp.707-709.

7. Lain, R.N., Thomas, P.E. and Huggins, J.: "The development of the industrial dc motor", Electronics and Power, Vol.27, No.10, October 1981, pp.735-738.

8. Lain, R.N.: "Drives to economy and efficiency", Electrical Review, Vol.211, No.11, October 1982, pp.47-48.

9. Sen, P.C.: "Thyristor DC Drives", Wiley, New York, 1981.

10. Robinson, C.E.: "Redesign of dc motors for applications with thyristor power supplies", IEEE Trans., Vol.IGA-4, No.5, Sept. 1968, pp.508-514.

11. Le Prince, J.: "Some problems in the design of dc machines supplied by semi-conductors", ACEC-Review, No.3-4, 1974, pp.3-16.

12. Pelly, B.R.: "Thyristor Phase-controlled Converters and Cyclo-Converters", Wiley, New York, 1971.

13. Dewan, S.B. and Straughen,A.: "Power Semiconductor Circuits", Wiley, Toronto, 1975.

14. Pearman, R.A.: "Power Electronics Solid State Motor Control", Reston (Prentice-Hall), Virginia, 1980.

15. Lukas, S.J.: "Microprocessor control of a dc drive", IEEE Conf. Rec. IAS Annual Meeting, Ohio, Sept/Oct, 1979, pp.881-885.

16. Ohmae, T., Matsuda, T., Suzuki, T., Azusawa, N., Kanigama, K. and Konishi, T.: "A microprocessor-controlled fast-response speed regulator with dual mode current loop for DCM drives", IEEE Trans., IA-16, No.3, May/June 1980, pp.388-394.

17. Chan, Y.T. and Plant, J.B.: "A microprocessor-based current controller for SCR-DC motor drives", IEEE Trans., IECI-27, No.3, Aug 1980, pp.169-176.

18. Tso, S.K. and Ho, P.T.: "Dedicated-microprocessor scheme for thyristor phase control of multiphase convertors", IEE Proc., Vol.128, Pt.B, No.2, March 1981, pp.101-108.

19. McMurray, W: "SCR DC to DC power converters", IEEE Inter. Conf. on Nonlinear Magnetics, Washington DC, April 1963.

20. Beasley, J. and White, G.: "The use of thyristors for the control of a DC traction motor operated from a 600 volt line supply", IEE Conf. Pub. No. 17, 'Power Applications of Controllable Semiconductor Devices', Pt.1, Nov 1965, pp.187-195.

21. Kalis, H. and Lemmrich, J.: "DC-chopper with switching reliability and without limitation of the adjustable mark space ratio", IEE Conf. Pub. No.53, 'Power Thyristors and their Applications', Pt.1, May 1965, pp.208-215.

22. Bailey, A.R. and Varley, J.R.: "The use of high frequency choppers for traction purposes", ibid., Pt.1, May 1965, pp.271-276.

23. Jauquet, C., Gouchiere, J. and Hologne, H.: "DC choppers for railway applications", ibid., Pt.1, May 1965, pp.289-296.

24. Berman, B.: "Design considerations pertaining to a battery powered regenerative system", IEEE Trans., 1A - 8, No.2, Mar/Apr 1972, pp.184-189.

25. Berman, B.: "All solid-state method for implementing a traction drive control", IEEE Trans., 1A-8, No.2, Mar/Apr 1972, pp.195-202.

26. McMurray, W.: "Stepless solid-state controls for battery-powered dc electric vehicles", IFAC Symp. 'Control in Power Electronics and Electric Drives', 1974, pp.421-435.

27. Knoll, H.: "High-current transistor choppers", 2nd IFAC Symp., 'Control in Power Electronics and Electric Drives", 1977, pp.307-315.

28. Steigerwald, R.L.: "A two-quadrant transistor chopper for an electric vehicle drive", IEEE Trans., IA-16, No.4, July/Aug 1980, pp.535-541.

29. Ravishankar, K., Swamy, R.A. and Khargekar, A.K.: "Two quadrant multiphase chopper for battery driven vehicles", ASNE Inter. Conf. Proc. 'Drive Electric Amsterdam 82', Amsterdam, Oct 1982, pp.602-611.

30. Evans, P.D.: "Electric drives - present and future trends", I.Mech.E. Conf. Proc. 'Electric v Hydraulic Drives', London, Oct 1983, pp.9-14.

31. Dunford, W.G. and Dewan, S.B.: "The design of a control circuit for a two-quadrant chopper based on the motorola 6800 microprocessor", IEEE Trans., IA-16, No.4, July/Aug 1980, pp.495-500.

32. Dewan, S.B. and Mirbod, A.: "Microprocessor-based optimum control for four-quadrant chopper", IEEE Trans., IA-17, No.1, Jan/Feb 1981, pp.34-40.

33. Marino, P., Picardi, C. and Russo, A.: "AC characteristics in AC/DC/DC conversion", IEE Proc., Vol.130, Pt.B, No.3, May 1983, pp.201-206.

34. Bradley, D.A., Clark, C.D., Davis, R.M. and Jones, D.A.; "Adjustable-frequency inverters and their application to variable-speed drives", IEE Proc., Vol.111, No.11, Nov 1964, pp.1833-1846.

35. Murphy, J.M.D.: "Thyristor Control of AC Motors", Pergamon Press, Oxford 1978.

36. Stemmler, H.: "The use of static converters to vary the speed of three-phase drives without losses", Brown Boveri Rev., Vol.54, No.5, May/June 1967, pp.217-232.

37. Hultstrand, K.A.: "Newest entry static adjustable frequency drives", Control Engineering, April 1964, pp.57-63.

38. Schonung, A.: "Varying the speed of three-phase motors by means of static frequency changers", Brown Boveri Rev., Vol.51, No.8/9, Sept 1964, pp.540-554.

39. Schonung, A. and Stemmler, H.: "Static frequency changers with 'subharmonic' control in conjunction with reversible variable-speed ac drives", Brown Boveri Rev., Vol.51, No.819, Sept 1964, pp.555-577.

40. King, K.G.: "Variable frequency thyristor inverters for induction motor speed control", Direct Current, Vol.10, Feb 1965, pp.26-35.

41. Mikrytzki, B.: "The controlled slip static inverter drive", IEEE Trans., IGA-4, No.3, May/June 1968, pp.312-317.

42. Salihi, J.T.: "Simulation of controlled-slip variable-speed induction motor drive systems", IEEE Trans., IGA-5, No.2, Mar/Apr 1969, pp.149-157.

43. Tsivitse, P.J. and Klingshirn, E.A.: "Optimum voltage and frequency for polyphase induction motors operating with variable frequency power supplies", IEEE Trans., IGA-7, No.4, July/Aug 1971, pp.480-487.

44. Humphrey, A.J.: "Constant horsepower operation of induction motors", IEEE Trans., IGA-5, No.5, Sept/Oct 1969, pp.552-557.

45. Hazeltine, L.A.: British Patent No.218675, 1923.

46. Griffith, D.C. and Ulmer, R.M.: "A semiconductor variable speed ac motor drive", Electrical Engineering, New York, Vol.80, May 1961, pp.350-353.

47. Bowler, P.: "The application of a cycloconverter to the control of induction motors", IEE Conf. Pub. No.17, 'Power Applications of Controllable Semiconductor Devices", Pt.1, Nov 1965, pp.137-145.

48. Slabiak, W. and Lawson, L.J.: "Precise control of a three-phase squirrel-cage induction motor using a practical cycloconverter", IEEE Trans., IGA-2, No.4, July/Aug 1966, pp.274-280.

49. McMurray, W.: "The Theory and Design of Cycloconverters", MIT Press, London, 1972.

50. Davis, R.M.: "Power diode and thyristor circuits", IEE Monograph Series 7, Peter Peregrinus Ltd., Stevenage, 1979.

51. Jenkins, J.E.: "A modified cycloconverter for use with high frequency sources", IEE Conf. Pub. No. 53, 'Power Thyristors and their Applications", Pt.1, May 1969, pp.313-319.

52. Chen, H.H.: "A microprocessor control of a three-pulse cyclo-converter", IEEE Trans., IECI-24, No.3, Aug 1977, pp.226-230.

53. Singh, D. and Hoft, R.G.: "Microcomputer-controlled single-phase cycloconverter", IEEE Trans., IECI-25, No.3, Aug 1978, pp.233-238.

54. Tso, S.K., Spooner, E.D. and Cosgrove, J.: "Efficient microprocessor-based cycloconverter control", IEE Proc., Vol.127, Pt.B, No.3, May 1980, pp.190-196.

55. Cornish, L.S. and Tso, S.K.: "Use of triacs in naturally commutated cycloconverters", Proc.IEE, Vol.126, No.6, June 1979, pp.520-521.

56. Tso, S.K. and Leung, C.C.: "Microprocessor control of triac cyclo-converter", IEE Proc., Vol.130, Pt.B, No.3, May 1983, pp.193-200.

57. Pedder, D.A.G., Issawi, A.M. and Bolton, H.R.: "A solid state, variable-frequency, 3-phase power source with individual harmonic control", IEEE Trans., Vol.IECI-24, No.1, Feb 1977, pp.100-107.

58. Ward, E.E.: "Invertor suitable for operation over a range of frequency", Proc.IEE, Vol.111, No.8, Aug 1964, pp.1423-1434.

59. Farrer, W. and Miskin, J.D.: "Quasi-sine-wave fully regenerative invertor", Proc.IEE, Vol.120, No.9, Sep 1973, pp.969-976.

60. Williams, K.H.: "Simple 3 phase ac motor control system for motors below 5 hp", IEE Conf. Pub. No.53, 'Power Thyristors and their Applications", Pt.1, May 1969, pp.320-327.

61. Green, R.M. and Boys, J.T.: "Inverter ac-drive efficiency", Proc.IEE, Vol.129, Pt.B, No.2, March 1982, pp.75-81.

62. Norton, G.J. and O'Callaghan, D.F.: "Transistorised inverters for standard 20 HP induction motor drive", IEE Conf. Pub. No.154, 'Power Semiconductors and their Applications', Sept 1977, pp.45-49.

63. Evans, P.D. and Hill-Cottingham, R.J.: "Some aspects of power transistor inverter design", Electric Power Applications, Vol.2, No.3, June 1979, pp.73-80.

64. Eastham, J.F., Daniels, A.R. and Lipczynski, R.T.: "A novel power inverter configuration", IEEE Conf. Rec. IAS Annual Meeting, Cincinnati, Vol.2, Sept/Oct 1980, pp.748-751.

65. Yair, A. and Ben-Uri, J.: "New 3-phase invertor with three thyristors", Proc.IEE, Vol.118, No.7, July 1971, pp.901-905.

66. Eastham, J.F.: British Patent Application 29692/75.

CHAPTER 2

BEHAVIOUR OF THE DELTA INVERTER WITH PASSIVE LOADS

2.1 Introduction

The previous chapter introduced a new type of three-phase inverter - the delta inverter. The basic circuit configuration given in Fig.2.1 shows the three limbs of the inverter, each of which contains an antiparallel transistor-diode pair and a dc supply. This configuration has conceivably the minimum number of power devices and related drive circuitry possible for a three-phase inverter system. In comparison with the conventional three-phase bridge inverter, Fig.2.2, the device count has been halved, although at the expense of requiring three isolated dc supplies instead of one.

With a new type of inverter such as the delta inverter, where the modes of operation are likely to be relatively complex, a thorough understanding of the circuits essential characteristics with the simplest types of loads is advisable before considering, for instance, the load presented by an induction motor. This chapter thus analyses the operation of the delta inverter under passive load conditions with 'purely' resistive, 'purely' inductive and RL loads. Of these, the first two can be handled graphically and analytically in a relatively convenient manner and this enables the limits to be ascertained within which the RL loads with intermediate time constants operate.

The delta inverter circuit used for the experimental work was substantially as shown in Fig.2.1, using 36 volt traction batteries as the dc sources. The power devices were monolithic Darlington transistors, with principal characteristics $I_{C(mean)}$ = 50A, $I_{C(max)}$ = 100A, $V_{CEO(sus)}$ = 450V and high power fast recovery diodes with a mean forward current capability of 70A. These devices were chosen, such that they would operate well within their ratings throughout, so that no problems were likely, and because their characteristics were already well understood. In order that a large number of different transistor switching waveforms could be investigated, a microprocessor system was produced to generate the switching sequences using open loop control. This system was found to be both convenient and versatile. Balanced three-phase conditions were observed throughout, both in switching waveforms and loads.

Some of the material contained in this chapter has been presented in a paper reproduced in Appendix 1. This led to a published discussion, Appendix 2. A recent conference paper has also been published, Appendix 3.

2.2 The Delta Inverter with Resistive Load

This section describes the behaviour of the inverter under ideally purely resistive load conditions, i.e. loads with negligible inductance. In practical terms, to model such resistances requires special construction; here, a bifilar technique, whereby, for each load, a piece of resistance wire with the required total resistance (5 or 10Ω) was bent in half and twisted together to reduce inductance to acceptably low levels.

With purely resistive loads the behaviour of the delta inverter can be obtained by inspection. Fig.2.3 shows the inverter with a star connected load. From an examination of either Fig.2.1 or Fig.2.3 it can be seen that under balanced three-phase conditions, where each of the three transistors is switched on for an identical conduction period (spaced 120^{o} apart), there is a maximum limit of 240^{o} conduction. Beyond this, three transistors would be on simultaneously, providing a destructive short circuit path for the three supplies. Tests have thus been carried out between a minimum conduction angle of 120^{o} (for which at least one device is always on) and a maximum of 240^{o}.

It is apparent that with negligible load inductance the feedback diodes will be inoperative and that, further, the shape (and consequently the harmonic content) of the voltage and current waveforms must be identical.

Consider, first, the three output voltages of the inverter, the line voltages, that apply whether the load is star or delta connected. It can be seen from Fig.2.3 that there are three possible voltage levels. For example, V_{RB} will be $+ V_D$ whenever T_1 is On, $- \frac{1}{2} V_D$ if either T_2 or T_3 is On and $- 2 V_D$ if both T_2 and T_3 are On. With delta connected loads these voltages are the load phase voltages in the usual way. For the star connected load, five voltage levels of the load phase voltage can be identified. These are, in the case of V_{RN}:

a) $+ \frac{1}{2} V_D$ when only T_1 is On

b) $+ V_D$ when T_1 and T_3 are On

c) Zero when T_1 and T_2 are On, or only T_3 is On

d) $- \frac{1}{2} V_D$ when only T_2 is On

e) $- V_D$ when T_2 and T_3 are On

In terms of the load, for every star load there is an equivalent delta load, so the overall behaviour of the system is not affected by the load configuration.

Fig.2.4 illustrates the resultant phase and line voltages that are possible. Fig.2.4a shows the transistor switching sequences with 120^{o}, an intermediate 180^{o} and 240^{o} conduction. Only voltage levels $+ \frac{1}{2} V_D$, $- \frac{1}{2} V_D$ and zero are present in the phase voltage with 120^{o} conduction, Fig.2.4b, and $+ V_D$ and $- \frac{1}{2} V_D$ in the line, Fig.2.4c. Any intermediate conduction angle between 120^{o} and 240^{o} will contain all five possible phase voltage levels, Fig.2.4d, and all three line voltage levels, Fig.2.4e. Finally, with 240^{o} conduction, voltage levels $+ V_D$, $- V_D$ and zero are present in the phase voltage, Fig.2.4f, and only $+ V_D$ and $- 2V_D$ in the line, Fig.2.4g. Oscillograms for these three conditions, showing the line voltages for 120^{o}, 180^{o} and 240^{o} conduction, are given in Fig.2.5a, b and c. It can be seen that these voltage waveforms correlate substantially with the predictions in Fig.2.4 for the idealised case.

For an intermediate conduction angle (180^{o}), Fig.2.6b, c, d and e respectively show a phase voltage (V_{RN}), a line voltage (V_{RB}) and the current and voltage of transistor T_1. From this, the maximum transistor current for any conduction angle greater than 120^{o} is $3I_D$, where $I_D = V_D/R_D$ and R_D is the equivalent line resistance. Similarly, the maximum voltage across each transistor is $V_{CE} = 3V_D$. For 120^{o} conduction the 'maximum' transistor current and voltage are $\frac{3}{2} I_D$ and $\frac{3}{2} V_D$, respectively.

An expression can be derived for the harmonic content of the line voltage with conduction angle θ between 120^{o} and 240^{o}. The analysis

is done using the standard Fourier series:

$$f(t) = C_0 + \sum_{n=1}^{\infty} (a_n \cos n\omega t + b_n \sin n\omega t) \qquad (2.1)$$

where

$$C_0 = \frac{1}{T} \int_0^T f(t)\, dt \qquad (2.2)$$

$$a_n = \frac{2}{T} \int_0^T f(t) \cos n\omega t\, dt \qquad (2.3)$$

$$b_n = \frac{2}{T} \int_0^T f(t) \sin n\omega t\, dt \qquad (2.4)$$

With reference to Fig.2.6c:

$$f(t) = C_0 + \sum_{n=1}^{\infty} a_n \cos n\omega t \qquad (2.5)$$

and using (2.2) $C_0 = 0$

and using (2.3)

$$\hat{V}_n = a_n = \frac{2}{\pi} \left\{ \int_0^{\frac{\theta}{2}} V_D \cos n\theta\, d\theta + \int_{\frac{\theta}{2}}^{\frac{4\pi}{3}-\frac{\theta}{2}} \frac{V_D}{2} \cos n\theta\, d\theta + \int_{\frac{4\pi}{3}-\frac{\theta}{2}}^{\pi} 2V_D \cos n\theta\, d\theta \right\}$$

from which

$$\hat{V}_n = \frac{6V_D}{\pi n} \sin \frac{2\pi n}{3} \cos n \left(\frac{2\pi}{3} - \frac{\theta}{2}\right) \qquad (2.6)$$

Using (2.6), the values of peak line voltage normalised to the dc supply voltage, $\frac{\hat{V}_n}{V_D}$, were computed. These results, together with the corresponding experimental results, are shown in Fig.2.7, for the first eight harmonics. No triplen harmonics appear because of three-phase symmetry. There is close agreement between the theoretical and

experimental results. It is apparent that the low order harmonics, especially the 2nd and 4th, can have relatively high amplitudes in the basic inverter waveforms. Whilst the amplitude of the fundamental doubles from 120^{o} to 240^{o} conduction, at 240^{o} the other unwanted harmonics are at a maximum. There is some scope for harmonic improvement by means of conduction angle control, e.g. zero 2nd harmonic (but maximum 4th harmonic) at 150^{o}. In general, however, harmonic improvement by some other means is required.

2.3 The Delta Inverter with Inductive Load

In practical terms, a purely inductive load, which by definition has an infinite time constant, is not feasible since all ordinary inductors have some resistance. However, the standard iron cored chokes used for the experimental work in this section were in most respects adequate models of pure inductors, i.e. their time constants were very long compared with the switching time periods under consideration. A typical inductive load used had the measured parameters, $L = 24$ mH and $R = 75$ mΩ, giving a load time constant $\tau = 0.3$s, compared with a switching period $T = 10$ mS (at 100 Hz).

In attempting to predict the delta inverter behaviour with inductive load, three basic principal conditions must be observed: the current changes linearly, the rate of change being proportional to applied voltage, $di/dt = V/L$; the average energy dissipated in an inductance over a cycle must be zero and, consequently, the time average power dissipation from the supplies must also be zero.

It is easier to explain the operation of the delta inverter under these conditions with reference to a delta connected load, Fig.2.1. It should be noted that the three diodes do not allow free-wheeling current from the load, in the usual sense of the word, but

provide feedback paths to the supply voltage sources and thus their action is that of flywheel diodes.

Considering the same transistor switching waveforms as in Section 2.2, there appear to be two distinct modes of operation with inductive loads. One mode extends from 240^{o} down to 160^{o} conduction, producing invariant current and voltage waveforms. Below 160^{o} the shape of the current and voltage change as the conduction angle changes. The two cases are considered separately.

2.3.1 $160^{o} \leq \theta \leq 240^{o}$

Taking one cycle under steady operating conditions and referring to Fig.2.1 and 2.8b, if T_1 is switched ON, current starts to rise in load L_a being driven by voltage $+ V_D$. At some point T_1 is switched OFF. The current I_a must continue flowing in the positive direction. The current flywheels through diodes D_2 and D_3, decreasing at twice the rate against $- 2V_D$. Provided that $\theta \geq 180^{o}$, the energy in the inductor is sufficient to maintain this decreasing current until such time as T_2 and T_3 are both ON together. The current then increases negatively with the voltage still being held at $- 2V_D$ by these transistors. When T_2 is switched OFF, the current flywheels through D_1, decreasing at the original rate against $- V_D$, until the current reaches zero and T_1 takes over again.

Fig.2.8b shows the resulting load voltage and current at 240^{o} conduction. It can be seen that the integral of both voltage and current with time over a cycle is zero and thus the average energy dissipation is zero. However, for $160^{o} \leq \theta < 180^{o}$, whilst the load current and voltage are the same, the mechanism is slightly different. As shown in Fig.2.8c, for 160^{o} conduction, the current flywheeling through D_2 and D_3 reaches zero before T_3 has been switched ON but the

voltage across L_a remains clamped at $-2V_D$ because T_2 is ON and current from L_c is still flywheeling through D_3.

From Fig.2.1, if a delta-star transformation is done, then I_R becomes an equivalent phase current. Hence, since $I_R = I_a - I_b$, this current can be determined directly, given the load currents I_a and I_b. Fig.2.9 shows the three load currents for a delta connected load at 180^o conduction, from which the line current I_R is drawn, Fig.2.9c. Similarly, by adding up the currents in all three loads which flow through T_1 or D_1, the transistor and diode currents may be determined. For one antiparallel pair, the current and voltage are shown in Fig.2.9d. These waveforms indicate that the constraint, that the time average battery power dissipated must be zero, applies.

An examination of the oscillograms in Fig.2.10, of the actual transistor and diode waveforms at 180^o conduction, shows some discrepancy between the practical and ideal cases. Comparing Figs.2.9d and 2.10, it can be seen that once the transistor has been turned on (i.e. base current has been applied), it contributes reverse current, which it was expected the diode would carry. Consider the point marked with a * on Fig.2.10. At this point the transistor is turned on and reverse current, which was flowing in the diode, immediately begins to flow through the transistor. Fig.2.11 shows an equivalent circuit of the antiparallel pair under such a regenerating load condition. Reverse inductive load current, i_L, has just been flywheeling through the diode, but as the transistor switched on, v_{CE} reverse biased the diode which then ceased conducting. Now, i_B must remain constant, since the voltage across R_B is clamped, hence

$$i'_B = i_B = \frac{V_{BB} - 2v_{BE}}{R_B} \qquad (2.7)$$

and since

$$i'_B = i_L + i_E \qquad (2.8)$$

in effect, as i_L increases it contributes to i'_B at the expense of a decreasing i_E. Assuming i_E is still greater than zero, the two base emitter junctions are forward biased, resulting in a net positive collector emitter voltage of around 0.7V. If, however, i_L is greater than i_E, the base emitter junctions are no longer clamped on and the base current, now flowing into the collector (with $- i_C$ flowing through the main supply into the load) can increase to a value defined by

$$i_B = \frac{V_{BB}}{R_B} \qquad (2.9)$$

At this point v_{CE} is reversed to the extent of the driver transistor's base collector forward junction voltage. The flywheel diode is consequently forward biased and carries any remaining excess current (this can be seen in Fig.2.10 as the smaller pair of diode current pulses).

This phenomenon of transistor reverse current carrying capability is not unique to the delta inverter and can occur in other circuits with antiparallel transistor-diode pairs. The effect is particularly noticeable in Fig.2.10 because the load currents are the same order of magnitude as the base drive currents. However, it is of little interest to the load or the inverter operation, as to which of the antiparallel pair carries the current.

Returning to an examination of the load voltages for the range of conduction angles under consideration; comparing Fig.2.8b and c with Fig.2.4g, the load voltages are identical to the load voltage for a purely resistive load with 240^{o} conduction. Thus, letting $\theta = \frac{4\pi}{3}$ in (2.6), gives the peak amplitude of the n^{th} harmonic of the line voltage with inductive load, as:

$$\hat{V}_n = \frac{6V_D}{\pi n} \sin \frac{2\pi n}{3} \quad \text{for } 160^{o} \leq \theta \leq 240^{o} \qquad (2.10)$$

The normalised harmonic amplitudes are therefore shown in Fig.2.7 at $\theta = 240^{o}$.

2.3.2 $120^{o} \leq \theta \leq 160^{o}$

From the foregoing, between 240^{o} and 180^{o} conduction the operation of the inverter is relatively simple. Reducing the conduction angle below 180^{o} (within the range $160^{o} \leq \theta \leq 180^{o}$) introduced a slight complication, in that the flywheel current under $-2V_D$ from a load was not maintained by flowing through two diodes over the required period. Since the total sum of currents flowing through one of the diodes reduced to zero, it was only because, as this diode subsequently went off, the corresponding transistor was on, that $-2V_D$ remained clamped across the load.

Further reducing the conduction angle below 160^{o} has the following effect. Taking the condition just mentioned, assuming in Fig.2.1 that $-2V_D$ is clamped across L_a because current is flywheeling through D_3 and T_2 is ON. D_3 is being held ON by a negative phase current in L_c. With T_2 being ON and positive current flowing through it, eventually all the current in L_c is supplied by T_2 and D_3 unclamps. L_a and L_c are now connected in series across leg 2 and the voltage across L_a, V_a, becomes $-\frac{1}{2} V_D$.

This mechanism accounts for the final complication in the basic inverter operation with inductive load. A full set of waveforms for a general conduction angle between 120^{o} and 160^{o} can be deduced, as shown in Fig.2.12 (for 140^{o}). Taking the phase current I_a: it was found, and will be shown, that the angle α from the point when T_1 is switched ON until positive current begins to flow in L_a, is constant at 40^{o}, whatever the conduction angle within the considered range. The shape of the load current can then be inferred as follows. From Fig.2.12:

a) Up to point p current rises in L_a under $+V_D$. At p, T_1 is switched OFF and the current in L_a flywheels through D_2 and D_3, reducing under $-2V_D$. During this period from p to q current in L_b is rising from a negative value, first through D_2 and then, going positive, through T_2. The phase current I_c, which is negative throughout this period, is decreasing through D_3.

b) From q to r, current in L_a has become negative with $-2V_D$ still clamped across it, due to T_2 and D_3. For angle γ the current flowing in L_a is due to a component of current in T_2. The phase current flowing in L_c is the sum of this current, which is increasing negatively in L_c, and the current in D_3 which must therefore be decreasing negatively (as the voltage across L_c is clamped at $+V_D$). These two current components are shown by dotted lines. Throughout most of the period from p to t, phase current I_b is rising through T_2 under $+V_D$ and need not further enter the situation.

c) At point r, D_3 unclamps and subsequently there is $-\frac{1}{2} V_D$ across L_a and across L_c.

d) Until point s, the voltage across L_a remains at $-\frac{1}{2} V_D$, then T_3 is switched ON, which clamps $-2V_D$ across L_a and $+V_D$ across L_c.

e) Finally, at point t, T_2 switches OFF and the sequence of events from p to t repeats with phase b taking the place of phase a and phases b and c being replaced by c and a, respectively.

Again, a delta-star transformation on the load makes the line current, Fig.2.12e, equivalent to the load current with star connected load.

As at one end of this range, 160^o conduction represented a simplified waveshape limit for this mode of conduction, so to at the other end of the range. Fig.2.13, then, shows the waveforms for 120^o conduction. Taking L_a again, the two diodes carrying the flywheel current both unclamp at the same time, since I_c has also reached zero. T_2 thus takes over providing the phase current through L_a, until switched OFF, when the current flywheels through D_1, until this current in turn reaches zero and T_3 takes over.

Having intuitively found the general shape of the waveforms, it is possible to derive expressions which give all the angles for any conduction angle between 120^o and 160^o. Returning to Fig.2.12, the angles that are required are α, β, γ and δ, which will completely define the waveforms. Consider the currents I_u, I_v and I_w, as marked. By inspection:

$$I_u = (\theta - \alpha)k \qquad (2.11)$$

$$= -\beta\, 2k$$

which gives $\theta - \alpha = 2\beta$ (2.12)

$$I_v = -(\alpha - (\theta - 120^o))k \qquad (2.13)$$

$$I_w = -(\gamma 2k + (\beta + \gamma)k) \qquad (2.14)$$

$$= -(\gamma 2k + \frac{\delta k}{2} + (\theta - 120^o)2k)$$

which gives $\beta + \gamma = \frac{\delta}{2} + 2(\theta - 120^o)$ (2.15)

(where k is defined as the current gradient due to one battery voltage, V_D, across one inductor and angles are in degrees).

Since at any instant in time, the sum of the load currents must be zero, then:

$$I_u + I_v + I_w = 0 \qquad (2.16)$$

Using (2.11), (2.13) and (2.14) in (2.16)

$$2\theta - 2\alpha - 3\gamma - \beta - 120^o = 0 \qquad (2.17)$$

and from Fig.2.12

$$\beta + \gamma + \delta = 240^o - \theta \qquad (2.18)$$

Subsituting the value of δ from (2.18) into (2.15) gives

$$\gamma = \theta - \beta - 80^o \qquad (2.19)$$

Substituting the value of γ from (2.19) into (2.17) gives

$$2\alpha = 120^o + 2\beta - \theta \qquad (2.20)$$

and substituting the value of β from (2.12) into (2.20) gives

$$3\alpha = 120^o \qquad (2.21)$$

hence:

$$\alpha = 40^o \qquad (2.22)$$

$$\beta = \tfrac{1}{2}(\theta - 40^o) \qquad (2.23)$$

$$\gamma = \frac{\theta}{2} - 60^{o} \qquad (2.24)$$

$$\delta = 320^{o} - 2\theta \qquad (2.25)$$

For $120^{o} \leq \theta \leq 160^{o}$ equations (2.22) to (2.25) completely define the waveforms.

2.3.3 Summary

From sections 2.3.1 and 2.3.2 it is possible to theoretically predict the operation of the inverter with inductive load, for any conduction angle between 120^{o} and 240^{o}. Oscillograms of the actual load currents and voltages for a delta connected load with conduction angles of 120^{o}, 150^{o} and 180^{o} are shown in Fig.2.14. The table given in Fig.2.15 compares the predicted and experimental values of α, β, γ and δ for conduction angles between 120^{o} and 160^{o}, taken from similar oscilloscope traces to those shown in Fig.2.14. The experimental results are a general confirmation of the predicted values and agree, in the main, to within 20% or less. Predictions were made for an ideal system and thus discrepancies due to loss mechanisms and non ideal components within the inverter and load are expected. The angle α remains constant, being, as predicted, independent of the conduction angle.

2.4 The Delta Inverter with RL Load

Having examined the inverter with purely resistive loads, that have a zero time constant, and inductive loads, that have an infinite time constant, then the inverter behaviour with loads having intermediate time constants will lie between these two limits.

The use of the inverter with inductive load, over a range of conduction angles, has particularly shown that the output voltages of

the inverter can be load dependent. Under these load dependent conditions, as soon as the load currents start taking flywheel paths, prediction of the circuit operation necessitates a knowledge of the load time constant. Although predictions of these conditions is, in principle, straightforward, it has not been undertaken in the present work.

This section gives a brief general view of the operation with RL loads, particularly related to highlighting the conditions under which sufficient parameters are defined (in effect, the load voltages), to make prediction, analysis and control of the circuit operation practicable, in general, irrespective of the type of load.

The experimental RL loads were made up using combinations of the non inductive resistors and iron cored chokes used in the previous two sections. This made determination of the real and imaginary parts of the loads easier. Thus loads were used having a range of time constants from about 0.1 mS to 10 mS, using a fundamental supply frequency of 100 Hz (period 10 mS).

Applying a step change in voltage across a load, with final value V, then the current through the load will attempt to rise or decay, from its initial value I_0, to a steady state value of $\frac{V}{R}$ within five time constants. The current being specified by:

$$i(t) = I_0 e^{-R/L\ t} + \frac{V}{R}(1 - e^{-R/L\ t}) \qquad (2.26)$$

The oscillograms of Fig.2.16 show the load voltage and current of a fairly resistive ($\tau \simeq 0.4$ mS) and a fairly inductive ($\tau \simeq 2.3$ mS) delta connected load, for 180^o and 240^o conduction. It can be seen that the behaviour of the current conforms to (2.26) and that, given sufficient time, does reach a steady state value.

Consider, first, 180^{o} conduction, Fig.2.16a and b. For both these load conditions, the voltages have the same general shape and thus the conduction mechanisms are the same. Comparing a fairly resistive load, Fig.2.16a, with Fig.2.5b, for a purely resistive load, and the general similarity is clear - having accounted for the current with fairly resistive load taking approximately 2 mS (five time constants) to reach any steady value. The effect of the inductance within this load is, however, to utilise the diode paths; either with reverse load current through two diodes or with forward load current through one diode. The conduction paths and changeover conditions follow the general scheme outlined in section 2.3.2 (for an inductive load with a conduction angle between 120^{o} and 160^{o}). The fairly inductive load behaves in the same way but the flywheel paths are maintained for longer and now the similarity between this current waveform and the triangular waveform for a purely inductive load, Fig.2.14c (with 180^{o} conduction), is becoming apparent.

Contrasting the case of 240^{o} conduction with that of 180^{o}, however, and it can be seen that whilst the flywheel paths are still utilised with 240^{o} conduction, the voltage waveform remains identical to that of 240^{o} conduction with purely resistive load - or, for that matter, with purely inductive load. 240^{o} conduction is the special case, where two of the three transistors of the inverter are always on. Examining Fig.2.1 shows that with two devices always on, all the load voltages are clamped. With a total of 240^{o} conduction per device, two devices always on, the load voltages are thus defined by the transistor switching sequence, and are load independent.

To investigate the effect on the harmonic content, of altering the load, a graph of current harmonics is shown in Fig.2.17 for 180^{o}

and 240° conduction. Load time constant is used as the abscissae and the fundamental frequency is again 100 Hz. The current harmonics are normalised to the amplitude of the fundamental current, as otherwise some accounting of the relative load impedances must be made.

With a large amount of inductance in the load, the harmonics for both conduction angles converge - since, with a purely inductive load, both current waveforms are identical. Towards the resistive end, whilst the harmonics for 240° show a smooth transition, the changes with 180° are less regular. Essentially the current harmonics for 240° conduction show the effect of a constant voltage waveform, identical voltage harmonics, across a changing load. Whereas the current harmonics for 180° conduction show the combination of a changing load and a consequential changing voltage waveform. However, a largely resistive load with 180° conduction does have a better harmonic content in comparison with 240° conduction, principally a much reduced 2nd harmonic, which is advantageous when considering harmonic losses.

2.5 Conclusions

This chapter has investigated the operation of the delta inverter with passive loads. The two simplest types of load, purely resistive and purely inductive, have been treated analytically. These being the extremes, zero and infinite time constants, set the limits within which intermediate RL loads were studied. Conduction angles between 120°, one transistor always on, and 240°, two transistors always on, were employed.

With a purely resistive load, operation at any conduction angle was straightforward. The introduction of inductance, which necessitates use of the flywheel paths, considerably complicates the inverter operation,

particularly at lower conduction angles. However, the limiting conduction angle of 240^{o} was shown to be a special case, whereby, regardless of load and consequent flywheel paths used, the operation becomes completely defined, as the output voltages are clamped according to the transistor switching sequence.

Investigation of the output harmonics with resistive load shows a poor performance with 240^{o} conduction. As the load becomes more inductive, with high conduction angles (160^{o} and above), the harmonic contents tend to the same values; the limiting case being 240^{o} conduction, where the voltage harmonics are constant and independent of the load. Principally because of the presence of even harmonics, particularly the 2nd harmonic, then, in general, the harmonic performance of the delta inverter is poorer than that of the conventional inverter.

Where a higher harmonic content can be accepted, the minimal component count of the delta inverter may make it advantageous. For efficient operation in an ac drive system, these initial results suggest harmonic improvement is necessary. Although plain 240^{o} conduction has a relatively poor harmonic performance, the ability in this condition, where two devices are always on, to be able to accurately predict the inverter operation, regardless of load, appears to considerably ease the task of developing effective control schemes and of improving the harmonic content.

CHAPTER 3

HARMONIC IMPROVEMENT-SINUSOIDAL PULSE-WIDTH MODULATION

3.1 Introduction

The raw output waveforms of the delta inverter, that were described in the previous chapter, may be adequate for some applications - such a resulting system being advantageous in terms of its overall simplicity. However, for many applications the relatively high harmonic content of these waveforms will give a low system efficiency and consequent high running costs. One of the principal applications for inverters is for ac machine control, and excessive additional harmonic losses can require motors to be significantly derated.

A number of methods are available for reducing harmonics. Some of these methods are briefly reviewed but the main investigation is restricted to sinusoidal pulse-width modulation (PWM). It is shown how this may be implemented on the delta inverter and comparisons with implementation on the conventional three-phase bridge inverter are made.

In selecting a method to reduce inverter harmonics a number of factors must be considered. Much depends on the nature of the load and the level of harmonics that can be tolerated. As the work involving the delta inverter is concerned with ac drives (in particular, the three-phase squirrel cage induction motor), a simplified assumption is made regarding the frequency dependent nature of the load and low order harmonics are taken as being most troublesome.

3.1.1 Filters

Directly filtering the inverter output does not appear attractive, due to the likely size, weight and cost of the filter components required to meet adequate performance specifications. The low order harmonics, which are particularly troublesome, being relatively close to the fundamental, are difficult to filter effectively. Direct filtering with the inverter under variable frequency operation is particularly difficult. If, however, the low order harmonics of a system can be reduced or eliminated by other means, then subsequent filtering of the remaining high order harmonics may be possible.

3.1.2 Multiple inverter/transformer connected systems

Systems have been described and developed which use a number of inverters, combining their outputs via suitable transformer connections, to reduce or eliminate harmonics. As examples, two methods may be mentioned: using a number of single-phase inverters, suitably combining their outputs by means of transformer connections[1,2] or, alternatively, the outputs of a number of conventional three-phase inverters with suitable phase shifts may be combined using a three-phase transformer connection[3,4,5].

Such schemes have advantages, particularly where the power devices are not fast enough for methods such as PWM. At low power levels initial cost and comparatively low efficiency appear to make such schemes uneconomical, while bulk and weight factors also appear unattractive. At high power levels and when a change in voltage level is also required, such methods may be necessary or advantageous.

3.1.3 Current control

A number of general methods of harmonic improvement are available for inverters, which rely on altering the switching sequence of the devices by some prescribed algorithm. Filtering of high frequency components may be incorporated but otherwise little additional penalties need be paid in weight or bulk. One such group of schemes are those of current control (and, similarly, methods grouped under the heading of voltage control).

The requirement of current control schemes is to suitably switch the inverter such that the load current waveform improves. Consider the method of current feedback[6]. By closed loop control, a signal proportional to the actual load current is compared with a reference sinusoid and the inverter devices switched accordingly, to keep the resultant error within set limits. For variable speed drives this method requires two feedback signals, load current and motor speed.

It is inferred that the delta inverter could operate under such a strategy, requiring only an understanding of the nature of the delta inverter's interdependent switching. However, to investigate the action of the inverter with various switching algorithms, the method is not particularly suitable. The need for feedback signals and careful initial setting-up of the control seems, in general, disadvantageous. Also, when considering variable speed operation, it is desirable to have a constant level of flux loading in the motor which is not readily achievable without monitoring motor speed and, as mentioned above, an extra feedback signal is then required.

3.1.4 Voltage control

These methods rely on the assumption that the harmonic losses within the motor are dependent on the level of harmonic distortion present in the inverter output voltage waveforms. Control does not rely on feedback signals but is done directly within the inverter. Variable speed operation is also straightforward (in principle), though requiring incorporation of a constant V/f ratio to maintain constant flux loading. Within this type of control, methods are grouped, here, under two headings: those of selective harmonic reduction and those of pulse-width modulation. At high switching frequencies the methods presumably become very similar, as they are attempting to achieve the same thing, a voltage waveform with low harmonic distortion, approaching pure fundamental in the limit. The PWM method has been adopted for the present work because it is the traditional method of control and the regular switching frequency allows the variation of voltage with frequency to be incorporated with relative ease. Consideration is given to synchronous PWM, where the modulation is synchronised to the inverter output. The implementation of selective harmonic reduction on the delta inverter is, however, discussed in Appendix 5.

3.2 Pulse-Width Modulation

The initial investigations of implementing sinusoidal pulse-width modulation techniques on power inverters related to the work done in the communications field, on what was more generally called pulse-duration modulation. Pulse communication was developed during the second world war, following which a number of papers appeared that theoretically investigated these pulse modulation techniques and the

spectra they produced - of particular interest being those related to PWM[7,8,9]. The techniques are now presented in standard text-books, such as those by Black[10] and Rowe[11]. The treatment by Black, for instance, was followed by Bowes[12,13] in the seventies, relating the work to the development of modulation techniques for the standard power inverter.

Whilst within the field of power inverters and ac drives the techniques of PWM are being universally accepted and developed at the present time, the system has not been so accepted in the communications field. The anomaly is due to the shift in emphasis between the needs of the two disciplines: communications being more concerned with the transmission of information and power inverters with the transmission, as efficiently as possible, of power. As an example, an ac drive must convert a dc power source into the mechanical output power of an ac motor; and for a given motor design the efficiency of the inverter and the quality of its output are crucial to optimise the drive. Within a PWM waveform in relation to the modulated information there is a large amount of power stored - which is necessary with an inverter to effectively supply the load. However, both disciplines are concerned with losses and distortion caused by modulation and thus the resultant harmonic spectra must be adequate for efficient implementation.

Effective sinusoidal PWM requires relatively high device switching frequencies. Schonung and Stemmler[14], introducing work on 'sub-harmonic' control, state the necessity of having sufficiently fast devices to make possible the design of drives which combine the simple and robust construction of the squirrel cage induction motor with the

control qualities of the rectifier fed dc motor. While Mokrytzki[15] states that the choice of PWM involves balancing the losses in the inverter, incurred in using high switching frequencies, against improved performance and reduced losses in the motor resulting from this high frequency switching. At the time of writing, the improved switching speeds of bipolar power transistors have reduced inverter losses to a relatively low level.

Both Schonung and Stemmler and Mokrytzki discuss the supply parameters to the load in terms of the flux and hence the voltage-time area. Mokrytzki discusses the relationship between the 'idealised modulating method', where each individual pulse width of a train of pulses is made proportional to the area of a sine wave modulating signal represented by its position, and the subharmonic method, using a high frequency triangular voltage carrier wave and a sinusoidal modulating signal. However, purely considering the quality of supply to the load, the optimising factor seems to be the reduction of unwanted harmonic components resulting from the improved modulated output wave shape.

Two methods of generating voltage controlled sinusoidal PWM have been predominant up to the present time - termed natural sampling and uniform or regular sampling. Wilson and Yeamans[16] have described both, numerically and analytically, although the investigation of (particularly) regular sampling, analytically, is not straightforward and not conclusive.

Natural sampling is represented in Fig.3.1. The intersection of a high frequency triangular carrier wave and a sinusoidal modulating signal determines the widths of each pulse in the modulated output

pulse train. The method follows directly from an analogue implementation of PWM. The approach in the present work is to consider the average value of a pulse as its width or mark-space ratio is varied, which, being a linear function, can be represented by a ramp. Thus, for each pulse, the simultaneous solution of the ramp functions and the sinusoidal modulating function determines the pulse widths. The time average value of each modulated pulse becomes equal to the value of the modulating signal at some instant in time determined by the modulating signal.

Fig.3.1 shows the use of double edge modulation, so called because using a triangular carrier waveform results in both edges of the unmodulated pulse waveform being modulated. However, the use of a sawtooth carrier results in only one edge of each pulse being modulated. This is illustrated in Fig.3.2 for natural sampling. Whilst one edge is modulated the other edge of the pulse remains fixed and periodic, thus single edge modulation. In Fig.3.2 the lagging edge of each pulse is modulated, lagging edge modulation, but equally well the leading edge could be modulated.

Uniform sampling is represented in Fig.3.3 and 3.4. In each case a stepped waveform is generated by regularly sampling the modulating sinusoid. The intersection of the triangular carrier and the stepped waveform determines the pulse widths. This has the advantage that the equations determining the pulse widths are numerically easier to solve than the corresponding expressions for natural sampling, making the waveforms easier to generate digitally. Fig.3.3 and 3.4 show, respectively, symmetrical sampling, in which both edges of each pulse are modulated by the same amount, and asymmetric sampling, in which the leading and lagging edges of each pulse are modulated independently.

The waveforms illustrated in Figs. 3.1-3.4 can be applied directly when considering implementing sinusoidal PWM on either the single- or three-phase bridge inverters and this is discussed in section 3.3. Applying sinusoidal PWM to the delta inverter is not as straightforward and the necessary changes to the modulating structure due to the delta inverter geometry are discussed in section 3.4. Section 3.5 describes various types of modulation that can be used, including natural and uniform sampling, and section 3.6 summarises the theoretical results of spectrum analysis with both types of inverter.

Some of the information in the proceeding sections is also contained in a paper entitled "Sinusoidal Pulse-Width Modulation Strategy for the Delta Inverter", scheduled for publication in July/August 1984 by the IEEE, and is reproduced in Appendix 4.

3.3 PWM Applied to Conventional Inverter Circuits

The generation of single-phase sinusoidal PWM is considered using two circuits, as illustrated in Figs. 3.5a and b, the single-phase centre-tapped or half bridge inverter and the single-phase bridge inverter, respectively. In the case of the half bridge circuit the load voltage can be switched between $+\frac{V_B}{2}$ and $-\frac{V_B}{2}$ by turning on either T_1 or T_2. Thus the modulated pulse trains of Figs. 3.1-3.4 can be synthesised directly. In a similar manner with the full bridge circuit, load voltages of $+V_B$ or $-V_B$ can be produced by switching on T_1 and T_4 or T_2 and T_3, respectively. However, by considering a notional reference potential, as shown in Fig.3.5b, the voltages at point A and point B may independently be controlled by considering the circuit composed of two half bridge inverters, each with sinusoidal PWM. The phase shift between these two inverters may, for example, provide amplitude control of the resultant load voltage. The full bridge also has a OV state available.

The conventional three-phase bridge inverter illustrated in Fig.3.6 can be considered (again) as simply three single-phase centre-tapped inverters with a notional reference potential, as shown. Thus the three-phase voltage set, of V_{RG}, V_{YG} and V_{BG}, is generated using T_1 and T_4, T_3 and T_6 and T_5 and T_2, respectively. For three-phase symmetry each of the three switching voltages need only be phase displaced from each other by $\pm 120^{o}$.

Considering, first, single edge modulation, then from the diagram of Fig.3.7, showing a general pulse of a single edge modulated pulse train, an expression can be derived for the harmonic spectra applicable to the voltages of the above three-phase voltage set (with a similar derivation for the single-phase circuits). Given there are p pulses per cycle of the modulating sinusoid, then the period of a pulse is given by $\Delta = \frac{2\pi}{p}$, as shown in Fig.3.7. A 50-50 mark-space ratio represents an average value of zero for the pulse. Thus, in this case, for the k^{th} pulse, the lagging edge is modulated by an angle δ_k about this mid position defined by α_k from the beginning of the modulation cycle. Using the exponential form of the Fourier series, for generality:

$$C_n = \frac{1}{2\pi} \int_{\lambda}^{\lambda+2\pi} f(\theta) e^{-jn\theta} \, d\theta \qquad (3.1)$$

then the amplitude of the n^{th} harmonic due to the k^{th} pulse, is given by,

$$C_{n_k} = \frac{1}{2\pi} \left\{ \int_{\alpha_k - \frac{\Delta}{2}}^{\alpha_k + \delta_k} \frac{V_B}{2} e^{-jn\theta} \, d\theta + \int_{\alpha_k + \delta_k}^{\alpha_k + \frac{\Delta}{2}} - \frac{V_B}{2} e^{-jn\theta} \, d\theta \right\} \qquad (3.2)$$

which on simplification gives,

$$C_{n_k} = \frac{jV_B}{2\pi n} e^{jn\alpha_k} \left\{ e^{-jn\delta_k} - \cos n \frac{\Delta}{2} \right\} \qquad (3.3)$$

Summing over a complete cycle (that is, for p pulses), then the amplitude of the n^{th} harmonic of the single edge modulated output voltage waveform, as described, is given by,

$$\hat{V}_n = \sum_{k=1}^{p} \frac{jV_B}{2\pi n} e^{-jn\alpha_k} \left\{ e^{-jn\delta_k} - \cos n \frac{\Delta}{2} \right\} \qquad (3.4)$$

In a similar way the treatment follows for double edge modulation. Fig. 3.8 shows a general pulse with the leading and lagging edges respectively modulated by δ_{k1} and δ_{k2}, where the modulated pulse is a centrally placed pulse, width $\frac{\Delta}{2}$. Hence,

$$C_{n_k} = \frac{1}{2\pi} \left\{ \int_{\alpha_k - \frac{\Delta}{2}}^{\alpha_k - \frac{\Delta}{4} - \delta_{k1}} - \frac{V_B}{2} e^{-jn\theta} \, d\theta + \int_{\alpha_k - \frac{\Delta}{4} - \delta_{k1}}^{\alpha_k + \frac{\Delta}{4} + \delta_{k2}} \frac{V_B}{2} e^{-jn\theta} \, d\theta \right.$$

$$\left. + \int_{\alpha_k + \frac{\Delta}{4} + \delta_{k2}}^{\alpha_k + \frac{\Delta}{2}} - \frac{V_B}{2} e^{-jn\theta} \, d\theta \right\} \qquad (3.5)$$

which on simplification and summing over a cycle, gives the amplitude of the n^{th} harmonic of a double edge modulated output voltage waveform as

$$\hat{V}_n = \sum_{k=1}^{p} jV_B e^{-jn(\alpha_k + \frac{\Delta}{4})} \left\{ e^{-jn\delta_{k2}} - e^{jn\delta_{k1}} + j \sin n \frac{\Delta}{2} \right\} \qquad (3.6)$$

In both cases, for single and double edge modulation, α_k is defined by:

$$\alpha_k = \frac{\pi}{p} (2k - 1) \qquad (3.7)$$

and respective δ_k s depend on the type of modulation employed (though shown in Figs. 3.7 and 3.8 as natural sampling).

Considering the n^{th} harmonic of one of the three 'phase' voltages, V_{RG}, V_{YG} and V_{BG}, the expression for a line voltage follows directly

i.e. given $V_{RY} = V_{RG} - V_{YG}$ etc.

then from three-phase symmetry,

$$V_{RY} = (1 - e^{jn\frac{2\pi}{3}}) V_{RG} \qquad (3.8)$$

Expression (3.8) has the effect of multiplying the amplitude of all the harmonics, defined by $\hat{V}_n$, by $\sqrt{3}$ and of eliminating all triplen harmonics of the fundamental frequency. Further, where the modulation process introduces a particular unwanted harmonic component at a frequency related to the carrier frequency (unmodulated pulse train frequency), a suitable choice of carrier frequency eliminates this unwanted component if it becomes a triplen.

3.4 PWM Applied to the Delta Inverter

When considering implementing sinusoidal pulse-width modulation on the delta inverter, the interrelated nature of the inverter's switching makes it necessary to sequence the resultant three-phase modulated switching waveforms in a manner peculiar to the delta inverter. Since it is the voltages that are being modulated it follows that these must be defined at all times irrespective of the type of load and whether currents are flywheeling. Thus, as implied in Chapter 2, this necessitates that two out of the three transistors of the inverter are on at any one time. This constraint, then, makes available only the two line voltage

states of $+V_D$ and $-2V_D$. In contrast with the symmetry of the three-phase bridge inverter, which has voltage states of $\pm V_B/2$ and zero, the delta inverter output voltages give rise to unequal rates of rise and fall of current. However, it has been shown in Chapter 2 that these output voltages, when applied to a star connected load, in the normal way give rise to load voltages of $\pm V_D$ and zero. This investigation of PWM with the delta inverter restricts analysis to the simpler two voltage state output waveforms, that apply, whatever the load configuration - the output voltages being, as can be seen from the circuit of Fig. 3.9, the line voltages.

Given the asymmetry of the delta inverter's available voltage states, there remains a further problem due to the inverter configuration, which puts more serious constraints on the type of modulation strategy that can be implemented. The problem can be summarised by saying that the three line voltages cannot be modulated independently because of the rule that two devices must always be on.

The solutions adopted to produce sinusoidal PWM on the delta inverter are different for single and double edge modulation. Since, also, the modulation processes become somewhat complex, these two methods are dealt with separately in sections 3.4.1 and 3.4.2.

3.4.1 Single edge modulation

Referring to Fig. 3.9, taking one line voltage such as V_a, then if T_1 is On this voltage is clamped at $+V_D$ and is similarly clamped at $-2V_D$ if T_2 and T_3 are On. Given three-phase symmetry, it follows that at any time if two devices are being controlled, the third device must be switched as a consequence of the other two, to maintain two devices always on, if all three output voltages are to be clamped. If two

particular devices are being modulated in such a way that the fundamental components of the two corresponding output voltages are two phases of a three-phase sinusoidal set, then the resulting third voltage must necessarily be the third member of that set. This principle may be thought of as the dual of an alternative arrangement[17] (referred to in Section 1.3.3) where two currents are modulated sinusoidally, and the third current, being the sum of the other two, is automatically the third phase of the current set. Considering three-phase symmetry then, it follows that each device is controlled for two thirds of a cycle and is switched as a consequence of the other two devices over the remaining third of a cycle. Thus control bands may be defined for each device, as shown in Fig. 3.10a.

The method of single edge modulation may be explained from Fig. 3.10b and c, which show the resultant unmodulated and modulated pulse trains, respectively. Over each section width Δ, as shown, each unmodulated pulse has an average value of zero, requiring a $\frac{2}{3} - \frac{1}{3}$ mark-space ratio. Taking the portion of a cycle from 0^{o} to 120^{o}, over which T_1 and T_2 have control bands, the unmodulated pulses of V_a are chosen such that they will be lagging edge modulated. From Fig. 3.10b it can be seen, however, that for the line voltage V_b (which corresponds to the control band of T_2) it is not possible for the pulses to be similarly orientated, as there would then be periods when both T_1 and T_2 were off together (and two of the three devices must be on at all times). Thus the pulses of V_b are placed as shown, to be leading edge modulated. T_3, being outside its control band, is switched so that V_c is $+V_D$ if either V_a or V_b are $-2V_D$.

From the foregoing, the resultant even symmetry of the two halves of each control band that can be seen in Fig. 3.10b suggest the adoption of a cosinusoidal modulating signal. The result of such modulation is shown in Fig. 3.10c. Each pulse within a control band is respectively either a leading or lagging single edge modulated pulse, modulated according to a cosine modulating wave whose positive maxima is at the mid-point of the respective control band. At any one time two devices are being cosinusoidally modulated, being within their respective control bands, producing fundamental components that are two phases of a three-phase set, whilst the third device must necessarily be switching to produce the required third member of this three-phase set. Switching occurring outside a control band is shown by dotted lines in Fig. 3.10c.

The required Fourier analysis need only be done over half a period because of the even symmetry. Taking voltage V_a from 0^o - 180^o, within this half period only two basic types of pulse exist - those occurring within the control band and those which occur outside the control band. A general pulse of each type is shown in Fig. 3.11a and b, respectively.

Fig. 3.11a shows a lagging edge modulated pulse. This k^{th} pulse is modulated about angle α_k by a modulating angle δ_k. The angle α_k is the angle from zero, the mid point of the control band, to a position $\frac{2}{3}\Delta$ from the beginning of the respective section. The angle δ_k may be positive or negative and is limited in range to $\pm \frac{\Delta}{3}$, which limits the average value over the section to within $\pm V_D$ and sets the corresponding upper limit on the amplitude of the cosinusoidal fundamental that can be modulated, as V_D. The amplitude of the n^{th} harmonic due to the k^{th} pulse of this type, $A_{n_{1_k}}$, can be found as follows.

Using the exponential form of the Fourier series and assuming half period even symmetry,

$$A_n = \mathrm{Re}\left\{ \frac{2}{\pi} \int_{\lambda}^{\lambda+\pi} f(\theta) e^{-jn\theta}\, d\theta \right\} \tag{3.9}$$

then from Fig. 3.11a

$$A_{n_{1_k}} = \mathrm{Re}\left\{ \frac{2}{\pi} \left\{ \int_{\alpha_k - \frac{2\Delta}{3}}^{\alpha_k+\delta_k} V_D e^{-jn\theta}\, d\theta + \int_{\alpha_k+\delta_k}^{\alpha_k + \frac{\Delta}{3}} -2V_D e^{-jn\theta}\, d\theta \right\} \right\} \tag{3.10}$$

which simplifies to give,

$$A_{n_{1_k}} = \mathrm{Re}\left\{ \frac{2jV_D}{\pi n} e^{-jn\alpha_k} \left\{ 3e^{-jn\delta_k} - e^{jn\frac{2\Delta}{3}} - 2e^{-jn\frac{\Delta}{3}} \right\} \right\} \tag{3.11}$$

where, $\Delta = \frac{2\pi}{p}$, for p pulses per cycle

$$\alpha_k = \Delta(k - \tfrac{1}{3}) \tag{3.12}$$

and δ_k depends on the type of modulation being used.

The amplitude of the n^{th} harmonic due to all the pulses of this type is found by summing over the control band,

$$\therefore\ A_{n_1} = \sum_{1}^{p/3} A_{n_{1_k}} \tag{3.13}$$

A typical k^{th} pulse that occurs outside the control band region is shown in Fig. 3.11b and can be similarly analysed. Thus the amplitude of the n^{th} harmonic due to the k^{th} pulse of this type, $A_{n_{2_k}}$, using (3.9), is given by,

$$A_{n_{2_k}} = \mathrm{Re}\left\{ \frac{2}{\pi} \left\{ \int_{\alpha_k - \frac{2\Delta}{3}}^{\alpha_k - \frac{\Delta}{3} - \delta_{k_1}} V_D\, e^{-jn\theta}\, d\theta + \int_{\alpha_k - \frac{\Delta}{3} - \delta_{k_1}}^{\alpha_k + \delta_{k_2}} -2V_D e^{-jn\theta}\, d\theta + \int_{\alpha_k + \delta_{k_2}}^{\alpha_k + \frac{\Delta}{3}} V_D\, e^{-jn\theta}\, d\theta \right\} \right\} \quad (3.14)$$

which simplifies to give,

$$A_{n_{2_k}} = \mathrm{Re}\left\{ \frac{2jV_D}{\pi n} e^{-jn\alpha_k} \left\{ 3e^{jn(\frac{\Delta}{3} + \delta_{k_1})} - 3e^{-jn\delta_{k_2}} - e^{jn\frac{2\Delta}{3}} + e^{-jn\frac{\Delta}{3}} \right\} \right\} \quad (3.15)$$

Examination of Fig. 3.10c shows that the angles δ_{k_1} and δ_{k_2} are related to corresponding angles δ_k in the control bands of the other two phases, from which relationships for k_1 and k_2 in terms of k can be found by inspection,

$$k_1 = \frac{2p}{3} - k + 1 \quad (3.16)$$

$$k_2 = k - \frac{p}{3} \quad (3.17)$$

A summation of all pulses of this type gives the corresponding amplitude of the n^{th} harmonic due to these pulses as,

$$A_{n_2} = \sum_{k=\frac{p}{3}+1}^{p/2} A_{n_{2_k}} \quad (3.18)$$

Thus the amplitude of the n^{th} harmonic of the line voltage due to this type of single edge modulation is given by

$$\hat{V}_n = A_{n_1} + A_{n_2} \quad (3.19)$$

Further useful simplification of these expressions to provide an analytical view of the performance of the delta inverter with single edge modulation was not found. The expressions can however be implemented on a computer to provide numerical results which are analysed in section 3.6.

Finally, an examination of Fig. 3.10 shows that it is practicable to swop the position of the leading and lagging edge modulated pulses within the control band. Thus for V_a, leading edge modulation can be used between 0^o and 120^o, provided lagging edge modulation is used in the other half of the control band, maintaining even symmetry. In the third of a cycle outside each control band the pulses must also be altered accordingly.

3.4.2 Double edge modulation

Conventionally, double edge modulation is employed with the three-phase bridge inverter. However, given that the implementation of single edge modulation on the delta inverter is not straightforward, the adoption of a form of double edge modulation requires considerable pulse manipulation from the standard form, due to the delta inverter configuration.

The method of approximating double edge modulation is shown in Fig. 3.12. Fig. 3.12a illustrates the position of the control bands of each switching device. An examination of Fig. 3.12b, showing the unmodulated pulse trains, reveals that, as with single edge modulation, even symmetry is maintained and that outside respective control bands each device is switched as a consequence of the other two devices, with two devices being on at all times. This suggests, as before, the use of a cosinusoidal modulating signal.

Ideally, taking a section width Δ, for double edge modulation, a pulse with zero average value, width $\frac{2\Delta}{3}$, would be centrally placed within this section. The leading and lagging edges of such a pulse then being individually modulated in accordance with the particular values of the modulating signal. This should occur for each pulse over the entire control band. From Fig. 3.12b it can be seen that these types of pulses only occur within the outer quarters of each control band (i.e. with device 1, for V_a, between 60^o and 120^o and between -60^o and -120^o). Having specified these positions for such pulses, over the remaining central half of each control band it is not possible to maintain this pattern and still keep only two devices on at all times. The solution shown splits each unmodulated pulse in two, leaving a central width $\frac{\Delta}{3}$ in each section and a pulse, width $\frac{\Delta}{3}$, on either side. Within each section the two available pulse edges of these two distinct pulse types occuring in each control band are then modulated, with the result as shown in Fig. 3.12c. Outside each control band a further type of pulse configuration is produced in order to maintain the necessary switching rule of two devices always on.

A comparison of Fig. 3.10 and Fig. 3.12 shows that for the same section width Δ the resultant switching frequency is greater for double edge modulation than for single edge modulation. A valid comparison between the two methods requires equivalence of switching frequencies.

In an analogous way to the method for single edge modulation, the position of the two types of pulses within the control band can be exchanged. Thus for V_a, the standard double edge modulated pulse can occur in the region from -60^o to $+60^o$. The portion of each cycle outside the control bands allow sufficient freedom to maintain the switching rule with this alternative arrangement.

The remainder of this section is devoted to a derivation of similar expressions to those given in section 3.4.1 for the harmonic content, in this case, of the double edge modulated waveforms. The resultant expressions are more cumbersome and there appears less likelihood of further useful simplification.

The three basic pulse types which occur within the double edge modulated waveform are illustrated in Figs. 3.13a, b and c. In each case α_k has been defined as being to the centre of each section, as shown. As before, the resultant harmonic spectrum of the waveform is found by summing the effect of each type of pulse, and because of even symmetry a half cycle need only be considered. Fig. 3.13a shows the type of pulse occurring between 0^o and 60^o in Fig. 3.12c. For this general k^{th} pulse, assuming even symmetry, and using (3.9)

$$A_n = \mathrm{Re}\left\{ \frac{2}{\pi} \int_{\lambda}^{\lambda+\pi} f(\theta) e^{-jn\theta} \, d\theta \right\},$$

then,

$$A_{n_{1_k}} = \mathrm{Re}\left\{ \frac{2}{\pi} \left\{ \int_{\alpha_k - \frac{\Delta}{2}}^{\alpha_k - \frac{\Delta}{6} + \beta_k} V_D \, e^{-jn\theta} \, d\theta + \int_{\alpha_k - \frac{\Delta}{6} + \beta_k}^{\alpha_k + \frac{\Delta}{6} - \gamma_k} - 2V_D e^{-jn\theta} \, d\theta \right.\right.$$

$$\left.\left. + \int_{\alpha_k + \frac{\Delta}{6} - \gamma_k}^{\alpha_k + \frac{\Delta}{2}} V_D e^{-jn\theta} \, d\theta \right\}\right\} \quad (3.20)$$

which becomes,

$$A_{n_{1_k}} = \mathrm{Re}\left\{ \frac{2jV_D}{\pi n} \, e^{-jn\alpha_k} \left\{ 3(e^{-jn(\beta_k - \frac{\Delta}{6})} - e^{-jn(-\gamma_k + \frac{\Delta}{6})}) \right.\right.$$

$$\left.\left. - 2j \sin n\frac{\Delta}{2} \right\}\right\} \quad (3.21)$$

and summing for all pulses of this type,

$$A_{n_1} = \sum_{k=1}^{p/6} A_{n_{1_k}} \tag{3.22}$$

Similarly, Fig. 3.13b shows the type of pulses occurring between 60^o and 120^o. From which,

$$A_{n_{2_k}} = \mathrm{Re}\left\{\frac{2}{\pi}\left\{\int_{\alpha_k-\frac{\Delta}{2}}^{\alpha_k-\frac{\Delta}{3}-\delta_k} -2V_D e^{-jn\theta}\,d\theta + \int_{\alpha_k-\frac{\Delta}{3}-\delta_k}^{\alpha_k+\frac{\Delta}{3}+\varepsilon_k} V_D e^{-jn\theta}\,d\theta + \int_{\alpha_k+\frac{\Delta}{3}+\varepsilon_k}^{\alpha_k+\frac{\Delta}{2}} -2V_D e^{-jn\theta}\,d\theta\right\}\right\} \tag{3.23}$$

which becomes,

$$A_{n_{2_k}} = \mathrm{Re}\left\{\frac{2jV_D}{\pi n} e^{-jn\alpha_k}\left\{3(e^{-jn(\frac{\Delta}{3}+\varepsilon_k)} - e^{jn(\delta_k+\frac{\Delta}{3})}) + 4j\sin n\frac{\Delta}{2}\right\}\right\} \tag{3.24}$$

and summing for all pulses of this type,

$$A_{n_2} = \sum_{k=\frac{p}{6}+1}^{p/3} A_{n_{2_k}} \tag{3.25}$$

Finally, using Fig. 3.13c, the harmonic components due to pulses outside the control band can be found. Hence,

$$A_{n_{3_k}} = \mathrm{Re}\left\{\frac{2}{\pi}\left\{\int_{\alpha_k-\frac{\Delta}{2}}^{\alpha_k-\frac{\Delta}{3}-\varepsilon_{k_1}} V_D e^{-jn\theta}\,d\theta + \int_{\alpha_k-\frac{\Delta}{3}-\varepsilon_{k_1}}^{\alpha_k-\frac{\Delta}{6}+\beta_{k_2}} -2V_D e^{-jn\theta}\,d\theta\right.\right.$$

$$\left.\left. + \int_{\alpha_k-\frac{\Delta}{6}+\beta_{k_2}}^{\alpha_k+\frac{\Delta}{6}-\gamma_{k_2}} V_D e^{-jn\theta}\,d\theta + \int_{\alpha_k+\frac{\Delta}{6}-\gamma_{k_2}}^{\alpha_k+\frac{\Delta}{3}+\delta_{k_1}} -2V_D e^{-jn\theta}\,d\theta\right\}\right\}$$

$$+ \int_{\alpha_k + \frac{\Delta}{3} + \delta_{k_1}}^{\alpha_k + \frac{\Delta}{2}} V_D e^{-jn\theta} \, d\theta \Bigg\} \Bigg\} \quad (3.26)$$

which becomes,

$$A_{n_{3_k}} = \mathrm{Re} \left\{ \frac{2jV_D}{\pi n} e^{-jn\alpha_k} \left\{ 3(-e^{-jn(\beta_{k_2} - \frac{\Delta}{6})} + e^{-jn(-\gamma_{k_2} + \frac{\Delta}{6})} - e^{-jn(\delta_{k_1} + \frac{\Delta}{3})} \right.\right.$$

$$\left.\left. + e^{jn(\epsilon_{k_1} + \frac{\Delta}{3})}) - 2j \sin n \frac{\Delta}{2} \right\} \right\} \quad (3.27)$$

and summing for all pulses of this type,

$$A_{n_3} = \sum_{k = \frac{p}{3} + 1}^{p/2} A_{n_{3_k}} \quad (3.28)$$

The values of k_1 and k_2 are as defined by (3.16) and (3.17). Whilst $\Delta = \frac{2\pi}{p}$ for p pulses per cycle, $\alpha_k = \Delta(k - \frac{1}{2})$ and δ_k again depends on the type of modulation being used.

From these expressions the amplitude of the n^{th} harmonic of the line voltage due to this type of double edge modulation is given by,

$$\hat{V}_n = A_{n_1} + A_{n_2} + A_{n_3} \quad (3.29)$$

which, as with the similar expression for single edge modulation, can be used for numerical evaluation of the harmonic content.

3.5 Types of Modulation

The initial work on PWM with power inverters and converters carried out during the 1960's[14,15] had to use analogue circuitry to generate the switching waveforms; combining triangular carrier waves and sinu-

soidal modulating signals. The introduction of LSI (large scale integration) and microprocessors has allowed a much more flexible approach to switching strategies and the complexity of modulation algorithms that can be implemented. Various methods have been presented which attempt to optimise performance, particularly trying with the modulation to take into account the exact nature of the load[18,19]. Having shown that there are a number of pulse train configurations that can be applied to the delta inverter, various methods of modulating the individual pulse widths are available.

Little has been published of a detailed nature classifying the various available modulation methods, particularly in the case of single edge modulation. The approach with the delta inverter has therefore been to investigate fundamental methods of modulation which seem valid ways of producing sinusoidal PWM. It was surmised that the effect on harmonic content due to the delta inverter's configuration would be significant and so the consideration of a number of different types of modulation seems essential.

Four methods of modulation are presented. The first two consider equivalence, between the modulating and the modulated waveforms, of average value, section 3.5.1, and of volt-seconds, section 3.5.2. The latter two methods analyse the conventional modulation techniques of natural and uniform sampling (sections 3.5.3 and 3.5.4, respectively), which depend on equality between the modulated signal and instantaneous sampled values of the modulating signal - these two sampling techniques have already been briefly described in this chapter. Each method is presented with relation to single edge modulation, expressions being derived for the respective values of δ_k, the modulating angle. Equivalent expressions for double edge modulation may be directly derived.

Each type of modulation is presented with reference to the delta inverter. The derived equations can, however, be applied to the three-phase bridge inverter provided account is taken of the change in voltage levels between the two inverters, from $+V_D$ and $-2V_D$ to $+\frac{V_B}{2}$ and $-\frac{V_B}{2}$. Sinusoidal PWM is also conventionally applied to the bridge inverter in relation to a sine wave modulating signal.

3.5.1 A method of linear piecewise approximation

This modulation technique is illustrated for lagging edge modulation in Fig. 3.14. Over each section width Δ the average value of the co-sinusoidal modulating signal is found, equivalent to assuming a linear approximation of the cosine over each section. The width of each corresponding pulse of the inverter pulse train is then modulated such that the average value of the two waveforms over each section are identical. Thus from Fig. 3.14, for the k^{th} section,

$$\frac{\omega_1 - 2\omega_2}{\Delta} = \frac{\cos(k\Delta) + \cos(k\Delta - \Delta)}{2} \qquad (3.30)$$

(taking V_D as unity)

and $\omega_1 + \omega_2 = \Delta$ (3.31)

thus substituting for ω_2 and given $\delta_k = \omega_1 - \frac{2\Delta}{3}$,

then $$\delta_k = \frac{\Delta}{3} \cos\frac{\Delta}{2} \cos(k\Delta - \frac{\Delta}{2}) \qquad (3.32)$$

and given $\alpha_k = k\Delta - \frac{\Delta}{3}$,

$$\delta_k = \frac{\Delta}{3} \cos\frac{\Delta}{2} \cos(\alpha_k - \frac{\Delta}{6}) \qquad (3.33)$$

Using (3.33) the corresponding modulating angles can be found over a complete cycle.

3.5.2 A method of equal areas

Given that the volt-seconds applied to a coil is proportional to the flux, it follows that by equating volt-seconds the modulated signal should produce a resultant load machine flux approximately following the sinusoidal nature of the modulating signal. Referring again to Fig. 3.14, which is approximately to scale. Over width Δ the volt-seconds of the modulating signal are given by,

$$\omega_1 - 2\omega_2 = \int_{k\Delta-\Delta}^{k\Delta} \cos\theta \, d\theta$$

$$= \sin(k\Delta) - \sin(k\Delta - \Delta) \qquad (3.34)$$

(again assuming V_D is unity)
and simplifying in a similar manner to section 3.5.1, using (3.31) and substituting for ω_2 gives,

$$\delta_k = \frac{2}{3} \sin\frac{\Delta}{2} \cos(\alpha_k - \frac{\Delta}{6}) \qquad (3.35)$$

As discussed briefly in section 3.2, modulating using (3.35) would appear attractive due to the effect on the flux waveform but consideration must be given to the overall harmonic losses within the load.

3.5.3 Natural sampling

The ramp (line AB) shown in Fig. 3.15 represents the change in average value of a pulse, as its width is varied, from a minimum value of $-2V_D$ across the section to a maximum of $+V_D$. The intersection of this ramp function and the cosinusoidal modulating function gives the required solution point. The modulating angle, shown on Fig. 3.15 as $\delta_k(NAT)$, is defined as being from α_k to this point and will be within the limits $\pm \frac{\Delta}{3}$ (the maximum amplitude of the cosinusoidal modulating signal being V_D).

The equation for the line AB from Fig. 3.15 is found using the expression,

$$y - y_1 = m(\theta - \theta_1) \tag{3.36}$$

Thus using the point $(\alpha_k,0)$ and assuming V_D is unity (3.36) gives,

$$y = \frac{3}{\Delta}(\theta - \alpha_k) \tag{3.37}$$

and the modulating signal is represented by,

$$y = \cos\theta \tag{3.38}$$

Equating (3.37) and (3.38) to find the solution point gives

$$\cos\theta = \frac{3}{\Delta}(\theta - \alpha_k) \tag{3.39}$$

and given that at this point,

$$\theta = \alpha_k + \delta_k \tag{3.40}$$

then (3.39) gives,

$$\delta_k = \frac{\Delta}{3}\cos(\alpha_k + \delta_k) \tag{3.41}$$

An iterative process readily solves (3.41) for δ_k. Although solution by computer of such an expression is straightforward, the solution in real time by some form of microprocessor control system presents problems due to the time taken in the iterative process.

3.5.4 Uniform sampling

In contrast to natural sampling where, in effect, the modulating signal is sampled at positions determined by the modulating signal itself, in uniform sampling the modulating signal is sampled at regular intervals - as has been stated. As a consequence, the iterative steps for determining

the solution with natural sampling are not necessary with uniform sampling.

From Fig. 3.15 it can be seen that the modulating cosine is sampled at the position corresponding to a zero time average modulated pulse. Line CD represents this value, and its intersection with line AB, the ramp function, gives the solution point (and hence δ_k(UNI), as shown). Using the equation for the ramp (3.37), then the simultaneous solution is given by,

$$\cos(\alpha_k) = \frac{3}{\Delta}(\theta - \alpha_k) \qquad (3.42)$$

from which

$$\delta_k = \frac{\Delta}{3}\cos(\alpha_k) \qquad (3.43)$$

Comparison of this equation with the expression for δ_k when using natural sampling (3.41) shows the simplification that results from using uniform sampling.

3.6 Comparison of Modulation Methods

This section summarises the theoretical results obtained for both single and double edge modulation techniques used on the delta and bridge inverters. Since expressions for the various modulation techniques are complex, straightforward analytic comparisons were not made. Consequently, computed results have been presented in graphical form. The results shown for both inverters, but particularly the bridge inverter, are not an exhaustive list, being intended to show the practicality of using sinusoidal PWM on the delta inverter, and the comparative merit of each of the various available modulation techniques.

Two forms of comparison have been used to illustrate the harmonic performance of the methods. First, using modulation producing an identical switching frequency, the harmonic spectra are presented for each technique. The results for single edge modulation are given in section 3.6.1, and for double edge modulation in section 3.6.2. Secondly, a form of harmonic summation is used which compares performance over a large range of switching frequencies for both single and double edge modulation - section 3.6.3.

With the delta inverter each modulation technique requires an exact number of pulses within each 60^{o} period. The number of pulses allowed within each cycle is thus limited to certain discrete values. Thus, given a section width Δ, where $60^{o}/\Delta$ is a whole number, then the number of pulses per cycle are given by:

For single edge modulation, $$p = \frac{360^{o}}{\Delta} \qquad (3.44)$$

For double edge modulation, $$p = (\frac{240^{o}}{\Delta}) + (\frac{120^{o}}{\Delta} . 2) + 2$$

$$= \frac{480^{o}}{\Delta} + 2 \qquad (3.45)$$

The values of p are therefore constrained to the following sequences:

For single edge modulation, $p = 6, 12, 18, 24, 30, 36, 42 \ldots$ (3.46)

For double edge modulation, $p = 10, 18, 26, 34, 42, 50, 58 \ldots$ (3.47)

An identical number of pulses per cycle must be used for valid comparison between the different methods (as inverter losses must be balanced against the reduction of additional harmonic losses in the load - both of which, in general, increase with switching frequency). Hence, although in practice inverter losses may be small, a theoretical comparison between single and double edge modulation with the delta inverter is

limited to the following values of p:

$$p = 18, 42, 66, 90 \ldots\ldots \qquad (3.48)$$

To illustrate the differences in the produced harmonics of the various methods, particularly the differences in the low order harmonics, a moderately low value of p has been chosen, 18 pulses per cycle. Considering a 50 Hz fundamental, this value of p represents a relatively low switching frequency but is in general high enough, such that the major spectral components that remain as the number of pulses per cycle are increased to very large values, are clearly identifiable. At very low carrier ratios (ratio of carrier to modulating frequency) distinct harmonic clusters that appear around each carrier harmonic may overlap and somewhat complicate the spectra - each resulting spectral component can, however, be thought of as the sum of the overlapping components[16].

3.6.1 The spectra resulting from single edge modulation techniques

From section 3.5 it is useful to summarise the expressions for δ_k with both inverters using single, lagging edge modulation. This is done in Table 1 below.

Type of Modulation	Delta Inverter	Bridge Inverter
Linear piecewise	$\frac{\Delta}{3} \cos \frac{\Delta}{2} \cos(\alpha_k - \frac{\Delta}{6})$	$\frac{\Delta}{2} \cos \frac{\Delta}{2} \sin(\alpha_k)$
Equal Area	$\frac{2}{3} \sin \frac{\Delta}{2} \cos(\alpha_k - \frac{\Delta}{6})$	$\sin \frac{\Delta}{2} \sin(\alpha_k)$
Natural Sampling	$\frac{\Delta}{3} \cos(\alpha_k + \delta_k)$	$\frac{\Delta}{2} \sin(\alpha_k + \delta_k)$
Uniform Sampling	$\frac{\Delta}{3} \cos(\alpha_k)$	$\frac{\Delta}{2} \sin(\alpha_k)$
	$\alpha_k = k\Delta - \frac{\Delta}{3}$	$\alpha_k = k\Delta - \frac{\Delta}{2}$

Table 1 Comparison of the expressions for the modulating angle δ_k, using both types of inverter. k = 1,2,3,4,...p.

The bridge inverter has simpler harmonic spectra. The two graphs of Fig. 3.16 and Fig. 3.17 show the result of lagging edge modulation on the bridge inverter using natural and uniform sampling, respectively. Ideally the amplitude of the fundamental of the bridge inverter line voltage should be 0.866 V_B ($\sqrt{3}$ x 0.5 V_B). In all cases this figure has been made unity and the harmonics normalised accordingly. The spectra are then comparable with the subsequent graphs for the delta inverter. As explained in section 3.3, triplen harmonics do not exist in the line voltage. As the chosen number of pulses per cycle, 18, is a triplen harmonic, the spectral components expected at the carrier frequency and its multiples do not exist. However, as shown, sidebands appear at the carrier frequency ± multiples of the modulation frequency - provided they are not themselves triplens. This is shown particularly well with natural sampling. The harmonic spectra with uniform sampling (Fig. 3.17) is somewhat more complex. Returning to Fig. 3.3 or 3.4 shows that the uniform sampling technique does not sample the modulating sinusoid but an intermediate stepped waveform. The difference in spectra between natural and uniform sampling is thought to be predominantly due to the extra harmonic components added by this stepped waveform. With single edge modulation the most detrimental result of this difference is the production of about 8% second harmonic (with respect to the amplitude of the fundamental) when using uniform sampling, as shown. This discrepancy increases as the carrier ratio is decreased (for instance the percentage of second harmonic increases to over 20% with six pulses per cycle), but as the carrier ratio tends to infinity the two sampled waveforms become similar, as the stepped waveform more accurately represents the sinusoid.

An examination of the respective expressions in Table 1 shows that the derived modulating angles for linear piecewise, equal area and uniform sampling will be approximately the same, given that $\cos \frac{\Delta}{2} \simeq 1$ and $\sin \frac{\Delta}{2} \simeq \frac{\Delta}{2}$, if Δ is small. Thus the spectra for the linear piecewise and equal area techniques using lagging edge modulation with the bridge inverter are virtually identical to the spectra produced by uniform sampling shown in Fig. 3.17, and have therefore not been shown separately.

In order to attempt an explanation of the harmonics appearing with the delta inverter, consider first the graphs shown in Fig. 3.18. The spectra shown using solid lines corresponds to the line voltage spectra of Fig. 3.16 for naturally sampled lagging edge modulation with the bridge inverter, but is for the pseudo phase voltage (the phase voltage taking the neutral point as the centre of the dc supply, as explained in section 3.3). This spectra has components at the carrier frequency and its harmonics (which are triplens here, and would be suppressed in the line voltage spectra), and sidebands at ± multiples of the modulating frequency. The spectra shown using dotted lines, again illustrates naturally sampled lagging edge modulation. Unlike the pseudo phase voltage spectra utilising voltage states of $\pm \frac{V_B}{2}$, this spectra has been produced by modifying the modulation to generate the harmonics that would result if the voltage states $+V_B$ and $-2V_B$ were available. The same unit amplitude modulating signal is used. Apart from the voltage levels, no change has been made in pulse train geometry between the two spectra and so the dotted harmonics in Fig. 3.18 represent those for the pseudo phase voltage of a bridge inverter with a dc supply of $3V_B$ and a notional reference potential asymmetrically tapped V_B down from the top of this assumed battery stack. This modified spectrum illustrates conventional lagging edge modulation employing the voltage states available on the delta inverter but without the changes in pulse train geometry necessary with the delta inverter. Thus from Fig. 3.18 the effect of just

changing the available voltage levels produces a change in the carrier associated components of the spectra. In particular, the amplitude of the carrier frequency component rises from approximately 44% to 105% of the fundamental.

The spectra produced using the delta inverter with naturally sampled single edge modulation (configured as in Fig. 3.10) is shown in Fig. 3.19. Comparing this graph with the spectra of the line voltage of the conventional inverter, Fig. 3.16, shows that, in both cases, the triplen harmonics are absent and the harmonics are negligible up to the tenth (at this switching frequency, corresponding to 18 pulses/cycle). However, the delta inverter has a very large harmonic at just above the carrier frequency (no harmonic appearing at the carrier frequency as this is a triplen). The magnitude of this harmonic is similar to that occurring at the carrier frequency for the pseudo phase voltage of the bridge inverter with voltage states of $+V_B$ and $-2V_B$, Fig. 3.18. The amplitude of this component again being comparable (slightly greater) than the amplitude of the fundamental. Thus, given the delta inverter voltage level constraints of $+V_D$ and $-2V_D$, the modulation strategy employed is reasonably successful. A major factor in determining the pulses/cycle with such modulation is the minimum frequency at which this large harmonic component can be tolerated.

The harmonic spectra produced with the delta inverter by the other types of single edge modulation, for uniform sampling, linear piecewise and equal area, are shown in Fig. 3.20, Fig. 3.21 and Fig. 3.22, respectively. Again, as with the bridge inverter, all three spectra are similar and the low order harmonic performance is not as good as that for natural sampling. With uniform sampling the amplitude of the second harmonic has been reduced at the expense of the other low order harmonics.

3.6.2 The spectra resulting from double edge modulation techniques

The harmonic spectrum which results from using double edge natural sampling on the bridge inverter is shown in Fig. 3.23. These results agree with those given in ref. (16), which are for any number of pulses per cycle greater than nine (as above 9 pulses/cycle with this sampling technique the harmonic amplitudes are approximately independent of the carrier ratio). Under such conditions the quoted Fourier sine series becomes approximately

$$b_n = \frac{2}{j\pi} J_k\left(\frac{j\pi}{2}\right) \qquad \text{where } j + k \text{ is odd} \qquad (3.49)$$

(when the no. of pulses/cycle tends to infinity to eliminate coincident sidebands of adjacent carrier harmonics)

J_k ( ) is a Bessel function of the first kind, order k

j is the j^{th} carrier harmonic

k is the k^{th} sideband

n = jp + k (n and p as previously defined)

A comparison of Fig. 3.23 with the equivalent spectrum for single edge modulation (Fig. 3.16) shows the reduction in the number of sidebands that results from using double edge modulation.

Considering uniform sampling with double edge modulation on the bridge inverter, asymmetric modulation is used as this is closer to the type of double edge modulation employed on the delta inverter. Examining the results for natural and uniform sampling, Figs. 3.23 and 3.24, respectively, there is no significant difference between the two at this carrier ratio. The lower sideband of the carrier frequency is most critical since this contains the lowest frequency significant harmonic. Whilst the amplitude of this harmonic is fixed with natural sampling,

(above 9 pulse/cycle), when using uniform sampling the amplitude is slightly smaller and depends on the carrier ratio (as stated by Bowes[13]). It can be seen that the sidebands occurring with uniform sampling are less symmetrical, and the spectra is much more dependent on the carrier ratio (until this becomes very high). A simple analytic expression for the spectrum with uniform sampling has not been found; an expression has been quoted [13] but is not easy to handle for comparison purposes. It can, however, be shown that the amplitude of the fundamental is not directly proportional to the depth of modulation, being a non-linear function of both modulation depth and frequency ratio (although it is stated that the non linearity is not significant).

Similar spectra are presented in Fig. 3.25 and Fig. 3.26 for double edge modulation with the delta inverter using natural and uniform sampling. From both these spectra it is obvious that the degree of alteration necessary in the modulated pulse trains to accommodate the constraints imposed by the delta inverter geometry, lead to a poor harmonic performance.

3.6.3 Comparative performance of the modulation methods

If the load being driven by the inverter is assumed to be purely frequency dependent, inductive, then a quantity referred to as the weighted harmonic voltage distortion (σ) can be used to summarise and compare the various modulation methods that have been described. Consider an expression which gives a summation of the current harmonics normalised to the fundamental,

$$\frac{\sum_{n=2}^{\infty} (\text{rms harmonic current})}{\text{fundamental current}} \qquad (3.50)$$

when assuming the frequency dependence of the load this may be written as

$$\sigma = \frac{\sqrt{\sum_{n=2}^{\infty} \left(\frac{V_n}{n}\right)^2}}{V_1} \qquad (3.51)$$

In practice (3.51) was used for the weighted harmonic voltage distortion in the range n = 2 to 500.

The results of using this expression on various modulation methods with both the delta and bridge inverters are shown in Fig. 3.27. Best performance, as expected, is given by the bridge inverter with double edge and then single edge modulation. Single edge modulation is best with the delta inverter, with natural and uniform sampling in the region of 10% better than the linear piecewise and equal area techniques. The graph is drawn for a wide range of pulses/cycle, since with variable speed operation such a wide range may have to be considered. Above about 150 pulses/cycle the delta inverter may be used with less than 1% harmonic distortion whilst a similar point for the bridge inverter is about 50 pulses/cycle (with the delta inverter using single edge modulation and the bridge inverter using double edge modulation). Taking a typical figure of, say, 36 pulses/cycle, which at 50 Hz requires a switching frequency of 1.8 kHz, then the best distortion figures for the respective methods are 3.9% with the delta inverter and 1.3% with the bridge inverter. These levels of distortion are very low, particularly when considering a comparison with the unmodulated output of either inverter.

3.7 Conclusions

One method of harmonic improvement has been considered in detail in this chapter - sinusoidal PWM. By applying sinusoidal PWM to the delta inverter it was shown that theoretically this inverter configuration can produce a high quality output. The purity of this output is only dependent on the acceptable maximum device switching speed. From this it appears possible to produce a highly efficient inverter-motor system using a three device inverter, with no inherent harmonic problems. An investigation of an ac drive system is given in the next chapter.

Although a successful method of implementing double edge modulation has not been found (results being poorer than those with single edge modulation), the single edge modulation method produces acceptable results. Conventionally, natural and uniform sampling have been proposed for analogue and digital implementations, respectively. Both these methods can be adopted on the delta inverter, which suggests that established techniques and technology can be adapted to a delta inverter PWM system.

A comparison with the conventional three-phase bridge inverter has shown that whilst results for the delta inverter are not as good, differences are not substantial considering the low distortion figures obtainable with either inverter. The price paid for the resultant harmonic improvement with both inverters is in increased control circuit complexity and higher inverter switching losses (the latter being dependent on the switching devices used).

3.8 References

1. Kernick, A., Roof, J.L. and Heinrich, T.M.: "Static inverter with neutralisation of harmonics", AIEE Trans., Vol.81, Pt.II, (App. and Ind.), May 1962, pp.59-68.

2. Anderson, D.L., Willis, A.E. and Winkler, C.E.: "Advanced static inverter utilising digital techniques and harmonic cancellation", NASA Technical Note, D-602, 1962.

3. Murphy, J.M.D.: "Thyristor Control of AC Motors", Pergamon Press, Oxford, 1978.

4. Flairty, C.W.: "A 50-kVA adjustable frequency 24 phase controlled rectifier inverter", Direct Current 6, 278, 1961, pp.278-282.

5. Sriraghavan, S.M., Pradhan, B.D. and Revankar, G.N.: "Three-phase pulse-amplitude and width-modulated inverter system", IEE Proc., Vol.128, Pt.B, No.3, May 1981, pp.167-171.

6. Daniels, A.R. and Slattery, D.T.: "Application of power transistors to polyphase regenerative power convertors", IEE Proc., Vol.125, No.7, July 1978, pp.643-647.

7. Fredendall, G.L., Schlesinger, K. and Schroeder, A.C.: "Transmission of television sound on the picture carrier", IRE Proc., Vol.34, Feb. 1946, pp.49-61.

8. Fitch, E.: "The spectrum of modulated pulses", IEE Jour., Vol.94, Pt.IIIA, 1947, pp.556-564.

9. Kretzmer, E.R.: "Distortion in pulse-duration modulation", IRE Proc., Vol.35, Nov. 1947, pp.1049-1053.

10. Black, H.S.: "Modulation Theory", Van Nostrand, New Jersey, 1962.

11. Rowe, H.E.: "Signals and Noise in Communication Systems", Van Nostrand, New Jersey, 1965.

12. Bowes, S.R. and Bird, B.M.: "Novel approach to the analysis and synthesis of modulation processes in power convertors", IEE Proc., Vol.122, No.5, May 1975, pp.507-513.

13. Bowes, S.R.: "New sinusoidal pulsewidth - modulated inverter", IEE Proc., Vol.122, No.11, Nov. 1975, pp.1279-1285.

14. Schonung, A. and Stemmler, H.: "Static frequency changer with "subharmonic" control in conjunction with reversible variable-speed ac drives", Brown and Boveri Review, Aug/Sept 1964, pp.555-577.

15. Mokrytzki, B.: "Pulse width modulated inverters for ac motor drives", IEEE Trans., Vol.IGA-3, No.6, Nov/Dec 1967, pp.493-503.

16. Wilson, J.W.A. and Yeamans, J.A.: "Intrinsic harmonics of idealized inverter PWM systems", IEEE Conf. Rec. Annual IAS Meeting, Oct. 1976, pp.967-973.

17. Eastham, J.F., Daniels, A.R. and Lipczynski, R.T.: "A novel power inverter configuration", IEEE Conf. Rec. Annual IAS Meeting, Oct. 1980, pp.748-751.

18. Buja, G.S. and Indri, G.B.: "Optimal pulsewidth modulation for feeding ac motors", IEEE Trans., Vol.IA-13, No.1, Jan/Feb 1977, pp.38-44.

19. Casteel, J.B. and Holt, R.G.: "Optimum PWM waveforms of a micro-processor controlled inverter", IEEE Conf. Rec. Power Electronics Specialist Conference, June 1978, pp.243-250.

CHAPTER 4

THE DELTA INVERTER A.C. DRIVE SYSTEM

4.1 Introduction

Previous chapters have described the delta inverter circuit. Chapter 2 discussed the basic behaviour of the circuit with passive loads and Chapter 3 investigated possible methods of control to produce improved output waveforms. The present chapter continues the research programme by studying the operation of an induction machine when driven by the delta inverter.

The behaviour of induction machines with non-ideal supplies, most commonly produced by a conventional bridge inverter, is quite well documented[1,2,3,4,5,6]. Such considerations as variable frequency-variable speed operation and the effect of supply harmonics are of interest in this respect.

The induction machine is primarily a constant speed device when operated from the supply network, its rotational speed being closely related to the supply frequency. To achieve efficient variable speed operation a variable frequency supply is required and it is the function of an inverter to provide it.

The supply from an inverter is non-ideal, however, in that it is not purely sinusoidal. It can vary from square, or quasi-square, to sinusoidal pulse-width modulated, with numerous other intermediate configurations. All such techniques degrade the induction machine behaviour to some extent and optimisation of inverter supply waveforms is an important subject.

In view of the work in Chapters 2 and 3, the present chapter investigates both theoretically and experimentally the behaviour of an induction motor with different types of delta inverter waveforms. In Section 4.2 the induction machine is introduced. Then Section 4.3 and 4.4 describe the operation of the drive system, first using unmodulated waveforms and then with a selective harmonic reduction (SHR) technique. A comparison is then made with the unmodulated bridge inverter system and, following this, the delta inverter a.c. drive system with sinusoidal PWM is investigated in Section 4.6. The subsequent two sections discuss the VA capacity of the delta and bridge inverter systems and look at some general system considerations (outlining the design strategy behind the prototype delta inverter system and looking at some of the practical aspects of this inverter configuration).

4.2 The Induction Machine

The advantages of squirrel cage induction motors are well known[1,6], and include efficient and reliable operation. Their use as variable speed drives, achieved by means of an inverter supply, therefore holds significant potential advantages over dc machines which are most commonly used for this purposes (see also Chapter 1 and Appendix 3).

Induction machines are usually designed for use on mains frequency supplies and much of the design and analysis is concerned with single frequency operation. One interesting example of this is the use of the conventional "slip" parameter.

$$S = \frac{\omega_s - \omega_r}{\omega_s} \qquad (4.1)$$

This is in fact the rotor frequency (the difference between synchronous frequency and rotor speed) normalised to the "constant" supply frequency. The physical behaviour of the induction machine, however,

is influenced by the rotor frequency itself, i.e. $\omega_s - \omega_r$, and normalising this parameter to a single base frequency, when considering variable frequency operation, is not necessarily helpful (as under constant flux operation the torque produced by a given machine depends only on the rotor frequency and not on the supply frequency).

The best known equivalent electric circuit representation of an induction machine is the single-phase equivalent circuit. As shown in Fig.4.1, it applies for a single frequency balanced sinusoidal supply and for ideal windings sinusoidally distributed in space. Although other mmf harmonics can be considered by extending the equivalent circuit[7] the fundamental, only, has been considered in the present work. It is possible also, however, to examine the behaviour of induction machines with non-sinusoidal supplies by means of an extension to the single-phase equivalent circuit[1]. This is achieved by reducing the inverter voltage waveform into its time harmonic constituents so that each harmonic is represented by a three-phase balanced set of voltages. Each of these sets can then be applied to the single-phase equivalent circuit in turn, its parameters being suitably modified to correspond to the harmonic in question. The overall steady state effect can be arrived at by superposition in the usual way.

Considerable simplification of the equivalent circuit for the harmonic voltages is possible. The reactance of the leakage and magnetising inductances to the n^{th} harmonic are n times those to the fundamental. The slip of the rotor, as it appears in the equivalent circuit, with respect to the harmonic fields, depends upon the direction of rotation of these fields:

For forward rotating fields,

$$S_{n_f} = \frac{n\omega_s - \omega_r}{n\omega_s} = 1 - \frac{\omega_r}{n\omega_s} \qquad (4.2)$$

For backward rotating fields,

$$S_{n_b} = \frac{-n\omega_s - \omega_r}{-n\omega_s} = 1 + \frac{\omega_r}{n\omega_s} \qquad (4.3)$$

The resultant equivalent circuit for the n^{th} harmonic is shown in Fig. 4.2a. For higher order harmonics,

$$S_{n_f} \doteq S_{n_b} \doteq 1 \qquad (4.4)$$

i.e. with respect to the speed of rotation of the harmonic field the rotor is approximately at a standstill.

In addition, while the reactances increase with harmonic order, the resistances can be assumed to be substantially constant (skin effect will cause some modification, and mainly to the rotor resistance). Hence R_s and R_r are small compared with the reactances and the equivalent circuit reduces to Fig.4.2b. Furthermore, X_m is usually large compared to X_s and X_r which results in the final approximate equivalent circuit, Fig. 4.2c.

The circuit of Fig. 4.2c produces a simple model for the effect of harmonic components on induction motors. The result shown by this method is that the harmonic currents driven by the harmonic voltage components are limited mainly by the leakage inductances. As the reactances increase with frequency, however, high order harmonics are subject to increasing attenuation of their currents.

There are a number of limitations to this model. Most notable, probably the fact that the assumption of superposition precludes non-linear effects such as saturation. Local saturation, for instance tooth-tip saturation, tends to affect leakage inductance[7], and therefore harmonic currents under different load conditions. Also, the interaction of different harmonic currents and fluxes which produce pulsating torques with zero average level are not predicted directly by this model.

If the effects of these limitations are neglected then a "figure of merit" for the voltage harmonic waveforms can be used, which makes their comparison relatively straightforward. From Fig. 4.2c, the current due to the n^{th} voltage harmonic can be approximated as,

$$I_n = \frac{V_n}{n(X_s + X_r)} \tag{4.5}$$

and the total rms harmonic current can be written as,

$$I_{harm} = \sqrt{\sum_{n=2}^{\infty} I_n^2} \tag{4.6}$$

Hence, from (4.5) and (4.6),

$$I_{harm} \propto \sqrt{\sum_{n=2}^{\infty} \left(\frac{V_n}{n}\right)^2} \tag{4.7}$$

A comparison of (4.7) with (3.51) shows that the standard expression for the weighted harmonic voltage distortion can be used to compare the voltage harmonic waveforms with motor load, where,

$$\sigma = \frac{\sqrt{\sum_{n=2}^{\infty} \left(\frac{V_n}{n}\right)^2}}{V_1} = \frac{I_{harm}}{I_1} \tag{4.8}$$

For present purposes, this is especially convenient for the comparison of alternative delta inverter waveforms with one another, and with waveforms from the conventional bridge inverter.

A more comprehensive model of the induction machine is the three-phase coupled circuit model, as shown in Fig. 4.3. The machine is represented by the three stator phases each of which has a constant self inductance and a constant mutual inductance with the other two phases. Similarly the rotor has three phases (notional ones in the case of the squirrel cage rotor) with constant self and mutual inductances. The mutual inductances between the stator and rotor phases are time dependent, however, due to the angular rotation. This is perhaps the most general induction motor model from which the single-phase equivalent circuit can be derived for the specified balanced conditions[8].

The three-phase model can be used to complement the single-phase equivalent circuit. Whereas the single-phase circuit gives some understanding of behaviour with harmonics (albeit approximately), the three-phase circuit model allows simulation of performance to almost any degree of precision required. For the present purposes, therefore, this three-phase model was used for prediction of the delta inverter-induction motor system performance with various inverter waveforms. A relatively simple version was used, i.e. the mutual inductances were taken to vary sinusoidally in space, and all inductance parameters were constant.

The set of differential equations that result from this three-phase model were solved, in this instance, by representing the model as equivalent electrical circuits and using a circuit analysis computer package[9]. The particular package used was ASTAP[10] (Advanced

Statistical Analysis Program), an IBM package for the analysis of linear and non-linear large scale integrated and discrete electrical circuits. For the present work this allowed the modelling of both the motor and inverter as a complete equivalent electrical circuit. Thus the overall behaviour of the inverter-induction motor system could be investigated for any given set of inverter switching logic waveforms. An alternative method which could be used would be a computer based numerical time-step iterative technique, either for the motor alone, or for the motor-inverter system. It was thought to be more efficient to use an available software package, with its sophisticated built in options, than to write a new program for the purpose. Both methods are valid not only for steady state conditions but also for both transient and start-up conditions and to this extent, at least, the three-phase equivalent circuit is more general than the single-phase equivalent circuit.

4.3 The Drive System With Unmodulated Waveforms

The operation of the delta inverter ac drive system is investigated for two unmodulated waveforms with conduction angles of 180^{o} and 240^{o}. The output of the inverter with these two waveforms was applied to a conventional three-phase squirrel cage induction motor. The particular motor used had previously been investigated[8] and so its parameters were well known. The machine was a conventional induction motor rewound to have the following specifications at 50 Hz:

nominal power rating $\simeq$ 2 kW

rms line voltage $\simeq$ 84V

The motor was therefore comparatively lightly loaded when used with the delta inverter (because of the nominal 36V dc supplies).

Taking the motoring mode, typical oscillograms of line voltage and phase current with the motor star connected are shown in Figs. 4.4 and 4.5. Considering, first, the voltage waveforms, the simpler waveform is for 240^{o} conduction, Fig. 4.5a. This waveform illustrates how the line voltage is clamped, irrespective of the load, at $+V_D$ or $-2V_D$ with this conduction angle. In comparison, the line voltage with 180^{o} conduction, Fig. 4.4a, appears more complicated. Both voltage waveforms were taken at a relatively high value of rotor frequency of 10 Hz, 20% slip, for a 50 Hz supply. Returning to Chapter 2, a comparison of Fig. 4.4a with Fig. 2.19a shows that, as expected, the motor load is behaving in a similar manner to a "fairly resistive RL load" at 180^{o} conduction. The periods when flywheel paths are utilised are similar; the output voltages being respectively clamped but via a conduction mechanism that, as has already been shown, is load dependent.

Typical load currents under the corresponding conditions are shown in Figs. 4.4b and 4.5b, for 180^{o} and 240^{o} conduction, respectively. These were compared with predicted waveforms using the three-phase equivalent circuit of the motor, as referred to in Section 4.2. A computer simulation using the ASTAP circuit analysis package, modelling this equivalent circuit and the inverter, produces the load current waveforms of Figs. 4.6 and 4.7, for 180^{o} and 240^{o} conduction. Visual agreement is apparent for the shape of the actual and experimental waveforms at both conduction angles. Amplitude measurements correspond to within about 10% for the 180^{o} case and to approximately 16% for 240^{o} conduction. Principal zero crossings appear to be within about 3% in both cases.

Fig. 4.8 shows the corresponding device currents with 180^{o} conduction, while Fig. 4.9 shows the computed results at this conduction angle. As before, there is reasonably close agreement between the two. The effect on device conduction of altering the conduction angle is illustrated by comparing Fig. 4.9 with the results of computation for the 240^{o} case, Fig. 4.10. As expected, device utilisation is greater with 240^{o} conduction.

The measured system performance under motoring conditions and using unmodulated inverter waveforms is shown in Figs. 4.11 and 4.12 for 180^{o} and 240^{o} conduction, respectively. In both cases it can be seen that output torque and power characteristics are typical for induction machines. Most noticeable is the relatively low overall efficiency (i.e. from dc power input to motor shaft output power) and hence the comparatively high input power. This is not unexpected in view of the poor harmonic quality of the waveforms.

Comparing the 180^{o} conduction case (Fig. 4.11) with 240^{o} conduction (Fig. 4.12), it can be seen that the output torque at 5 Hz rotor frequency (0.1 slip) increases from approximately 2.4 Nm with 180^{o} conduction to 2.75 Nm at 240^{o} conduction. Taking nominal values of fundamental voltage as 1.43 V_D for 180^{o} and 1.65 V_D for 240^{o}, then the percentage increase in torque of just under 15% is considerably less than the percentage increase in voltage squared of 33%. This most probably arises from the poorer harmonic content at 240^{o} (for instance, see Section 2.4) and is reflected by the poorer efficiency at this point, i.e. 57% for 180^{o} and 41% for 240^{o}. These results have been included to provide reference conditions for unmodulated drive systems and are not suggested as useful operating conditions.

Theoretical torque curves have been included on Figs. 4.11 and 4.12, calculated from the single-phase equivalent circuit using the assumed fundamental components of voltage, only. The differences between these results and the measured torques provide further indications of the high level of harmonic losses present.

Although previous results (Figs. 4.4 to 4.12) have concentrated on system behaviour under motoring conditions, an example of regenerative behaviour is also given in Figs. 4.13 to 4.15. This is for device conduction of 240^{o} per cycle. It can be seen by comparing the actual phase current (Fig. 4.13) with the computed current using the three-phase equivalent circuit (Fig. 4.14a) that the current waveforms are generally predictable (with amplitudes, here, to within approximately 10%) and that regenerative operation is possible, as would be expected in an ac system. Computed device currents are shown in Fig. 4.14b and demonstrate the expected higher diode utilisation.

The results in Fig. 4.15, of system performance, are of expected shape and again demonstrate the low overall efficiency which was observed in motoring tests, and was attributed to the high harmonic content of the unmodulated inverter waveforms.

4.4 The Drive System with Selective Harmonic Reduction

To investigate how the delta inverter ac drive system performance can be improved by modulating the inverter output, a form of selective harmonic reduction (SHR) was implemented. The waveform with reduced low order harmonics derived in Appendix 5 with harmonic spectrum shown there in Fig. 4 was applied to the inverter. This particular modulation, as stated, improves the poor harmonic performance of the unmodulated inverter output with 240^{o} conduction by considerably suppressing low

order harmonics up to the tenth. The three output voltages were defined at all times by the transistor switching sequence, by ensuring that two transistors were always on.

Oscillograms of the inverter drive system operation are shown in Fig. 4.16. The switching pattern can be seen from the line voltage, Fig. 4.16a. The two current waveforms of Fig. 4.16b and c show the load current at synchronous speed and at 5 Hz rotor frequency (0.1 slip). The current can be considered as a fundamental sinusoid with ripple current due to the harmonics superimposed on it. A visual comparison of the two cases suggests that the ripple current remains substantially unchanged, suggesting that the harmonics are to a degree independent of slip, as has been demonstrated in Section 4.2.

Inspection of the unmodulated current with 240^{o} conduction, Fig. 4.5b, and the current of Fig. 4.16c indicates a reduction in low order harmonics. As shown in Fig. 4.17, this is at the expense of increased device switching. Computed results using the three-phase equivalent circuit are again in visual agreement, both for load current and device operation, Fig. 4.18a, b and c. Predicted results for the load current, Fig. 4.18a, agree with the actual current of Fig. 4.16c to within approximately 15% in amplitude, and to approximately 5% for principal zero crossings.

System performance is shown in Fig. 4.19, and this may be compared with the unmodulated case of 240^{o} conduction in Fig. 4.12. With SHR the torque has been considerably reduced at 5 Hz rotor frequency compared with the unmodulated case, due to the reduction in fundamental voltage. However, as in Section 4.3, taking the nominal values of fundamental voltage as 1.08 V_D with SHR and 1.65 V_D for 240^{o} unmodulated, then the

percentage increase in torque of 77% is again considerably less than the percentage increase in voltage squared of 134%, from using SHR to the unmodulated case. As before, this probably arises from the difference in harmonic content between the two waveforms, reflected in an improved efficiency with modulation, from 41% to 57%. As an indication of the relative harmonic contents, the theoretical weighted harmonic voltage distortion, σ, with unmodulated waveform is 0.263 and is 0.078 with the modulated waveform. In comparison with Fig. 4.11, it can be seen that improving the unmodulated 240^{o} waveform using this form of SHR has produced a system efficiency similar to that with unmodulated 180^{o} conduction. The operation with the modulated waveform, however, retains load independent inverter voltage waveforms. In a similar manner to graphs in Section 4.3, a theoretical torque curve has been included on Fig. 4.19, using the single-phase equivalent circuit with the assumed fundamental voltage component.

4.5 Comparison with the Unmodulated Bridge Inverter System

It is of interest at this stage to compare the conventional bridge inverter with the delta inverter under the control conditions described in the previous two sections. Clearly this is because the bridge inverter is the traditional circuit for producing a variable frequency output for variable speed ac drive systems.

The operation of the bridge inverter in this context is well known and described in the literature (for example Ref.(1) provides a good general description of its behaviour). However, one aspect of its behaviour which is relevant to the present comparison is stated briefly below. This is the inverter output waveform. The Fourier series which describes the output voltage between two terminals of the unmodulated

bridge inverter is typically,

$$\hat{V}_L = \frac{2\sqrt{3}}{\pi} V_B \left\{\sin(\omega t) - \frac{1}{5}\sin(5\omega t) + \frac{1}{7}\sin(7\omega t) - \frac{1}{11}\sin(11\omega t) + \ldots\right\} \quad (4.9)$$

The harmonic spectrum is illustrated in Fig. 4.20. All even harmonics and triplen harmonics are absent from this so called "quasi-square" waveform and the harmonics present, other than the fundamental, are given by the relationship,

$$(6K \pm 1) \qquad K = 1,2,\ldots,n$$

The harmonics appear as pairs in ascending order 5th and 7th; 11th and 13th... etc, with the respective harmonic amplitudes decreasing in inverse proportion to the harmonic number.

Using the figure of merit of the weighted harmonic voltage distortion, σ, for this waveform, it is evident that $\sigma = 0.046$.

The figures of merit for the conditions considered so far are summarised below in Table 4.1. A broad comparison from these and

		σ
Delta inverter:	180^o conduction *	.156
	240^o conduction	.263
	SHR (Section 4.4)	.078
Bridge inverter:	Unmodulated	.046

Table 4.1: Comparison of the weighted harmonic voltage distortion (summing to the 500th harmonic)

* This is for the ideal 180^o waveform (Fig. 2.9) and does not allow for the changes produced in it by the load.

previous results suggest two things. First, whereas the bridge inverter can be used successfully with unmodulated waveforms, the delta inverter is unlikely to produce an acceptable system without some form of modulation to reduce the harmonic content of the output waveforms. Secondly, the form of SHR applied to the delta inverter (Section 4.4) is of a similar quality to the unmodulated bridge inverter system. An experimental comparison of an unmodulated bridge inverter system and the delta inverter system with SHR was therefore undertaken.

From (4.9) the amplitude of the fundamental with the unmodulated bridge inverter is 1.10 V_B. By making V_B = 36V, the fundamental voltage and consequent main flux in the machine will be of a similar size to those due to the delta inverter waveform using SHR in Section 4.4, since the amplitude of the fundamental, in this case, is 1.08 V_D and V_D = 36V. In practical terms, with these relatively low voltage levels device volt-drops need to be taken into account. In this case the bridge inverter voltage must be reduced by $2V_{CE(sat)}$ and the delta inverter voltage by $V_{CE(sat)}$.

The resulting system performance of the bridge inverter drive system is shown in Fig. 4.21, under motoring conditions. This performance is compared with that shown in Fig. 4.19, for the delta inverter with SHR. The torque is approximately 1.45 Nm at 5 Hz rotor frequency in Fig. 4.21 compared with 1.55 Nm for the delta inverter system - this gives a percentage difference in torques of 6.9%. The corresponding difference in output voltages squared is approximately -2.7%. These small differences suggest the similarity of the two conditions and, it is thought, reflects the comparative low levels of harmonic distortion present in the two waveforms when compared with, say, the unmodulated

delta inverter waveforms. Theoretical predictions of torque (using the single-phase equivalent circuit and fundamental voltage only, as before) are shown for the unmodulated bridge inverter in Fig. 4.21 and, as with the delta inverter SHR case, it is thought that the relative accuracy of these suggest harmonic losses are considerably less than with, say, the unmodulated 240^{o} waveforms with the delta inverter (Fig. 4.12).

A comparison of system efficiencies can be made with reference to Fig. 4.22. This diagram shows the efficiency curves for the unmodulated delta inverter system, the delta inverter system with SHR and the unmodulated bridge inverter system. Summarised from this figure is the poor performance of the unmodulated delta inverter with 240^{o} conduction and the similarity between the delta inverter with 180^{o} conduction and with SHR. It can be seen from Fig. 4.22 that the efficiency with the bridge inverter is, as expected, higher than with the delta inverter. Taking 5 Hz rotor frequency, the bridge inverter has an overall system efficiency of approximately 63% compared with 57% for the delta inverter with SHR.

Following from these efficiency figures, it is useful to separate inverter losses from motor losses. Taking the delta inverter with SHR, an estimate of inverter losses was made and compared with that for the unmodulated bridge inverter system. The method of analysis adopted involved using a digital oscilloscope to record required waveforms, from which graphical estimates were then made of the various losses. This method is necessarily approximate. A rotor frequency of 5 Hz was again used.

Transistor on-state losses for the delta inverter were calculated from plots of I_C and $V_{CE(sat)}$. On-state losses per transistor were estimated at 7.8W and, in a similar manner, per diode at 0.5W. Thus total on-state

loss for the inverter was approximately 25W. The other major loss, particularly with a relatively high switching rate, is transistor loss on switching off. The voltage and current characteristics of a transistor as it switched off were recorded and from these the energy dissipated was estimated at 11 mJ each time the transistor switched off. This was done for the average current at switch off during a cycle. From this, switch off losses per transistor were estimated at 6.8W, total for the delta inverter of approximately 20W. Turn on losses were neglected as being relatively small compared with turn off losses. Total losses in the delta inverter came to 45W and 55W for the bridge inverter.

Under these similar experimental conditions the loss in the delta inverter appears less than that in the bridge inverter. The situation can be summarised by the results tabulated below, Table 4.2 (where motor loss = system loss - inverter loss).

Inverter	i/p Power	o/p Power	System loss	Inverter loss	Motor loss
Delta	765	438	327	45	282
Bridge	652	410	242	55	197

Table 4.2: Watts loss analysis for delta inverter with SHR and bridge inverter (unmodulated)

(Rotor frequency = 5 Hz. All powers in Watts)

Although the results in Table 4.2 are necessarily approximate, it seems likely that the difference in overall efficiency between the delta inverter with SHR and the bridge inverter can be attributed mainly to the difference in motor losses. These losses are assumed to be dependent upon the levels of harmonics associated with the two waveforms as indicated by the respective figures in Table 4.1.

It appears, therefore, that the technique of SHR, as implemented so far, does not enable the performance of the delta inverter to approach very closely in quality that of the unmodulated bridge inverter, even though it provides considerable improvement on the unmodulated delta inverter. It is instructive to establish the reasons for this.

The basis of choice of the SHR waveform was to minimise, as far as possible, using a small number of modulating pulses, the low order harmonics that were produced by the delta inverter - especially the low even harmonics, such as the 2nd and 4th. It can be seen from the respective spectra (Appendix 5, Fig. 4 for the delta inverter with SHR and Fig. 4.20 for the unmodulated bridge inverter) that the delta inverter waveform contains reduced amplitude harmonics up to the tenth, in comparison with the amplitude of both the 5th and 7th harmonics of the bridge inverter (although the delta inverter produces even harmonics, the 4th and 8th, but at low amplitude). An additional effect of the SHR modulating pulses, however, is to increase significantly the harmonics around the average switching frequency, which in the case investigated is 16 pulses/cycle, as shown in Fig.4, Appendix 5 . The "figure of merit" which has been used indicates the effect of these harmonics on additional copper loss, but does not include, completely, their effect on iron and stray loss. It appears from the results that these additional losses are significant, but a more detailed assessment of them is beyond the scope of the present work. The conclusion, however, seems to be that for SHR to be completely effective a greater number of modulating pulses than was first anticipated should be used so that the high amplitude harmonics that they produce are of a higher frequency. This being the case, an advantage of SHR, i.e. the use of a smaller number of modulating pulses to determine a few selective

harmonics, seems to be reduced. This feature, coupled with the complexity of combining voltage control with SHR, suggests that a form of regular modulation, such as sinusoidal pulse-width modulation, might be a better system to adopt for overall control of the delta inverter. In the following section experimental results are given for such a modulation system applied to the delta inverter, continuing from the theoretical work in Chapter 3.

4.6 The Drive System with Sinusoidal PWM

Preceding chapters suggested that sinusoidal PWM might be the most effective method for harmonic improvement with the delta inverter. Further, it seems easier to provide voltage control using PWM than with the other modulation technique described, selective harmonic reduction. Operation of the delta inverter ac drive system with PWM is now investigated.

Single edge modulation using natural sampling appeared the best PWM technique in the previous chapter, in terms of the theoretical harmonic spectra, and this type of modulation has been incorporated on the inverter drive system. A nominal switching frequency of 1.8 kHz was chosen to investigate behaviour, being a reasonably compatible frequency for the inverter power devices.

Practical results for the phase and line quantities resulting with this type of PWM applied to the inverter are illustrated in Fig.4.23. It can be seen from Fig.4.23a that the line voltage is clamped at either $+V_D$ or $-2V_D$ by the "two devices always on" rule, making this waveform and the inverter operation load independent. The relatively long period when switching is not occurring (marked as (P) on Fig. 4.23) is due to the fact that the smallest negative pulses required for strict

sinusoidal PWM have not been used because they are the same order of magnitude as the total turn off time of the power transistors. The total number of pulses per cycle was therefore 32, which corresponds to an average switching frequency of 1.6 kHz. The phase voltage that appears with a star connected load, Fig. 4.23b, shows that voltage states $+V_D$, $-V_D$ and zero are utilised. Typical current waveforms are shown in Fig. 4.23c and d, taken at 5 Hz rotor frequency, and give visual evidence of the sinusoidal nature of the delta inverter supply. This improvement in waveform is accomplished at the expense of an increased device switching rate, as shown in Fig. 4.24.

To measure, accurately, the efficiency of a machine which has a relatively high efficiency is difficult to achieve by measuring the input and output powers. For example, take the case of an 80% efficient machine, with an input power of 100 units, say, and an output power of 80 units. If these powers are each measured experimentally to an accuracy of 5% then the results would be in the range 100 ± 5 and 80 ± 4. The worst case combinations could therefore predict efficiencies of 72% or 88%. This can make comparison of efficiencies with different supply waveforms an unreliable procedure particularly where the two waveforms are similar, such as is suggested in the case when comparing a pure sinusoidal supply with a PWM sinusoidal supply. This problem is compounded in the present system when the electrical input power is a combination of pulse-width modulated voltage and current waveforms and the output power is derived from a torque transducer, i.e. input and output powers cannot be measured by the same instruments to achieve higher accuracy.

A more accurate method might be to measure power loss directly - in the present case this is a heat loss. While a direct calorimeter method would be difficult to achieve, in the present circumstances it was thought that measurement of machine temperature rise would be the most convenient system to use. It was assumed[11] that, within the temperature ranges encountered, heat loss was proportional to temperature rise, and although actual efficiencies were not calculated from temperature rise, at least the temperature rise produced by different supply waveforms can be compared quite accurately. This is thought to be an appropriate method because temperature rise of a machine is the limiting factor on its specific output and temperature rise considerations form an important part of the motor design process.

From the foregoing it is concluded that a comparison can be made of the motor efficiency when supplied by the inverter with PWM and by the standard mains three-phase, 50 Hz, sinusoidal supply, in terms of resultant temperature rise. Such a comparison appears to be an acceptable way of assessing the performance of the PWM system.

For these tests motor temperature was measured using a thermocouple fixed to the stator end windings. During each run, for comparison purposes, the rotor speed and measured shaft torque were kept approximately the same. To achieve this the fundamental voltages were within 2% - this itself is indicative of a low level of harmonic loss with the PWM waveform. The results using a star connected induction motor at 5 Hz rotor frequency are shown for the PWM and mains supplies, as temperature rise above ambient in Fig.4.25. The induction motor used produced just over ½ kW throughout the heat runs. The tests were continued for just under two hours, sufficiently long for the exponential temperature rise to approach steady state. The difference in

temperature rise above ambient between the two cases can be seen in Fig. 4.25 to be about 10%. This level of additional motor loss is not dissimilar to the order of additional loss produced by conventional inverters and for practical purposes would normally be within motor specification tolerances. For a motor with, say, 80% overall efficiency an increase of 10% in the losses results in a reduction of efficiency of only 2%, i.e. to 78%.

Voltage spectra for the test conditions are shown in Fig. 4.26. Fig. 4.26a shows the ideal theoretical harmonic spectrum (calculated using equation (3.19), section 3.4.1), while Fig. 4.26b is the measured voltage spectrum and compares the relative amplitudes of the harmonics. It can be seen that there is close agreement with the theoretical spectrum, although some very low amplitude harmonics also exist throughout the range of the measured spectrum. As with conventional inverter experience, these are due to some degradation of the theoretical waveform, and are mainly the result of practical considerations such as allowances for finite device switching times.

The results given in this section confirm the suggestion that the application of PWM to the delta inverter significantly improves the system performance. The equations given in Section 3.4.1 may be used as the basis to producing a suitably controlled system.

4.7 The Effect on Inverter VA Capacity of Using Sinusoidal PWM

It is suggested that a poor system efficiency need not be an inherent drawback of the delta inverter, since the previous section showed that implementation of sinusoidal PWM on the inverter may enable satisfactory efficiencies to be achieved. This was shown by comparing the operation of the delta inverter system with that of the ideal system using a mains quality three-phase sinusoidal supply. It appears

that the performance of such an inverter system depends to a large extent on the value of carrier ratio that can be used, and the trade-off between reducing harmonic losses in the ac machine and increasing switching losses in the inverter. Having made favourable conclusions on the overall system efficiency achievable, a number of further points need to be considered in order to assess the cost effectiveness and feasibility of using the delta inverter as a means of producing the supply for an ac drive.

On introducing the delta inverter in Chapter 1 emphasis was put on the reduced component count of the delta inverter. A comparison was made with the conventional three-phase bridge inverter and the regenerative chopper, two alternative drive circuits, which showed that the dc system has the benefit of a reduced component count over the conventional ac system. It was shown that, similarly, the delta inverter requires only half the number of power devices of the bridge inverter. This of itself may be a considerable advantage in terms of reliability and might be a major factor in choosing a delta inverter based system. In terms of cost, however, such advantage may depend to some extent on the level of utilisation of the main power devices. Therefore one form of assessment, that will be made here, is in terms of the relative silicon cost of the delta inverter.

The silicon cost of an inverter can be associated with the total switching capacity of the inverter. On this basis a comparison was made in Appendix 1 between the conventional bridge inverter and the delta inverter. Both inverters used unmodulated waveforms (240^{o} conduction with the delta inverter). It was shown that the switching capacity (from the total transistor rating in relation to the power delivered to the load) of both inverters was the same. A similar

investigation will be made here, but considering the inverters with sinusoidal PWM.

In both cases, a simplified comparison method is used, where the following assumptions are made:

a) For each inverter the voltage rating is related to the battery voltage and is independent of the nature of the load.

b) Since the output of a motor depends upon the kVA delivered to it, it is possible to assess the current rating of the devices in terms of the real power delivered to a resistive load.

These assumptions make the comparison necessarily approximate. However, the validity of the comparison is enhanced since the same assumptions are made for both inverters.

The results of this comparison are shown in Table 4.3 below. The dc supplies are taken as V_B for the bridge inverter and V_D for the delta inverter, as usual. Both inverters are taken to be working with PWM of the types previously described (see Chapter 3). Sufficiently high carrier ratios are assumed, such that the nominal values of fundamental voltages can be assumed, as shown in Table 4.3. Assuming the loads are delta connected with phase resistances R_B and R_D, respectively, then the total power delivered to the load follows directly. The minimum transistor voltage ratings are taken as equal to the maximum voltages the devices see during a cycle. Similarly, the minimum current rating, with the bridge inverter, is taken, with three devices on, as equivalent to the current due to V_B across $R_B/2$ and, with the delta inverter, is taken as due to $2V_D$ across a total resistance of $2/3\ R_D$.

	Bridge Inverter	Delta Inverter
1. RMS fundamental phase voltage	$\frac{V_B \sqrt{3}}{2\sqrt{2}}$	$\frac{V_D}{\sqrt{2}}$
2. RMS fundamental phase current	$\frac{V_B \sqrt{3}}{2\sqrt{2}\ R_B}$	$\frac{V_D}{\sqrt{2}\ R_D}$
3. Total power delivered to load	$3\ \frac{V_B^2\ 3}{8\ R_B}$	$3\ \frac{V_D^2}{2R_D}$
4. Minimum transistor voltage rating	V_B	$3V_D$
5. Minimum transistor current rating	$\frac{2V_B}{R_B}$	$\frac{3V_D}{R_D}$
6. Total installed VA rating of transistors	$6\ \frac{2V_B^2}{R_B}$	$3\ \frac{9V_D^2}{R_D}$
7. $\frac{\text{Total transistor rating}}{\text{Load power}}$	$\frac{32}{3}$	18

Table 4.3 Comparison of Total Transistor VA Ratings for Bridge and Delta Inverters with PWM

In comparison with the unmodulated case in Appendix 1, it can be seen that on the basis of this approximate comparison the total VA capacity of the delta inverter is substantially reduced. The ratio of total transistor rating to load power has increased from 6.6 to 18. The application of PWM to the bridge inverter also has a detrimental but less severe effect, the ratio increasing from 6.6 to 10.7. The changes in VA capacity are related to the changes in fundamental voltage levels of the waveforms for each inverter. Comparing between the two inverters it can be seen that the percentage reduction in fundamental when using PWM with the delta inverter is greater than with the bridge inverter and the theoretical silicon cost of the delta inverter consequently suffers. However, in most cases silicon cost is only one consideration and others such as the number of heat sinks, power diodes, base drives and base drive power supplies, all of which are halved for the delta inverter, must also be considered in an overall assessment.

4.8 Practical System Considerations

The major component blocks of the delta inverter are each investigated in this section. Although at first sight it might appear that radical design changes are necessary to conventional inverter design in order to accommodate the delta inverter circuit, in fact, based on recent inverter technology, most changes required for the delta inverter can, it appears, be made relatively straightforward.

One departure from conventional design is the requirement for three isolated dc supplies and the ramifications of this are discussed in Section 4.8.1. Section 4.8.2 shows, however, that conventional circuitry can be used for the power stages of the delta inverter. Control strategy requirement can, to a large extent, be approached in a similar

fashion to those methods adopted with, for instance, the bridge inverter and, from a practical point of view, may be simpler with only three devices to control - this is illustrated in Section 4.8.3. Similarly, it appears that methods of protection recently developed for the bridge inverter can be adapted to the delta inverter, again with some potential simplicity apparent due to the reduced component count of the delta inverter, Section 4.8.4.

4.8.1 The DC Sources

Two alternatives have been considered for the dc supplies to the delta inverter - either batteries or rectified ac. Generally, the appropriate choice is dictated by the application.

For stand alone traction applications, such as fork lift trucks and electric vehicles, batteries are used. Standard traction batteries were incorporated in the prototype delta inverter system. There appear no particular restrictions peculiar to this inverter on the choice of such power sources. These are conventionally batteries of the lead acid type, which are likely to remain popular for an indefinite time, due to numerous advantages, such as low cost, high reliability, performance and flexibility[12]. Of interest are the numerous other types under intensive world wide investigation[13] but only nickel cadmium batteries, as alternatives, are generally available at present.

Making a comparison between the conventional bridge inverter and the delta inverter: given a battery stack of a certain voltage and ampere-hour rating for the bridge inverter, then for the delta inverter this same stack can be split into three separate batteries, each of one third the total voltage. (An examination of the delta inverter circuit shows that it is possible to use only two batteries, by swopping the

position of the battery and antiparallel pair in one leg, where one stack has twice the voltage of the other and is centre tapped. This is actually shown in Fig. 4.34. The result is a possible marginal reduction in cabling). Assuming similar inverter/system efficiencies, the delta inverter system may work a comparable duty cycle, given that the average battery current per cycle will be similar (as battery capacity is affected by the level of the discharge current). The comparison is slightly more complicated since, whilst the battery stack of the bridge inverter has a continuous discharge current (with ripple), each battery of the delta inverter sees a form of pulsed discharge. It has been reported [14] that performance with some pulsed forms of discharge, in comparison with steady discharge, may not be unfavourable in terms of battery capacity, under certain conditions. However, filters could also be used to reduce battery ripple current.

If proposing a commercial battery fed delta inverter system, then consideration must be given to the method of battery charging. Whereas the conventional bridge inverter supply can be charged without disconnecting either the inverter or its load, this is not possible with the delta inverter. The delta inverter system requires two load terminals to be disconnected and the battery supplies can then be charged via the main flywheel diodes by inserting a charger into the delta "loop". These required functions are readily achieved by contactors.

Considering the use of rectified ac for inverter supplies, Fig. 4.27 shows one circuit which could be used with the bridge inverter. Rectified three-phase is usually more attractive because the ripple frequency is much higher than with a comparable single-phase supply. A 50 Hz single-phase full wave rectifier has a ripple frequency of 100 Hz, whereas the three-phase circuit has a ripple frequency of 300 Hz - the filter

requirement is therefore reduced. The rectifier in Fig. 4.27 has been shown supplied by a three-phase transformer but, where a change of voltage level is not required, could equally well be supplied directly from a suitable three-phase supply. As an alternative, to provide an adjustable dc link voltage, a phase controlled rectifier or chopper can be used.

Using a similar three-phase transformer, a suitable supply for the delta inverter could be made, as shown in Fig. 4.28. This circuit has the disadvantage of 100 Hz ripple on each of the three dc outputs, requiring larger filter components. Comparable performance with 300 Hz ripple requires three three-phase secondaries on the transformer, giving a circuit such as Fig. 4.29. This configuration has a small drawback in terms of transformer winding complexity, but the overall transformer size should be approximately the same for both cases, for any given power throughput. The use of a single-phase ac input supply might be considered for some electric traction applications, such as electric trains, where single-phase operation is used because of the simplification in current collection.

Again, assuming similar inverter/system efficiencies, then each of the delta inverter's three dc supply sections need only have one third the VA capability of the comparable bridge inverter supply. Thus transformer secondaries, rectifiers and filters may be derated. Using a rectified dc supply, energy from the flywheel paths in both inverters must be absorbed in the filter components and so, in both cases, ratings must be adequate. In general, such supplies are not suitable if a regenerative mode is necessary - this requires some form of anti-parallel or double converter to be incorporated usually (see Chapter 1).

4.8.2 The Inverter Power Electronics

A major advantage to the present prototype design of the delta inverter was the availability of relatively high power transistors. Until recently conventional designs would have had to incorporate thyristors as the main power devices. This would have produced the necessity for a reliable method of operation, and particularly commutation, within the delta inverter configuration.

The power transistors used in the prototype were manufactured by Toshiba, type 2SD 646 silicon triple mesa Darlington transistors, having a $V_{CEO(sus)}$ = 450V and $I_{C(max)}$ = 100A and requiring approximately 2.5A base current for saturation. The main flywheel diodes used were Westinghouse high power, fast recovery silicon diodes type SF5 GN/GR 71. Data shsets for both devices are reproduced in Appendix 6 .

The trend in semiconductor power electronic devices at the present time is one of rapid development - already, for instance, the 2SD 646 transistor has been superseded by the 2SD 646A which has improved performance with notably faster switching speeds. The power devices chosen for the prototype were not selected for optimum inverter design but rather to provide large voltage and current margins so that possible abnormal conditions in the delta inverter could be accommodated. In practice this was not found to be necessary, as ascertained throughout the present work. An important limitation of the incorporated devices is, however, their switching speed. In particular their relatively long turn-off time, made up of approximately 8 μS storage time and 5 μS fall time, limits the maximum switching frequency. Some further operational details of these devices can be obtained in Ref. (15).

A circuit diagram of the delta inverter showing the main components is given in Fig. 4.30, in which it can be seen that each separate leg of the inverter contains an antiparallel transistor-diode pair. Fig. 4.30 illustrates the positioning of non-inductive current shunts in the prototype, in this particular case when both capacitive and inductive snubber components[15] are present.

Base drive design for the power device switching can again follow upon conventional circuitry incorporated into bridge inverter systems. An available discrete in-house design of base drive was incorporated in the prototype inverter system. At the present time there are becoming available integrated circuit base drives (for example, the Thomson-EFCIC UAA 4002 control chip) which incorporate the facilities for overcurrent and out of saturation protection of the power devices and which allow the setting of minimum on and off times.

A photograph of the prototype inverter is shown in Fig. 4.31. Identifiable to the rear of the inverter are the three main heat sinks, one for each antiparallel pair assembly. The base drive and logic boards are on the upper rack.

4.8.3 The Control Strategy and Microprocessor Systems

The delta inverter requires a logic signal to the base drive supply of respective power transistors. Where the output waveforms are unmodulated a simple TTL logic circuit can be used. In practice it is advisable to incorporate protection against malfunction - in this case, to prevent all three power devices being told to be on together. Such a straightforward approach was initially adopted. However, the necessity to produce waveforms using various switching strategies makes this type of approach unpracticable.

To provide a versatile means of generating control signals a microprocessor system was adopted. In this case a Motorola M6800[16] microprocessor system was designed but most standard "off the shelf" systems could equally well perform the required functions.

An open loop control scheme was developed to produce the various switching techniques adopted throughout the present work. An outline of the approach taken now follows. A flowchart for the basic program is shown in Fig. 4.32. The microprocessor system clock frequency (from a crystal controlled 1 MHz, or optionally 2 MHz, oscillator) was used as the general timing reference. By varying the number of times a fixed delay loop in software was executed, variable time delays were produced. This can be distinguished in the flow chart as the inner loop, decrementing the contents of a microprocessor register. Each delay over which no output logic signal changes is separated and the length of time this state is invariant is translated into the required number of times the delay loop need be executed. The required output logic state over this time is fed out via a parallel interface device as the logic signals necessary for the base drives. In this way a complete cycle can be built up producing a data table which is executed serially to produce the periodic control signals in a continuous manner. By this method signals can be produced to generate waveforms from the simple unmodulated type to those with PWM.

Using the 1 MHz clock frequency, the basic program had a minimum time delay of 36 μS and resolution to 6 μS, there being no upper limit on the length of time delay possible (within practical limits). These two figures are obviously halved if a 2 MHz clock frequency were used. Given the relatively long switch off time of the power transistors,

approximately 13 μS, the program speed is adequate and can be further enhanced by programming changes, for instance, where dead bands of short duration are required. Special consideration must be given to provide dead bands (i.e. periods between one transistor being switched off and the next switching on) to allow for the power device switching times. As previously mentioned, with the delta inverter switching strategy of two devices always on, this necessitates guarding against all three devices being on together. (Similarly, two devices in any leg of the bridge inverter must never be on together). With the devices used, a dead band of approximately 20 μS was required.

A number of general solutions have been considered for extending these microprocessor techniques with the delta inverter to produce a closed loop system with PWM. In essence the basic problem appears one of real time processing requirements - if the microprocessor is continuously generating the control waveforms there may be little facility left for monitoring and updating computations. As those methods considered appropriate, discussed below, have already been developed and documented for conventional inverter design it was felt that the present work on the open loop PWM system for the delta inverter should not, however, be extended at this stage.

One suggested solution, which has been applied to the bridge inverter system[17], is to store the switching sequence for a complete cycle in a shift register circuit, in an appropriate format which can continuously be sent out to the inverter. Meanwhile the microprocessor can be left free to calculate data for a new cycle if or when a response is needed to a changing control parameter. This new data can be entered into the shift register circuit input whilst the original sequence is still controlling the switching, shifting out of the shift

register (i.e. using the first-in-first-out principle). In a similar way, a method of using DMA (direct memory access) transfer has been described[18], where the firing sequence for the thyristors of a bridge inverter are stored in system memory and are accessed directly in a manner transparent to the processor. Two alternating portions of memory are used - one supplying the firing circuits whilst the other can be being updated with a new sequence.

These two methods seem to lead naturally to the suggestion of a multimicroprocessor system. One such system has been described by Mauch and Ito[19]. In this example the main calculations are performed by a 16 bit microprocessor that passes information to a fast bipolar microprocessor which controls generation of the switching sequences.

Having developed a method of controlling the delta inverter system, then one further consideration is useful. In large induction machines it is sometimes necessary to trim out slight imbalance in the supply waveforms or subharmonic oscillations can occur - this may be particularly necessary because the machine has a relatively low impedance near zero frequency. The problem has also been recognised with the bridge inverter where an offset can be caused between the two devices of any one leg because, say, the resultant switching is not exactly 50:50 or voltage drops across the devices are not equal. Such subharmonics may also be inherently generated in some particular modulation techniques[20]. It has been recognised that when using PWM, then, if an unbalance is present, one method of controlling this is to adjust the modulation to compensate. It is therefore suggested that any unbalance that occurs with the delta inverter (and this may be due, for instance, to unequal supply voltages) can be similarly compensated for.

4.8.4 Fault Current Control

Compared with the thyristor the power transistor is a fairly delicate device and because of its relatively low overload capacity (i.e. in terms of peak to mean current rating) cannot be easily protected. In the case of a fault or circuit malfunction developing, fuses are invariably too slow.

Conceivably one of the worst faults that can occur in the bridge inverter is if both devices of the same leg are on together. A solution to this particular fault condition has recently been reported by Evans and Saied[21,22] and it is proposed in this section to show how that method can be adapted to protect the delta inverter in its analogous fault condition, when all three power devices are on together.

In its basic form, to protect the power devices of the bridge inverter a modification is made to the classic circuit arrangement of each leg of the inverter. The modified circuit can be thought of as the combination of a step-down chopper and a step-up chopper, as shown in Figs. 4.33a and b, respectively. Each of these circuits allows unidirectional current and power flow but in opposite directions. The combination of these two circuits produces the modified inverter leg shown in Fig. 4.33c. Conventionally an inductor is sometimes placed in the output line to control the rate of rise of fault current in the event of a load short-circuit but by moving the inductor to the position shown in the modified leg it can now control not only an output fault but also fault current due to both devices in a leg being on together.

A similar modification which is suggested for the delta inverter is shown in Fig. 4.34. In this proposed modified delta inverter configuration the positions of the antiparallel pair and dc supply in one

leg have been interchanged and a protection choke included. In the event of all three devices being simultaneously on together it can be seen that a suitable choice of inductance value should allow the protection choke to limit the rate of rise of current sufficiently to allow some form of inverter "shut-down" procedure to operate.

Preliminary computer simulations of the delta inverter-induction motor system subjected to a fault condition have been carried out. One example is given in Fig. 4.35. This example shows the delta inverter system with unmodulated 240^{o} conduction running at 10 Hz rotor frequency (as in Section 4.3) but with the on time of T_1 extended beyond 240^{o}, providing a short period during each cycle when all three devices are on together. A comparison of current waveforms in Fig. 4.35a with Fig. 4.10 shows the effect on the general transistor conduction of adding the inductor (in this example a value of 100 μH was used). Fig. 4.35b shows that during the period of the fault the current in all three transistors ramps up in a defined manner under the effect of approximately $3V_D$ across the protection choke. This produces the corresponding spike of current marked with a * in Fig. 4.35a. In this particular case the fault occurs when currents in both T_1 and T_2 are at a maximum when the degree of additional fault current that the devices can tolerate is most severely limited. It is suggested that the current in T_3 after the fault has been removed is contributed to by the discharging of the fault current established in the inductor, freewheeling through T_3 and D_3 with, therefore, a relatively long time constant, and by the increasing load current in T_3. A similar argument seems to follow earlier in the cycle when T_3 switches off at 6.67 mS and the choke current can freewheel in T_1 and D_1. This effect being similar to that which occurs in the modified bridge circuit.

There appears little effect on load current of this particular fault current protection procedure. This can be seen by comparing the waveform in Fig. 4.35c with the load current waveforms discussed in Section 4.3, shown in Fig. 4.7 for unmodulated 240^{o} conduction. The configuration shown in Fig. 4.34 can produce some unbalance in the load current and the choke should therefore be as small as possible, commensurate with satisfactory fault protection. To maintain balanced conditions compensation may also be possible via the modulation strategy as suggested in the conclusion of Section 4.8.3.

4.9 Conclusions

This Chapter has investigated the delta inverter ac drive system. The effect on the system of the relatively poor waveforms of the unmodulated inverter have been demonstrated. Implementation of the PWM strategy outlined in Chapter 3 has been shown to produce a significantly improved system performance as a consequence of the reduction in harmonics produced by this modulation.

The application of PWM to the delta inverter system makes possible a more favourable comparison with the performance of conventional inverters and may allow the obvious advantage with the delta inverter, of having a reduced component count, to be viewed more optimistically.

Some of the specific consequences of the delta inverter's reduced component count, such as the requirement for isolated dc supplies, have been discussed. Control and fault protection methods look practicable and in some respects a degree of simplicity seems to be introduced.

4.10 References

1. Murphy, J.M.D.: "Thyristor Control of AC Motors", Pergamon Press, Oxford, 1978.

2. Jain, G.C.: "The effect of voltage waveshape on the performance of a 3-phase induction motor", IEEE Trans., Vol.PAS-83, No.6, June 1964, pp.561-566.

3. Klingshirn, E.A. and Jordan, H.E.: "Polyphase induction motor performance and losses on nonsinusoidal voltage sources", IEEE Trans., Vol. PAS-87, No.3, March 1968, pp.624-631.

4. Chalmers, B.J. and Sarkar, B.R.: "Induction-motor losses due to nonsinusoidal supply waveforms", IEE Proc., Vol.115, No.12, Dec. 1968, pp.1777-1782.

5. McLean, G.W., Nix, G.F. and Alwash, S.R.: "Performance and design of induction motors with square-wave excitation", IEE Proc., Vol.116, No.8, Aug. 1969, pp.1405-1411.

6. Largiader, H.: "Design aspects of induction motors for traction applications with supply through static frequency changers", Brown and Boveri Rev., Vol.57, April 1970, pp.152-167.

7. Alger, P.L.: "The Nature of Induction Machines", Gordon and Breach, New York, 1965.

8. Al-Obaidi, H.A.: "The analysis of inverter fed induction machine systems", Ph.D. Thesis, University of Bath, 1982.

9. Evans, P.D. and Al-Obaidi, H.A.: "Simulation of inverter fed induction motor systems by means of circuit analysis computer packages", IEE Inter. Conf. 'Machines-Design and Applications', Vol.213, July 1982, pp.114-118.

10. IBM: "ASTAP - Program Reference Manual", Program No. 5796.PBH, 1972.

11. Say, M.G.: "Alternating Current Machines", Pitman, London, 4th ed., 1978.

12. Weissman, E.Y.: "Lead-Acid Storage Batteries", "Batteries", Vol.2, "Lead-Acid Batteries and Electric Vehicles" (Ed. by Kordesh, K.V.), Chap. 2, Marcel Dekker, New York, 1977, pp.1-200.

13. Rowlette, J.J. and Klose, G.J.: "New perspective on electric vehicle batteries", ASNE Inter. Conf. Proc. 'Drive Electric Amsterdam 82', Amsterdam, Oct. 1982, pp.195-204.

14. Jayne, M.G.: "The behaviour of lead-acid batteries under pulsed discharge conditions", Power Sources 6, 10th Inter. Symp., Brighton, Sept. 1976, Academic Press, London, 1977, pp.35-44.

15. Evans, P.D. and Hill-Cottingham, R.J.: "Some aspects of power transistor inverter design", IEE Electric Power Applications, Vol.2, No.3, June 1979, pp.73-80.

16. Motorola: "M6800 Microprocessor Applications Manual, 1975.

17. Humblet, L.C.P., De Buck, F.G.G. and De Valck, P.: "A realisation example of a microprocessor-driven PWM transistor inverter", IEE 2nd Inter. Conf. on Electrical Variable-Speed Drives, Sept. 1979, pp.151-156.

18. Rajashekara, K.S. and Vithayathil, J.: "Microprocessor based sinusoidal PWM inverter by DMA transfer", IEEE Trans., Vol.IE-29, No.1, Feb. 1982, pp.46-51.

19. Mauch, K. and Ito, M.R.: "A multimicroprocessor ac drive controller", IEEE Conf. Rec. Annual IAS Meeting, Oct. 1976, pp.634-640.

20. Bowes, S.R. and Bird, B.M.: "Novel approach to the analysis and synthesis of modulation processes in power convertors", IEE Proc., Vol.122, No.5, May 1975, pp.507-513.

21. Evans, P.D. and Saied, B.M.: "Fault-current control in power-conditioning units using power transistors", IEE Proc., Vol.128, Pt.B, No.6, Nov. 1981, pp.335-337.

22. Evans, P.D. and Saied, B.M.: "Protection methods for power-transistor circuits", IEE Proc., Vol.129, Pt.B, No.6, Nov. 1982, pp.359-363.

CHAPTER 5

CONCLUSIONS

A new type of inverter, the delta inverter, has been introduced and studied. Preceding chapters have described the behaviour of this inverter circuit and have established guidelines for its design to meet a specified performance. The suitability of the delta inverter for any given application can therefore be assessed. Detailed conclusions have already been presented for each chapter but the overall conclusions from the work are summarised below.

The prime feature of the delta inverter is the fact that it requires three main power devices and associated equipment. This compares with six devices required by a conventional three-phase bridge inverter for an ac drive. The potential therefore exists for halving the complexity of the power converter in an ac drive system.

The drawback of the delta inverter is, however, the need for three isolated dc sources. This possibly restricts its application to battery fed schemes, except for special circumstances. The need for control loops to ensure balanced charge and discharge rates for the three sources would therefore usually be required.

The natural output waveforms of the delta inverter are rich in harmonics and would be undesirable for most applications. However, a scheme for applying sinusoidal pulse-width modulation has been presented which produces high quality output waveforms. For example, a decrease in motor efficiency of about 2% was measured using sinusoidal PWM with a switching frequency of 1.6 kHz.

Alternative schemes for pulse-width modulation and equivalent techniques with mathematical and computer assessment of their properties comprise a significant portion of the thesis, principally in Chapter 3.

Throughout the study, attempts have been made to draw quantitative comparisons with the conventional bridge inverter. From the point of view of total installed switching capacity of semiconductor devices it is shown to be the same for both unmodulated inverters, but slightly greater when PWM is used.

Reliability of power semiconductor equipment is always an important consideration. Apart from the reduced component count of the delta inverter, which inherently provides better reliability, one further advantage is apparent. With the bridge inverter there are three possible fault paths - by a shoot through in each leg. In the delta inverter only one similar path exists, if all three devices conducted simultaneously. A rearrangement of the inverter circuit can control this fault.

The main purpose of the research programme described in this thesis was to attempt to reduce the complexity of the ac inverter. This was in order that induction machines could be used, instead of dc machines, in variable speed drive systems, without the cost and complexity of the ac controller detracting from the inherent advantages of the ac system.

The delta inverter has shown that the number of devices can be halved from six to three, and three is conceivably the minimum number of devices for a three-phase inverter. The requirement for three dc sources is clearly a disadvantage, compared to the bridge inverter, but the understanding of the delta inverter has now been taken to a

stage where the two alternative systems can be compared and assessed for practical applications.

It is difficult to foresee where possible economic applications for the delta inverter might lie, and these may indeed change in the future as the relative costs of the various components in a power control chain vary and as new applications arise.

Taking the two extreme ends of the power spectrum for example:

- there is the possibility of low power transformer fed ac drive systems in which three isolated dc sources can be derived quite readily and the low number of power semiconductor devices gives an overall cost advantage.
- at the higher power end, GTOs may be suitable alternative devices for the delta inverter and allow high voltage and high current operation without the need for thyristor commutation circuits.

APPENDIX 1

IEE Proceedings
Vol.127, Part B, No.6, Nov. 1980
Electric Power Applications

Paper Entitled,

"Delta Inverter"

by P.D. Evans, R.C. Dodson and J.F. Eastham

Delta inverter

P.D. Evans, B.Sc. (Eng.), D.I.C., Ph.D., A.C.G.I., R.C. Dodson, B.Sc., and
Prof. J.F. Eastham, D.Sc., Ph.D., F.R.S.E., C.Eng., F.I.E.E.

Indexing terms: *Motors, Power electronics*

Abstract: The delta inverter is a novel circuit which uses only three power transistors to produce a three-phase supply. Requiring approximately half the components of a conventional bridge inverter it therefore has potential cost and reliability advantages. The basic operating principles of the delta inverter are explained, using passive resistive and inductive loads. Some aspects of its performance are compared with a bridge inverter, and preliminary results with an induction motor are presented.

1 Introduction

The bridge inverter in Fig. 1 is commonly used to derive a variable frequency three-phase supply from a d.c. source. It is illustrated for comparison with an alternative inverter circuit, referred to here as the 'delta inverter',[1] which is shown in Fig. 2.

The main attraction of the delta inverter is the reduced number of components that it requires. Offsetting this advantage is the need for three isolated d.c. supplies. However, these may be derived from a battery source, if the stack is split into three sections.

The potential area of application for the delta inverter is therefore thought to be in the field of battery-fed variable-speed drive systems. These are used in industrial handling systems, such as fork-lift trucks and in battery vehicles. The latter have yet to become widely established, but are currently the subject of world-wide research and development activity.

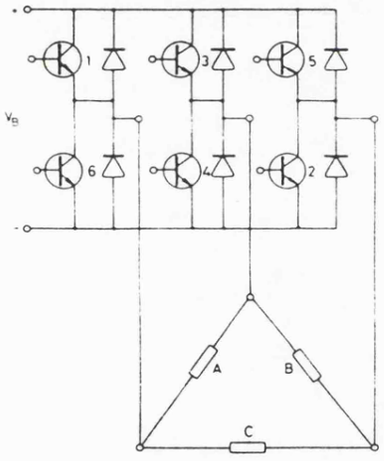

Fig. 1 *Bridge inverter and load*

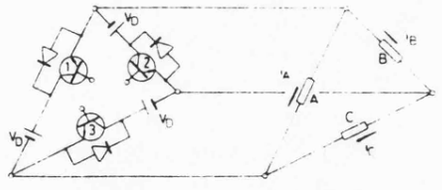

Fig. 2 *Delta inverter and load*

Paper 955B, first received 23rd January and in final form 10th July 1980

The authors are with the School of Electrical Engineering, University of Bath, Claverton Down, Bath, BA2 7AY, England

Most variable-speed systems use d.c. machines. One of the reasons for this is that, despite the well known drawbacks of d.c. machines, the controllers for them are relatively simple and reliable. They require a small number of solid-state devices. Induction machines, on the other hand, although being cheap and reliable compared to d.c. machines, require solid-state inverters to drive them. Broadly speaking, the conventional three-phase inverter for an induction motor is equivalent in solid-state component count to three regenerative d.c. choppers. The total cost of a variable-speed a.c. system is therefore dominated by the controller. As the overall reliability of a system is strongly dependent upon the number of components it contains, the inverter is also worse than its d.c. counterpart in this respect.

The delta inverter was therefore devised in an attempt to reduce the complexity of a three-phase inverter. It conceivably contains the minimum number of devices possible for a three-phase inverter system. This paper presents the results of a study which was undertaken to assess its feasibility.

2 Basic operation of the delta inverter

The modes of operation of the delta inverter are relatively complex and it has therefore been investigated experimentally and theoretically with two types of passive load. First, it was used to drive a 'purely' resistive load. This was constructed so that it had negligible inductance. Secondly, iron-cored chokes were used to provide a 'purely' inductive load. One advantage of these two loads is that they can be handled graphically and analytically in a relatively convenient manner. They also allow the essential characteristics of the delta inverter to be studied and set the limits within which an *RL* load with an intermediate time constant would operate. The description of the behaviour of the inverter assumes that the transistors and diodes behave as ideal devices.

Preliminary results have also shown that the delta inverter will operate in both the motoring and regenerating modes with an induction machine.

The prototype delta inverter was constructed using power transistors as the power switching elements. All tests were carried out under balanced three-phase conditions. For convenience, a microprocessor was used in an open-loop mode to generate the transistor switching signals. Peak device currents of around 20 A were used in the tests.

0143-7038/80/060333 + 08 $01·50/0

2.1 *Behaviour of the delta inverter with resistive load*

Each transistor in the delta inverter can remain on for up to two-thirds of a period ($\theta = 4\pi/3$). (If θ exceeds $4\pi/3$, three devices are on simultaneously and form a short-circuit path for the three supplies). Transistor conduction angles in the range $2\pi/3 \leqslant \theta \leqslant 4\pi/3$ have therefore been considered.

The feedback diodes are inoperative with a purely resistive load and the behaviour of the circuit can be ascertained by inspection. In Fig. 3*a* the transistor switching sequences are illustrated for a typical conduction angle within the above-mentioned range. The resulting voltage appearing across phase *A* (Fig. 2) of the delta-connected load is shown in Fig. 3*b*. Identical voltage waveforms appear across phases *B* and *C* but they are displaced progressively by $2\pi/3$ to form a three-phase set.

It can be seen that, in general, three voltage levels appear at each phase of the load. These are $+V_D$ when the transistor in its corresponding inverter leg is ON (transistor 1 for phase *A* etc.), $-0{\cdot}5V_D$ when either one of the other two inverter legs is ON, and $-2V_D$ when both the other legs are ON together. When $\theta = 2\pi/3$, only the voltage levels $+V_D$ and $-0{\cdot}5V_D$ occur, and when $\theta = 4\pi/3$, only $+V_D$ and $-2V_D$ occur. Oscillograms of the phase voltages for $\theta = 2\pi/3, \pi$ and $4\pi/3$ are shown in Fig. 4.

Transistor currents and voltages are shown in Fig. 3*c* and *d*, respectively. It can be seen that the maximum transistor current is $3I_D$ where $I_D = V_D/R_D$, R_D being the phase resistance. Similarly, the maximum voltage to which each transistor is exposed is $V_{CE} = 3V_D$.

The peak amplitude of the nth harmonic of the voltage waveform shown in Fig. 3*b* is given by

$$\hat{v}_n = \frac{6V_D}{\pi n} \sin\frac{2\pi n}{3} \cos n\left(\frac{2\pi}{3} - \frac{\theta}{2}\right) \qquad (1)$$

Theoretical and experimental values of $\hat{v}_n/V_D$ are compared in Fig. 5 for the range of θ under consideration. This figure shows that the low-order harmonics, especially the second and fourth, can have relatively high amplitudes in the basic inverter waveforms.

2.2 *Behaviour of the delta inverter with inductive load*

The operation of the delta inverter with a purely inductive load is less straightforward. Load voltage is no longer determined solely by the transistor switching pattern, as with the resistive load, but also depends upon the time constant of the load. For a purely inductive load (infinite time constant), the delta inverter appears to have two modes of behaviour which depend upon the transistor ON times. The operation for $8\pi/9 \leqslant \theta \leqslant 4\pi/3$ is different from $2\pi/3 \leqslant \theta \leqslant 8\pi/9$, and the two are discussed seperately below.

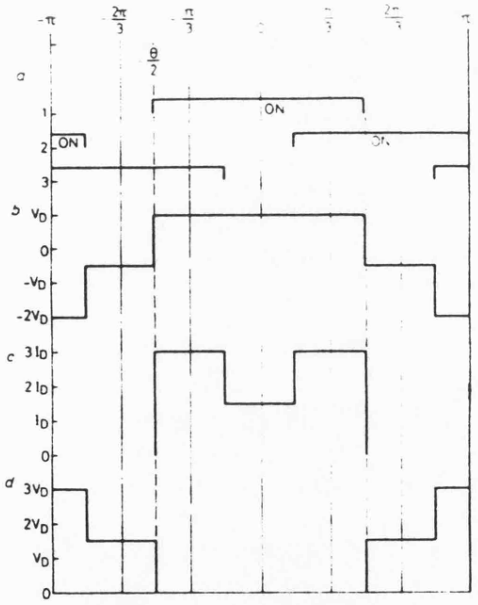

Fig. 3 *Behaviour of delta inverter with resistive load*

a Transistor switching sequence
b Phase *A* voltage
c Current in transistor 1
d Voltage across transistor 1

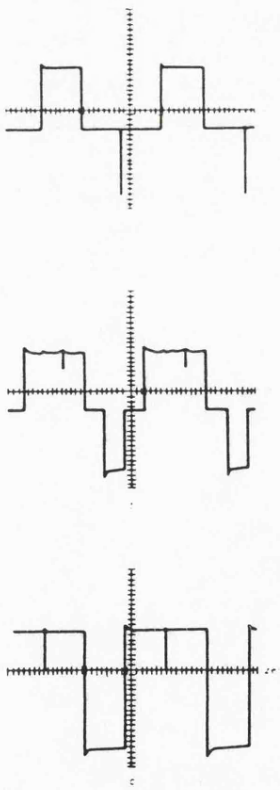

Fig. 4 *Phase voltage waveforms with resistive load*

(*a*) $\theta = 2\pi/3$
(*b*) $\theta = \pi$
(*c*) $\theta = 4\pi/3$

Voltage = 20 V/cm
Time = 2 ms/cm

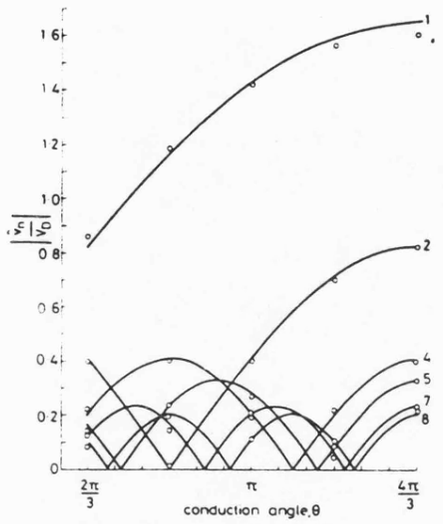

Fig. 5 *Harmonic content of phase voltage for range of conduction angles (resistive load)*

○ experimental results
– theoretical results

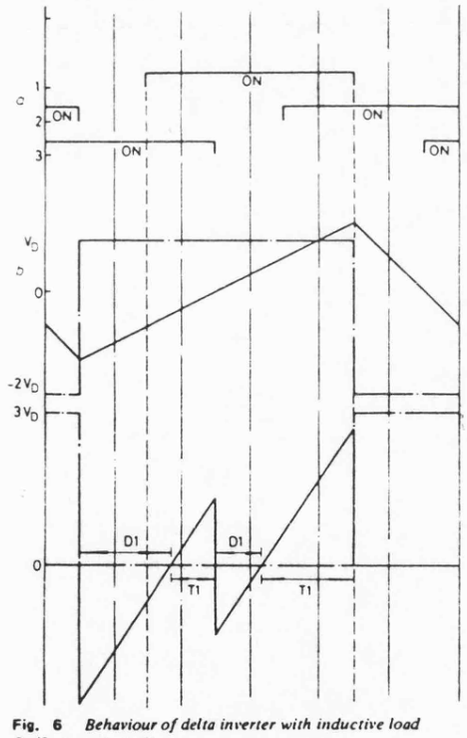

Fig. 6 *Behaviour of delta inverter with inductive load*
$8\pi/9 < \theta < 4\pi/3$

a Transistor switching sequence
b Phase voltage (– · –)
and phase current (———)
c Transistor and diode currents (———)
and transistor voltage (– · –)

2.2.1 $8\pi/9 \leqslant \theta \leqslant 4\pi/3$: For this range of conduction angles, the voltage and current waveforms do not change. They are illustrated for the case $\theta = \pi$ in Fig. 6. When transistor 1 turns off the forward current, it has been driving through phase *A* flywheels through the diodes of legs 2 and 3. The positive phase voltage is therefore $+V_D$ and negative voltage is $-2V_D$. Provided that $\theta > 8\pi/9$, the reverse voltage is held at $-2V_D$ by current flywheeling through the diode paths until *T2* and *T3* are both ON. The voltage is then held at $-2V_D$ by these two devices. When *T2* is subsequently switched OFF, phase *A* current flywheels through *D1*. This clamps phase *A* voltage at $+V_D$ and it is held at this value when *T1* is switched ON for the start of the next cycle.

The rates of change of phase current can be seen to be proportional to the phase voltage: this must be the case for an inductive load. The current rises linearly for two-thirds of the cycle under the effect of $+V_D$ and falls linearly at twice the rate against $-2V_D$ for the remaining one-third of the cycle. Under these conditions, the average energy dissipated in each phase inductance is zero. The corresponding transistor and diode currents are shown in Fig. 6*c*. This also indicates that the time-average battery power dissipated is zero. Oscillograms of transistor and diode currents and voltages are shown in Fig. 7. The traces in Fig. 7 differ to some extent from those derived for ideal

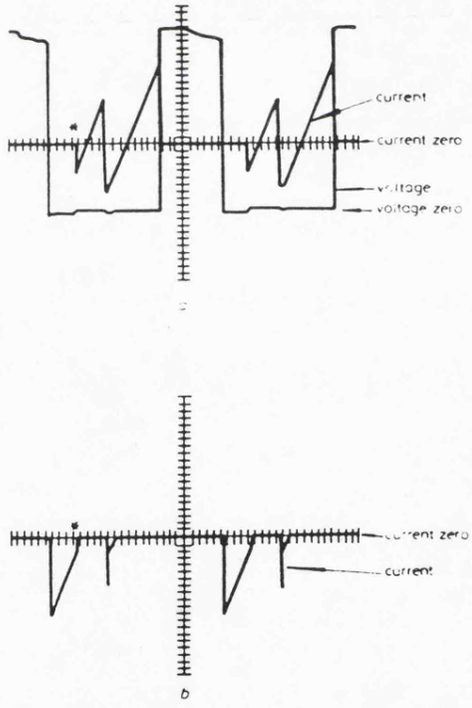

Fig. 7 *Transistor and diode performance with inductive load*

a Transistor
b Diode

Voltage = 20 V/cm
Current = 4 A/cm
Time = 2 ms/cm

devices in Fig. 6c. The first in each pair of triangular current pulses through the diode can be seen to be approximately correct. This occurs before the transistor has been turned on. The second in the pair is considerably reduced, however, as the transistor which has been turned on by this time appears to be carrying reverse current. This effect is explained in some detail in Appendix 8.1. It is not special to the delta inverter, however, and can occur in other circuits which contain the antiparallel arrangement of transistor and diode.

2.2.2 $2\pi/3 < \theta < 8\pi/9$: For this range of conduction angle, operation of the delta inverter is more complex, and the invariant current and voltage waveforms for the previous range are no longer maintained. Phase currents and voltages for the case $\theta = 7\pi/9$ are shown in Fig. 8. An explanation of them, which also makes reference to Fig. 2, is given below:-

(*a*) At point *p* in Fig. 8, transistor 1 switches off and phase *A* current flywheels through *D2* and *D3* for the period β. During this period, phase B current is rising linearly, flowing through *D2* and then *T2*, and phase *C* current is also rising linearly, flowing through *D3*.

(*b*) At point *q*, phase *A* current has reduced to zero and can no longer flow through *D2* and *D3*. However, the voltage across phase *A* remains clamped at $-2V_D$ because *T2* is on and because phase *C* current is still flywheeling through *D3*. The current through phase *A* must therefore continue to decrease at the same rate, thus becoming negative. This current is driven by *T2* during the period from *q* to *r* and the same current is driven through phase *C*. For angle γ, therefore, phase *C* current is made up of an increasing component through *T2* and a decreasing component through *D3*. (These compents are shown by fine dotted lines.)

(*c*) At point *r*, *T2* is providing all of phase *C* current. *D3* consequently unclamps and the voltages across phase *A* and phase *C* both change to $-V_D/2$. The currents through these phases therefore change at a correspondingly reduced rate during the period from *r* to *s*.

(*d*) At point *s*, *T3* switches on, thereby applying $-2V_D$ to phase *A* and causing $+V_D$ to appear across phase *C*.

(*e*) At point *t*, *T2* switches off and the sequence from *p* to *t* repeats itself with phase *B* taking the place of phase *A* and phases *B* and C being replaced by *C* and *A*, respectively. For these operating conditions, i.e. $2\pi/3 < \theta < 8\pi/9$, it can be shown that the angles α, β, γ and δ in Fig. 8*b* are related to θ by

$$\alpha = \frac{2}{9}\pi \tag{2a}$$

$$\beta = \frac{1}{2}\left(\theta - \frac{2}{9}\pi\right) \tag{2b}$$

$$\gamma = \frac{1}{2}\left(\theta - \frac{2}{3}\pi\right) \tag{2c}$$

$$\delta = \frac{16}{9}\pi - 2\theta \tag{2d}$$

Hence

θ	α	β	γ	δ
$\frac{1}{3}\pi$	$\frac{2}{9}\pi$	$\frac{1}{9}\pi$	0	$\frac{4}{9}\pi$
$\frac{7}{9}\pi$	$\frac{2}{9}\pi$	$\frac{1}{18}\pi$	$\frac{\pi}{18}$	$\frac{2}{9}\pi$
$\frac{8}{9}\pi$	$\frac{2}{9}\pi$	$\frac{2}{9}\pi$	$\frac{\pi}{9}$	0

Oscillograms of phase voltages and currents are shown in Fig. 9 for $\theta = 2\pi/3$, $5\pi/6$ and π.

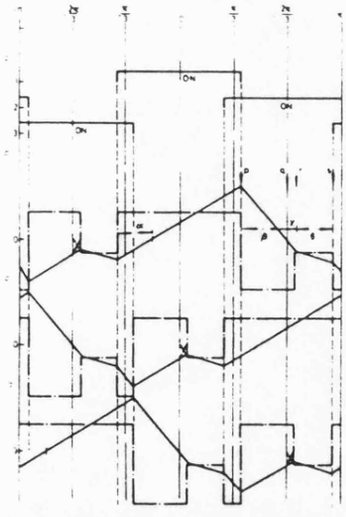

Fig. 8 *Behaviour of delta inverter with inductive load*
$\theta = 7\pi/9$

a Transistor switching sequence
b Phase A current (———) and voltage (– · –)
c Phase B current (———) and voltage (– · –)
d Phase C current (———) and voltage (– · –)

3 Comparison of bridge and delta inverters

3.1 Output waveforms

The main use of three-phase inverters is in motor drive systems. It is important therefore that the output waveform is low in unwanted harmonic components, as these increase the losses in the motor, without a commensurate increase in the net output power.

The voltage produced across the phase of a delta-connected load by a conventional bridge inverter is well known to be

$$V_{ph} = \frac{2\sqrt{3}}{\pi} V_B \left\{\cos(\omega t) - \frac{1}{5}\cos(5\omega t) + \frac{1}{7}\cos(7\omega t) - \frac{1}{11}\cos(11\omega t) + \ldots.\right\} \tag{3}$$

It is clear that this waveform contains no even or triplen harmonics. The first harmonic above the fundamental that occurs is the fifth. An induction motor will operate quite satisfactorily from this waveform. The main effect is that motor efficiency deteriorates by 5%-10% compared with that achieved from a sinusoidal supply, so that the motor has to be derated by the appropriate amount to ensure that its maximum rated temperature rise is not exceeded. However, the inverter waveform can be improved by the use of standard techniques such as sinusoidal pulse-width modulation. This removes or reduces prescribed harmonic components in order to improve motor efficiency.

The voltage waveform produced by a delta inverter for an inductive load $8\pi/9 \leq \theta \leq 4\pi/3$ can be shown from eqn. 3 to be

$$\dot{V}_{ph} = \frac{3\sqrt{3}}{\pi} V_D \{\cos(\omega t) - \tfrac{1}{2}\cos(2\omega t) + \tfrac{1}{4}\cos(4\omega t) - \tfrac{1}{5}\cos(5\omega t) + \ldots\} \quad (4)$$

Although the triplen harmonics are absent from this series, because of the balanced three-phase switching sequence, all other harmonics are present. It seems to be important therefore to improve the output waveform of the delta inverter before it is suitable for most drive applications. Standard techniques exist for achieving this. The most appropriate open-loop method is 'selective harmonic reduction', which was suggested by Turnbull[2] and has been extended by Patel and Hoft[3]. This technique requires the devices to be switched off at strategic points and for defined intervals during a cycle, in order to eliminate or reduce one or more harmonic components. An example of how this technique may be applied to the delta inverter is described as follows.

A motor load presents a substantially resistive impedance, but it also has an inductive component which controls its behaviour during the short modulating intervals. In conventional pulse-width modulation techniques, it is usual to relate the maximum length of the modulating intervals to the motor time constant. The behaviour of the delta inverter with an RL load that has a power factor of 0·8 at the fundamental frequency has therefore been examined. This precise load has been taken as a first-order approximation to a motor load. From Section 2.2, the basic voltage waveform is taken to be as shown in Fig. 6*b*. Switching the devices in the pattern shown in Fig. 10*a* produces the voltage waveform of Fib. 10*b*. The phase voltage during the modulating intervals is defined by the current paths through the flywheel diodes, as described in Section 2.2. The amplitude of the nth voltage harmonic, a_n, for the waveform shown in Fig. 10*b*, is given by

$$a_n = \frac{6V}{\pi n} \sin\frac{2\pi n}{3} \left\{1 - 4\sum_k \sin n\delta_k \sin n\left(\frac{2\pi}{3} - \alpha_k\right)\right\} \quad (5)$$

where there are k pairs of modulating pulses. For the example in Fig. 10, $k = 2$, and $\alpha_1 = 0{\cdot}44\pi$, $\alpha_2 = 0{\cdot}55\pi$ and $\delta_1 = \delta_2 = 0{\cdot}022\pi$. The effectiveness of this sample modulation in improving the voltage waveform is illustrated in

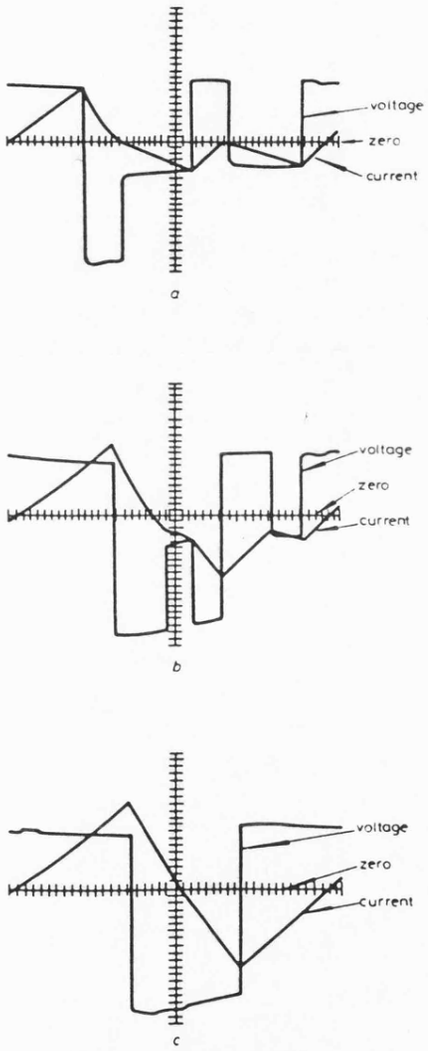

Fig. 9 *Phase voltage and current waveforms with inductive load*
(a) $\theta = 2\pi/3$
(b) $\theta = 5\pi/6$
(c) $\theta = \pi$
Voltage = 20 V/cm
Current = 2 A/cm
Time = 1 ms/cm

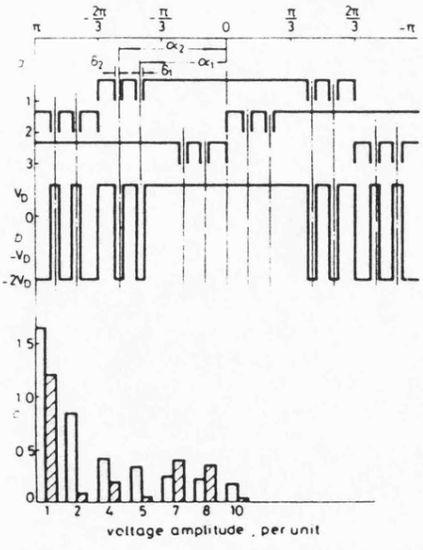

Fig. 10 *Effect of harmonic reduction technique*
a Transistor switching pattern
b Phase voltage
c Harmonic amplitudes

Fig. 10c. Although the amplitude of the fundamental also suffers some reduction, it can be seen that the second, fourth and fifth harmonics are substantially reduced. This method can be extended by incorporating many modulation intervals in the inverter waveform to eliminate or reduce the required number of harmonics. Taken to its limit, it can be seen that this method is not dissimilar to the so-called 'subharmonic' method of control.[4]

A second method of producing a near sinusoidal output from the delta inverter relies on closed-loop control. In essence, the output currents of the inverter are sensed and the inverter devices are switched according to a prescribed algorithm in order to maintain the output waveforms close to sinusoidal control signals. This is a well established method of control.[5] Its application to the delta inverter requires a switching algorithm for the three transistors which can be used to force two of the output currents to be sinusoidal. The third current then automatically takes the correct form for a balanced three-phase system. A switching algorithm which achieves this has been devised for the delta inverter.

It is clear that satisfactory operation of the delta inverter for motor-drive applications relies upon the use of efficient power transistors and compact and reliable control circuitry. Recent trends in the development of large transistors and microelectronics suggest that both of these are becoming more readily available.

3.2 *Installed power-transistor switching capacity*

The product of the total voltage and current ratings of devices required for an inverter gives some measure of the silicon cost for that inverter. The total transistor VA ratings for the bridge and delta inverters have therefore been compared. The comparison was made on the following basis:

(*a*) For each type of inverter the voltage rating is related to the battery voltage and is independent of the nature of the load.

(*b*) The output of a motor depends upon the real power delivered to it. The current rating of the devices was therefore fixed in terms of real power delivered to a resistive load.

These assumptions make the comparison necessarily approximate. However, the validity of the comparison is enhanced by the fact that the same assumptions have been made for both inverters.

Each transistor in the delta inverter has been assumed to be on for $\theta = 4\pi/3$. Both loads are delta-connected, R_D and R_B being the phase resistances for the delta and bridge inverters, respectively. The source connected to the bridge inverter has a voltage V_B, and V_D volts are connected in each of the three legs of the delta inverter. Calculations and results are given in Table 1.

On the basis of the above approximate comparison therefore, the total VA capacity of devices used in the bridge and delta inverters is the same. The delta inverter consequently has the merit of requiring half the number of power switches without requiring a greater total switching capacity.

3.3 *System considerations*

Some of the implications of using a delta inverter in a battery/inverter/motor system are described briefly as follows:

(*a*) *Motor:* there is no significant difference between the motor design for a bridge or delta inverter system; although naturally it must be wound for the appropriate voltage.

(*b*) *Inverter:* the delta inverter requires half the number of power transistors, flywheel diodes, heat sinks and base drives compared to a bridge inverter.

(*c*) *Battery:* three separate battery stacks are required for the delta inverter and this introduces extra complications. Battery wiring, filters and fuses are therefore increased threefold. Battery charging can however, be accomplished using a single charger provided that a three-way off-load isolator is incorporated in the system. If this is used to disconnect two of the motor leads and to break the delta inverter loop in one place, the three batteries can be charged as a single series stack, using the inverter flywheel diodes as connecting links.

An overall judgement of the delta inverter system therefore requires that the additional electromechanical complexities associated with the battery circuits are offset against the reduction in the components of the inverter circuit.

4 Behaviour of a delta inverter/induction-motor drive system

Some preliminary results have been obtained using a battery-fed delta inverter to drive a squirrel-cage induction motor. Tests were carried out with two transistor switching waveforms. First, with each device in the delta inverter conducting for two-thirds of a period (the Fourier series for the resulting voltage waveform, $\theta = 4\pi/3$, is given in eqn. 4). Secondly, incorporating two pairs of modulating pulses, precisely as illustrated in Fig. 10*b*, to obtain a reduction in unwanted voltage harmonics. The amplitudes of the voltage harmonics for the two waveforms are compared in Fig. 10*c*. The waveform in Fig. 10*b* was chosen to demonstrate that the principle of harmonic reduction can be applied to the delta inverter: it does not represent an optimised waveform.

Table 1: Comparison of total transistor *VA* ratings for bridge and delta inverters

	Bridge inverter	Delta inverter
1 R.M.S. fundamental phase voltage	$\frac{\sqrt{6}}{\pi} V_B$ (eqn. 3)	$\frac{3\sqrt{3}}{\sqrt{2}\pi} V_D$ (eqn. 4)
2 R.M.S. fundamental phase current	$\frac{\sqrt{6}}{\pi} \frac{V_B}{R_B}$	$\frac{3\sqrt{3}}{\sqrt{2}\pi} \frac{V_D}{R_D}$
3 Total power delivered to load	$3\frac{6}{R_B}\left(\frac{V_B}{\pi}\right)^2$	$3\frac{27}{2R_D}\left(\frac{V_D}{\pi}\right)^2$
4 Minimum transistor voltage rating	V_B	$3V_D$ (Fig. 3)
5 Minimum transistor current rating	$\frac{2V_B}{R_B}$	$\frac{3V_D}{R_D}$ (Fig. 3)
6 Total installed *VA* rating of transistors	$6\frac{2V_B^2}{R_B}$	$3\frac{9V_D^2}{R_D}$
7 Total transistor rating / Load power (line 6 ÷ line 3)	$\frac{2\pi^2}{3}$	$\frac{2\pi^2}{3}$

The results of the tests, using 36 V per inverter leg and a frequency of 50 Hz, are shown in Fig. 11. It can be seen that, as with conventional induction motor/inverter systems, the delta inverter is capable of returning generated power for the induction motor to the d.c. source.

The efficiency of the system when the transistor conduction angle $\theta = 4\pi/3$ can be seen to be poor – the overall system efficiency from batteries to motor shaft has a maximum value of around 40%. Incorporating the two pairs of modulating pulses in the switching waveform, however, boosts the system efficiency to 60%. The overall efficiency of the same induction motor with a conventional bridge inverter was around 70%. It seems possible therefore, that optimisation of the switching strategy for the delta inverter will enable an acceptable system efficiency to be achieved. This work is in progress.

Current waveforms obtained during the tests described above are illustrated in Fig. 12. A substantial improvement in the current waveform by the use of modulating pulses is evident.

5 Conclusions

The delta inverter appears to be a novel circuit and has features which make it an attractive proposition for some applications. In particular, its reduced component count should lead to lower manufacturing costs and improved reliability. Reservation about the reliability of solid-state controllers is one of their main drawbacks at the present time, and to be able to halve the number of devices in a circuit should make a real improvement in this area. A regenerative chopper for a d.c. machine (with a commutator) needs two main power switches. The delta inverter requires just one more to be able to accomplish motoring and regenerative control for a brushless a.c. machine.

Section 2 has described in some detail the basic behaviour of the delta inverter with passive resistive and inductive loads. This provides an introduction to the operating principles of a new circuit. Sufficient understanding can be gained from it to be able to approach the problem of driving more complex loads.

The 'raw' output waveform of the delta inverter has been shown to contain more harmonics than the conventional bridge inverter. Standard techniques exist to reduce the harmonic content of an inverter waveform and one example of how this may be achieved was given in Section 3. Preliminary results for a delta inverter/induction-motor drive system were presented in Section 4. They suggest that an acceptable drive system can be developed.

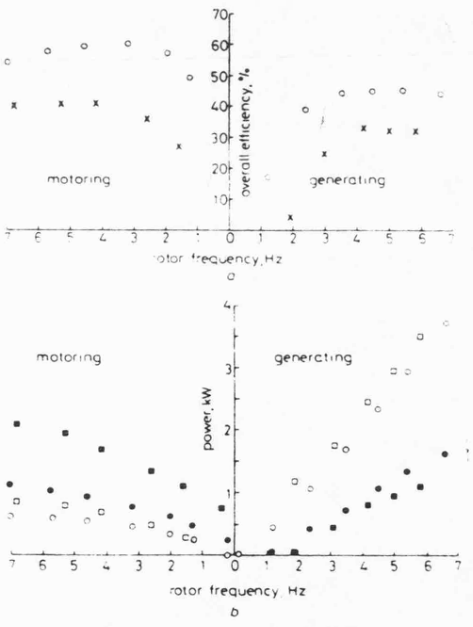

Fig. 11 *Performance of delta inverter/induction motor system*

a Overall system efficiency
X conduction angle = $4\pi/3$
conduction angle = $4\pi/3$, plus modulating pulses

b Mechanical and electrical power characteristics

	Conduction angle = $4\pi/3$	
	without modulating pulses	with modulating pulses
Mechanical power	○	○
Electrical power	■	●

6 Acknowledgments

The authors would like to thank KGEL for funding the work described in this paper. Thanks are also due to J. McCaig of the Electrical Engineering Workshop at the University of Bath, and B. Bowyer, each of whom helped with the construction of the prototype inverter.

7 References

1 EASTHAM, J.F.: British Patent Application 29692/75
2 TURNBULL, F.G.: 'Selected harmonic reduction in static d.c.-a.c. inverters', *IEEE Trans.*, 1964, CE-83, pp. 374–378
3 PATEL, H.S., and HOFT, R.G.: 'Generalised techniques of harmonic elimination and voltage control in thyristor inverters: Part I - harmonic elimination', *IEEE Trans.*, 1973, IA-9, pp. 310–317
4 SCHONUNG, A., and STEMMLER, H.: 'Static frequency changers with 'subharmonic' control in conjunction with rever-

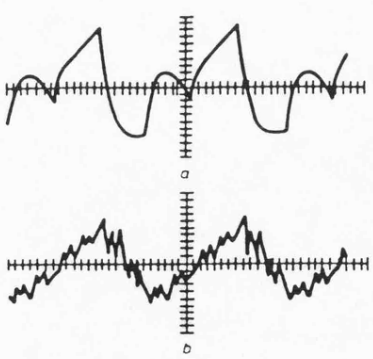

Fig. 12 *Motor current*

a Conduction angle = $4\pi/3$
b Conduction angle = $4\pi/3$, plus modulating pulses

Current = 40 A/cm
Time = 5 ms/cm

sible variable speed a.c. drives', *Brown Boveri Review*, August/September 1964, pp. 555–577
5 DANIELS, A.R., and SLATTERY, D.: 'Class ABD amplifier', *Electron. Lett.* 1974, 10, (17), p. 364

8 Appendix

8.1 Explanation of reverse transistor currents

The equivalent circuit in Fig. 13 illustrates the base drive supply, the driver and output devices of the monolithic darlington transistor and the flywheel diode. These comprise one antiparallel transistor-diode pair.

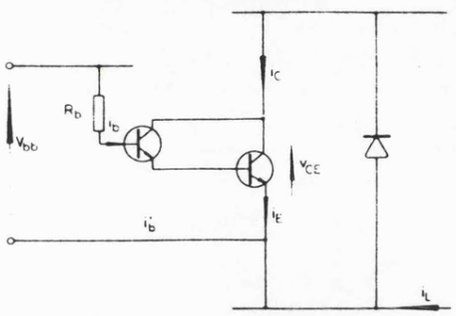

Fig. 13 *Equivalent circuit of antiparallel transistor-diode pair*

The period under consideration is when the transistor is ON, i.e. base current is flowing, but there is no forward collector current: the inductive load current i_L requires a flywheel path through the antiparallel pair. One such period starts at time * in Fig. 7.

Initially V_{CE} is positive, so that the diode is reverse biased. As i_L rises, i_E reduces so that i_B remains constant at a value defined by

$$i_B = \frac{V_{bb} - 2v_{be}}{R_b} \tag{6}$$

Therefore i_L contributes to i'_B at the expense of i_E, and the surplus component of i_B flows to the collector, forward-biasing the base collector junction of the driver transistor.

During this stage, when i_L is less than i_E, the two base emitter junctions and the base collector junctions are forward biased, resulting in a net positive collector emitter voltage of around 0·7 V.

The oscillograms of Fig. 7 were taken with load currents that were of the same order of magnitude as the base drive capability of the large power transistor. It was under these conditions that a reverse transistor current and a positive collector emitter voltage were observed.

When i_L exceeds i_E, the base emitter junctions cease to be clamped on, and the base current, all of which is now flowing to the collector, increases in order to supply the rising load current i_L. When the base current reaches a value defined by

$$i_b = \frac{V_{bb}}{R_b} \tag{7}$$

the collector emitter voltage is reversed to the extent of one forward junction voltage due to the base collector junction. The main flywheel diode consequently becomes forward biased and carries all further increase in i_L. However, the base drive continues to contribute to the load current to the extent defined by eqn. 7.

APPENDIX 2

IEE Proceedings
Vol.129, Part B, No.3, May 1982
Electric Power Applications

Discussion on Delta Inverter

Discussion on

Delta inverter

D.M. Brooks *(GEC Traction Ltd.):* I would like to begin by congratulating the authors on producing an excellent and stimulating paper on this novel form of inverter. To build a 3-phase inverter based on the use of only three switchable unidirectional devices would seem to be impossible; yet here it has been done.

The paper describes how the voltage waveform can undergo a sudden step change for certain conduction angles when the inverter is supplying an inductive load and, therefore, I wonder whether the PWM version could also have a sudden step change in voltage as the inductance of the load changed. I would also like to have the authors comments on whether or not the pulse-width modulation of the delta inverter needs to be done at a higher chopping rate than normal, in order to remove the asymmetry of the basic voltage waveform of the delta inverter.

G.A. Fisher *(British Rail Research):* This is a most interesting paper, showing an ingenious and novel inverter configuration which requires only three active or inverting switches. Compared with a bridge inverter drive where, generally, the cost of the power electronics far exceeds the cost of the motor(s), the delta inverter offers potential savings, especially for lower voltage and power applications. British Rail, in these costs-conscious times, is keen to see the development of cheaper power electronics for traction and for auxiliaries.

The authors' subsequent results with sine-wave PWM techniques are encouraging and demonstrate more of the delta inverter's potential.

In certain applications, the provision of three virtually isolated equal power supplies for a delta inverter may be uneconomical. I would like to suggest the following as a possible way of using one supply and transferring isolation to the load.

120° single-supply delta inverter with unipolar current

The circuit for up to 120° conduction is shown in Fig. A. The main switches (TR1–3), shown as transistors, are switched in sequence; for example, TR1, X, TR2, X, TR3, X, TR1 etc., where X denotes all switches off.

The case of 120° conduction, where there is always one transistor conducting and 'X' disappears from the sequence, is outlined below. When TR1 is on, TR2 and 3 being off, the supply V_D is impressed on the primary of phase A. The delta connection of the secondaries causes $-V_D$ to be impressed across phases B and C in series, which, for an 'ideal resistive load', gives $-V_D/2$ on each phase. This ideal waveform is given in Fig. B(i).

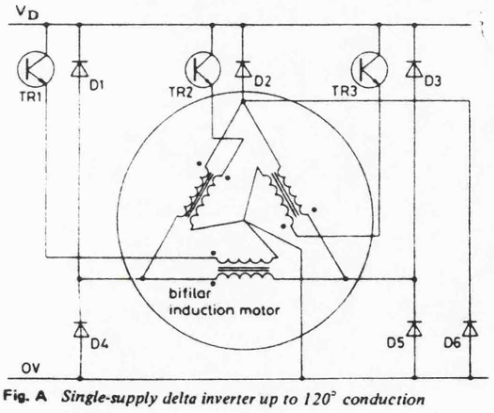

Fig. A *Single-supply delta inverter up to 120° conduction*

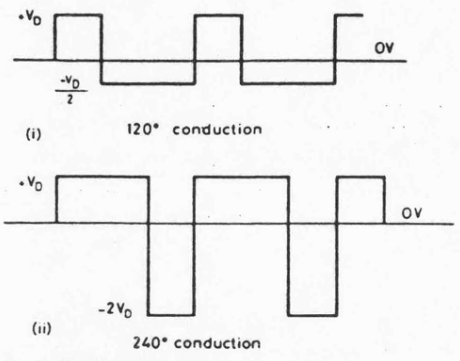

Fig. B *Idealised phase voltage*

240° single-supply delta inverter with unipolar current

The circuit is shown in Fig. C, in which diodes (D1–3) are replaced by thyristors (CSR1–3). The main switches and thryristors are sequenced as follows: TR1 + CSR1–3, TR1 and 2 + CSR3 and 1, TR2 + CSR1–3, TR2 and 3 + CSR1 and 2, TR3 + CSR1–3, TR3 and 1 + CSR2 and 3 etc., the thyristors being fired, but not necessarily conducting because of the direction of load current. This allows the voltage applied to the windings to be effectively doubled. The ideal waveform for resistive loads is shown in Fig. B(ii).

It should be noted that CSR1–3 and D4–6 form a rectifying bridge and not an inverting bridge. Consequently, the thyristors do not require forced commutation. This bridge should handle reactive and regenerative power.

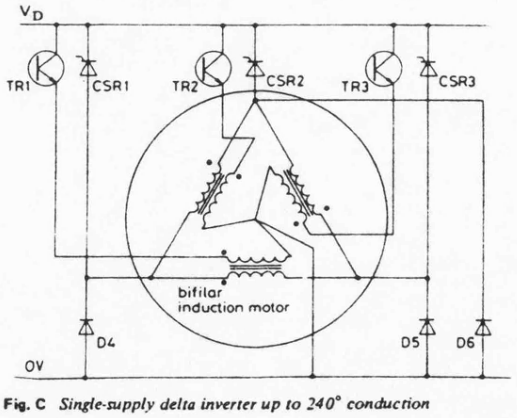

Fig. C *Single-supply delta inverter up to 240° conduction*

Comparative characteristics of single-supply delta inverter

(i) Only one supply is required

(ii) ripple current drawn from the supply will be at a higher frequency and of a lower RMS value

(iii) all the semiconductors have one terminal connected to a supply pole, so that only two isolated heatsinks are required. (It may be more convenient to replace D4–6 rather than D1–3 with thyristors. The circuit will still operate)

(iv) the motor, as shown, would be more expensive and have greater losses

Paper 955B by EVANS, P.D., DODSON, R.C., and EASTHAM, J.F. [See *IEE Proc. B, Electr. Power Appl.*, 1980, 127, (6), pp. 333–340.] Read before IEE Power Division Professional Group P6, 6th October 1981

(v) leakage between bifilar windings has a significant effect on detailed circuit design and cost

(vi) one inherent advantage of having leakage is the limit to the rate of rise of fault current

(vii) normal 3-phase loads, e.g. standard induction-motor or resistive load, may be coupled to the inverter via a bifilar transformer. This has been reported earlier [A]. The transformer should have lower leakage and permit the voltage to be stepped up or down if required. Isolation, using tertiary (non-bifilar) winding, is easy

(viii) instrumentation and control should be easier with a single supply.

Leakage inductance

The energy stored in leakage inductance is unlikely to be insignificant, and a more thorough appraisal of the problems is required. Bifilar winding should reduce the problems to a manageable level.

PWM delta inverters

The results for PWM, described at the meeting (to be the subject of a future paper), showed that, when compared with a bridge inverter operating at the same chopping frequency, the delta inverter produces higher ripple. I believe this arises because the delta inverter imposes V_D, $-V_D/2$ or $-2V_D$ on the motor windings but never zero. I should like to suggest the following adaptation, which permits the output line voltages to be zero.

By connecting the motor terminals to each other, via three thyristors arranged cyclically, then, when all the main switches are off, firing of the thyristors will short-circuit the motor, all main switches being off. Normally, the thyristors will be forward biased and only these will conduct. Commutation may be achieved by appropriate sequencing of the inverting (transistors) switches. This adaptation should apply to the basic delta inverter and the single-supply configurations where the thyristors may be connected to any of the sets of windings.

I should be grateful for the authors' comments on these ideas.

C. Oates *(GEC Rectifiers Ltd.):* Three main comments are given.

History

To demonstrate the point that there is nothing in the world that is new, the English Electric Company, Stafford, used the delta inverter circuit form in 1963 for the Appleby Frodingham steel rolling mill. The scheme was used for a low-frequency motor drive and would have been one of the last contracts to still use mercury arc rectifiers (contract AEM4060, shown on drawing S5500 13877). There was concern at the time over the presence of circulating currents in the load and the schemes were not reused.

DC currents

If a purely inductive load is considered with switching at π radians, the following results shown in Fig. D can be obtained:

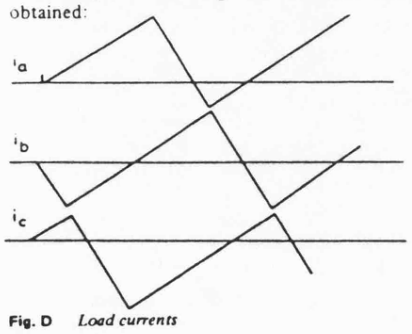

Fig. D *Load currents*

The disparity in the DC levels between phases A and C is equal and opposite and related to the starting conditions. Since this is not present for a resistive load, it is to be expected that, under steady state conditions on an LR load, it would decay away with the time constant L/R. Tracing the case for the inductive load through to the currents in the transistors, we have the situation shown in Fig. E.

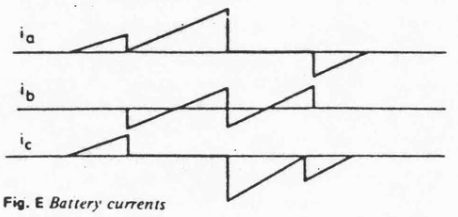

Fig. E *Battery currents*

From this, it can be seen that there is an instant when one transistor and one diode is taking twice the current that one would expect in the steady state.

Since, in the steady state, these will settle down, owing to any resistance present, in the transient conditions one would expect in servomotor control, would changing modulation patterns, frequency etc. be likely to create problems?

Harmonics

In Fig. 10 of the paper, the pattern of the modulating waveform is symmetrical about 0°. This is to be expected when cancelling odd harmonics; however, to cancel even harmonics, it might be expected that some asymmetry is required. It is interesting to note that the waveform shown in Fig. 12*b* is similar to that shown for the purely inductive case, and thus it is suggested that some of the improvement demonstrated is caused by the increased frequency of modulation rather than any harmonic cancellation principles.

H.R. Bolton *(Imperial College, London):* Any suggestion for reducing inverter complexity is valuable and is worth investigating fully. The authors are to be congratulated on a paper which, in my view, is comprehensive, objective and concise. Their Table 1 makes the point that the total VA transistor rating per output kW for the delta inverter is identical to that of the standard bridge inverter. Some readers might feel put off the delta inverter by the apparent need for devices of triple voltage rating for given rail voltage, so I would think that the authors should reinforce the point that for the delta inverter, if one uses the original battery stack divided into three portions, the device voltage rating required is, of course, no greater. The device current rating, in this case, is doubled and, in this and similar cases, the authors would certainly seem justified in claiming an advantage for the delta inverter with its halved device count. If one compared inverters with V_D comparable to V_B, would the present cost penalty on high-voltage devices perhaps tend to more than offset the benefits?

Even-order harmonics can be a nuisance. The second and fourth time harmonics set up fields whose speeds are rather low compared with the usual harmonic fields encountered, and the corresponding harmonic torque contributions will tend to be correspondingly more significant. Have the authors considered the use of the delta inverter with reluctance and synchronous machines? If autopiloted, conductor work (dampers) can often be omitted, and time harmonics do not then give rise to significant loss, at least in the rotor.

P.D. Evans, R.C. Dodson and J.F. Eastham *(in reply):* We thank Mr Brooks for his introductory comments and for his contribution to the discussion. The 'step change' to which he draws attention, which appears in Figs. 8 and 9 of our

paper, occurs with inductive loads when the conduction angle of each device is less than 160°. This condition produces significant portions of each cycle when only one device is conducting, so that the three voltages are not defined by the control signals but depend on diode conduction paths. The method of sinusiodal pulse-width modulation relies on the fact that two devices are switched on at all times, so that the three output voltages are completely defined by the switching signals. Under these conditions, therefore, we would not expect to experience step changes and have, in fact, not done so in our experimental work.

Mr Brooks is largely correct in thinking that the delta inverter theoretically requires a higher chopping rate than normal to remove the inherently greater asymmetry of the basic waveform. We have found, however, that satisfactory performance can be achieved by using chopping frequencies which are within the normal practical range. For example, if

$$\sqrt{\sum_{n=1}^{\infty}\left(\frac{V_n}{n}\right)^2}$$

is used as a figure of merit – it is representative of the RMS harmonic current – then, for 50 pulses per cycle (2.5 kHz switching frequency for 50 Hz fundamental), this figure of merit is around 1% for a conventional bridge inverter with double-edge sinusoidal modulation and just under 3% for the delta inverter with single-edge modulation.

We would like to thank Mr Fisher for his kind comments and are pleased that he supports our view that efforts should be made to reduce the complexity of the solid-state controllers for AC drives.

Our general view is that a 3-phase inverter supply can be produced, either by the conventional and well established bridge inverter which uses a single DC supply and six controlled devices, or by the delta inverter which uses three DC supplies and three controlled devices, or by a single-supply, 3-device, centre-tapped winding arrangement. The conventional bridge inverter has many advantages and is well established for mainstream applications, but it was thought to be important, at the present stage in the development of power electronics, to evaluate the last two alternatives. After a preliminary consideration of them, we postponed the study of the centre-tapped version in favour of the delta inverter under discussion, and we hope that this has now been brought to a stage at which informed evaluation of it can be made.

Mr Fisher's suggestions for arrangements using centre-tapped windings are fascinating, but we hesitate to comment critically on them without a very detailed study. We agree with his willingness to mix power transistors and naturally commutated thyristor in a circuit, because there is a general tendency to treat them as mutually exclusive alternatives. We have two main reservations on the use of centre-tapped windings. First, if the windings are bifilar wound in order to minimise leakage inductance between them, it is difficult to provide secure and reliable insulation between them. If, however, they are wound separately, in order to provide good separation, then their leakage inductance increases significantly. Secondly, the operation of an inverter circuit in a pulse-width-modulation mode with centre-tapped windings is not altogether straightforward. This, we believe, would constitute an important area of study in an investigation of this type of circuit.

Concerning the use of thyristors to provide a zero voltage condition, this amounts to the provision of controllable freewheel diodes which bypass the power supplies. We have not tried this experimentally, but it appears to be a method of reducing the motor-current ripple.

We thank Dr. Oates for his contribution. As we understand it, the 'inverter' for the Appleby Frodingham steel rolling mill was a phase-controlled type of circuit – a cycloconvertor – producing a low-frequency supply. In this respect it appears to belong to the class of delta-connected AC voltage controllers, some of which are described by Dewan [B].

The transient conditions described seem to be the standard type. In a workable control system for the delta inverter, such as the sinusoidal pulse-width modulation we have described, two devices are on at all times. This defines the three output voltages and the currents are therefore correspondingly defined.

The fact that switching one device affects two voltages, and the need to retain 3-phase symmetry, places some constraints on the pulsing pattern to achieve harmonic cancellation. The pattern suggested in Fig. 10*a* of our paper contains some compromise on these requirements and provides the reduction in even harmonics illustrated in Fig. 10*c*.

The relationship between the current waveform in Fig. 12*b* and the inductive current waveform is not thought to be direct. More important is the comparison between the current waveform in Fig. 12*a*, obtained with an induction motor, with no harmonic reduction, and that in Fig. 12*b* with the induction machine under the same conditions, but with the harmonic cancellation described in Fig. 10.

We would like to thank Dr. Bolton for his comments on our paper, and for clarification of the point about the required device voltage rating. Power semiconductor devices are at a relatively early stage in their development and we hesitate to comment on their economics because they are changing rapidly.

Although we have not investigated the possible use of the delta inverter with reluctance or synchronous machines, we are inclined to agree with Dr. Bolton that optimisation of their behaviour using the harmonic components of an inverter supply is an interesting and possibly fruitful area of work.

References

A YAIR, A., and BEN-URI, J.: 'New 3-phase invertor with three thyristors', *Proc. IEE*, 1971, **118**, (7), pp. 901–905

B DEWAN, S.B., and STRAUGHAN, A.: 'Power semiconductor circuits' (Wiley, 1975)

DC111 B

APPENDIX 3

Proceedings
Europe's International Conference on
Electric Road Vehicle Systems
"Drive Electric Amsterdam 82"
Amsterdam 25-28 October 1982

Paper Entitled

"The Delta Inverter"

by P.D. Evans, R.C. Dodson and J.F. Eastham

THE DELTA INVERTER

P D Evans, R C Dodson & J F Eastham, University of Bath, Bath, BA2 7AY UK

ABSTRACT
The paper compares briefly a.c. and d.c. drive systems for electric vehicles in order to emphasise that it is difficult to benefit from the clear advantages of a.c. machines over d.c. machines because of the more complicated power controller required for variable frequency a.c. control. A three-phase inverter consists essentially of three regenerative choppers.

An examination of alternative three phase inverter configurations is shown to reveal two alternative circuits each of which only requires three main power semiconductor devices. One of them, the delta inverter, is described in some detail and its general performance and method of control is explained. It is shown that satisfactory operation in a motor drive system can be expected.

INTRODUCTION

Most existing systems for electric and hybrid vehicles utilise d.c. motors to produce the motive power from the battery energy source. The main reason for this is that the solid state power controller - usually some form of chopper - is a relatively simple arrangement. The basic chopper requires one main power switch, shown as a power transistor in Figure 1(a), and a regenerative system which allows energy to be returned to the battery requires two main devices, as shown in Figure 1(b). The d.c. machine can therefore operate at full output when connected directly to the battery via the solid state switch. Smooth and reliable variable speed operation is also possible by varying the average value of voltage applied to the motor by means of the time-ratio control action of the chopper.

The solid state controller for a d.c. machine is therefore a simple and effective item of equipment. It is generally recognised, however, that an a.c. machine, especially a squirrel cage induction motor, would be preferable to a d.c. machine. There are a number of reasons for this:

- Induction motors are invariable smaller, lower cost machines. It is thought particularly that d.c. machines do not lend themselves to mass production techniques, whereas induction motors, and solid rotor synchronous machines, are cheaper options which would respond to automotive production methods.

- The induction motor requires less maintenance than a d.c. machine, mainly because of the absence of brushgear and commutator. (In view of the generally short operating life of a vehicle it is possible, however, that d.c. machine design practice, which is accustomed to meeting the long term operational requirements of industrial applications, can readily provide high reliability and low maintenance schedules.)

- Induction machines, having simple, strong rotors can operate at high speeds, thereby enhancing power to weight ratio. Operation up to 6000 rpm or so is simple to achieve and allows existing automotive gearboxes to be used. Although

the optimum overall economic arrangement is difficult to predict it has been suggested (1) that speeds in the range 10,000 rpm to 15,000 rpm are advantageous. In this context some synchronous machine designs have been proposed (2) for high speed operation. In these machines both the field and a.c. windings are stationary and the rotor is a passive steel member. A disc-geometry version of this machine allows the rotor to be attached permanently to the mechanical transmission system and the stator to be a stationary bolt-on unit.

- The a.c. system is possibly safer under fault conditions because any controller failure diminishes the output of an a.c. machine. If the main device of a chopper switches on and latches on when not so required however, then full torque is produced by the d.c. motor.

- It is probably simpler to improve the overall operating efficiency of an a.c. motor than it is for a d.c. machine. This is of particular importance in battery electric vehicles where savings in battery weight (or alternatively increased range) can be directly offset against the cost of higher efficiency machines.

The power controller for an a.c. machine is, however, a much more complex piece of equipment than a d.c. controller. This is because it has to convert the d.c. battery output to an a.c. supply. The a.c. supply must have a variable frequency so that variable speed is possible and the a.c. voltage must also change, maintaining the voltage/frequency ratio approximately constant in order that the rated flux loading of the machine is used over the full speed range. In addition, the a.c. supply so produced must approximate closely to the sinusoidal in order that motor efficiency is not adversely affected.

The conventional circuit for this type of power conversion is the three phase bridge inverter, illustrated in Figure 2. The greater complexity of the a.c. controller is clear, by comparison with Figure 1: it consists essentially of three regenerative choppers. The inverter therefore, with all the associated equipment such as base drives, power supplies and control and protection circuits, is a relatively complex piece of equipment. Apart from its high cost, it is also difficult to achieve high reliability.

The "delta inverter" (3), the subject of the present paper, arose from an attempt to reduce the cost and complexity of a.c. controllers. The general configuration of the delta inverter is shown in Figure 3. It can be used to produce a three phase, variable voltage, variable frequency supply suitable for an a.c. machine. As can be seen, it requires half the number of main components of a bridge inverter - three instead of six, and being an a.c. controller operates naturally in the regenerative mode. This type of a.c. power controller therefore only requires one more device than a regenerative d.c. system.

ORIGINS OF DELTA INVERTER CIRCUIT

The basic 'building blocks' for the most common forms of power controllers are suggested in Figure 4. Figure 4(a) is a step-down chopper; Figure 4(b) is a step-up chopper; and Figure 4(c), which is a combination of (a) and (b) is the regenerative chopper. Two

regenerative choppers make up a single phase inverter and, as already stated, three of them constitute the three phase inverter.

The delta inverter owes its origin to different building blocks however, and these are perhaps less well known. They are illustrated in Figure 5. In Figure 5(a) energy transferred from the battery source to the load when the power switch is ON, flywheels into a separate battery when the switch is OFF. The mutual arrangement of three such circuits enables bidirectional currents to be controlled through a three phase load, as shown in Figure 5(b). It can be seen therefore that the delta inverter is of a different type to conventional circuits and consequently has different operating characteristics and control requirements. It can also be seen how the three isolated d.c. sources act together with the three power switches. While the requirement for three isolated d.c. sources is not usually convenient for conventional mains-fed systems, for battery systems the stack can be subdivided into three separate sections. Figure 5(c) shows a further development, however, in which coupled windings are used so that a modified building block is produced which now requires only one battery source. For a motor drive, therefore, if centre tapped windings are used, a system appears which retains the benefit of three main switches and also requires one battery supply. Some preliminary work on this type of system has been published by Yair and Ben Uri (4).

OPERATION, CONTROL AND PERFORMANCE

The method of operation of the delta inverter is not straightforward, primarily because the change in state of one power switch can alter two output voltages. However, if attention is limited to the condition when two devices are ON at all times, ie each device is ON for two thirds of a cycle, then the three output voltages are fully defined at all times. Under these conditions when T1, say, is ON then the output voltage V_{RY} is equal to $+V_S$, when T2 and T3 are ON, then V_{RY} is equal to $-2V_S$. The switching pattern and the output voltages for these conditions are shown on Figure 6. The Fourier series which describes this voltage waveform can be shown to be:

$$V_R = \frac{3\sqrt{3}}{\pi} \cdot V_S \cdot \cos(\omega t) - \tfrac{1}{2}\cos(2\omega t) + \frac{1}{4}\cos(4\omega t) - \frac{1}{5}\cos(5\omega t) + \ldots$$

or, expressed in another way, the amplitude of the nth harmonic present in the waveform is given by:

$$a_n = \frac{6V_S}{\pi n} \sin\frac{2\pi n}{3}$$

This shows that the natural output waveform of the delta inverter is rich in harmonics. Both odd and even harmonics are present. Only harmonics which are multiples of three are absent, a consequence of the three phase switching pattern. In this respect the delta inverter compares unfavourably with the bridge inverter. The harmonics present in the "quasisquare" output of a bridge inverter are in the series:

$$1, \quad 5, \quad 7, \quad 11, \quad 13, \quad \ldots\ldots 6k \pm 1 \ldots\ldots$$

The waveform shown in Figure 6, the natural output of the delta inverter, has been found to be unsatisfactory for an efficient motor drive system. An overall efficiency of around 40% was recorded on a small prototype system.

However, a number of techniques exist by which waveforms can be improved, and one such method has been applied successfully to the delta inverter. A modified form of sinusoidal pulse width modulation has been implemented, which enables a high waveform quality to be achieved.

The principles behind the use of sinusoidal pulse-width modulation with the delta inverter are of some interest. In the first place, as described above, if two devices are ON at all instants in time (neglecting for present purposes the safety zones during switching of devices) then all three output voltages are completely defined. Secondly, if two of the output voltages are modulated so that they constitute two phases of a three phase set, the resulting third output voltage must be the third member of that set. Briefly, therefore, during the ON time for each device, as defined in Figure 6, each device is switched to produce a sinusoidally pulse-width modulated pattern corresponding to its part of a three phase set. During the time when it would be OFF, according to Figure 6, it can be switched ON if either of the other two devices is OFF, in order to ensure that two devices are always ON.

This method was implemented on a 0.75kW prototype system, using single edge modulation and was found to operate very successfully. For convenience, a microprocessor was used to generate the switching control signals. The effectiveness of this sinusoidal pulse width modulation was checked by direct comparison with a mains-derived sinusoidal waveform. An induction motor was operated under equivalent conditions with both supply systems and its temperature rise was monitored. (Measurement of motor loss in terms of temperature rise was thought to be more reliable and direct than by calculation of efficiency from the measurement of input and output powers.)

It was found with these tests that motor temperature rise was approximately 10% higher with the inverter supply than with the 'ideal' sinusoidal supply. This was thought to be an encouraging result, and further improvement is likely to be possible. It means that motor loss is around 10% greater. In terms of efficiency this means that a motor efficiency of, for example, 80% would be degraded to 78%.

Motor currents produced during the inverter-fed tests were typical for this type of supply. They consisted essentially of a three phase fundamental set on which was superimposed a ripple at the switching frequency.

SYSTEM CONSIDERATIONS

It has been established above that the delta inverter can be controlled in such a way that satisfactory motor performance is possible. From a system point of view, however, the great simplification in the power semiconductor equipment that the delta inverter offers must be balanced against some additional complications it introduces. Some of the more important of these are discussed briefly below:

(i) Battery Wiring. The need for three battery sections increases the power cabling connected with the battery stack.

(ii) Battery Charging. Although the delta inverter itself can presumably be used as a battery charger from a three phase supply of suitable voltage rating a simpler solution is also possible. This requires the motor to be disconnected from the inverter (or at least, two of the motor cables) and for the delta inverter loop to be broken in one place. All three batteries can then be charged in series, via the flywheel diodes.

(iii) Filters. Three filters are required, one for each battery section, in order to reduce supply impedance and to smooth out the current demand from the battery.

The main problems introduced by the delta inverter are therefore of a conventional nature and the net benefits, or otherwise, of the delta scheme depend upon an overall system assessment which includes these effects.

CONCLUSIONS

The complexity of inverters has to a large extent prevented the inherent advantages of induction machines over d.c. machines being exploited, especially in electric vehicle drive systems. An investigation of alternative solutions has shown that there appear to be three basic methods by which a variable-voltage, variable frequency three phase supply can be produced. The first uses the conventional bridge inverter which requires a single battery stack and six main power devices. The second is the delta inverter which requires three main devices but three battery sections. Both these methods operate with standard types of motor. The third appears to permit the use of three devices with a single stack providing a special machine with centre-tapped windings is used. The design of conventional inverters is relatively well known and the work described in the present paper now enables the delta inverter to be evaluated and compared in overall system studies. Although some preliminary work has been reported on the third system, further study would be required before a full evaluation of its operation and control can be made.

ACKNOWLEDGEMENTS

The authors would like to thank KGEL Ltd, Coldharbour Farm, Goring Heath, Reading, RG8 7SY, England, for funding the research described in this paper.

REFERENCES

1. Agarwal, P D and Levy, I M: "A High Performance A.C. Electric Drive System", Paper 670178, Automotive Engineering Congress and Exposition, Detroit, Michigan, USA, January 1967.

2. Evans, P D and Eastham, J F: "Disc Geometry Homopolar Sychronous Machine", IEE Proc., Vol.127, Pt.B, No.5, September 1980.

3. Evans, P D, Dodson, R C and Eastham, J F: "Delta Inverter", IEE Proc., Vol.127, Pt.B, No.6, November 1980.

4. Yair, A and Ben-Uri, J: "New 3-Phase Inverter with Three Thyristors", Proc.IEE, Vol.118, No.7, July 1971.

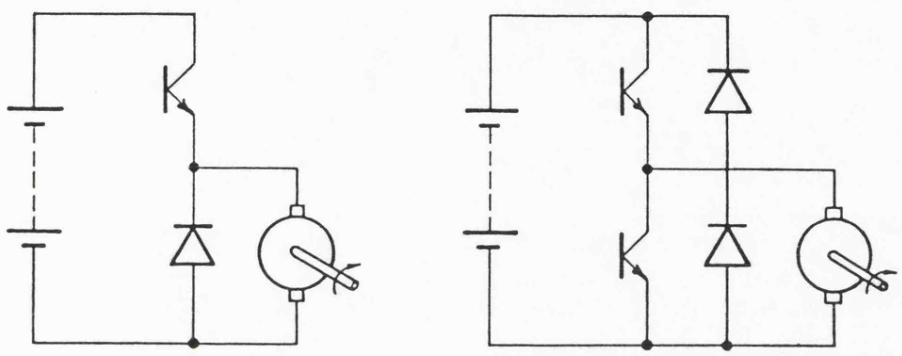

(a) Simple Chopper (b) Regenerative Chopper

Figure 1 Schematics of DC Controllers

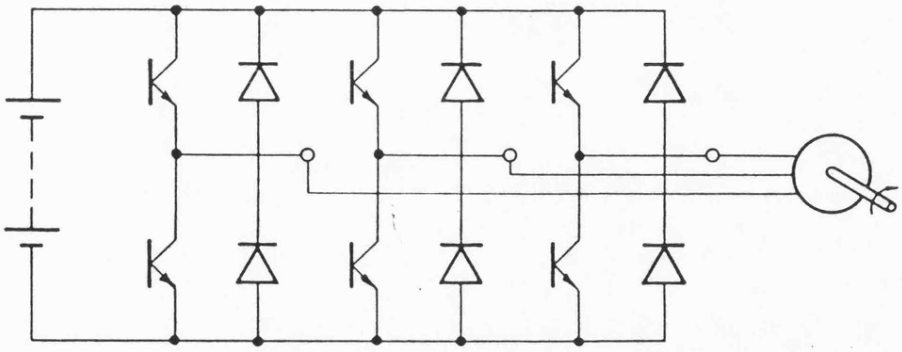

Figure 2 Schematic of 3-Phase Inverter for AC Machine Control

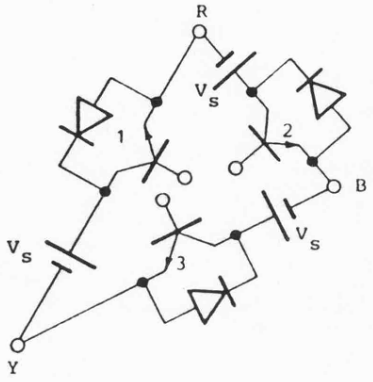

Figure 3 Schematic of Delta Inverter

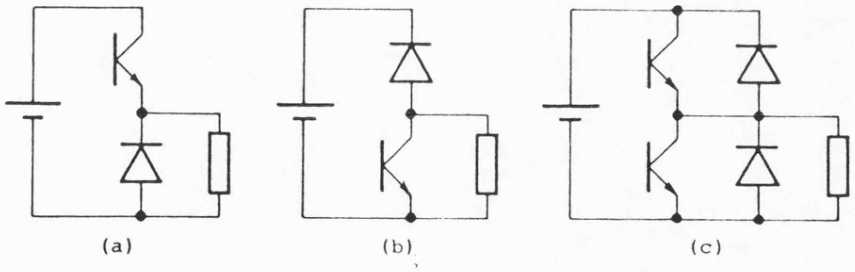

Figure 4 Building Blocks for Conventional Inverter

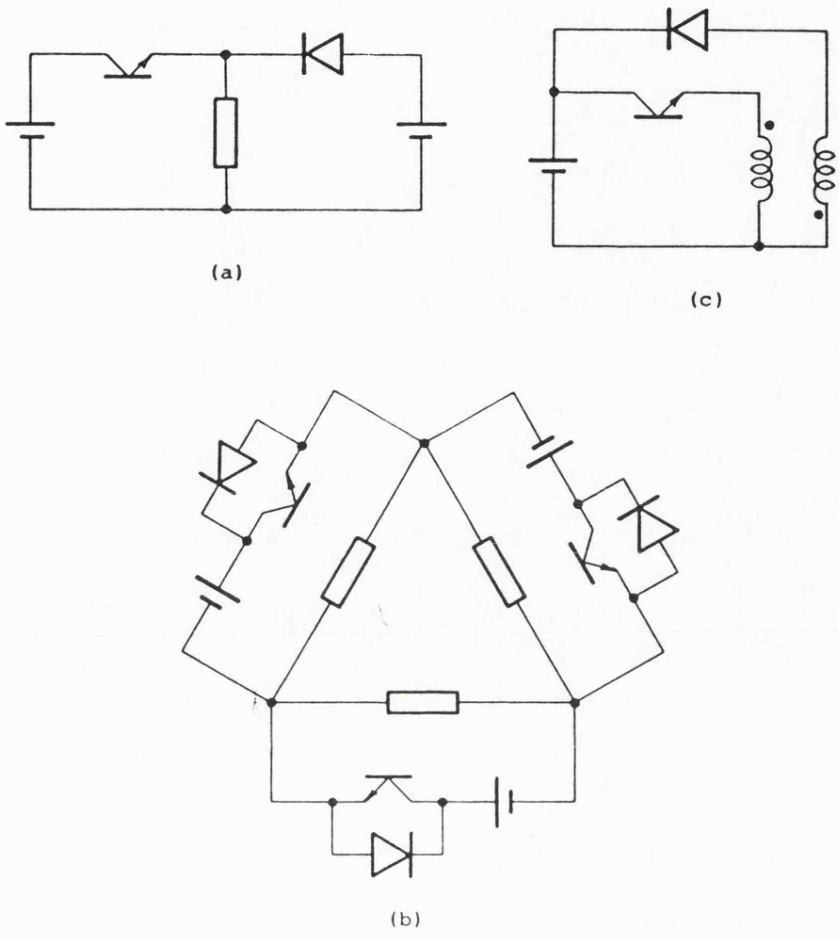

Figure 5 Building Blocks for Delta Inverter

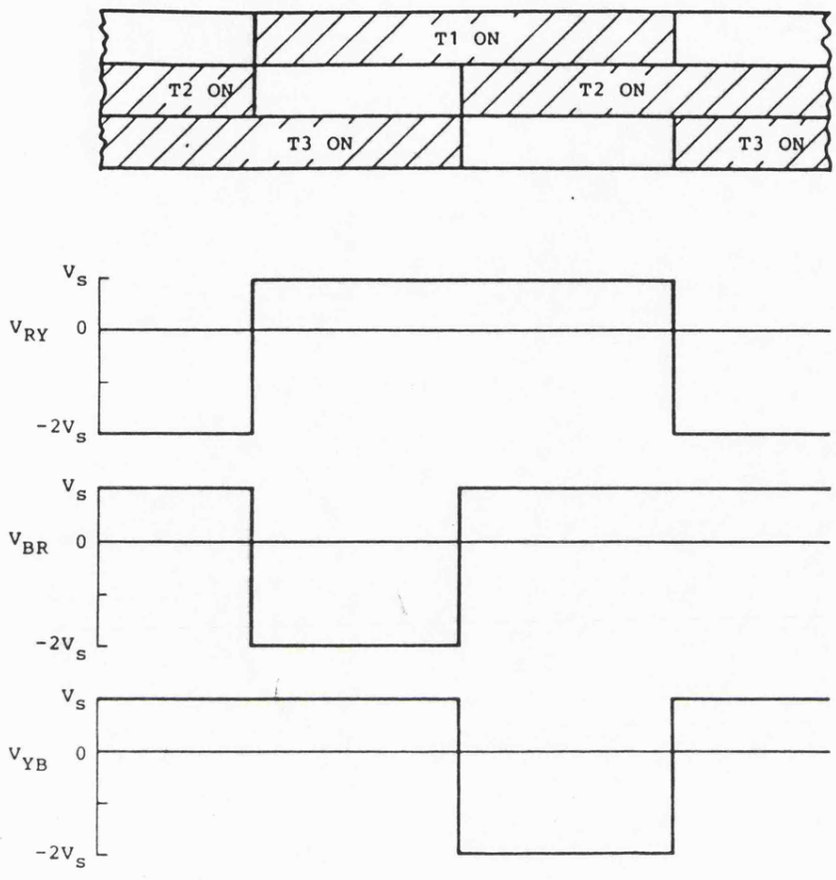

Figure 6 Basic Delta Inverter Switching Waveforms

APPENDIX 4

Manuscript of Paper Scheduled
for publication July/Aug 1984,
in IEEE Trans on Industrial Applications

Paper Entitled
"Sinusoidal Pulse-Width Modulation Strategy
for the Delta Inverter"
by P.D. Evans, R.C. Dodson and J.F. Eastham

SINUSOIDAL PULSE-WIDTH MODULATION STRATEGY FOR THE DELTA INVERTER

BY

P D Evans, BSc(Eng), DIC, PhD, ACGI

R C Dodson, BSc

Professor J F Eastham, DSc, PhD, FRSE, CEng, FIEE

School of Electrical Engineering
University of Bath
Claverton Down
BATH BA2 7AY

ABSTRACT

A method by which sinusoidal pulse-width modulation can be implemented on the delta inverter is described. Analysis of the resulting waveforms, in terms of the exponential form of the Fourier series, is provided, along with a comparison of harmonic content with a conventional sinusoidally modulated waveform. Experimental results consist of temperature rise measurements for an induction motor under delta inverter and mains supply conditions, voltage harmonic measurements and motor current waveforms.

1. Introduction

The development of power semiconductor devices in recent years has given rise to solid state power control units, usually known as inverters, for use with a.c. induction machines in variable speed drive applications. The d.c. machine has traditionally been used for these duties because its speed can be changed relatively simply, by controlling the average voltage applied to its terminal. The advantages of the induction machine over the d.c. machine are well known, and include smaller size, lower cost and greater reliability. To achieve efficient variable speed operation with it, however, it is necessary to provide an a.c. supply in which both the voltage amplitude and frequency can be varied. This is usually achieved by means of the three phase inverter which uses six main power semiconductor switches. The cost and complexity of this type of controller tends to negate the inherent advantages of the induction machine.

Alternative inverter configurations which are potentially less complex are therefore of some interest.

An earlier paper introduced the delta inverter[1]. This form of three phase inverter, shown in Figure 1, uses three main power semiconductor switches. Although this is half the number of components of the bridge inverter, this arrangement also requires three separate d.c. sources. For this reason the delta inverter is thought to be most suitable for battery fed systems, such as electric vehicles.

Another paper[2] has suggested that three devices can be operated with a single d.c. source providing bifilar machine windings are used.

A detailed examination of this form of inverter in a motor drive application has not yet been reported.

It seems, therefore, that three phase solid state supplies can be produced in three main ways. The first is the conventional bridge inverter which requires six main power switches and a single d.c. source, and appears to be pre-eminent for many applications. The second is the delta inverter which requires three main power switches and three d.c. sources. Both these systems operate with conventional machines. The third apparently can use three power switches and a single d.c. source in conjunction with bifilar motor windings.

Another paper has also shown that four devices, together with a centre-tapped supply, can also be used to produce a three phase supply under special control conditions[3].

The earlier paper on the delta inverter[1] described its basic operating conditions and presented some preliminary results with an induction motor drive system. It was demonstrated, however, that the natural output waveform was rich in harmonics and that improvements would be necessary for an efficient system. The present paper describes the technique by which sinusoidal pulse-width modulation can be implemented with the delta inverter, thus reducing the harmonic content of its output waveform to acceptable levels.

This paper, together with the earlier one[1] enables the design of a delta inverter-induction motor drive system to be undertaken. Comparison with alternative systems to meet a given specification therefore becomes possible.

2. SINUSOIDAL PULSE-WIDTH MODULATION

2.1 Introduction

Sinusoidal pulse-width modulation is a well known waveshaping method for power inverters. In a conventional three phase bridge inverter each 'leg' voltage can be controlled independently and the problem of implementing sinusoidal pulse-width modulation reduces in principle to one of generating and applying the required control signals.

In the delta inverter shown in Figure 1 the problem is less straightforward. This is because operation of one device affects more than one output voltage - and under some conditions it was shown[1] that an output voltage can depend upon the load time constant. The problem is therefore to establish a basic method by which sinusoidal pulse-width modulation can be achieved on the delta inverter. Although several types of sinusoidal pulse-width modulation are possible and were studied theoretically, single-edge modulation appeared to produce marginally better results. This is a relatively simple form of modulation, and was therefore chosen in order to establish the principles of the method.

2.2 Application to the Delta Inverter

Development of a sinusoidal pulse-width modulation strategy for the delta inverter starts from the observation that if at any instant in time* two devices are ON, the three output voltages of the inverter are completely defined, and the sum of these voltages is zero. Under these conditions a line voltage is always $+V_D$ when its corresponding device is ON and always $-2V_D$ when it is OFF. For example, V_A is $+V_D$ when T1 is ON and $-2V_D$ when T2 and T3 are ON.

* It has been assumed in this part of the discussion that the devices switch instantaneously.

A further consideration is that if for a portion of the cycle two particular devices are modulated in such a way as to make the fundamental components of two corresponding output voltages two of a three phase sinusoidal set, then the resulting third voltage must necessarily be the third member of that set. (This principle may be thought of as the dual of an alternative arrangement[3] where two currents are modulated sinusoidally, and the third current, being the sum of the two, is automatically the third phase of the current set.)

Figure 2 illustrates how these principles are applied to produce sinusoidal pulse-width modulation for the delta inverter. This figure is for twelve modulating pulses per cycle (carrier frequency to modulating frequency ratio of twelve). This small number has been chosen only for illustrative purposes in order that the drawing, which is approximately to scale, can show individual pulses in detail: it is not suggested that twelve pulses per cycle is an optimum number. A 'control band' extending over two-thirds of a cycle is defined for each device, and two control bands exist at all times throughout the cycle. During its control band a device is switched to produce a sinusoidally modulated waveform for its corresponding output. It can be seen that, as defined in Figure 2, T1 is switched during the first and last portions of the cycle, to produce a cosinusoidal fundamental waveform for V_A with its positive maximum at the zero reference of the figure. In view of the available voltage states, ie $+V_D$ and $-2V_D$, the modulation must be adjusted accordingly. For example, to produce zero average voltage during a modulating pulse a mark to space ratio of 2:1 is required. The corresponding waveforms for

V_B and V_C during the control bands of their devices T_2 and T_3 respectively are also shown as full line portions of the waveforms in Figure 2.

Outside its control band a device is only switched ON if this is required to fulfil the condition that two devices are always ON. For example, during the first one-third of the cycle shown T3 is only ON when either T1 or T2 is OFF. The resulting waveform for V_C during this portion is shown as a dotted line. The equivalent waveform for V_A is also shown dotted.

Calculation of the voltage spectrum produced by this type of waveform was made by summing the effect of each individual modulating pulse. Two characteristic shapes of modulating pulse exist. The first, shown in Figure 3(a), is the typical single-edge modulated pulse occurring during the control band region of each line voltage. The k^{th} pulse shown in Figure 3(a) is characterised by a position α_k and modulation angle δ_k. The amplitude, $A_{n_{1_k}}$, of the nth harmonic due to the k^{th} pulse of this type occurring in the control band region of a cycle, assuming even symmetry, is given by:

$$A_{n_{1_k}} = 2.\mathrm{Re}\left\{\frac{jV_D}{\pi n}\ e^{-jn\alpha_k}\ \left\{3e^{-jn\delta_k} - e^{+jn\frac{2\Delta}{3}} - 2e^{-jn\frac{\Delta}{3}}\right\}\right\} \quad \ldots (1)$$

where $\Delta = \frac{2\pi}{p}$, for p pulses per cycle

$$\alpha_k = \Delta\ (k - \tfrac{1}{3})$$

$$\delta_k = \frac{m\Delta}{3}\cos\ (\alpha_k + \delta_k) \quad \text{where m is the depth of modulation.}$$

The resultant amplitude of the nth harmonic A_{n_1}, due to all the single-edge modulated pulses in the control band region, is given by the summation:

$$A_{n_1} = \sum_{k=1}^{p/3} A_{n_{1_k}} \quad \ldots (2)$$

Outside the control band region, the pulse shapes - shown dotted in Figure 2 - have the characteristic shape illustrated in Figure 3(b). As explained above, these shapes are a consequence of the modulation of the other two devices during their control band regions. The amplitude, $A_{n_{2_k}}$, of the nth harmonic due to a pulse of this type, again assuming even symmetry, is given by:

$$A_{n_{2_k}} = 2.\mathrm{Re}\left\{\frac{jV_D}{\pi n} \cdot e^{-jn\alpha_k}\left\{3e^{jn(\frac{\Delta}{3} + \delta_{k_1})} - 3e^{-jn\delta_{k_2}} - e^{jn\frac{2\Delta}{3}} + e^{-jn\frac{\Delta}{3}}\right\}\right\} \quad \ldots (3)$$

where $k_1 = \frac{2p}{3} - k + 1$

$k_2 = k - \frac{p}{3}$

and the overall effect of pulses of this type, expressed by A_{n_2}, is given by the summation:

$$A_{n_2} = \sum_{k=p/3+1}^{p/2} A_{n_{2_k}} \quad \ldots (4)$$

Equations 1,2,3 and 4 can be used to define completely the harmonic voltage spectrum produced by the proposed modulation method in terms of the supply voltages, the depth of modulation and the number of pulses per cycle. Although further useful analytical simplification of these equations was not obtained, it is a simple matter to implement them on a computer in order to obtain required results.

2.3 Comparison with Conventional Sinusoidal Pulse-Width Modulation

The resulting waveform from the delta inverter with sinusoidal pulse-width modulation has irregularities that do not appear with an equivalent type of modulation from a conventional three phase bridge

inverter. It is of interest therefore to compare theoretically the spectra for the two types.

The basis of comparison was taken to be the term:

$$\sqrt{\sum_{n=2}^{\infty} \left(\frac{V_n}{n}\right)^2}$$

where V_n is the amplitude of the nth harmonic, the amplitude of the fundamental being taken as unity. In practice the summation was carried out over the first five hundred terms. This term is representative of the additional rms current that would be driven by the voltage harmonic source, and is therefore representative of additional stator and rotor copper loss.

For the delta inverter the type of waveform described in the previous section was used. For the bridge inverter, however, double-edge modulation was assumed as this is the method which is most commonly used.

The results of computations for a range of modulating pulses per cycle are shown in Figure 4. (The product of the number of modulating pulses per cycle and the power frequency is the switching frequency of the devices.) It is clear from these results that although the delta inverter harmonic content is higher than that of the conventional inverter, nevertheless low levels of harmonics can be achieved with reasonable switching frequencies.

3. EXPERIMENTAL INVESTIGATION

A prototype system comprising a power transistor delta inverter, a microprocessor control system and a squirrel cage induction motor was used for experimental assessment of the proposed sinusoidal pulse-width modulation technique. The delta inverter leg voltage was 36V, the star-connected induction motor produced about 0.75kW (1 hp) and the fundamental and switching frequencies were 50Hz and 1.8kHz respectively.

Motor temperature rise was used as the basis of assessment of the modulation strategy, and for this purpose a thermocouple was affixed to the stator end windings. The results of heat runs for a mains-quality sinusoidal supply and for the delta inverter supply are shown in Figure 5. For comparison purposes the rotor speed and the measured shaft torque were kept the same throughout each run. It can be seen that the temperature rise with the delta inverter supply was about 10% greater than with the sinusoidal supply. This is not dissimilar to the order of additional loss produced by conventional inverters, and for practical purposes would normally be within motor specification tolerances.

Visual evidence of the sinusoidal nature of the delta inverter supply is provided in Figure 6. This is a typical set of motor currents recorded during heat run tests.

The theoretical voltage spectrum for the practical tests is illustrated in Figure 7a. This characteristically contains the

fundamental, and sideband clusters around the switching frequency and its harmonics. Figure 7(b) is the measured voltage spectrum, and compares the relative amplitudes of the harmonics. It can be seen that there is close agreement with the theoretical spectrum, although some low amplitude harmonics also exist throughout the range. As with conventional inverter experience, these are due to some degradation of the theoretical waveform, and are mainly the result of practical considerations such as allowances for finite device switching times.

4. CONCLUSIONS

A method by which sinusoidal pulse-width modulation can be applied in the delta inverter has been proposed and explained. It has been shown both theoretically and experimentally to provide acceptable waveforms for a motor drive system.

Expressions which define the voltage harmonic amplitudes in terms of supply voltage, depth of modulation and number of pulses per cycle, equations 1-4, have been developed. This aspect of system design can therefore be undertaken quite readily.

Motor temperature rise was used as the main basis of evaluation of the modulation strategy because by this method all additional machine losses due to the inverter supply are taken into account. According to the tests the total losses were increased by around 10% due to the non-ideal nature of the supply. This is comparable with the additional loss caused by more conventional inverter systems. [An increase of 10% in

losses in a motor operating at 85% efficiency, say, would cause a small deterioration in actual efficiency to just over 83.5%.]

This modulation strategy can therefore be applied with some confidence and overcomes a problem of the delta inverter which was the high harmonic content of its natural output waveforms.

5. ACKNOWLEDGEMENTS

The authors would like to acknowledge with thanks the financial support of KGEL Ltd for the research on the Delta Inverter.

6. REFERENCES

(1) Evans, P.D., Dodson, R.C. and Eastham, J.F.: "Delta Inverter", IEE Proc., Vol.127, Pt.B, No.6, November 1980, pp.333-340.

(2) Yair, A. and Ben-Uri, J.: "New 3-phase inverter with three thyristors", IEE Proc., Vol.118, No.7, July 1971, pp.901-905.

(3) Eastham, J.F., Daniels, A.R. and Lipczynski, R.T.: "A Novel Power Inverter Configuration", IEEE Industry Applications Society, Annual Meeting, Cincinnati, 1980.

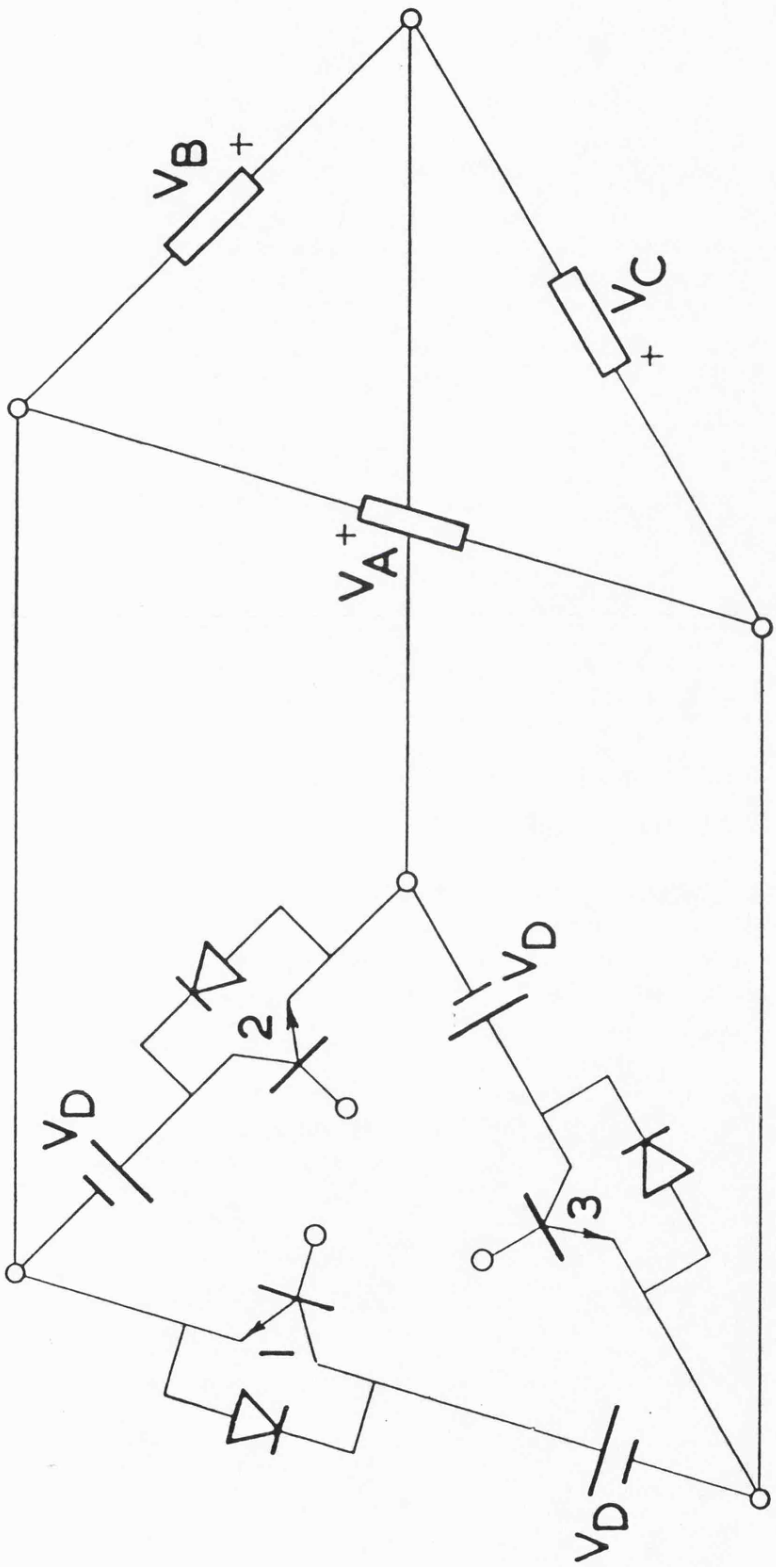

Figure 1 Delta inverter and load

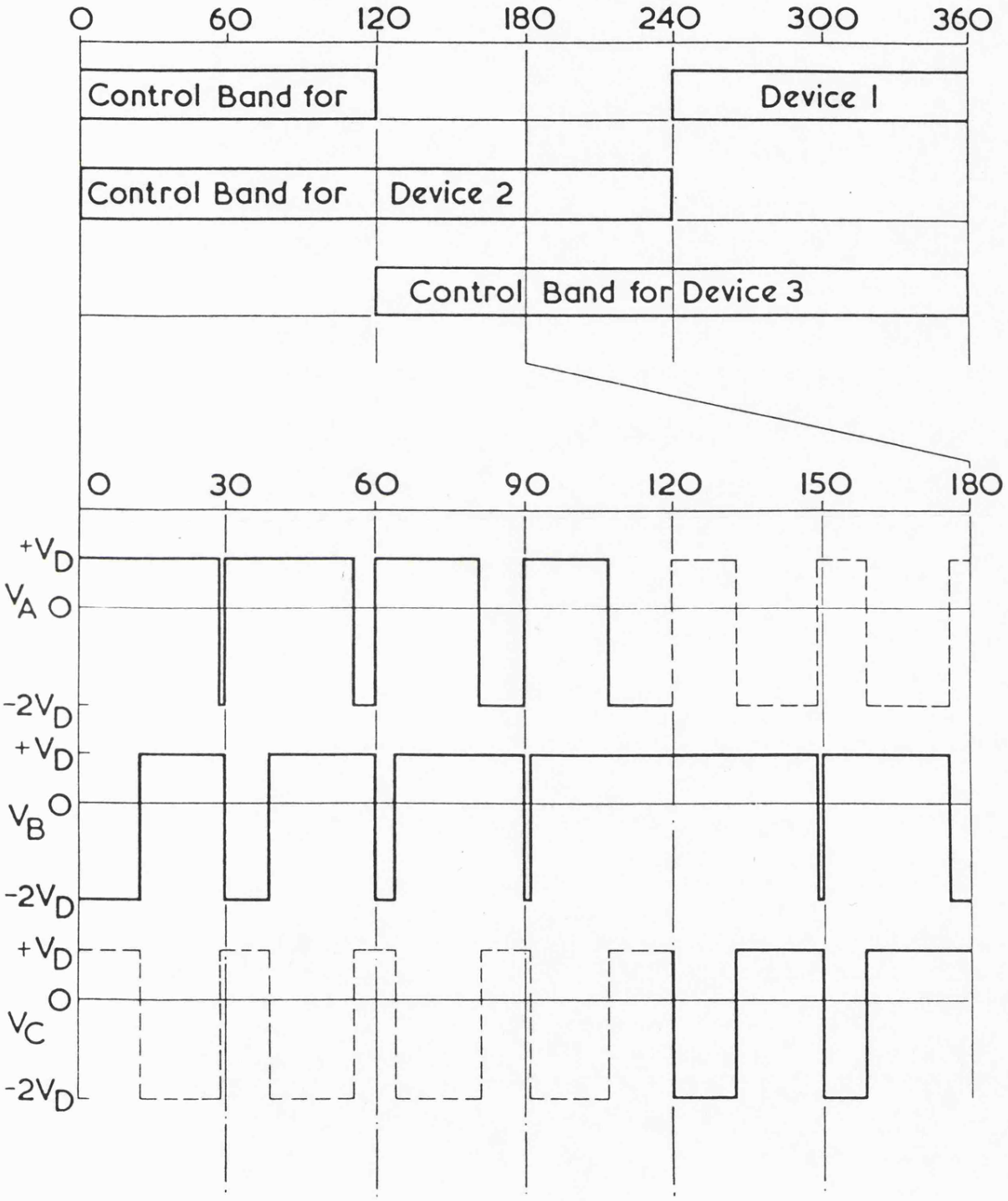

Figure 2 Sinusoidal pulse-width modulation strategy

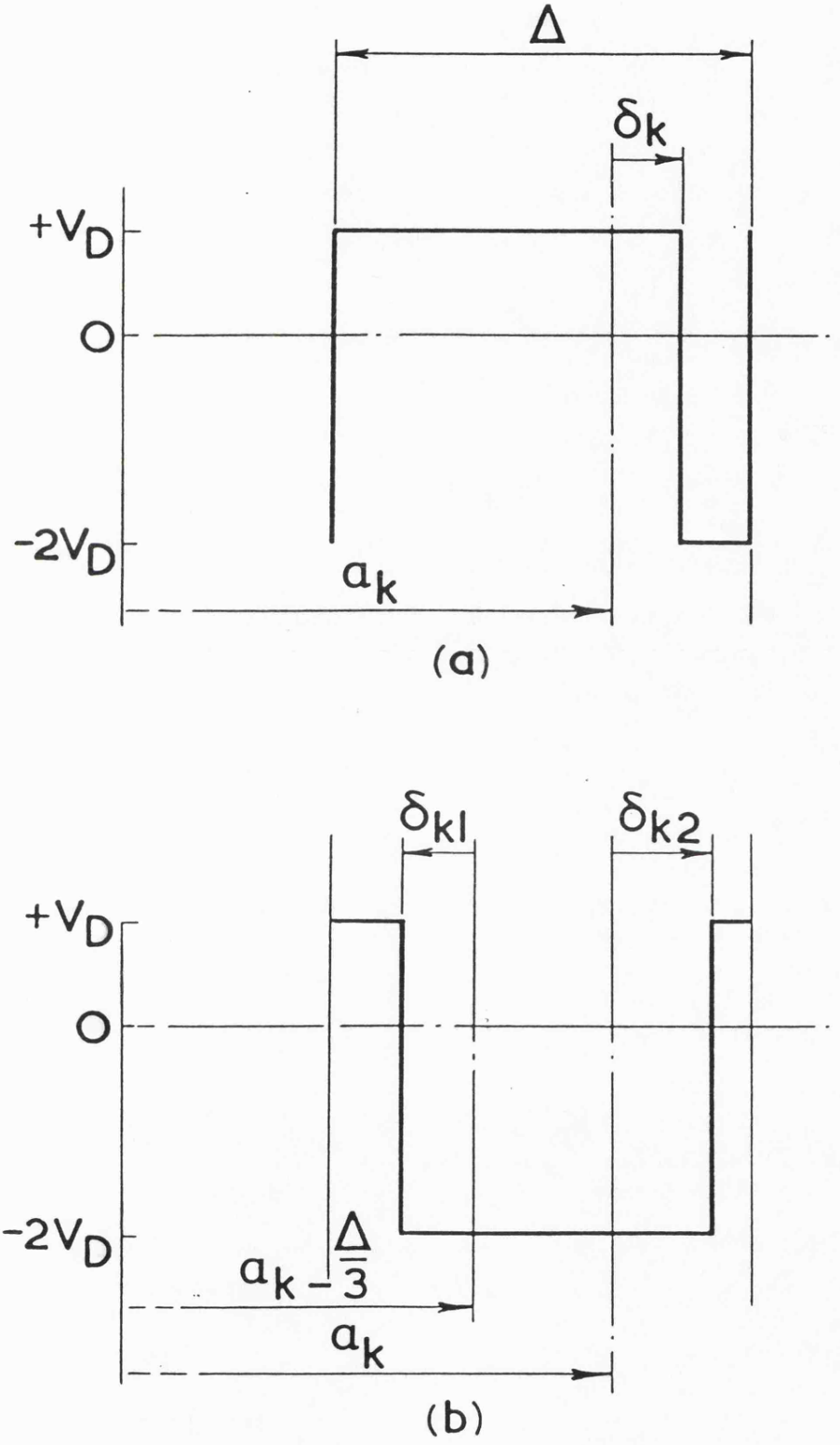

Figure 3 Modulating pulse shapes

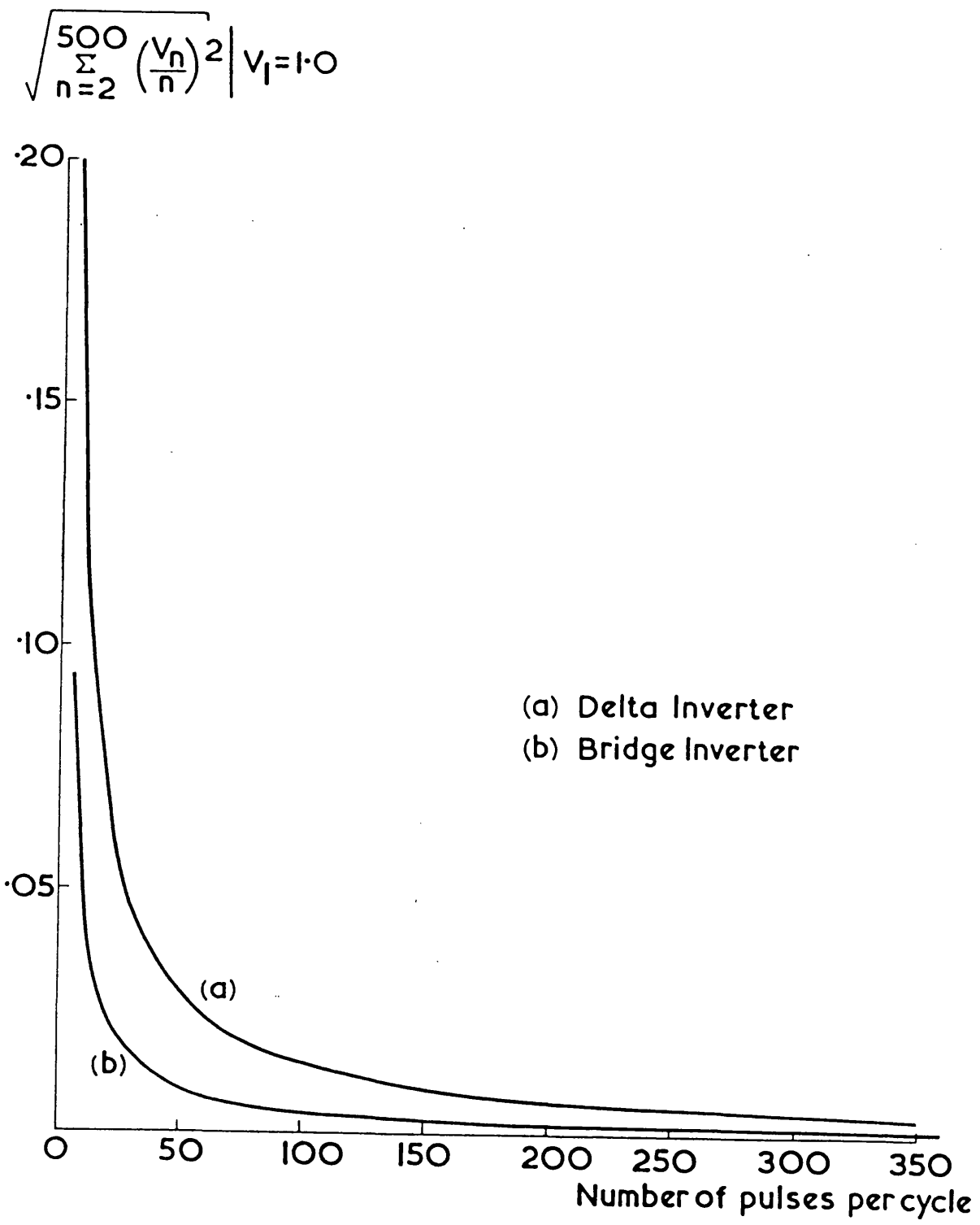

Figure 4 Comparison of bridge and delta inverter waveforms

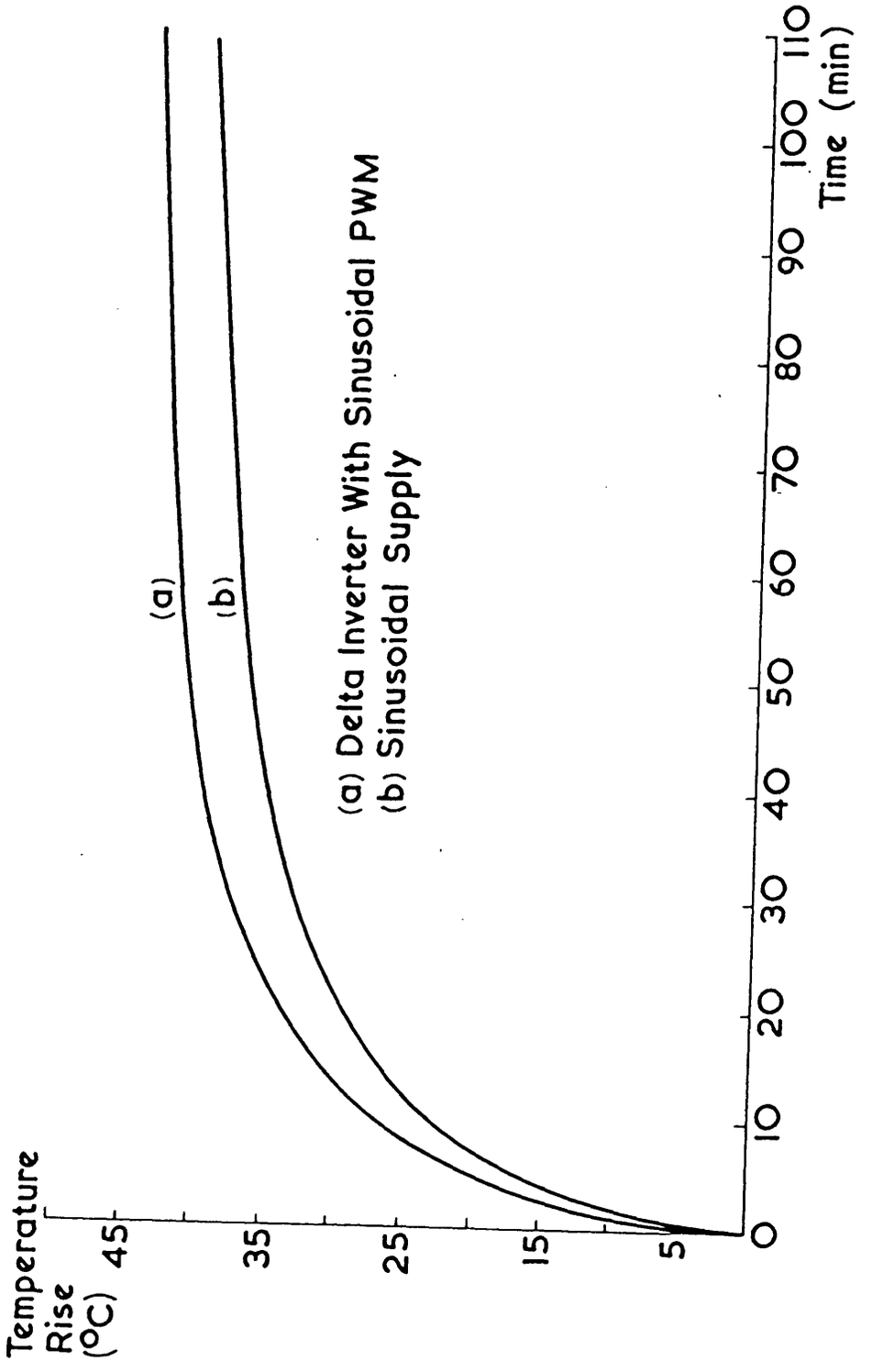

Figure 5 End-winding temperature rise

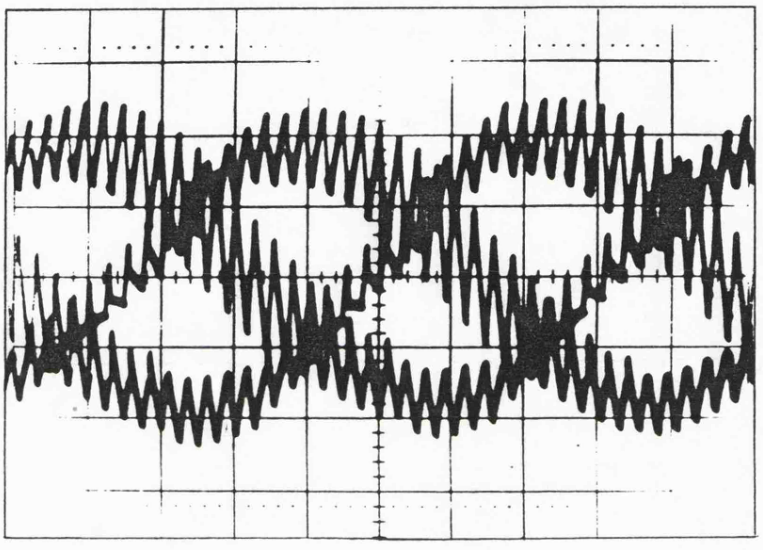

Current: 10 A/cm
Time: 2 mS/cm

Figure 6 Motor current waveforms with delta inverter supply

(a)

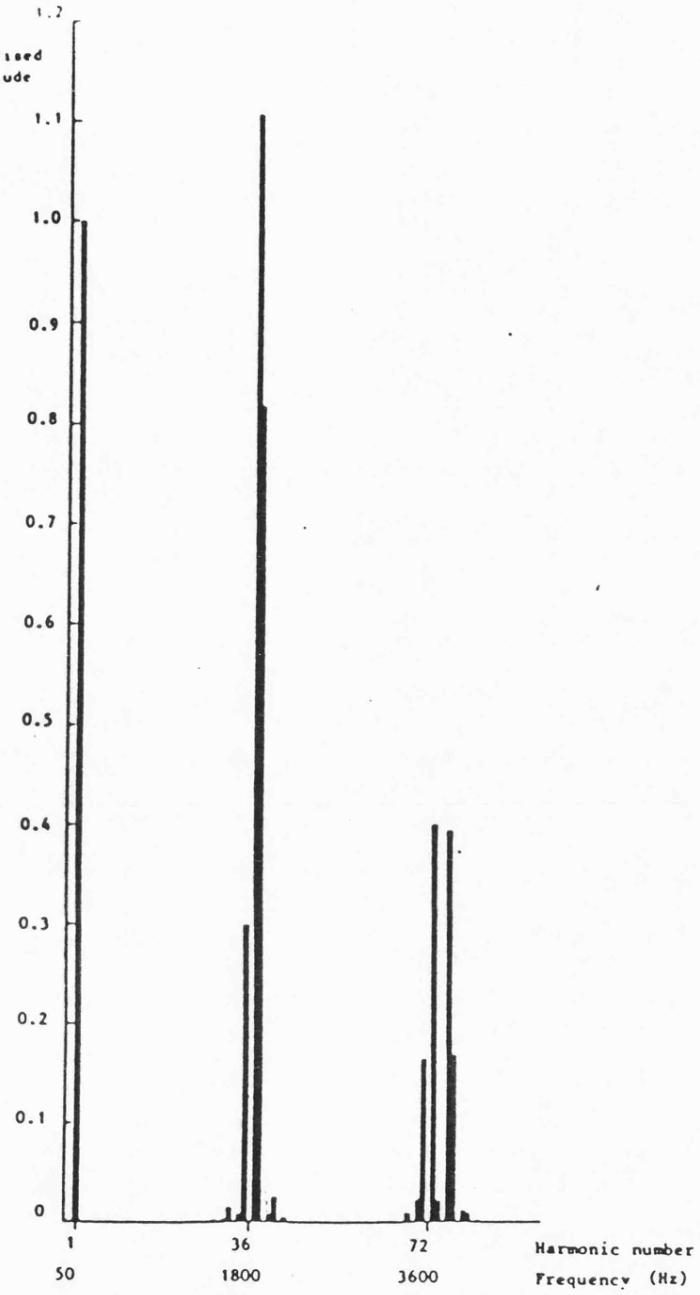

(b)

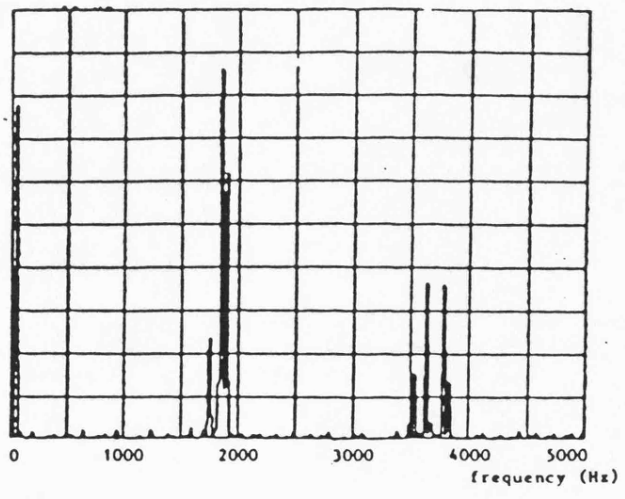

Figure 7 (a) Theoretical voltage spectrum for delta inverter
(b) Measured voltage spectrum for delta inverter

APPENDIX 5

SELECTIVE HARMONIC REDUCTION

The method of selective harmonic reduction was first described by Turnbull[1]. Taking the unmodulated square wave output voltage of a conventional single-phase inverter and performing four additional load voltage reversals, symmetrically, during each half cycle of the fundamental produces two unknowns into the waveform definition. Turnbull refers to the result as introducing "notches" into the output waveform and the resultant unknowns are therefore, in effect, "notch" position and "notch" width. With two unknowns, two equations putting two harmonics to zero can thus be simultaneously satisfied. Patel and Hoft[2,3] describe this technique as "chopping" the square wave output and extend the work to eliminate M harmonics by chopping M times per half cycle. However, the technique requires the solution of a number of simultaneous, non-linear, transcendental equations which is not straightforward, particularly as the number of equations becomes large.

Application to the delta inverter of the simple case to eliminate two harmonics is illustrated in Fig.1. The basic waveform of unmodulated 240^{o} conduction is employed, where the voltages are defined by the transistor switching sequence, two devices always on. Consider the switching sequence for T_1 in Fig.1a. Unmodulated conduction extends from -120^{o} to $+120^{o}$ (termed, for convenience, the control band) but the waveform is "chopped" between 60^{o} and 120^{o} producing a "notch", as defined by angles α_1 and δ_1, in both positive and negative halves of the control band. The other two transistors are treated in an identical

manner and all three resultant switching waveforms are then modified to maintain two devices always on. Three-phase symmetry is maintained throughout. As a result of this procedure the output line voltage of the inverter appears as shown in Fig.1b. This waveform can also be considered as the addition of the two component waveforms in Fig.1c and Fig.1d.

Taking the two component waveforms of the line voltage separately then, assuming even symmetry, for Fig.1c the harmonic content is given by:

$$a_{n_1} = \frac{6V_D}{\pi n} \sin \frac{2\pi n}{3} \qquad (1)$$

(i.e. the unmodulated 240^o case).

And for Fig.1d:

$$a_{n_2} = \frac{2}{\pi} \left\{ \int_{\alpha_1 - \delta_1}^{\alpha_1 + \delta_1} - 3V_D \cos n\theta \, d\theta + \int_{\frac{4\pi}{3} - \alpha_1 - \delta_1}^{\frac{4\pi}{3} - \alpha_1 + \delta_1} 3V_D \cos n\theta \, d\theta \right\}$$

$$= - \frac{24}{\pi n} V_D \left\{ \sin \frac{2\pi n}{3} \sin n\delta \sin n \left(\frac{2\pi}{3} - \alpha\right) \right\} \qquad (2)$$

Thus the expression for the harmonic content of the line voltage is given by:

$$a_n = a_{n_1} + a_{n_2}$$

$$= \frac{6V_D}{\pi n} \sin \frac{2\pi n}{3} \left\{ 1 - 4 \sin n\delta \sin n \left(\frac{2\pi}{3} - \alpha\right) \right\} \qquad (3)$$

To solve expression (3) for α and δ, two harmonics are put to zero. Putting the 2nd and 4th harmonics to zero, which are the lowest

order harmonics and most troublesome, results in two simultaneous equations:

$$\left.\begin{aligned} 1 - 4 \sin 2\delta \sin 2\left(\frac{2\pi}{3} - \alpha\right) &= 0 \\ 1 - 4 \sin 4\delta \sin 4\left(\frac{2\pi}{3} - \alpha\right) &= 0 \end{aligned}\right\} \qquad (4)$$

As these equations are non-linear and transcendental, numerical techniques are used for solution. The basic Newton Raphson technique converges satisfactorily, giving identical results to those obtained using a NAG (Numerical Algorithm Group) computer package, C05NAF[4], based on a fortran subroutine given by Powell[5,6] which combines the Newton Raphson and steepest descent methods for numeric solution. As a result, for zero 2nd and 4th harmonics in the line voltage of the delta inverter, $\alpha = 82.5^{o}$ and $\delta = 7.5^{o}$.

This technique can be used to eliminate any two harmonics but elimination of the 2nd and 4th are most sensible. Fig.2 shows the harmonic spectrum of unmodulated 240^{o} conduction and this can be compared with Fig.3 which shows the result of this selective harmonic reduction (SHR) technique. It can be seen that whilst the 2nd and 4th harmonics have been eliminated, higher order harmonics are adversely affected and the amplitude of the fundamental is reduced. Whilst a reduced fundamental is not necessarily a problem (this can be compensated for by a suitable choice of rated load voltage), taken together with an increase in high order harmonics, it suggests some form of optimisation technique for overall harmonic performance needs to be adopted. This problem is discussed in Chapter 3.

Attempts were made to use 2 pairs of notches to eliminate the first four harmonics in the delta inverter waveform. This proved difficult for two reasons. Firstly, although the numerical methods

could be easily extended, initial estimates could not be found that would lead to convergence and, secondly, because the delta inverter configuration puts further constraints upon the numerical method. An examination of the region 0^{o} to 120^{o}, say, in Fig.1a shows that if T_1 is off anytime between 60^{o} and 120^{o} then during its off time T_2 must correspondingly not be off or the condition that two transistors must always be on is violated and the inverter operation becomes load dependent. This leads to restrictions on the way the angles α and δ may change as the numeric technique automatically seeks convergence.

The problem of solving non linear simultaneous equations has received considerable attention within the mathematics discipline[7,8,9] and of particular interest, in the context of the present work, Branin[10,11] describes a method of finding multiple solutions of such equations. Whilst this suggests that considerable extension of this SHR technique applied to the delta inverter could be attempted, the technique of sinusoidal pulse-width modulation appears to offer significant advantages in terms of overall optimisation of the harmonic performance of the delta inverter system, not least in the ease of procurement of the solutions for the switching waveforms. Chapter 3 discusses implementation of sinusoidal PWM to the delta inverter.

One advantage of SHR, however, appears to be the techniques ability to optimise harmonic performance using the minimum of switching waveform complexity. In an attempt to show this, a switching waveform containing four pairs of modulated pulses in the control band was chosen which represented a good, but not optimal, harmonic performance. With reference to Fig.1, the respective values of α and δ for the four "notches" become $58^{o}/2^{o}$, $85^{o}/4^{o}$, $105^{o}/2.5^{o}$ and $114^{o}/2.5^{o}$. When these

values are implemented (still maintaining two devices always on), the resultant theoretical spectrum is as shown in Fig.4. It can be seen that the waveform was chosen for its effectiveness in reducing the low order harmonics present in the delta inverter line voltage, up to the tenth. Again, in comparison with unmodulated 240^{o} conduction, Fig.2, higher order harmonics are increased and the fundamental amplitude is reduced. The performance of a delta inverter AC drive system incorporating this switching waveform is investigated in Chapter 4.

References

1. Turnbull, F.G.: "Selected harmonic reduction in static DC-AC inverters", IEEE Trans., Vol.CE-83, 1964, pp.374-378.

2. Patel, H.S. and Hoft, R.G.: "Generalised techniques of harmonic elimination and voltage control in thyristor inverters: Part I - harmonic elimination", IEEE Trans., Vol.IA-9, No.3, May/June 1973, pp.310-317.

3. Patel, H.S. and Hoft, R.G.: "Generalized techniques of harmonic elimination and voltage control in thyristor inverters: Part II - voltage control techniques", IEEE Trans., Vol.IA-10, No.5, Sept/Oct 1974, pp.666-673.

4. Numerical Algorithm Group (NAG) Fortran Library Manual, Vol.1, Mk.5, Jan 1976.

5. Powell, M.J.D.: "A Fortran subroutine for solving systems of non-linear algebraic equations", Harwell Report, AERE, R5947, HMSO, 1968 (also published in (6)).

6. Powell, M.J.D.: "A hybrid method for non-linear equations", published in Rabinowitz, P.: "Numerical Methods for Non-linear Equations", Gordon and Breach, 1970, pp.87-114.

7. Spang, H.A.: "A review of minimization techniques for non-linear functions", SIAM Review, Vol.4, No.4, Oct 1962, pp.343-365.

8. Broyden, C.G.: "A class of methods for solving non-linear simultaneous equations", Math. Comp., Vol.19, 1965, pp.577-593.

9. Broyden, C.G.: "A new method of solving non-linear simultaneous equations", Comp. Journal, Vol.12, 1969, pp.94-99.

10. Branin, F.H. and Hoo, S.K.: "A method for finding multiple extrema of a function of n variables", Proc. of Conf. on Numerical Methods for Non-linear Optimisation, University of Dundee, June/July 1971, Published in: "Numerical Methods of Non-Linear Optimisation", Academic Press, London, Aug 1972, pp.231-237.

11. Branin, F.H.: "Widely convergent method for finding multiple solutions of simultaneous non-linear equations", IBM J. Res. Develop., Sept 1972, pp.504-522.

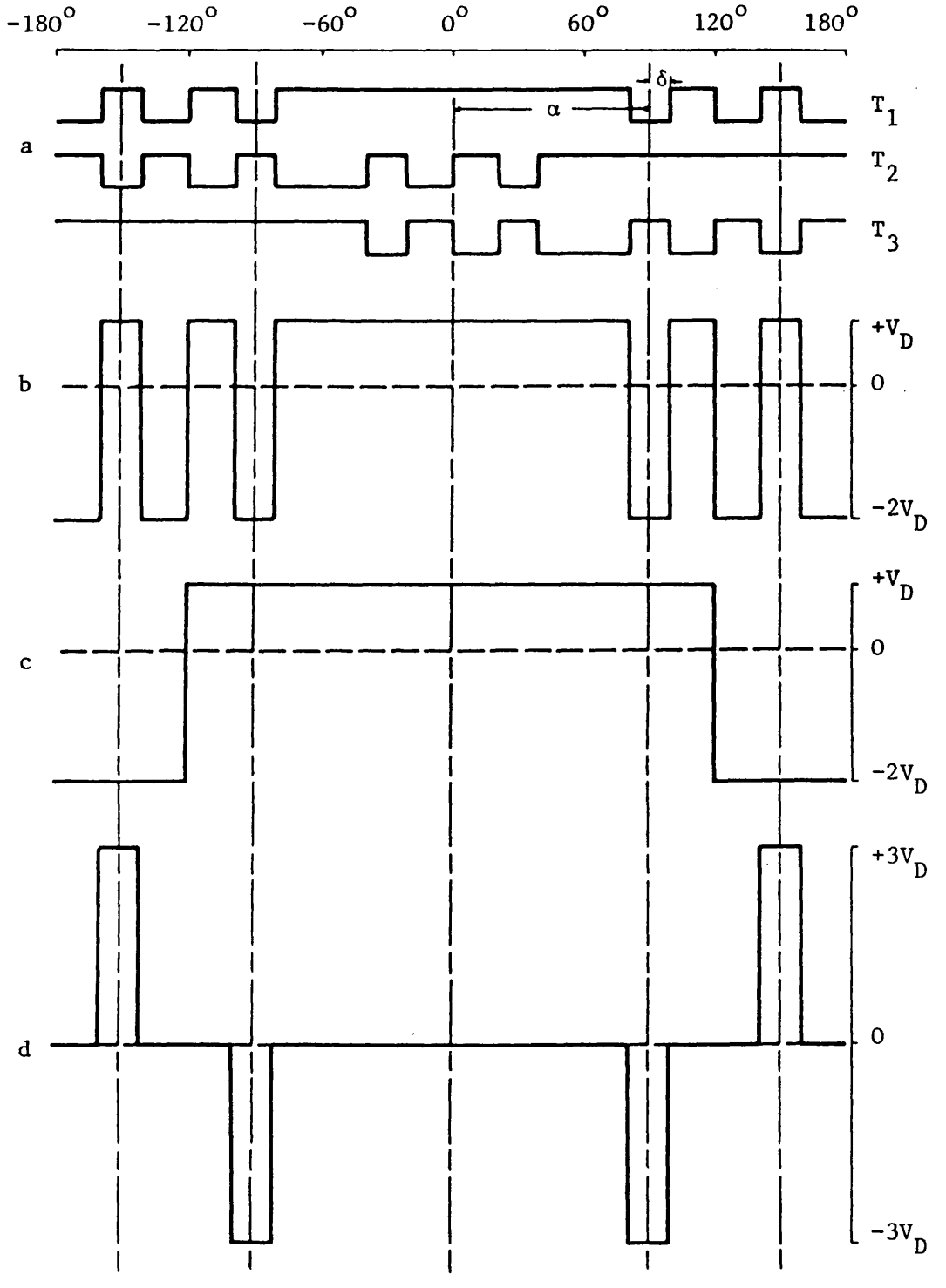

Fig.1 Delta Inverter with Selective Harmonic Reduction

a) Transistor switching sequence
b) Line voltage (V_a)
c) Component waveform - unmodulated 240° conduction
d) Component waveform - pulses to combine with c, giving b

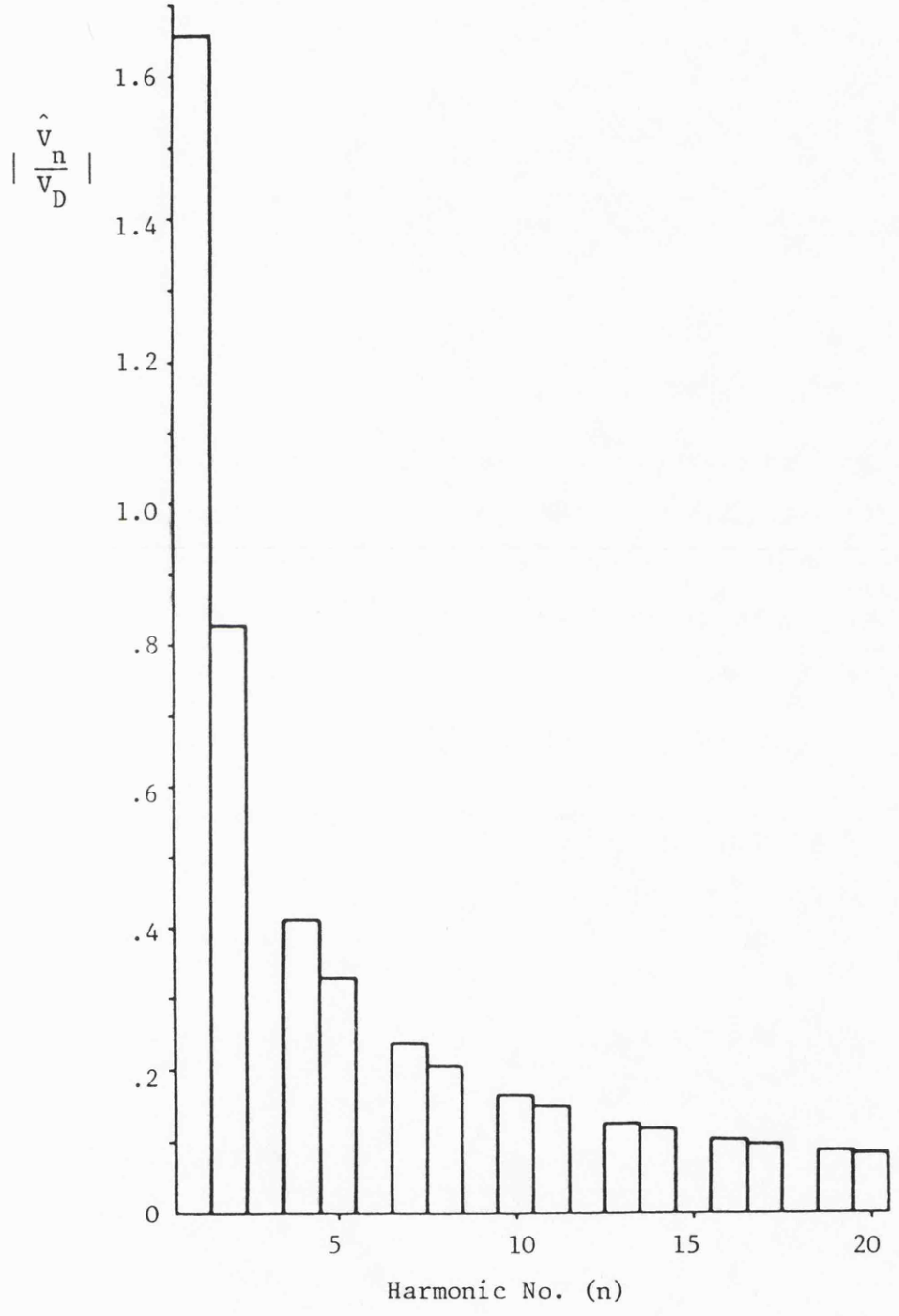

Fig.2 Delta Inverter with Unmodulated 240° Conduction - Theoretical Line Voltage Spectrum

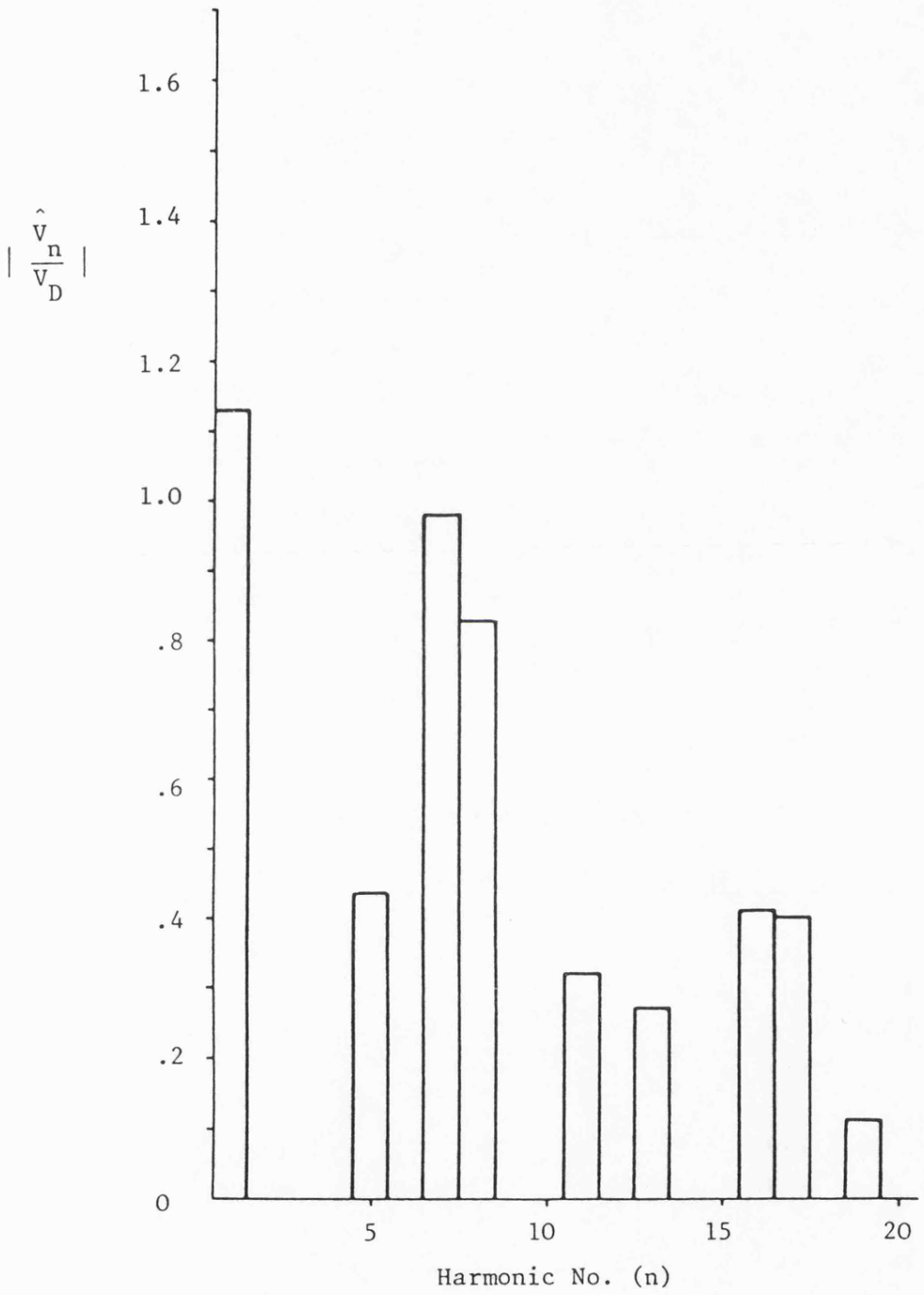

Fig.3 Delta Inverter with Selective Harmonic Reduction - Theoretical Line Voltage Spectrum with Zero 2nd and 4th Harmonics

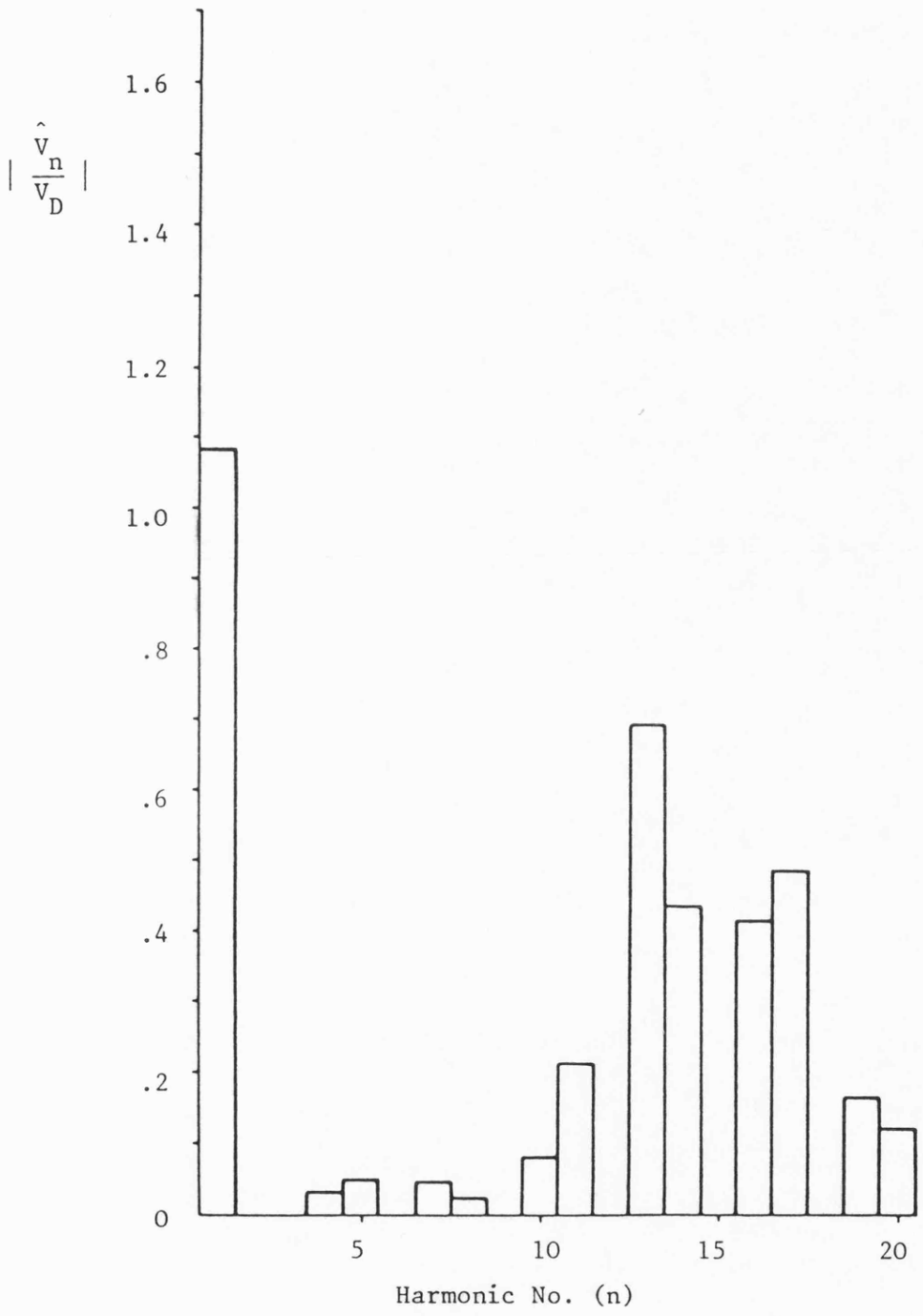

Fig.4 Delta Inverter with Selective Harmonic Reduction - Theoretical Line Voltage Spectrum with Reduced Low Order Harmonics

APPENDIX 6

Data sheets for:

Power transistors : Toshiba 2SD646

Power diodes : Westinghouse SF5GN/GR 71

SEMICONDUCTOR

TECHNICAL DATA

TOSHIBA GIANT TRANSISTOR (SI-TR)

2 S D 6 4 6 (S2517)

SILICON NPN TRIPLE MESA

HIGH POWER SWITCHING APPLICATION

INDUSTRIAL APPLICATION

MAXIMUM RATINGS : (25 °C)

Voltages	SYMBOL		UNITS
Collector to Base	VCBO	600	Volts
Collector to Emitter	VCE(SUS)	450	Volts
Emitter to Base	VEBO	5	Volts
Current			
Collector (DC)	IC	50	A
Collector (Peak)	IC	100	A
Base	IB	3	A
Dissipation			
Collector	PC	400	W
Temperature			
Junction	Tj	150	°C
Storage	Tstg	-40~150	°C

Unit in mm

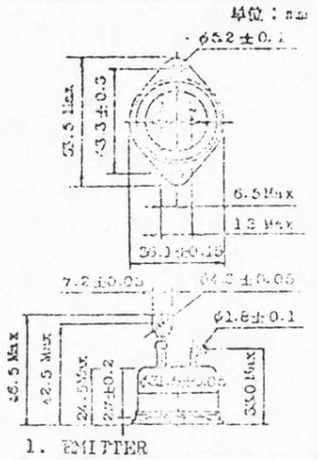

1. EMITTER
2. BASE
COLLECTOR (CASE)

JEDEC	
EIAJ	
TOSHIBA	2-32A1A

ELECTRICAL CHARACTERISTICS : (25 °C)

	SYMBOL	MIN.	TYP.	MAX.	UNITS
Forward Current Transfer Ratio (1) (VCE = 5V, IC = 50A) (VCE = 5V, IC = 30A)	hFE	150 -	- 700	- -	
Collector to Emitter Sustaining Voltage (IC = 0.5A, L = 40mH)	VCEO(SUS)	450	-	-	Volts
Collector to Emitter Saturation Voltage(1) (IC = 50A, IB = 1A)	VCE(sat)	-	-	2.0	Volts
Base to Emitter Saturation Voltage(1) (IC = 50A, IB = 1A)	VBE(sat)	-	-	2.5	Volts
Collector Cut-off Current (VCB = 600V, IE = 0)	ICBO	-	-	1.0	mA
Emitter Cut-off Current (VEB = 5V, IC = 0)	IEBO	-	-	40	mA
Output Capacitance, Common Base (VC = 50V, IE = 0, f = 1MHz)	Cob	-	600	-	pF
Switching Time — Turn on Time	ton	-	1.5	-	μS
Storage Time	tstg	-	8	-	μS
Fall Time (IC = 50A, IB1=-IB2=1A, VC=300V)	tf	-	5	-	μS

(1) Pulse Test : Pulse Width = 300μS, Duty Cycle = 2%

安全動作領域 ASO

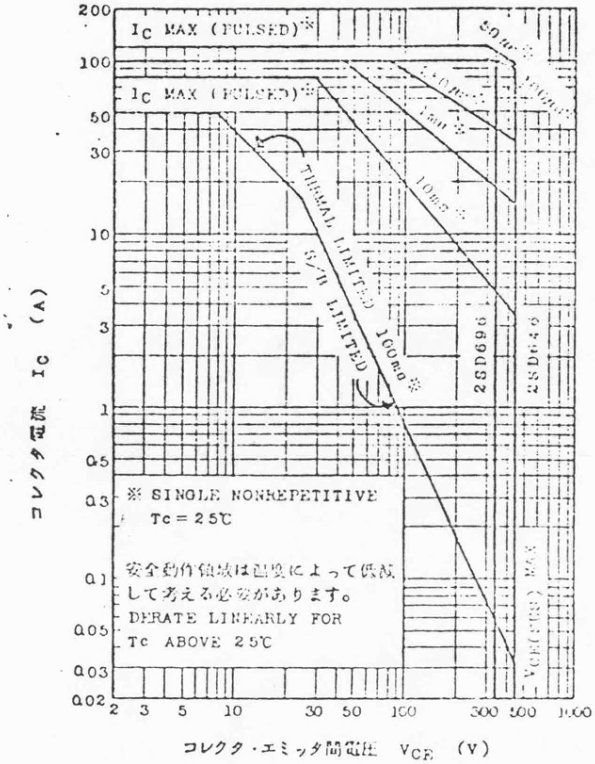

$h_{FE} - I_C$

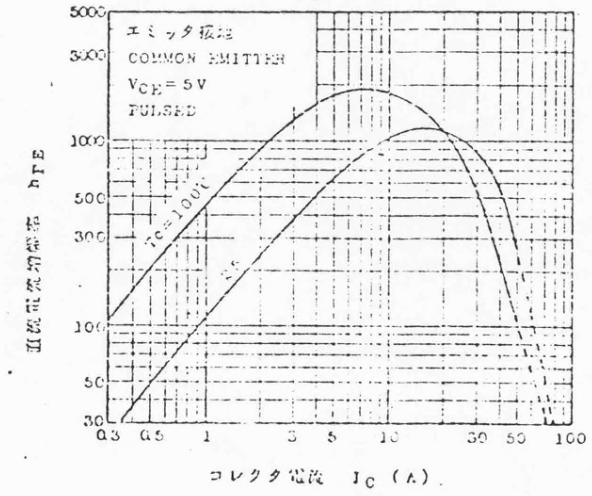

SWITCHING TIME – I_C

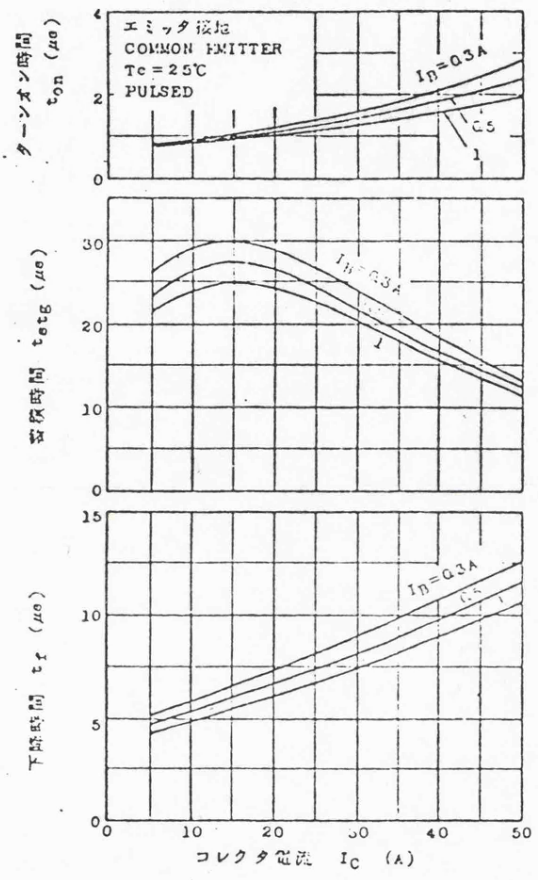

MAXIMUM TRANSIENT THERMAL IMPEDANCE (JUNCTION TO CASE)

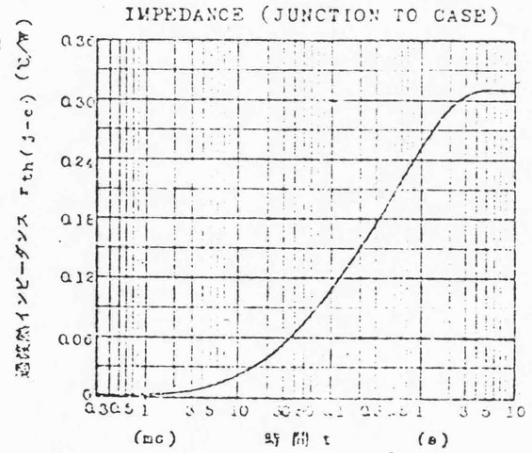

High Power Fast Recovery Silicon Diodes
Type SFxGN/GR – BN/BR71

Mean forward current 70 amperes

This publication details the basic ratings of the type SFxBR/GR71 diode and includes characteristics of reverse recovery performance and stored reverse charge. These ratings should be read in conjunction with publication D/WB/HP.

This diode has been specifically designed for high frequency rectification and for those applications requiring a fast reverse recovery coupled with a low recovery charge. e.g. inverters, choppers and ultra sonic systems, etc.

Figures 1-5 give the basic ratings and Figures 6 and 7 show the reverse recovery time T_{RR} and stored reverse charge Q_r as a function of the rate of change of forward current di/dt at a junction temperature of 150°C. Figures 8-10 give the amount of derating to be applied to the peak forward current for a variety of base temperatures and di/dt values.

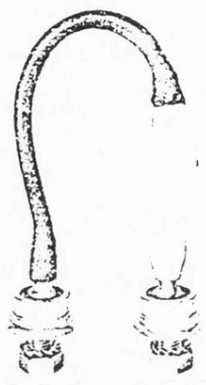

SFxBN/BR71 SFxGN/GR71

VOLTAGE RATINGS

Voltage class	V_{RRM}	V_{RSM}
1	100	150
2	200	300
3	300	400
4	400	500
5	500	600

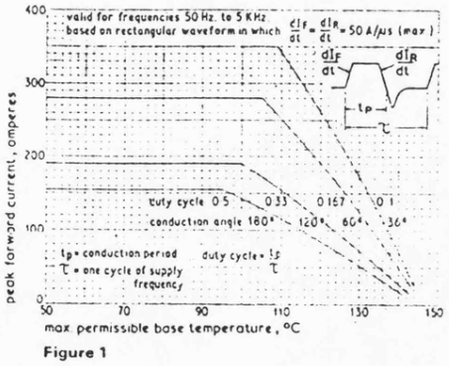

Figure 1

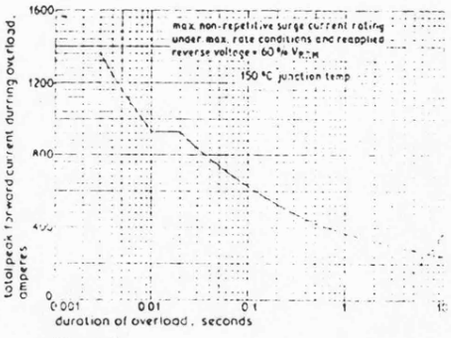

Figure 2

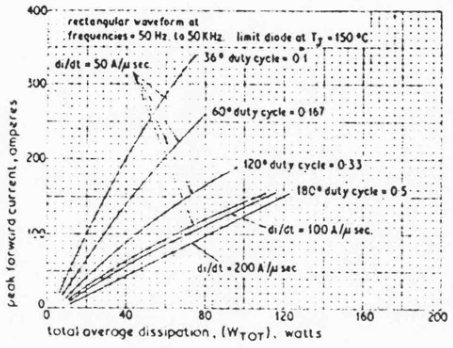

Figure 3

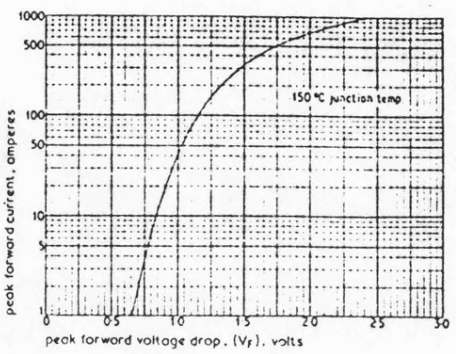

Figure 4

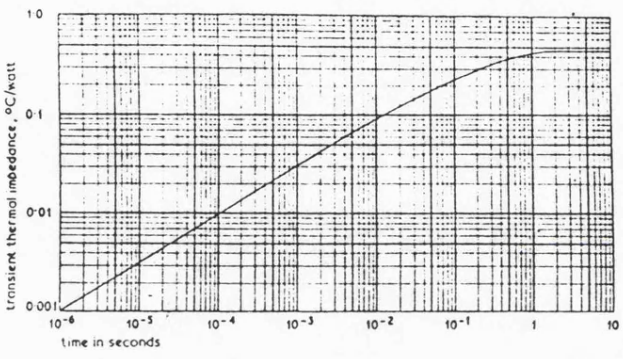

Figure 5

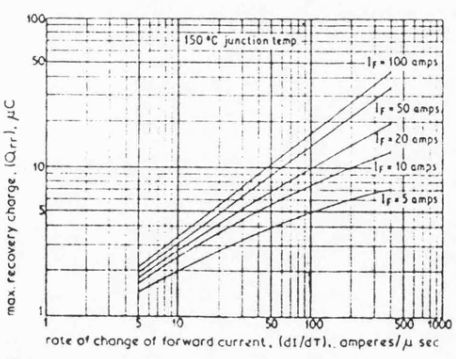

Figure 6

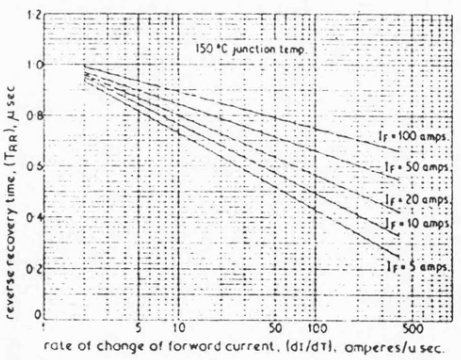

Figure 7

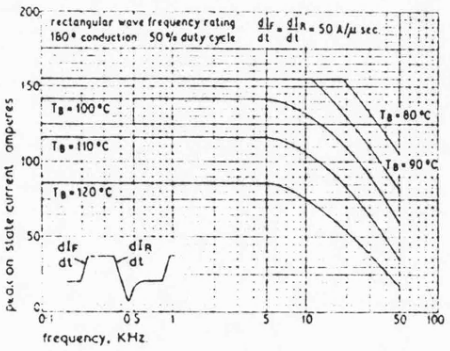

Figure 8

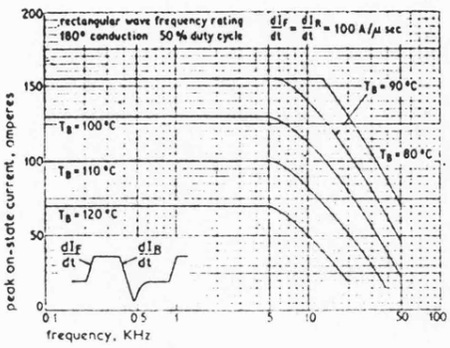

Figure 9

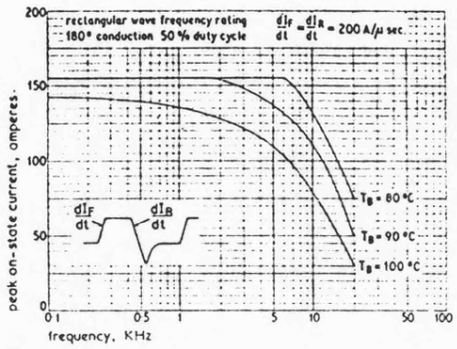

Figure 10

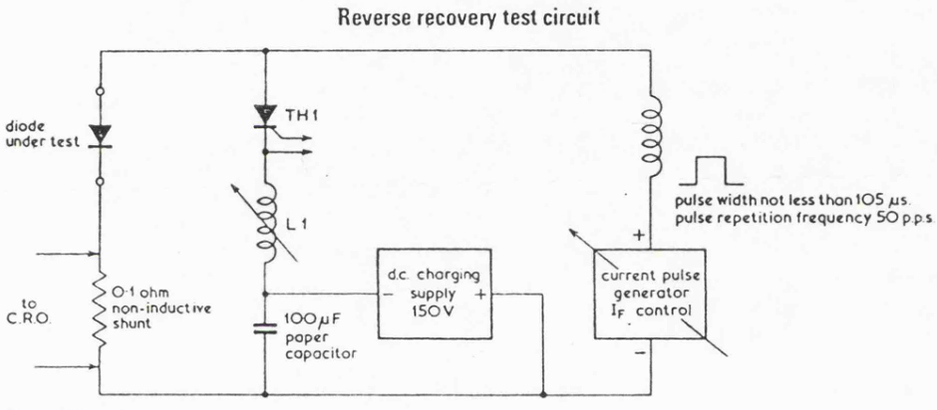

Figure 11

Figure 11 shows a basic recovery test circuit used in the measurement of the reverse recovery and stored charge performance for rectangular waveform. The value of I_{FM} used in these measurements is 100 amperes and is read across the non-inductive shunt by means of an oscilloscope.

The forward current is set by adjusting the Current Pulse amplitude and thyristor TH1 is fired 100 μS after initiation of the forward current pulse. The reverse di/dt is set by adjusting the value of inductance L1.

The method used to estimate the recovery time is that suggested in the draft I.E.C. document, issued as B.S. document No. 70/24886. The reverse current waveform is established as shown in Figure 12. A tangent is drawn at points 0·9 I_{RR} and 0·5 I_{RR} and the reverse recovery time t_{RR} is defined as the period between the point where the curve initially crosses the datum line to the point where the tangent crosses the datum line.

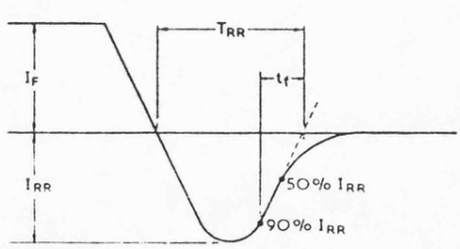

Figure 12

The same draft document recommends the following relation for calculating the stored charge Q_{rr}: $Q_{rr} = 0{\cdot}5 T_{RR} \times I_{RR}$.

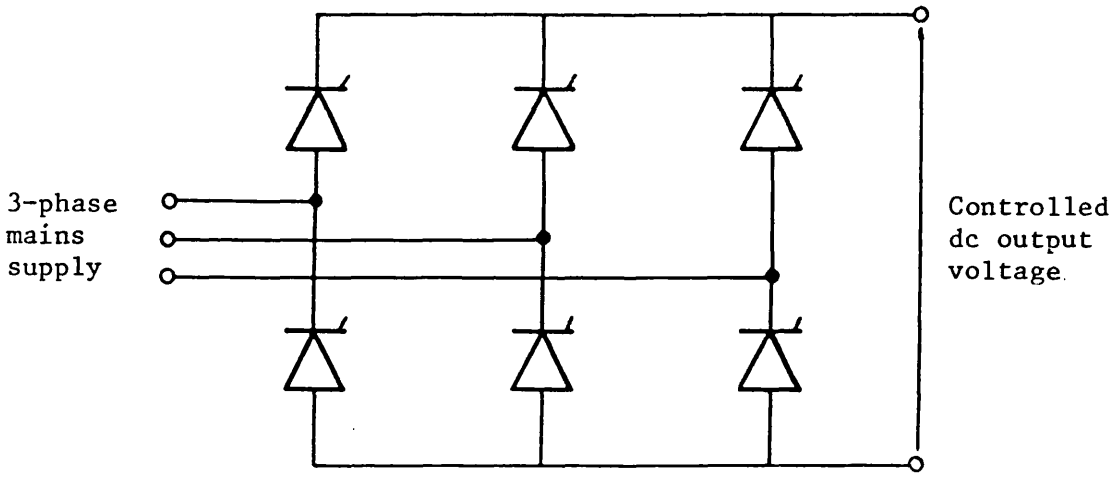

Fig. 1.1 Three-phase, phase controlled rectifier bridge

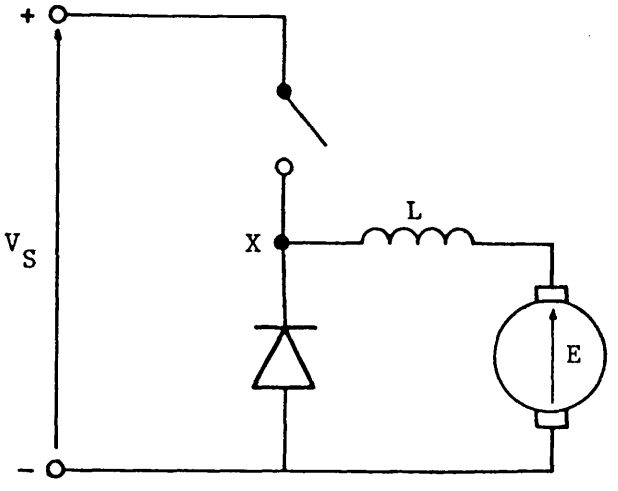

Fig. 1.2 Step-down chopper

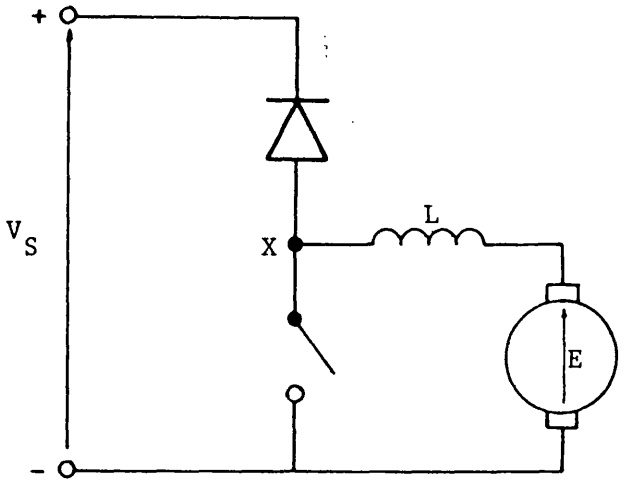

Fig. 1.3 Step-up chopper

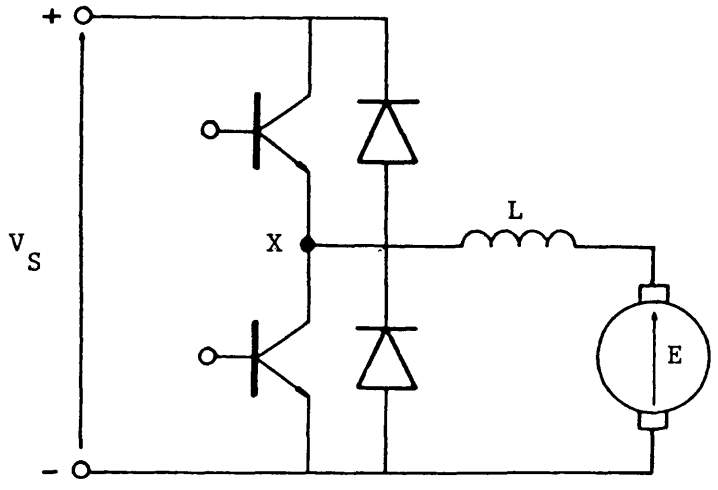

Fig. 1.4 Regenerative chopper

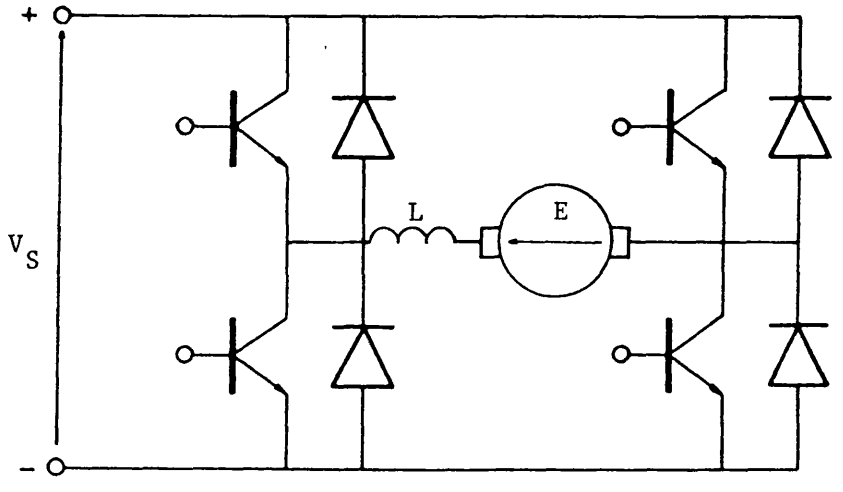

Fig. 1.5 Four-quadrant chopper

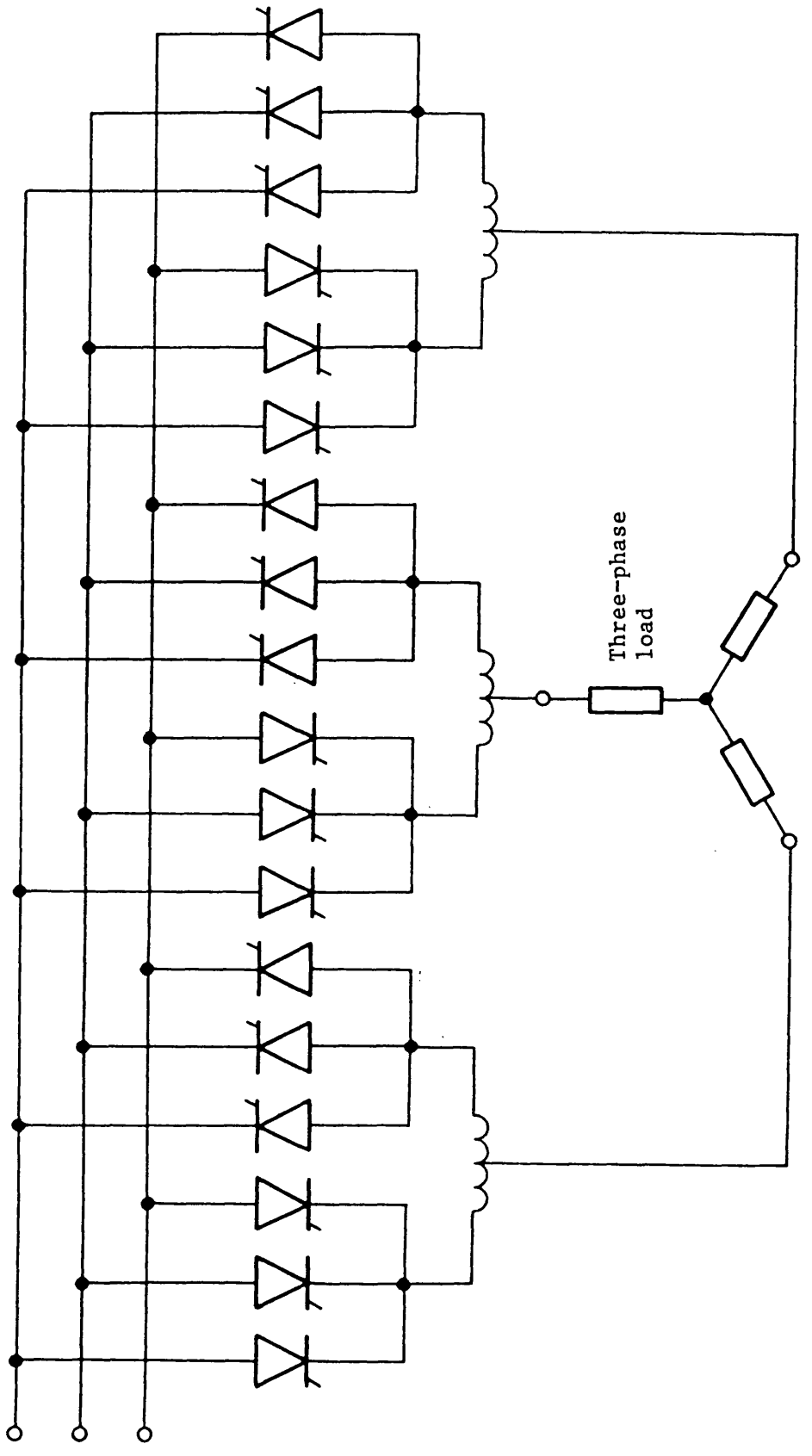

Fig. 1.6 Three-phase to three-phase cycloconverter

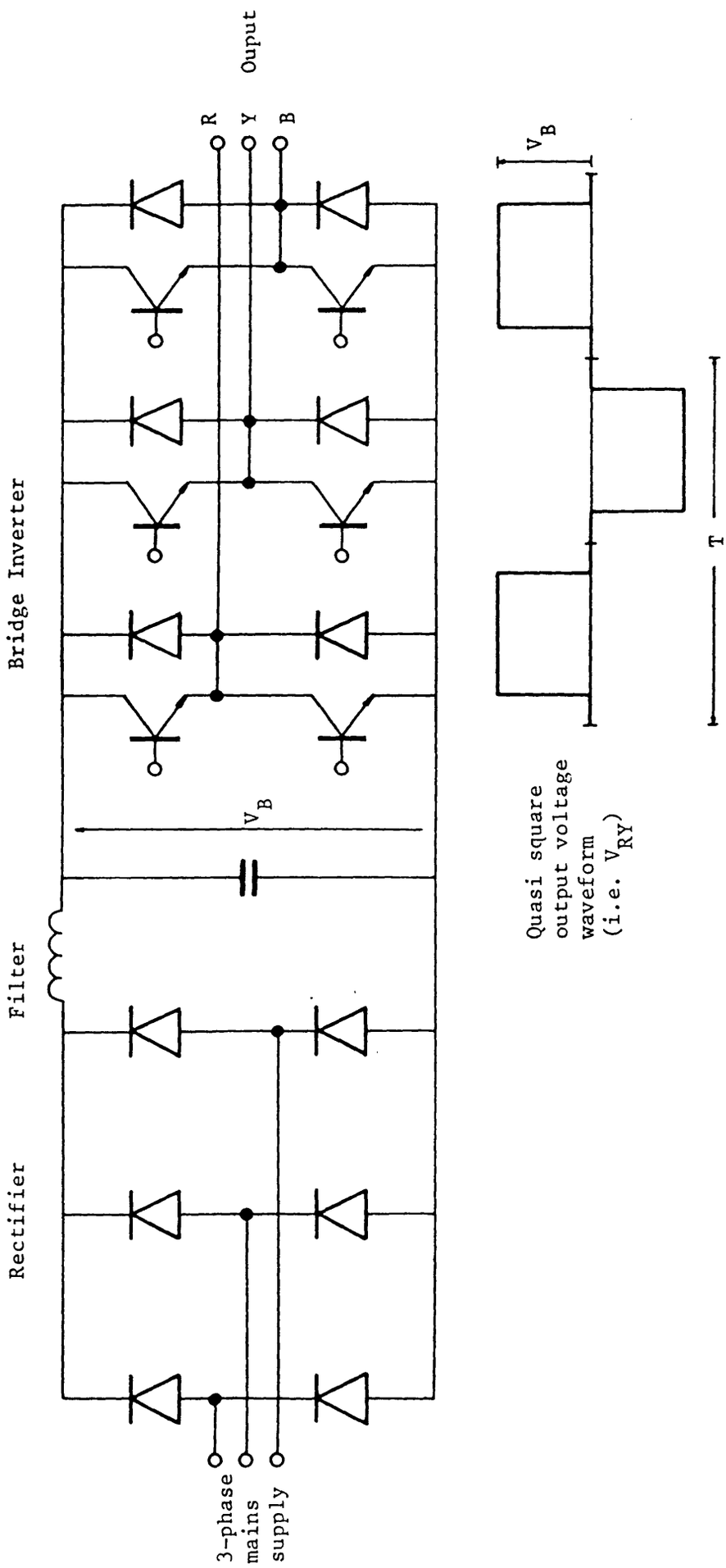

Fig. 1.7 DC link converter and unmodulated output voltage waveform

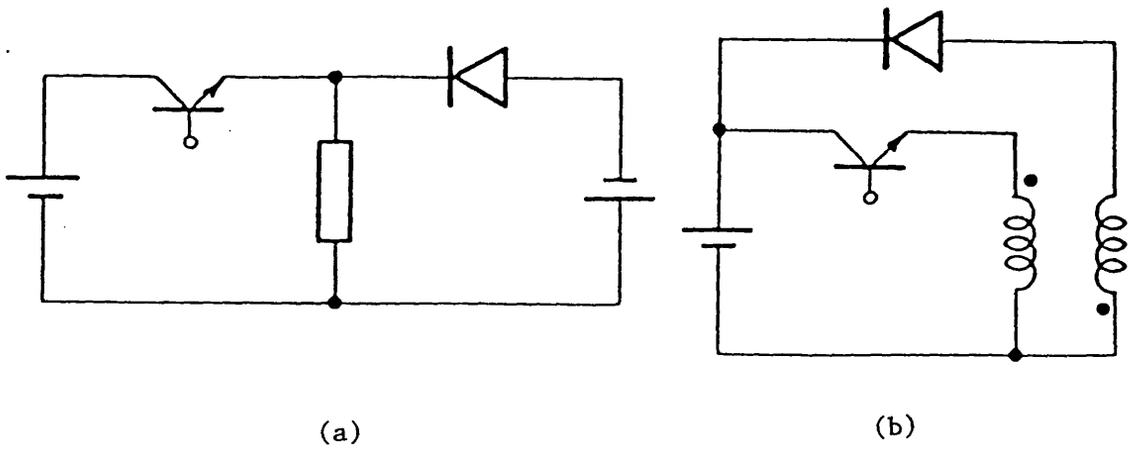

(a) (b)

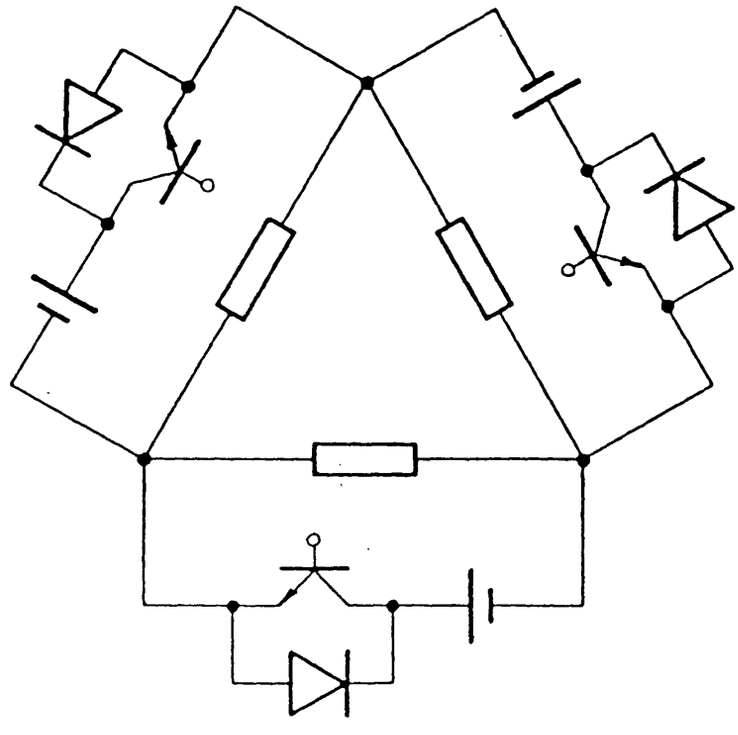

(c)

Fig. 1.8 Alternative inverter building blocks

a) Proposed building block
b) Modified building block with coupled windings
c) Three-phase arrangement using building block (a)
   - the delta inverter

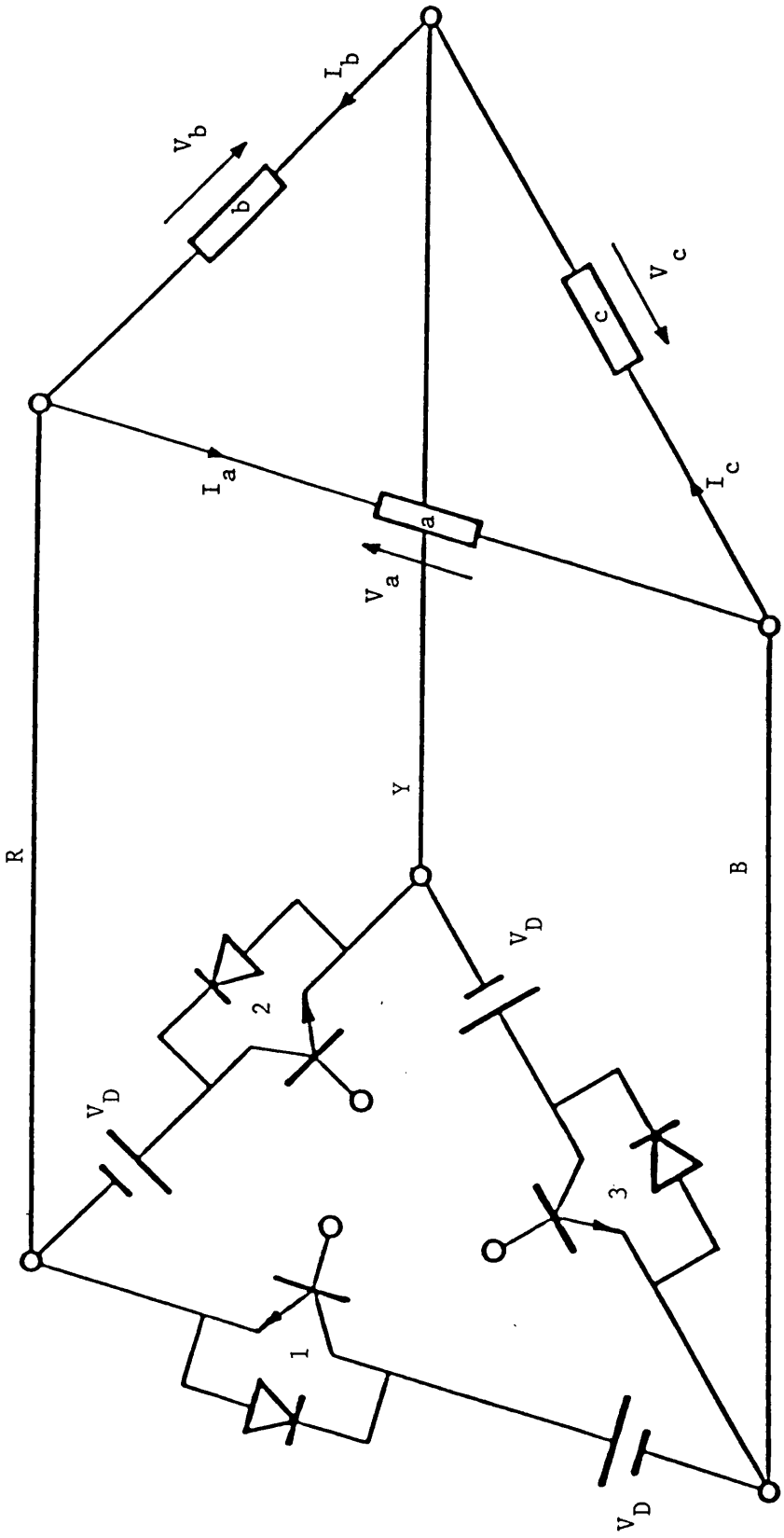

Fig. 2.1 Delta inverter and load

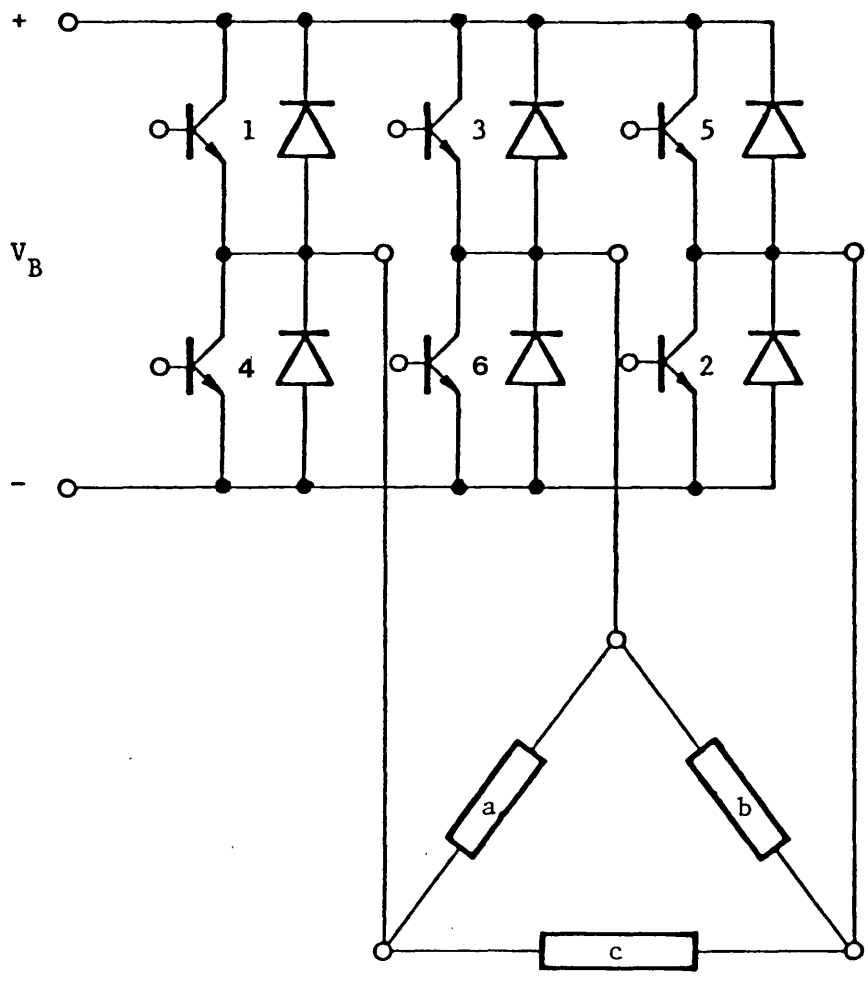

Fig. 2.2 Bridge inverter and load

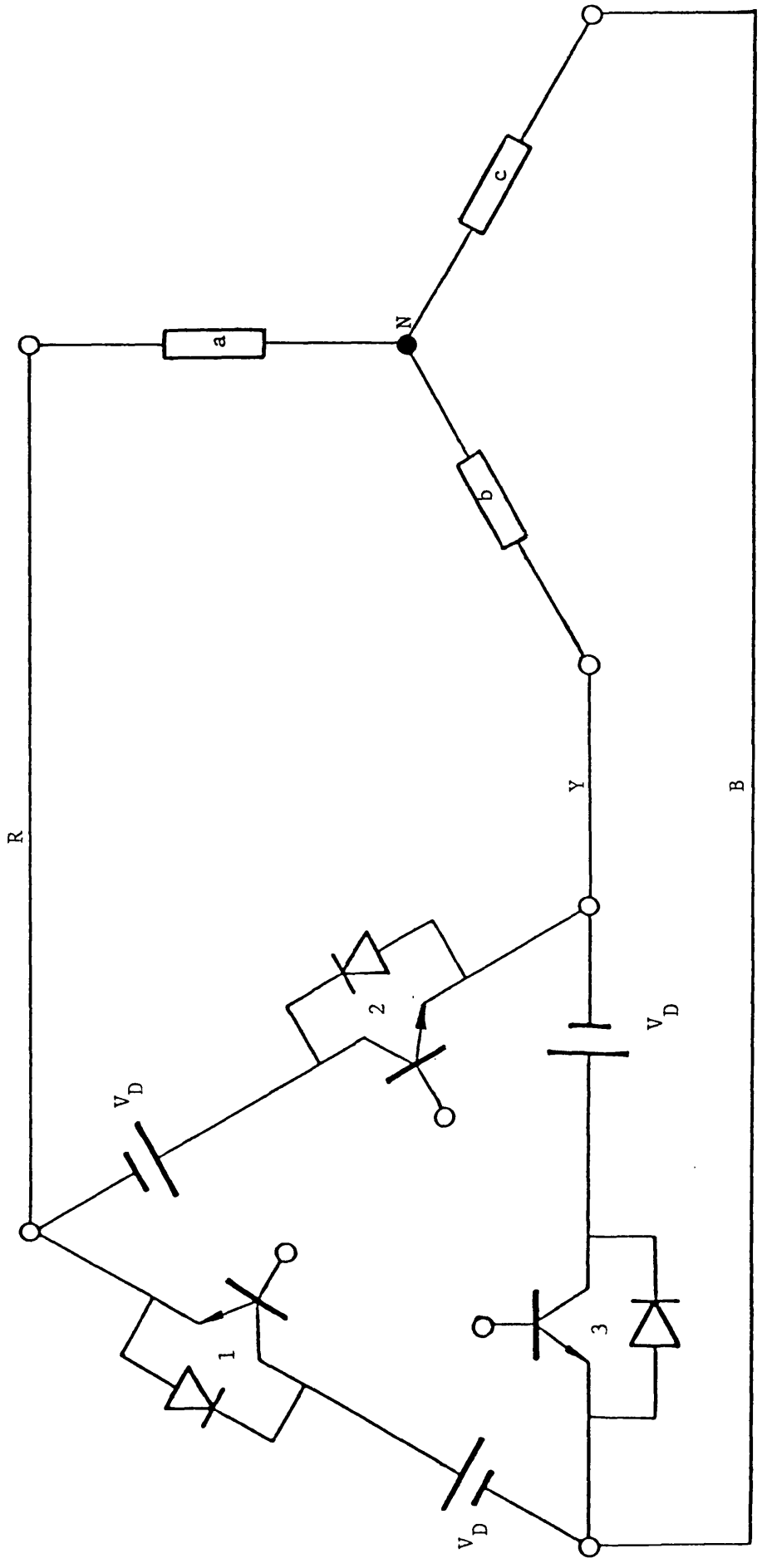

Fig. 2.3 Delta inverter with star connected load

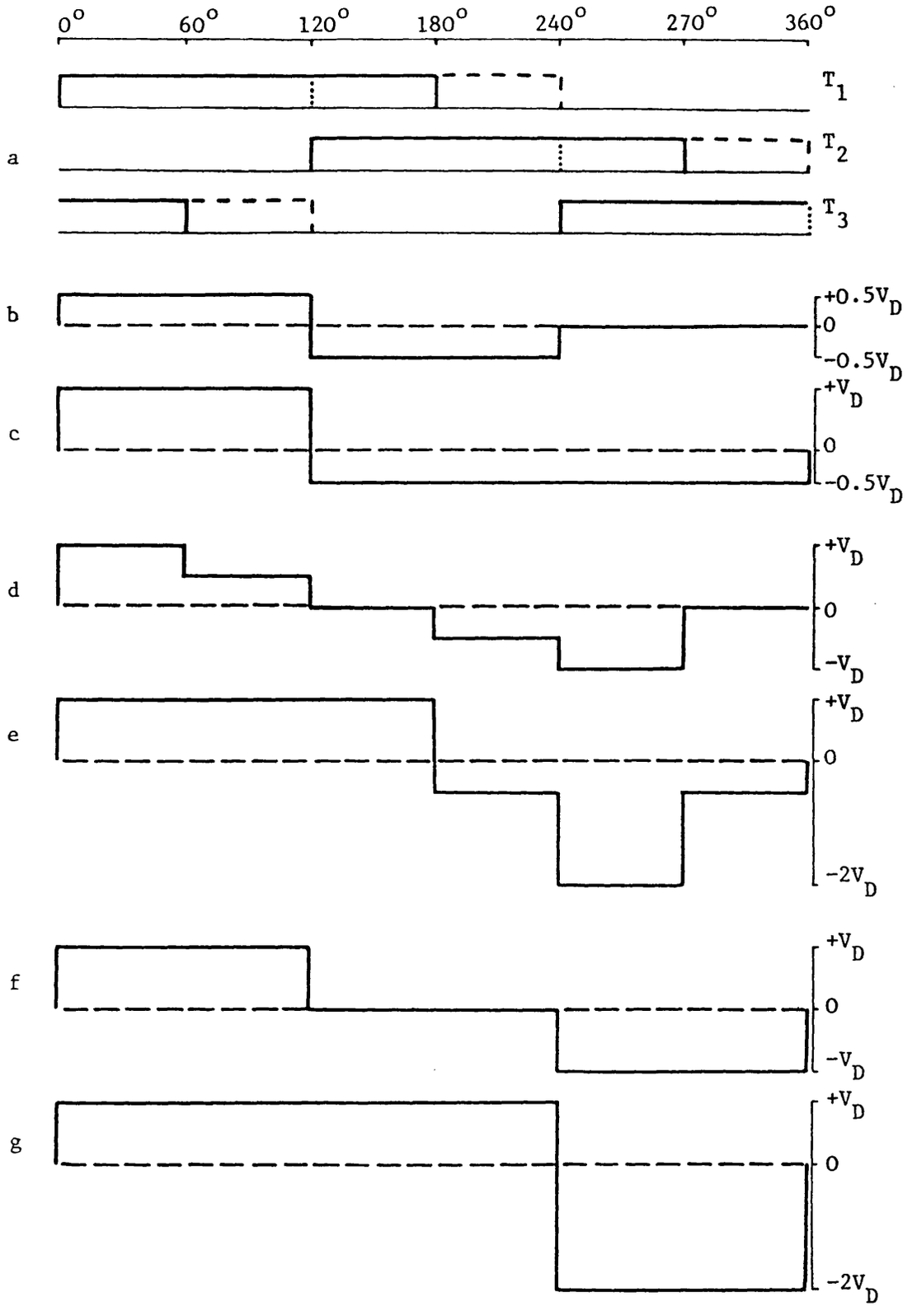

Fig. 2.4 Delta inverter with resistive load

a Transistor switching sequences 120°, 180°, 240°

b 120°, phase voltage V_{RN}

c 120°, line voltage V_{RB}

d 180°, phase voltage V_{RN}

e 180°, line voltage V_{RB}

f 240°, phase voltage V_{RN}

g 240°, line voltage V_{RB}

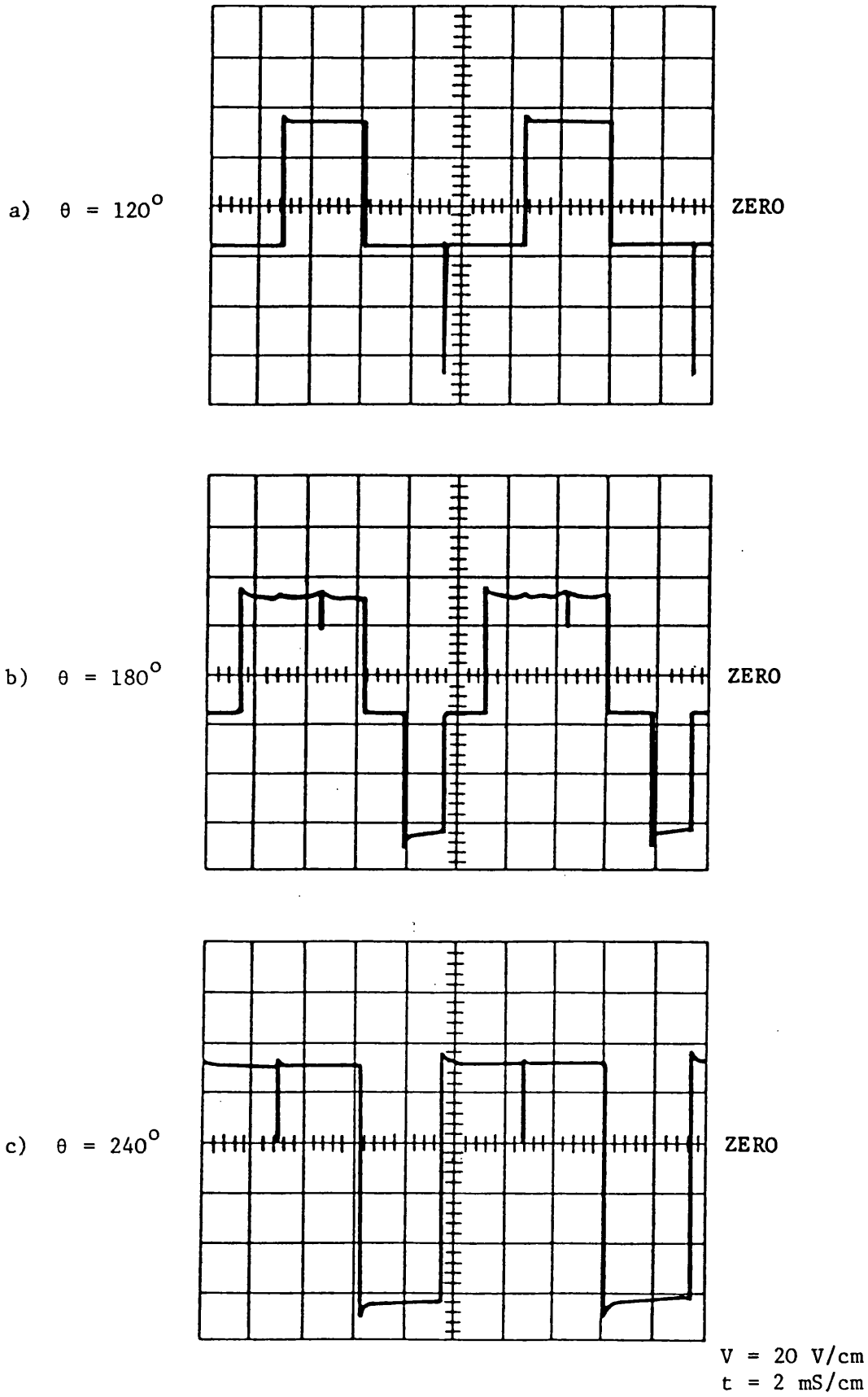

Fig. 2.5 Delta inverter with resistive load, line voltages

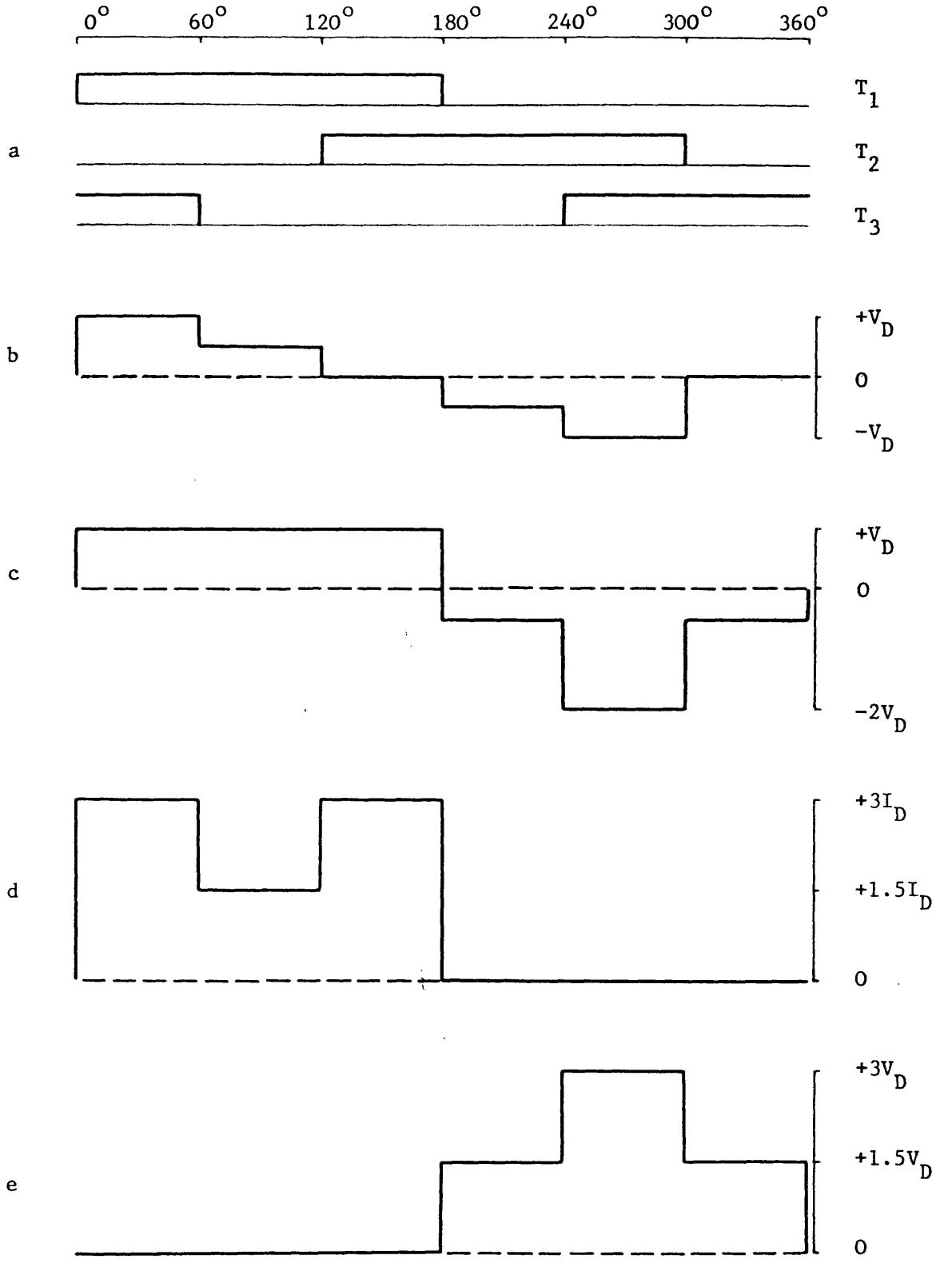

Fig. 2.6 Delta inverter with resistive load, 180° conduction

a Transistor switching sequence

b Phase voltage V_{RN}

c Line voltage V_{RB}

d Current in transistor T_1 (I_E)

e Voltage across transistor T_1 (V_{CE})

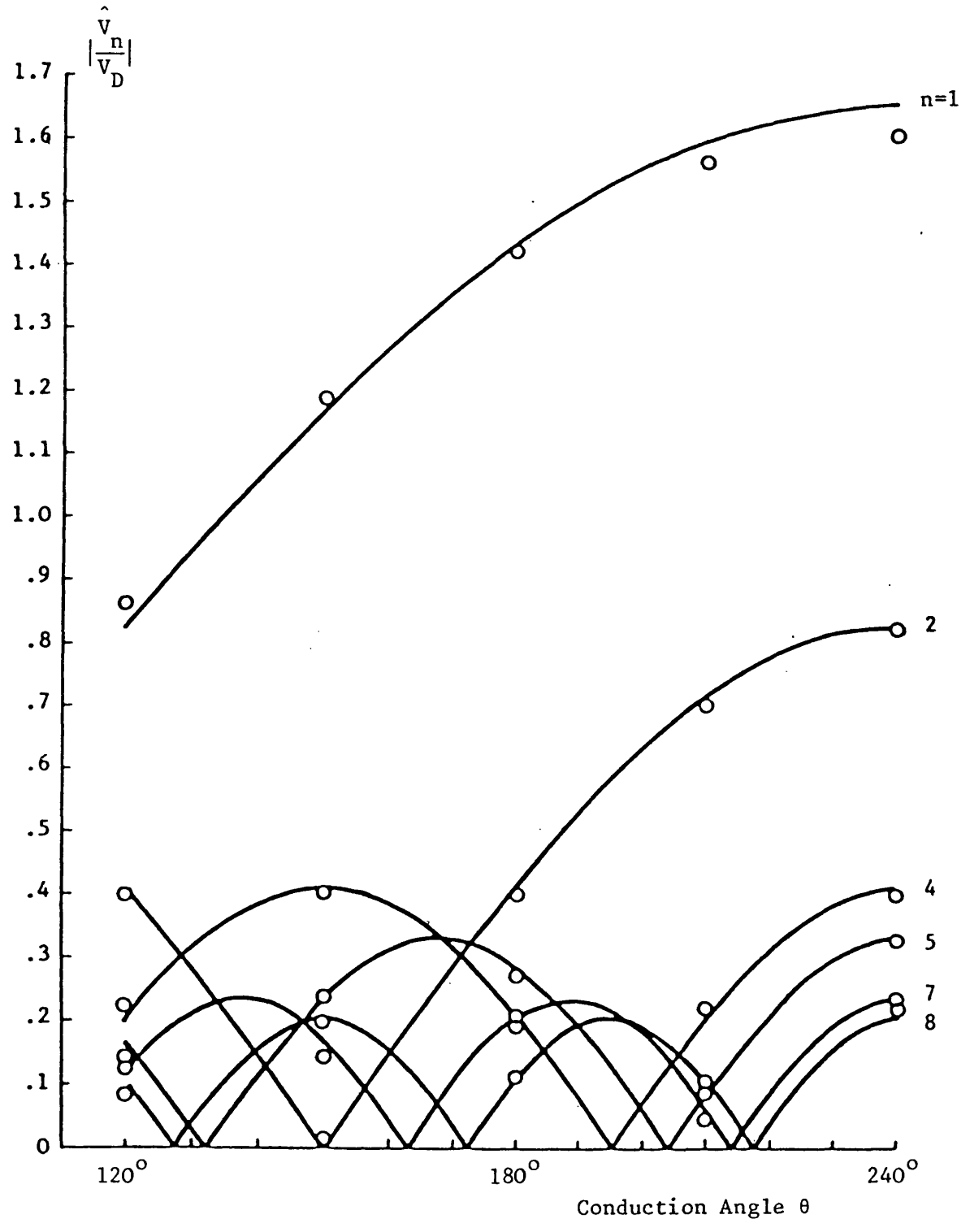

Fig. 2.7 Delta inverter with resistive load.
Harmonic content of line voltage for range of conduction angles.

O Experimental result

— Theoretical result

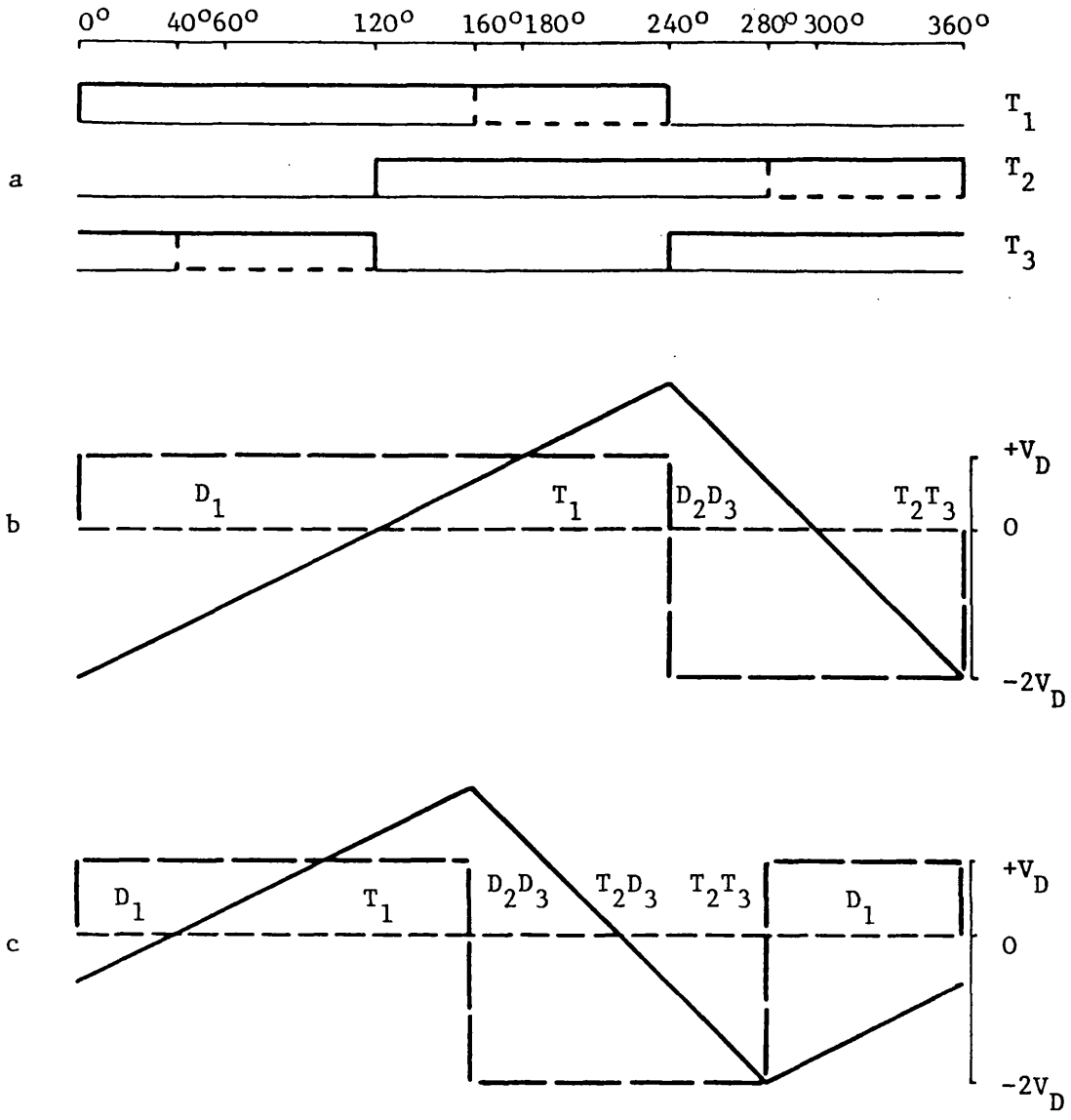

Fig. 2.8 Delta inverter with inductive load $160^{\circ} \leq \theta \leq 240^{\circ}$

a Transistor switching sequence

b Load voltage and current, 240° conduction

c Load voltage and current, 160° conduction

——— voltage

——— current

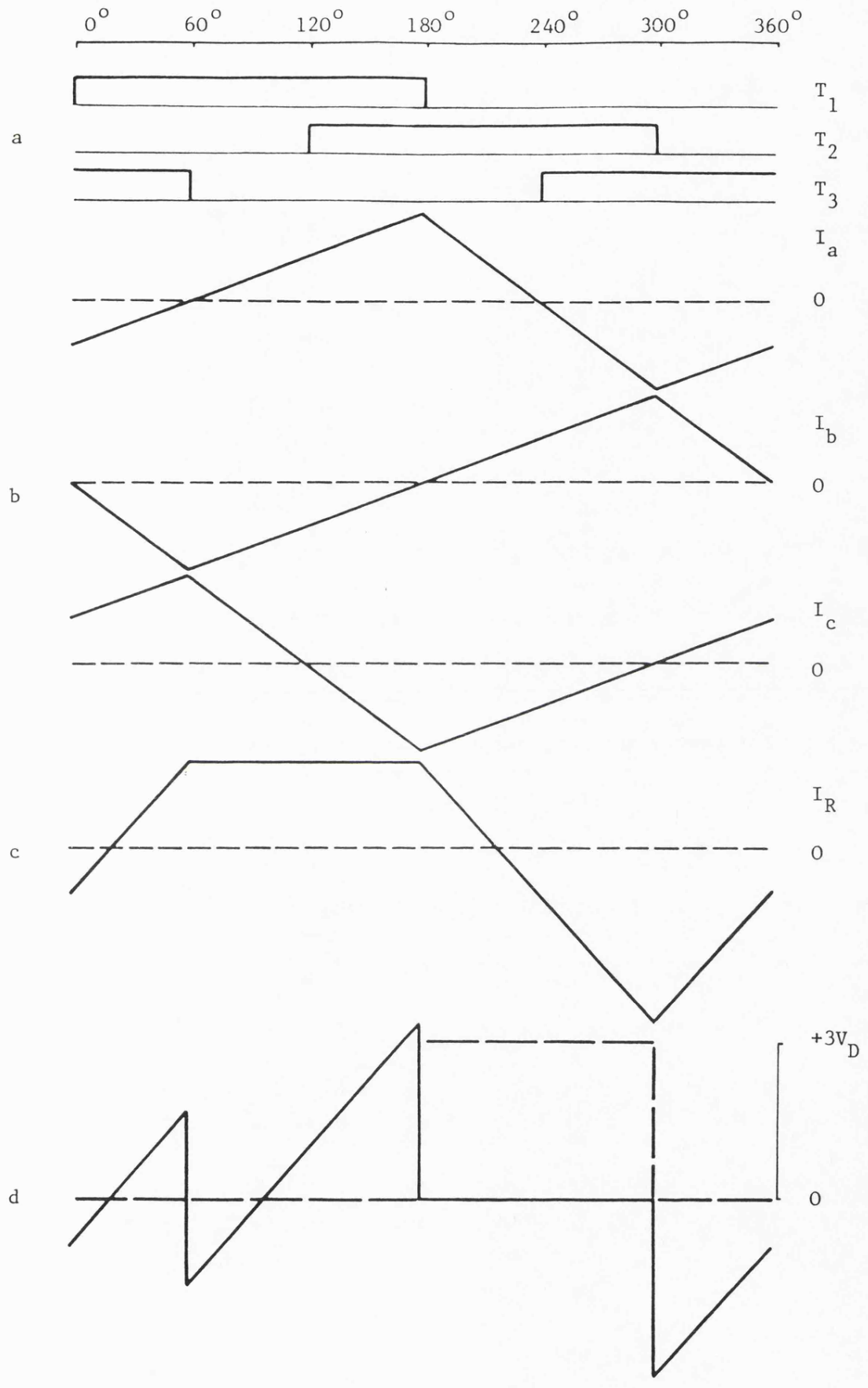

Fig. 2.9 Delta inverter with inductive load, $\theta = 180^\circ$

a Transistor switching sequence

b Load currents

c Line current

d Transistor and diode currents (————) and voltage (—— ——)

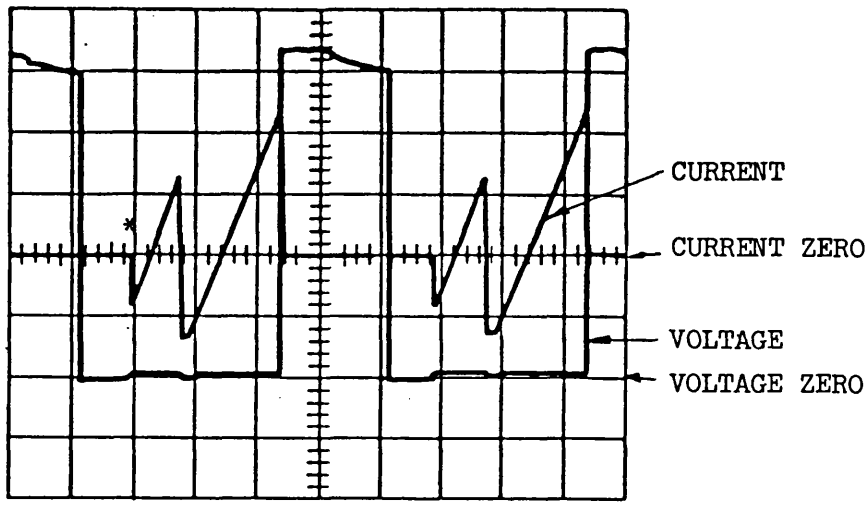

(a) TRANSISTOR

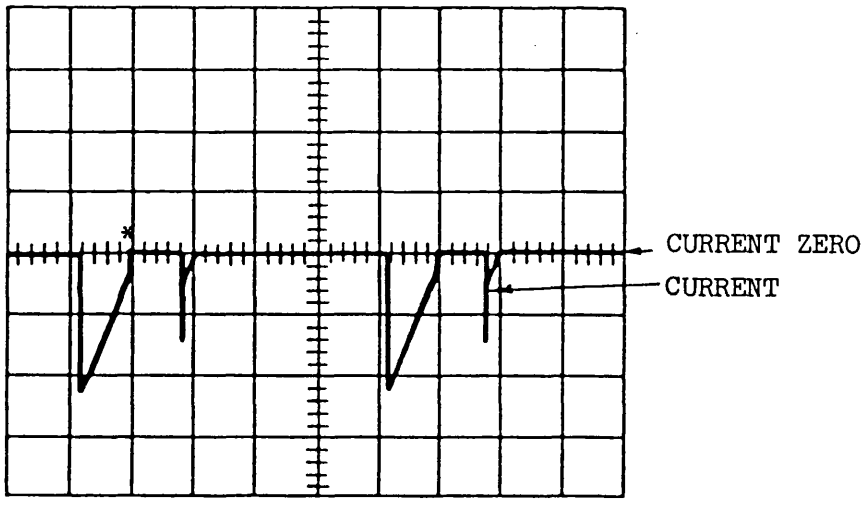

(b) DIODE

V = 20V/cm
i = 4A/cm
t = 2mS/cm

Fig. 2.10 Transistor and diode performance with inductive load, $\theta = 180^{o}$

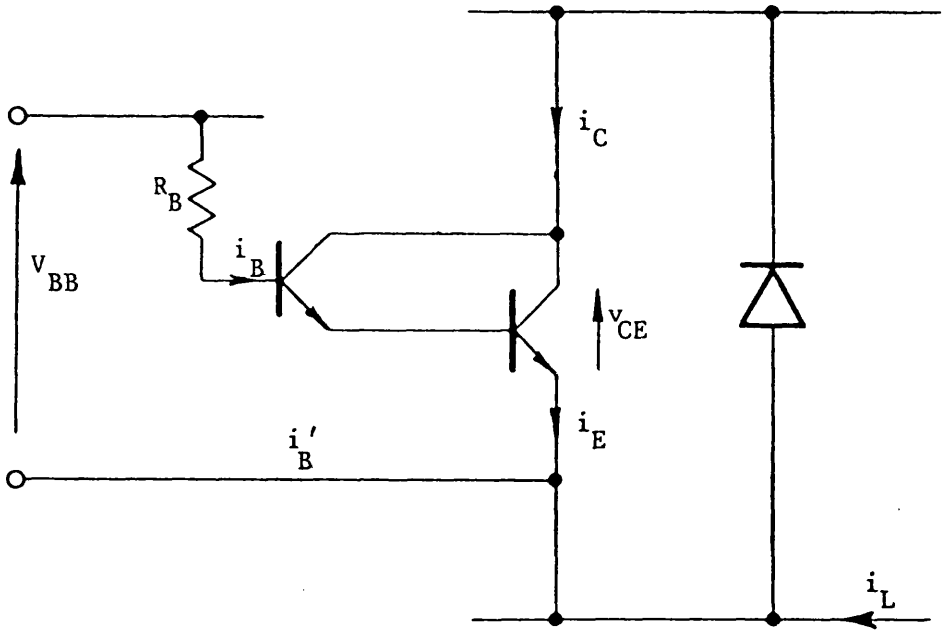

Fig. 2.11 Equivalent circuit of anti-parallel transistor-diode pair

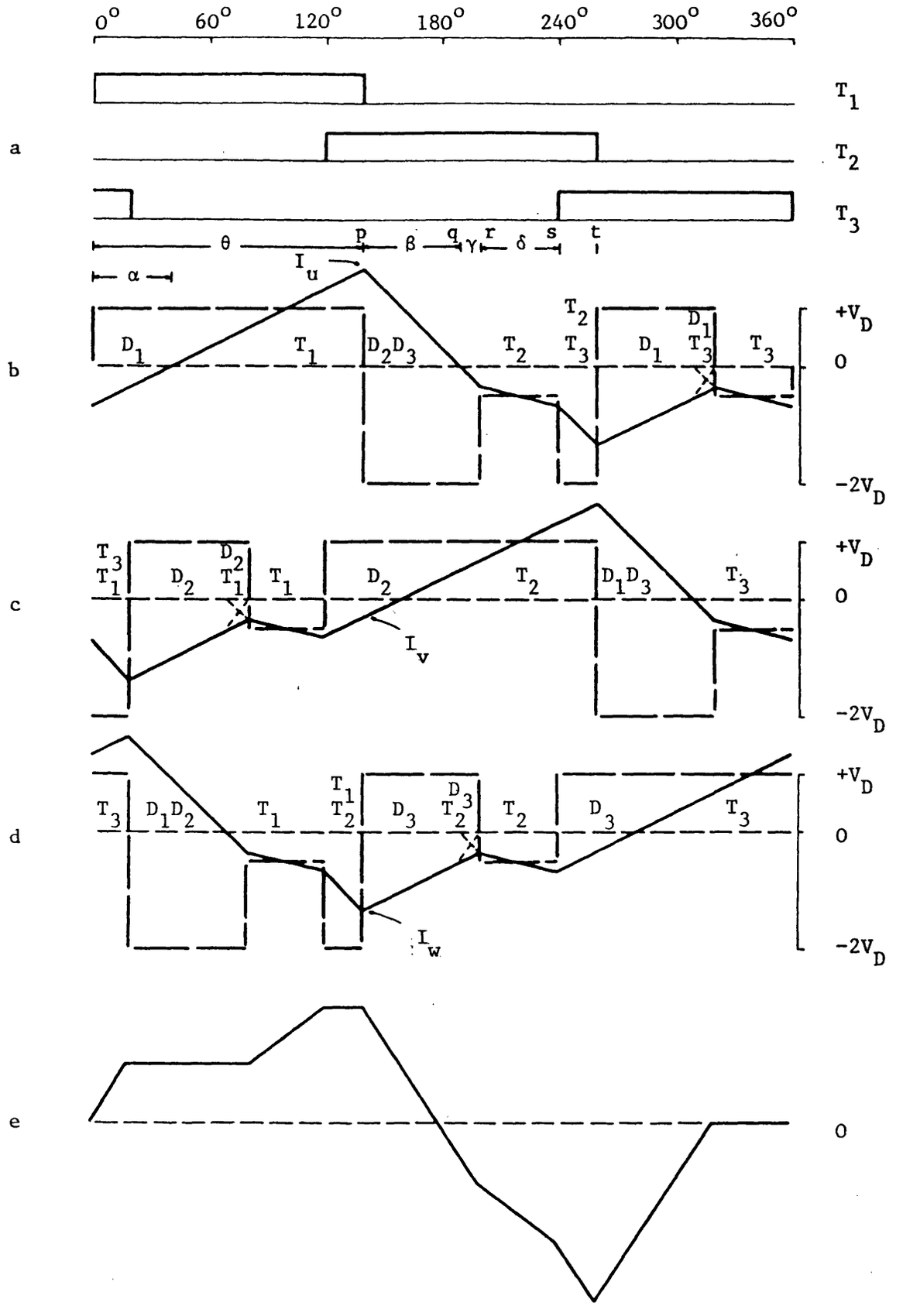

Fig. 2.12 Delta inverter with inductive load $\theta = 140^{\circ}$

a Transistor switching sequence

b Load a, voltage and current

c Load b, voltage and current

d Load c, voltage and current

e Line current I_R

——— voltage

——— current

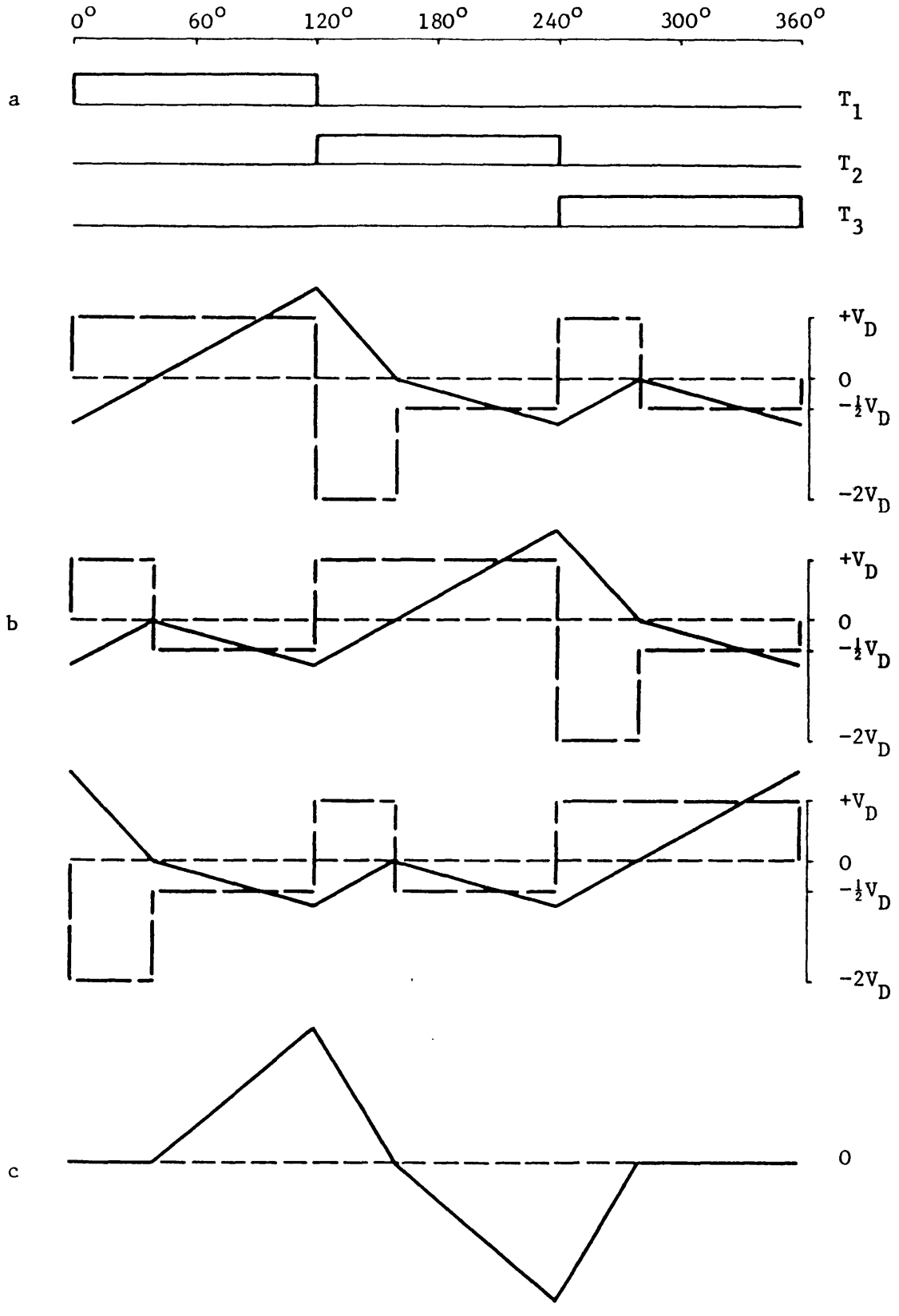

Fig. 2.13 Delta inverter with inductive load $\theta = 120^{\circ}$

a Transistor switching sequence
b Load a, voltage and current
c Load b, voltage and current
d Load c, voltage and current
e Line current I_R

—— —— voltage
——— current

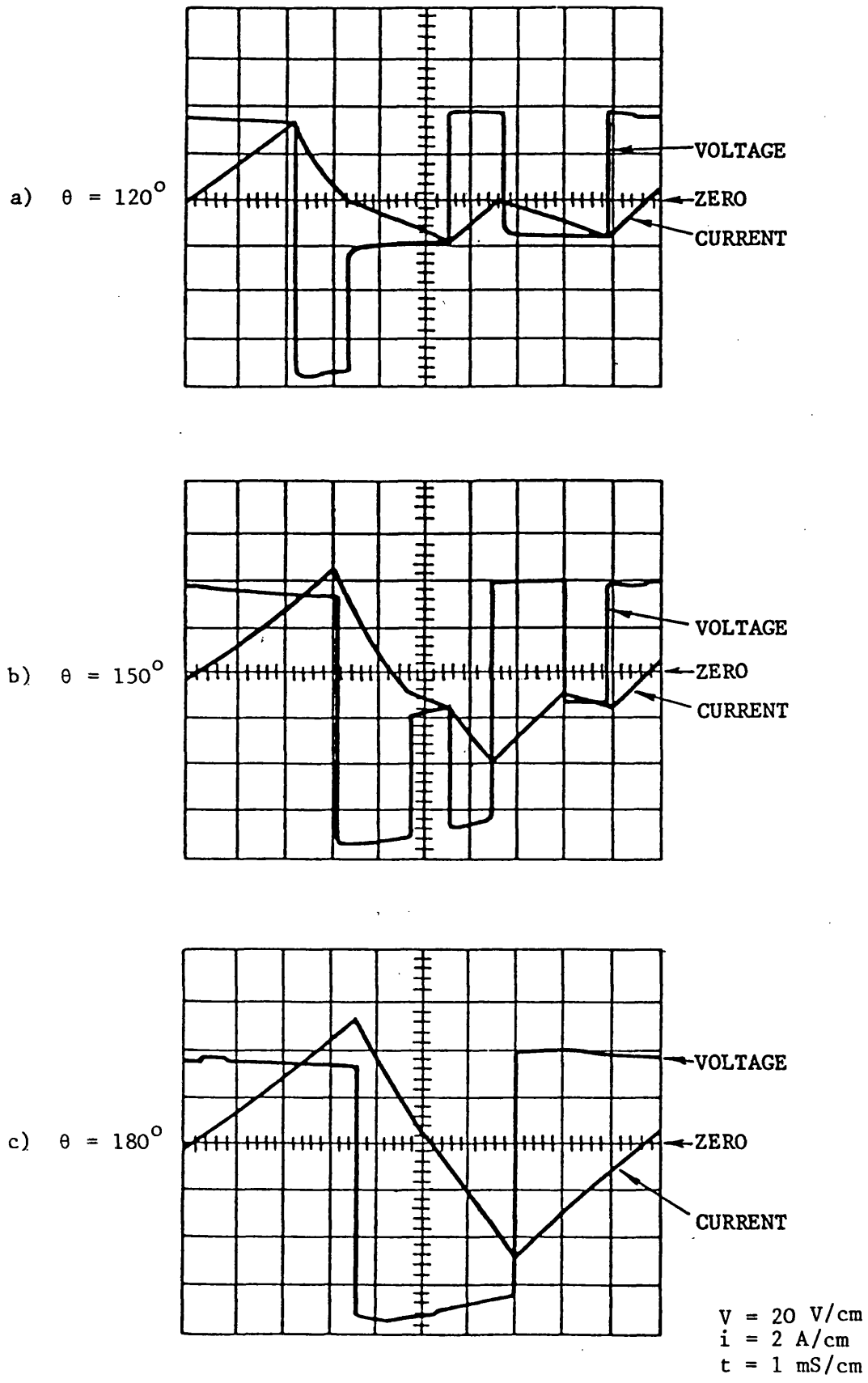

Fig. 2.14 Delta inverter with inductive load, load waveforms

	α		β		γ		δ	
θ	THEO	EXP	THEO	EXP	THEO	EXP	THEO	EXP
120°	40°	36°	40°	36°	0°	0°	80°	87°
140°	40°	36°	50°	46°	10°	7°	40°	50°
150°	40°	36°	55°	48°	15°	12°	20°	34°
160°	40°	36°	60°	51°	20°	15°	0°	15°

Note Experimental results were measured from an oscilloscope and are thus approximate

Fig. 2.15 Comparison of theoretical and experimental values of waveform angles with inductive load (see Fig. 2.12)

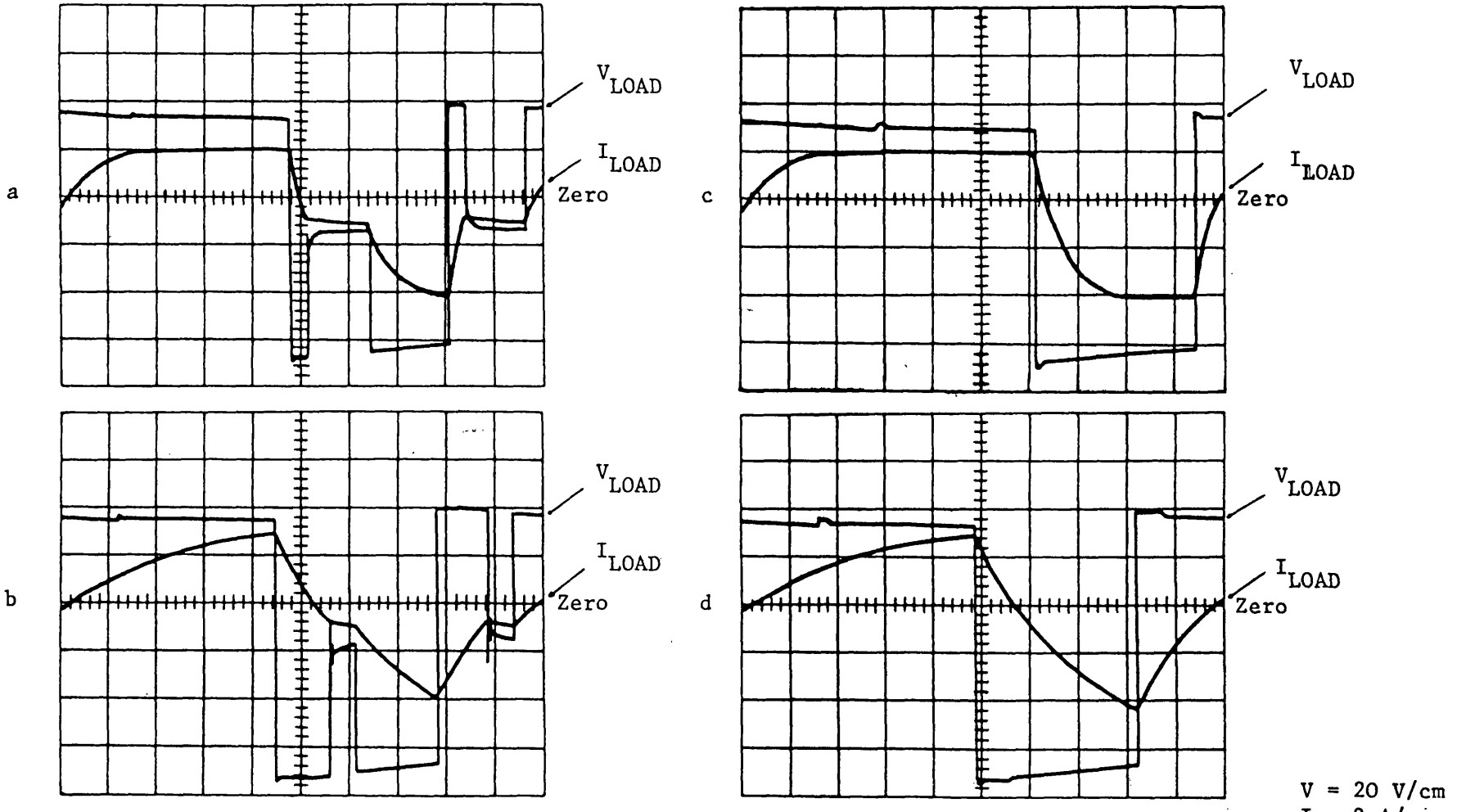

Fig. 2.16 Delta inverter with R-L load

a) Fairly resistive (T ≈ .4 mS)
b) Fairly inductive (T ≈ 2.3 mS)
} 180^{o} conduction

c) Fairly resistive (T ≈ .4 mS)
d) Fairly inductive (T ≈ 2.3 mS)
} 240^{o} conduction

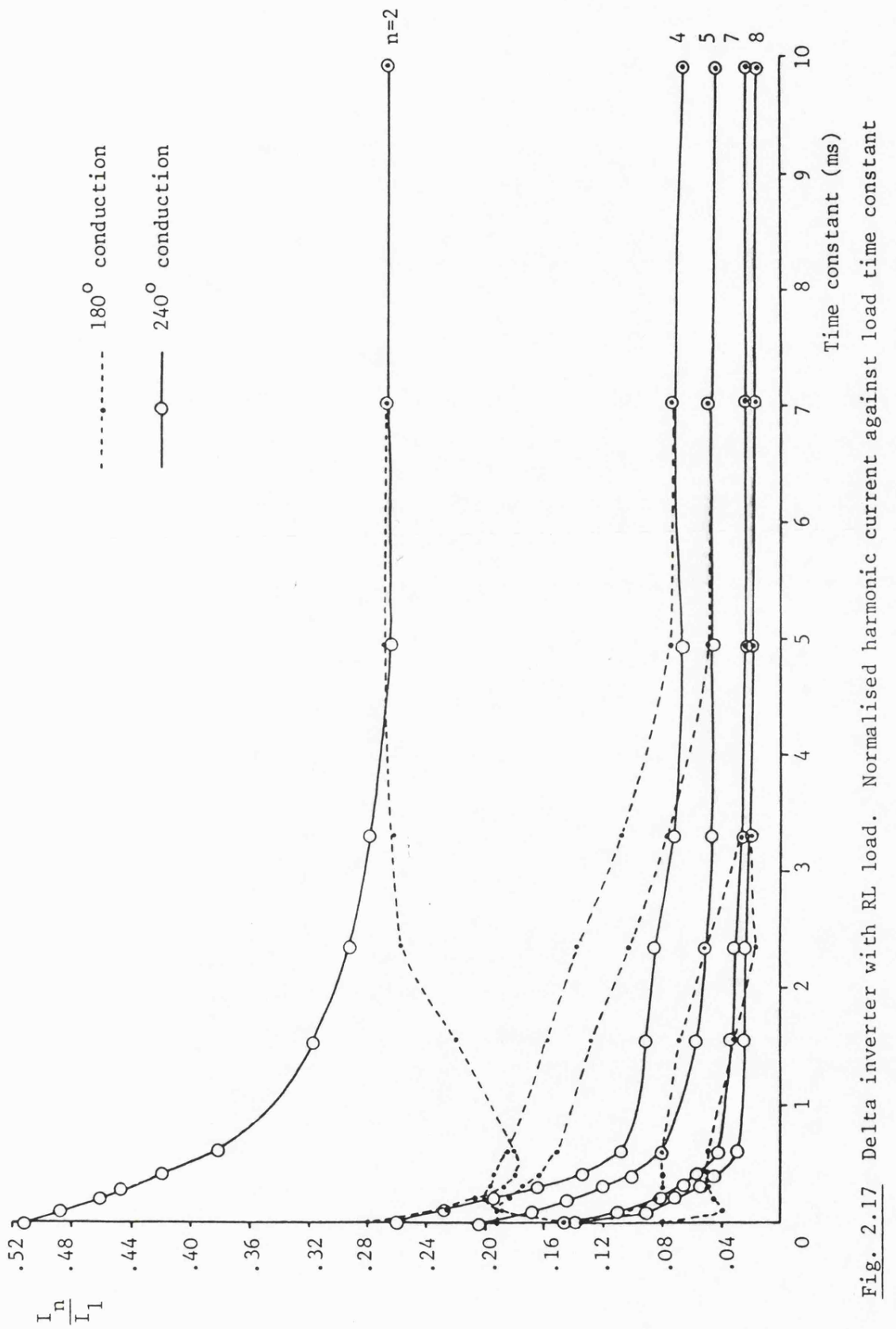

Fig. 2.17 Delta inverter with RL load. Normalised harmonic current against load time constant

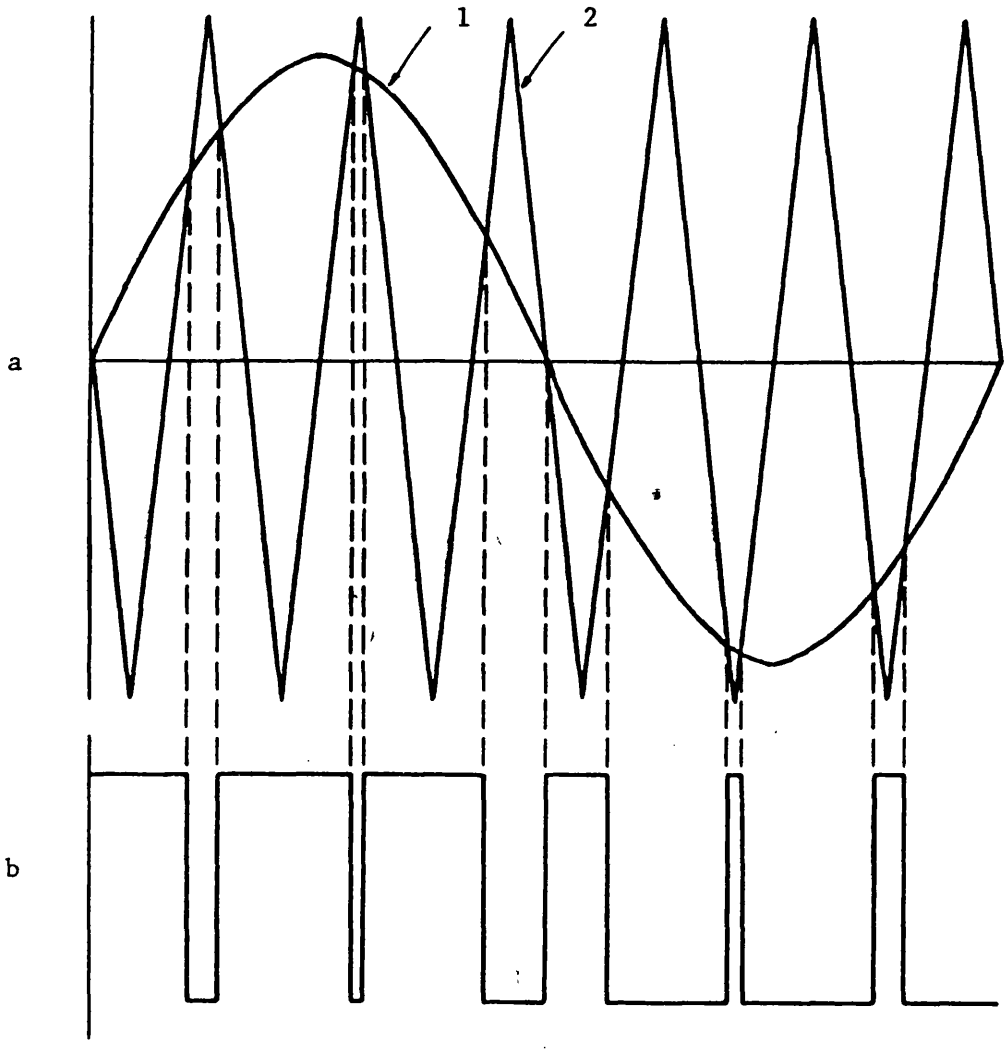

Fig. 3.1 Natural Sampling with Double Edge Modulation

a) Modulating sinusoid (1) and triangular carrier (2)
b) Modulated pulse train

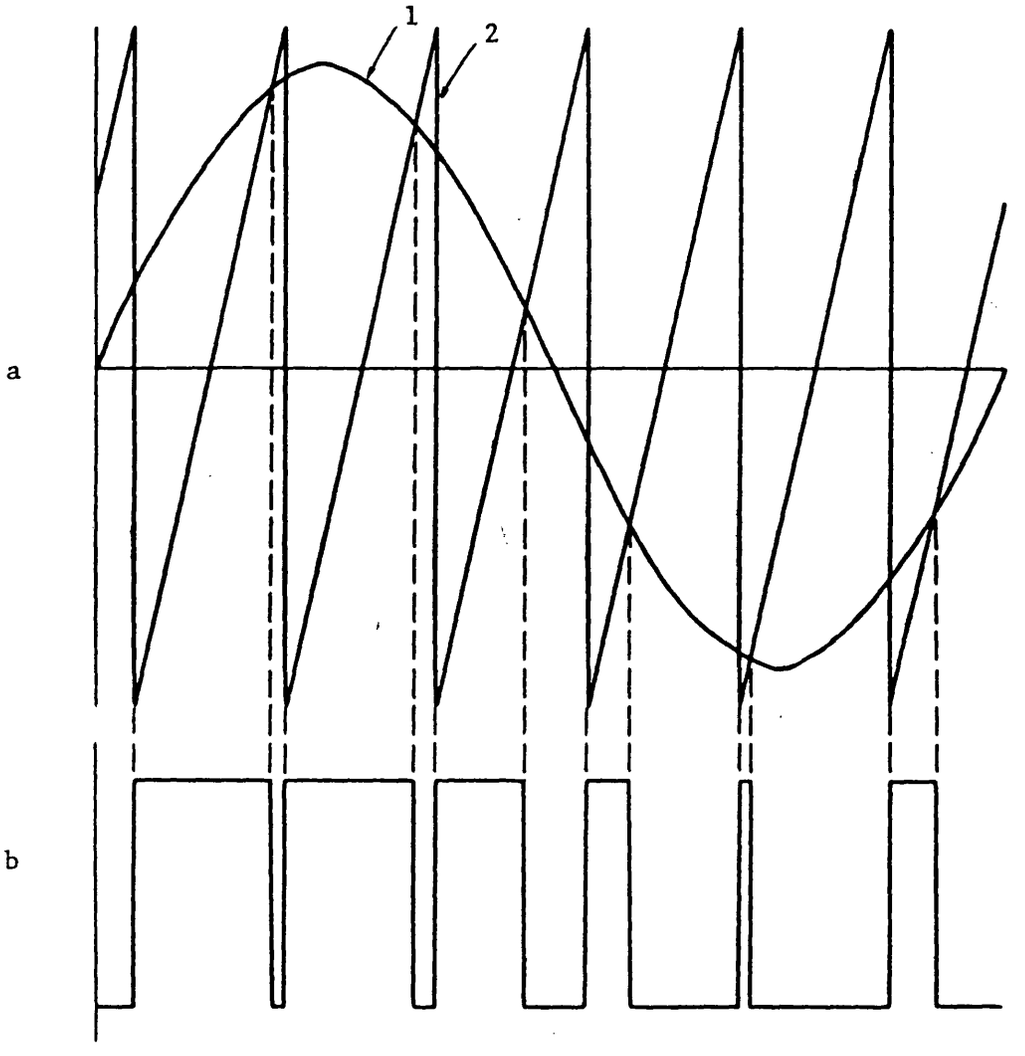

Fig. 3.2 Natural Sampling with Single (Lagging) Edge Modulation

a) Modulating sinusoid (1) and sawtooth carrier (2)
b) Modulated pulse train

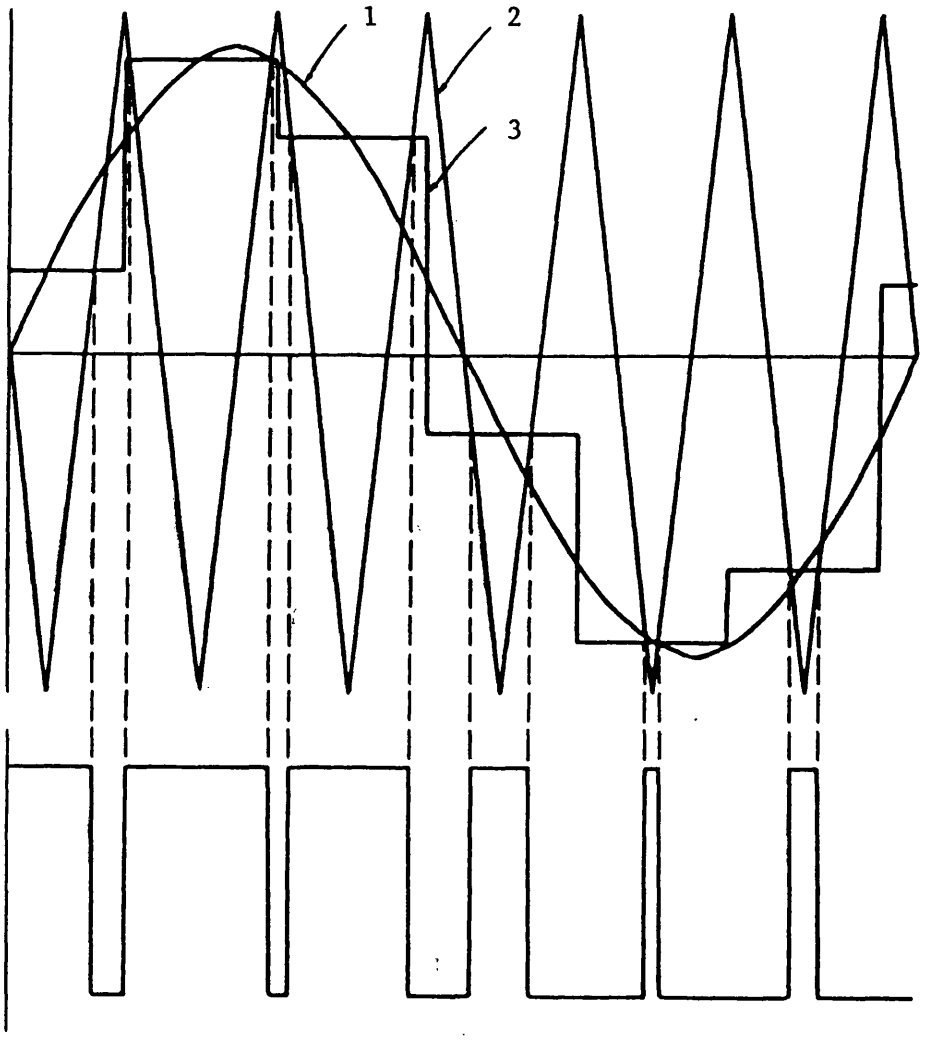

Fig. 3.3 Uniform Sampling with Symmetric Double Edge Modulation

a) Modulating sinusoid (1), triangular carrier (2) and stepped waveform (3)
b) Modulated pulse train

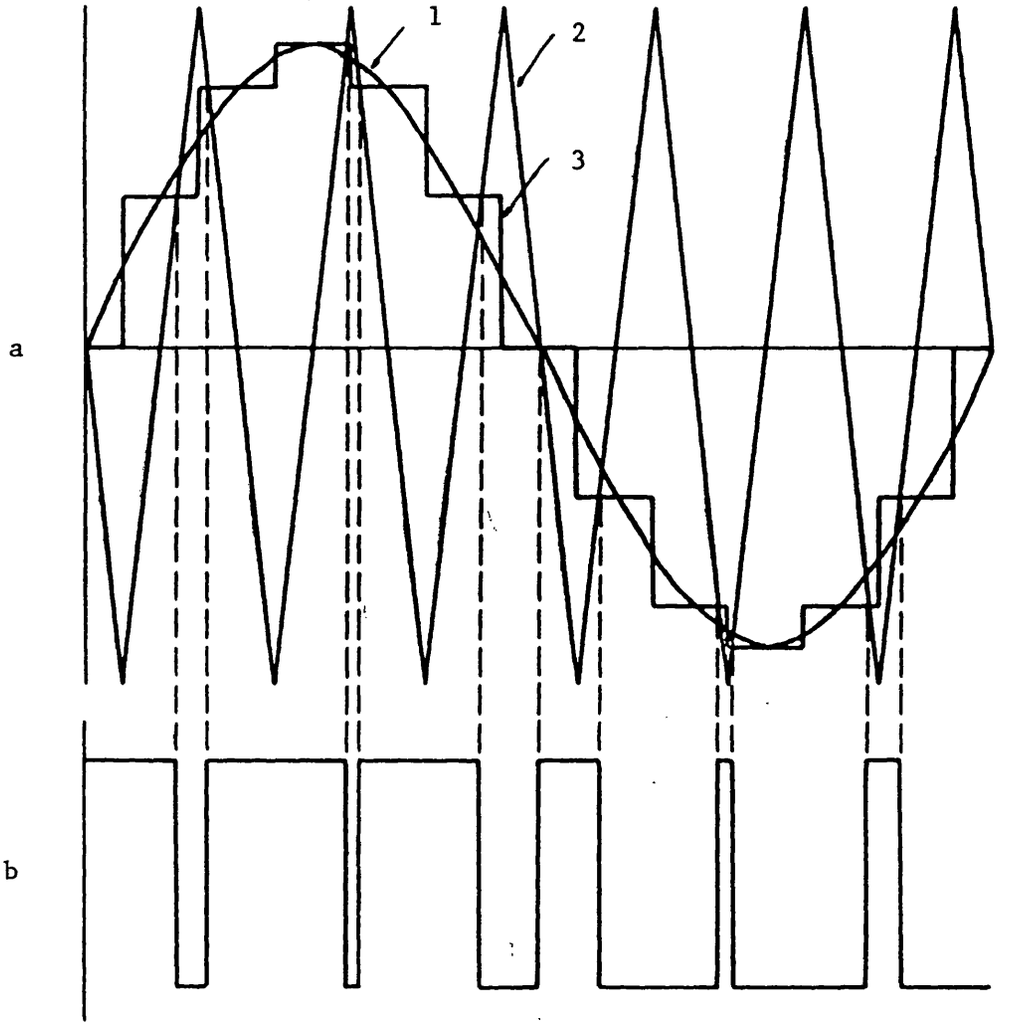

Fig. 3.4 Uniform Sampling with Asymmetric Double Edge Modulation

a) Modulating Sinusoid (1), triangular carrier (2), and stepped waveform (3)
b) Modulated pulse train

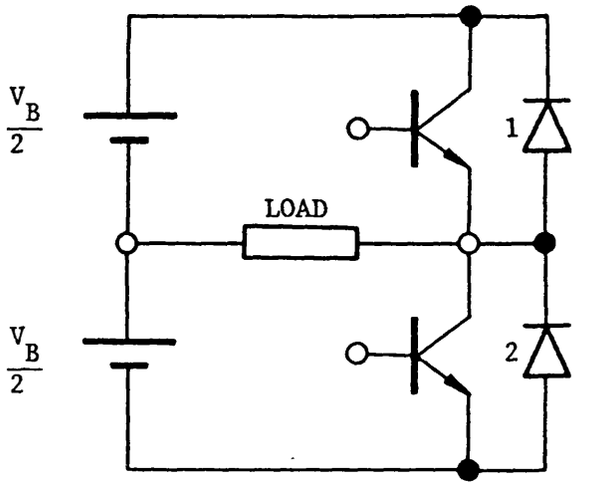

Fig. 3.5a Single-phase Centre-tapped or Half Bridge Inverter

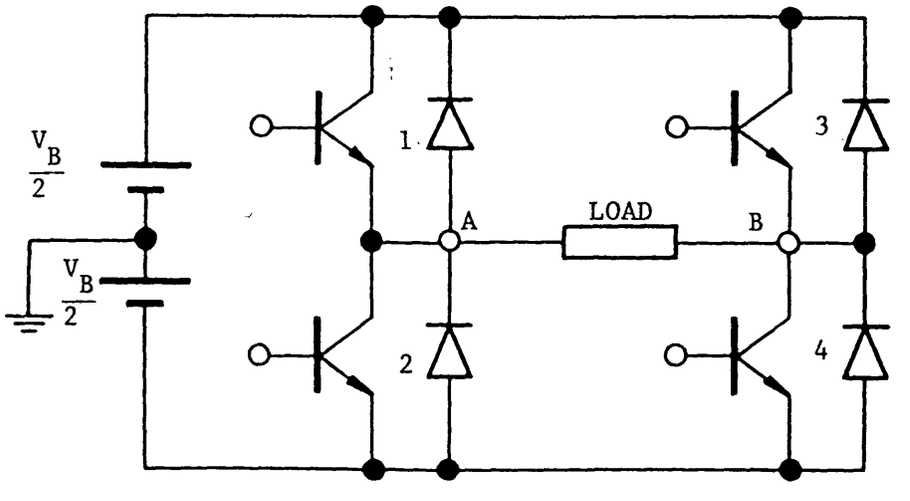

Fig. 3.5b Single-phase Bridge Inverter

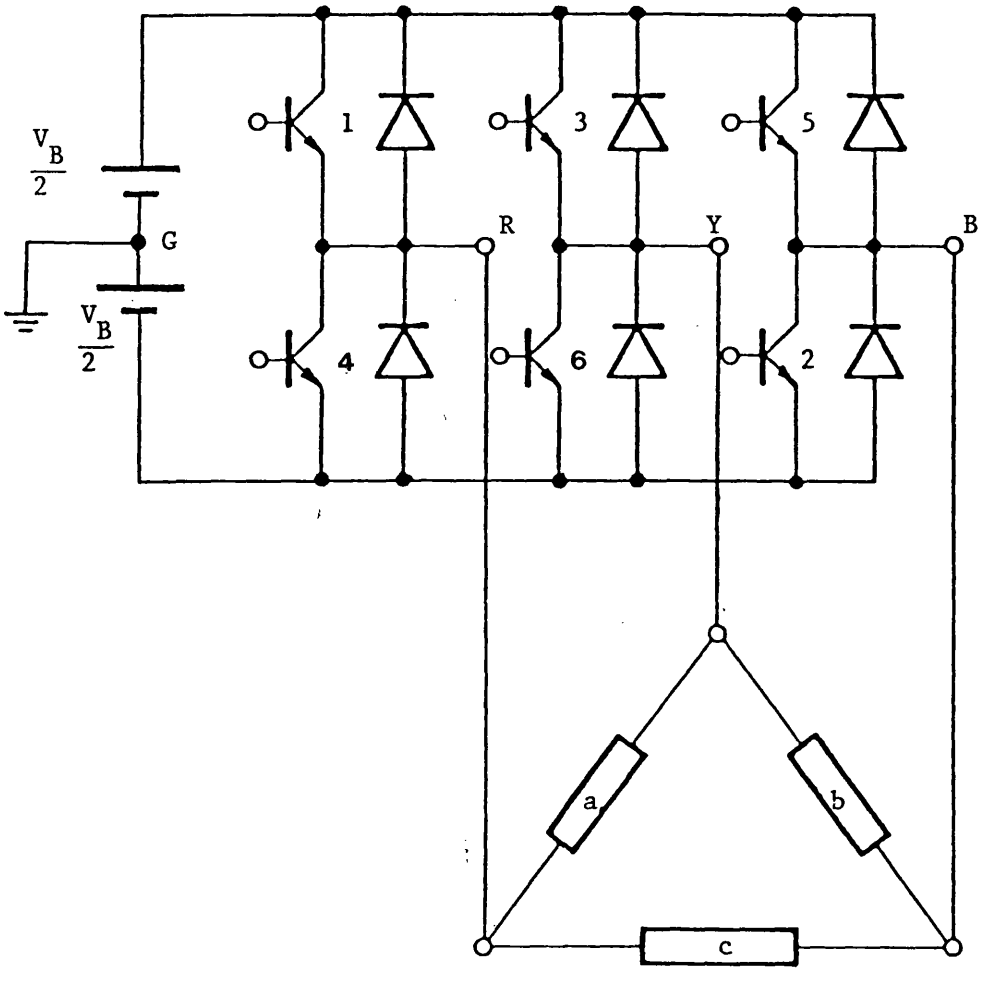

Fig. 3.6 Three-phase Bridge Inverter

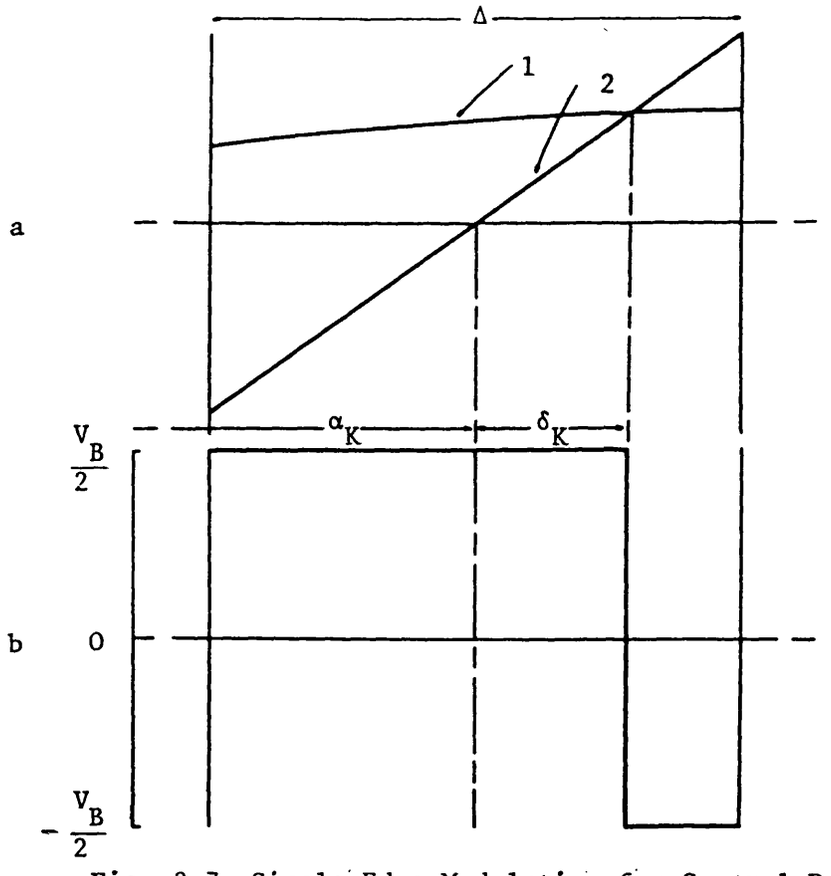

Fig. 3.7 Single Edge Modulation for General Pulse - Bridge Inverter

a) Modulating sinusoid (1) and sawtooth (ramp) carrier (2)
b) Modulated pulse

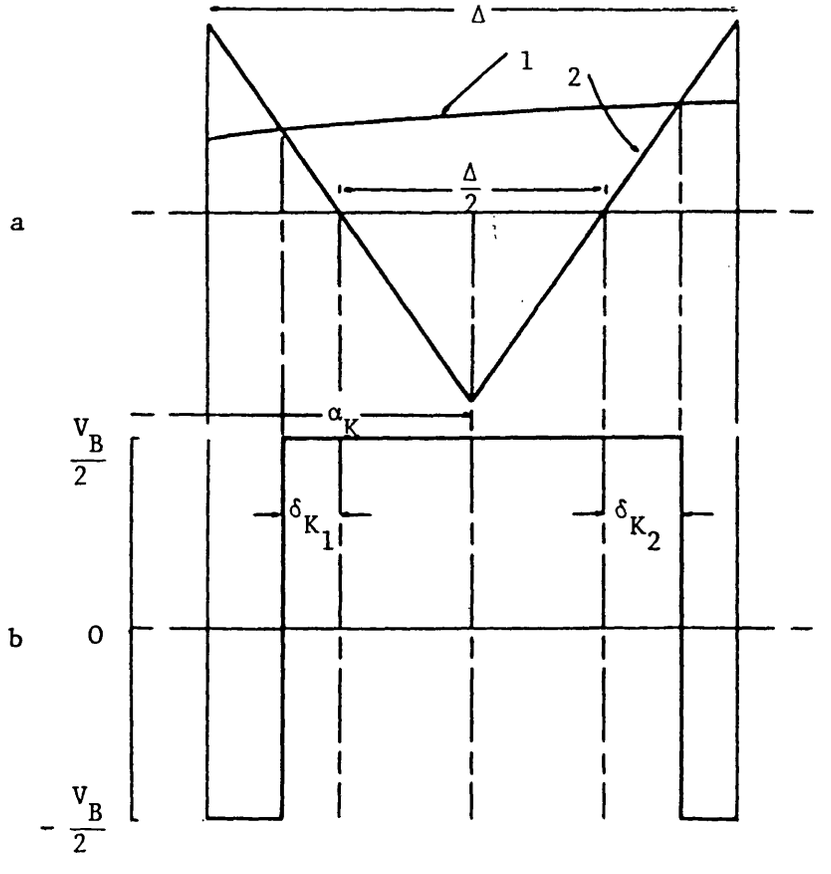

Fig. 3.8 Double Edge Modulation for General Pulse - Bridge Inverter

a) Modulating sinusoid (1) and triangular carrier (2)
b) Modulated pulse

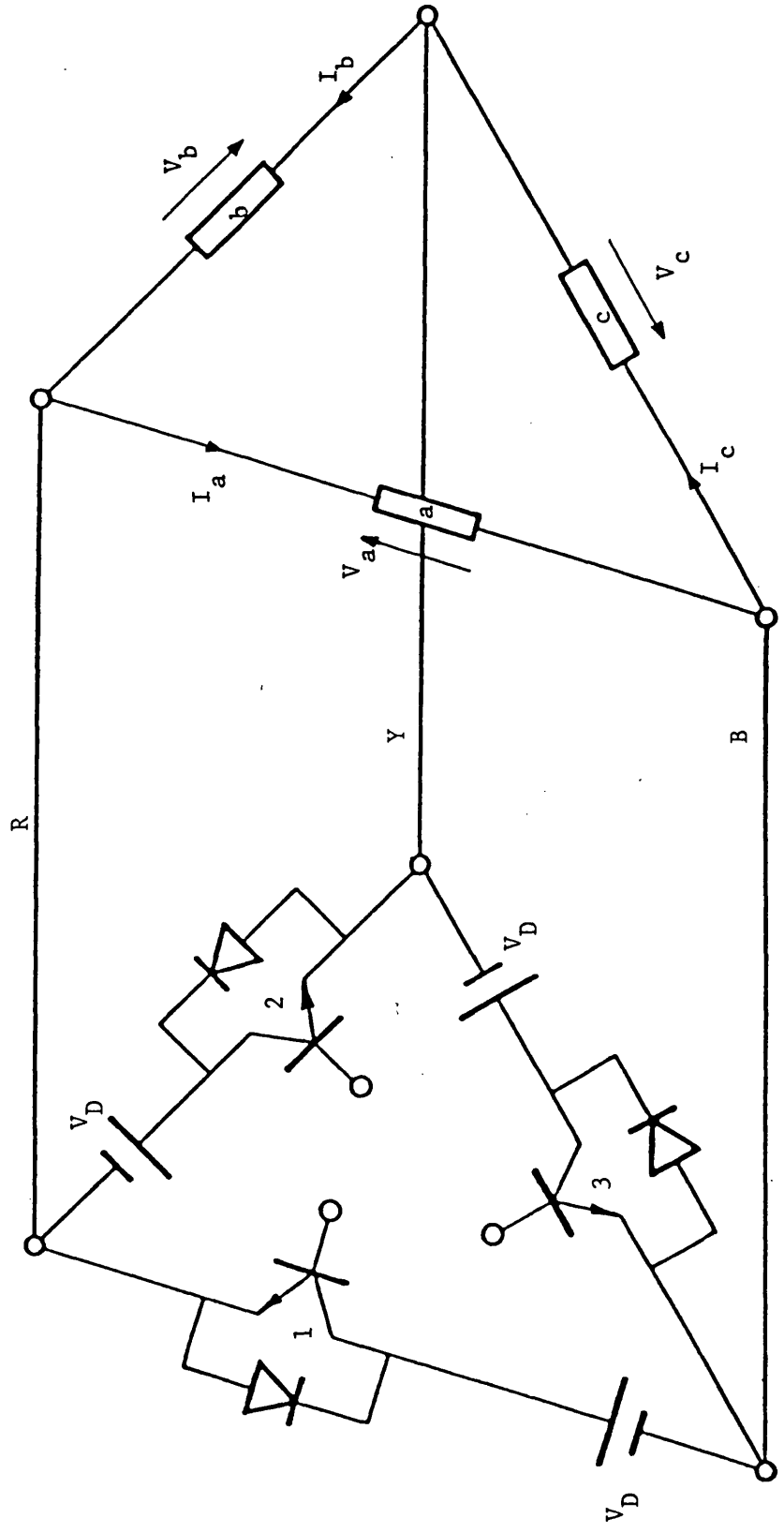

Fig. 3.9 Delta Inverter and Load

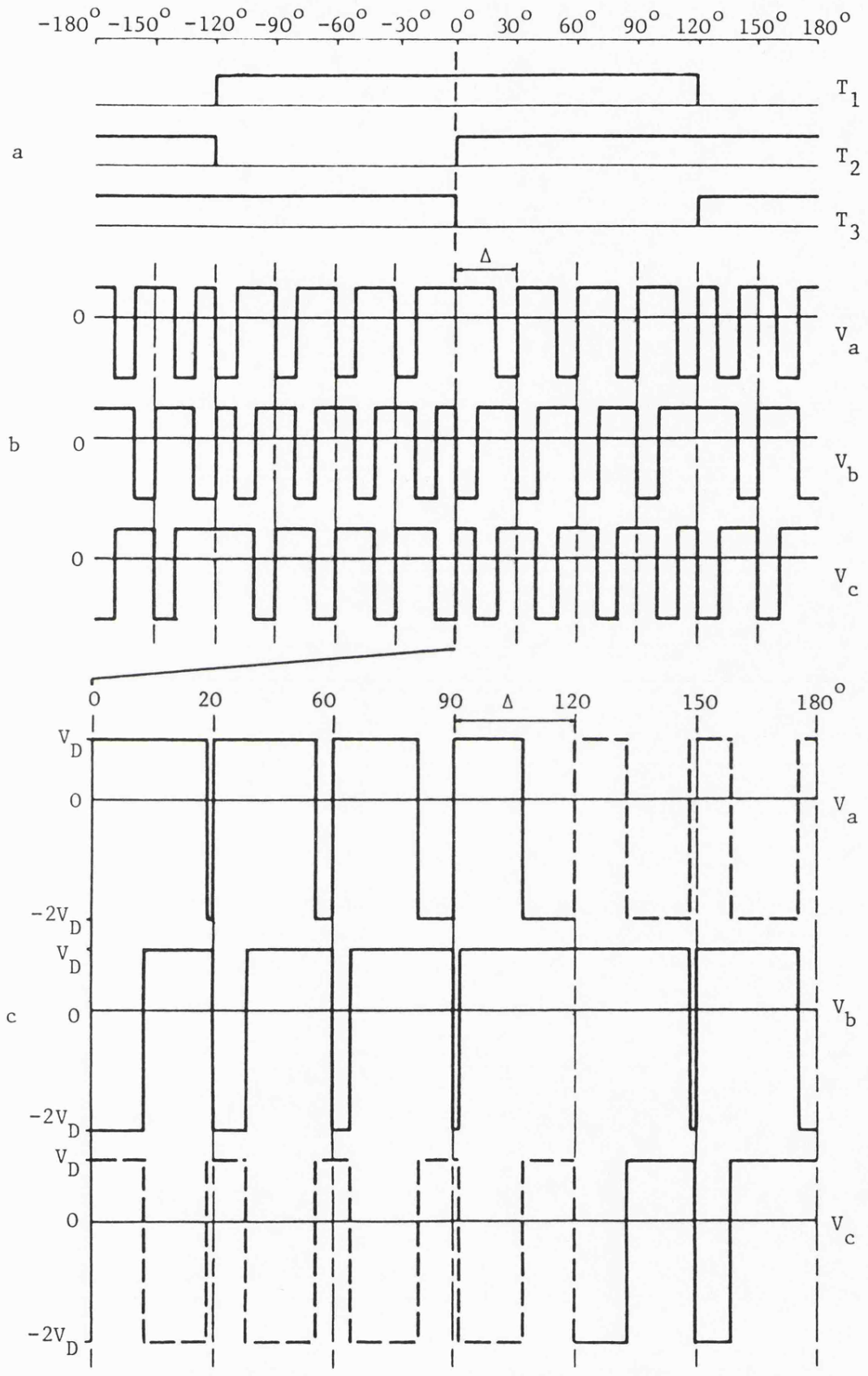

Fig. 3.10 Single Edge Modulation with Delta Inverter

a) Control bands
b) Unmodulated pulse trains (line voltages)
c) Modulated pulse trains (line voltages)

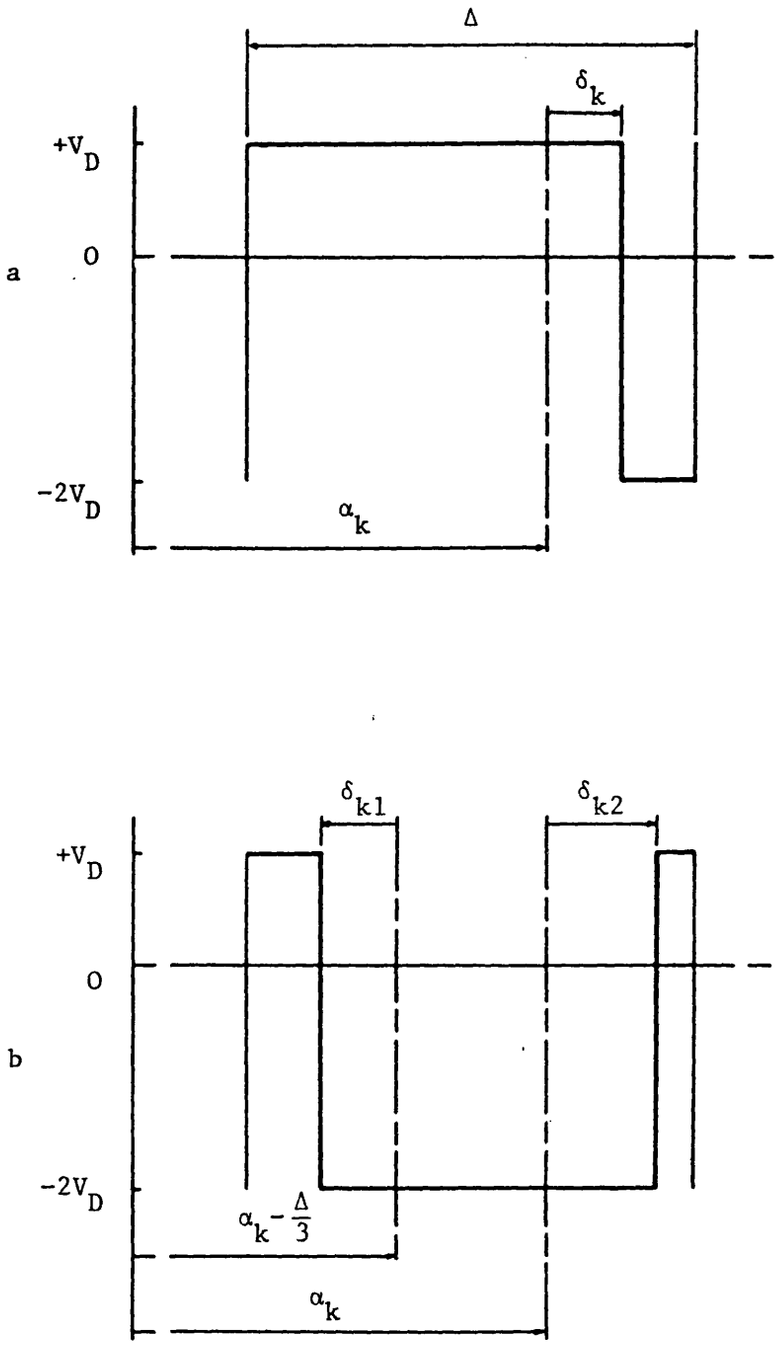

Fig. 3.11 Modulating Pulse Shapes, Single Edge Modulation

a) General pulse within control band
b) General pulse outside control band

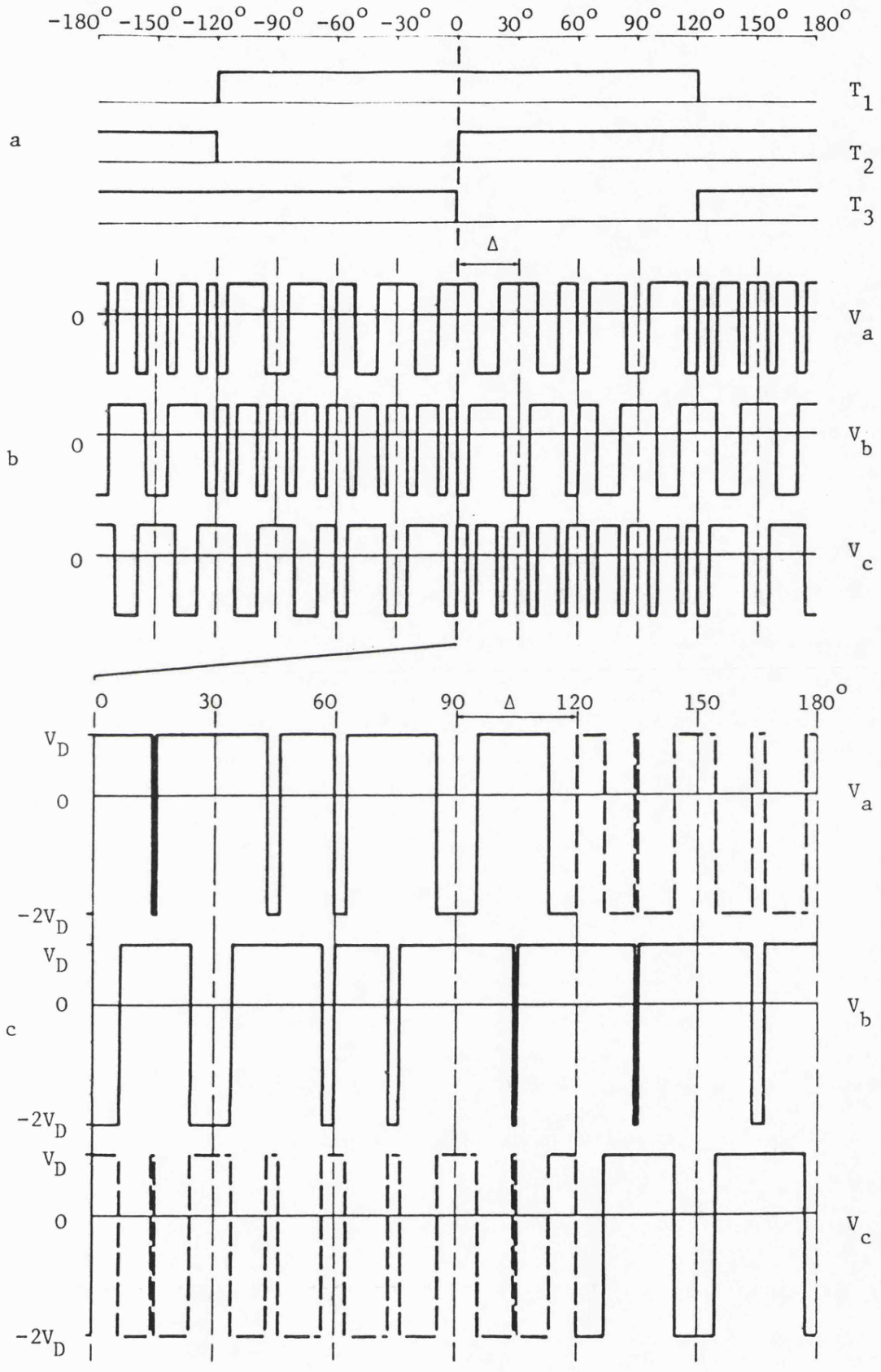

Fig. 3.12 Double Edge Modulation with Delta Inverter

a) Control bands
b) Unmodulated pulse trains (line voltages)
c) Modulated pulse trains (line voltages)

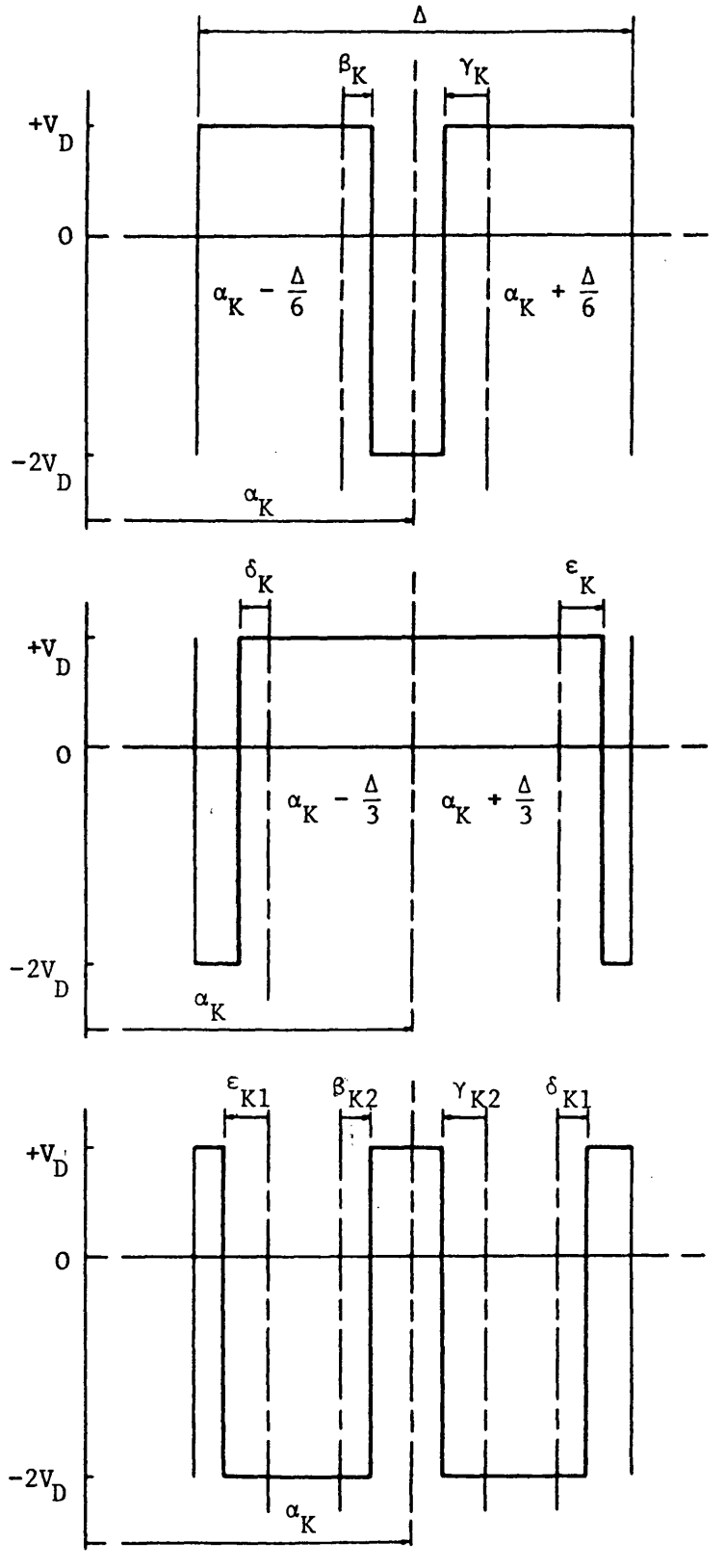

Fig. 3.13 Modulating Pulse Shapes, Double Edge Modulation

a) General pulse within control band (0-60°)
b) General pulse within control band (60-120°)
c) General pulse outside control band

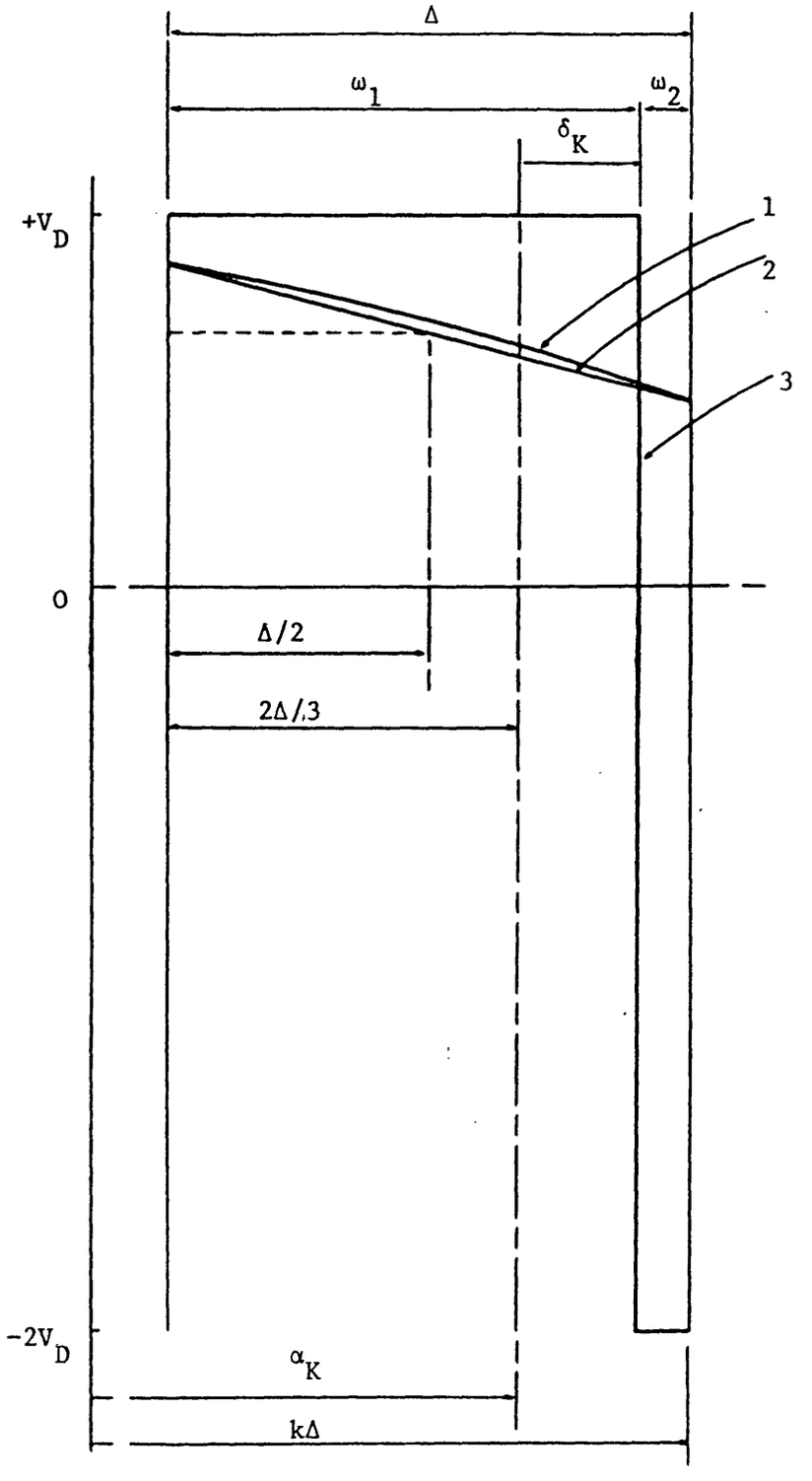

Fig. 3.14 General Pulse for Lagging Edge Modulation
- Method of Linear Piecewise and Equal Area

1) Cosinusoidal modulating signal
2) Linear approximation to modulating signal
3) Resultant modulated pulse for both methods

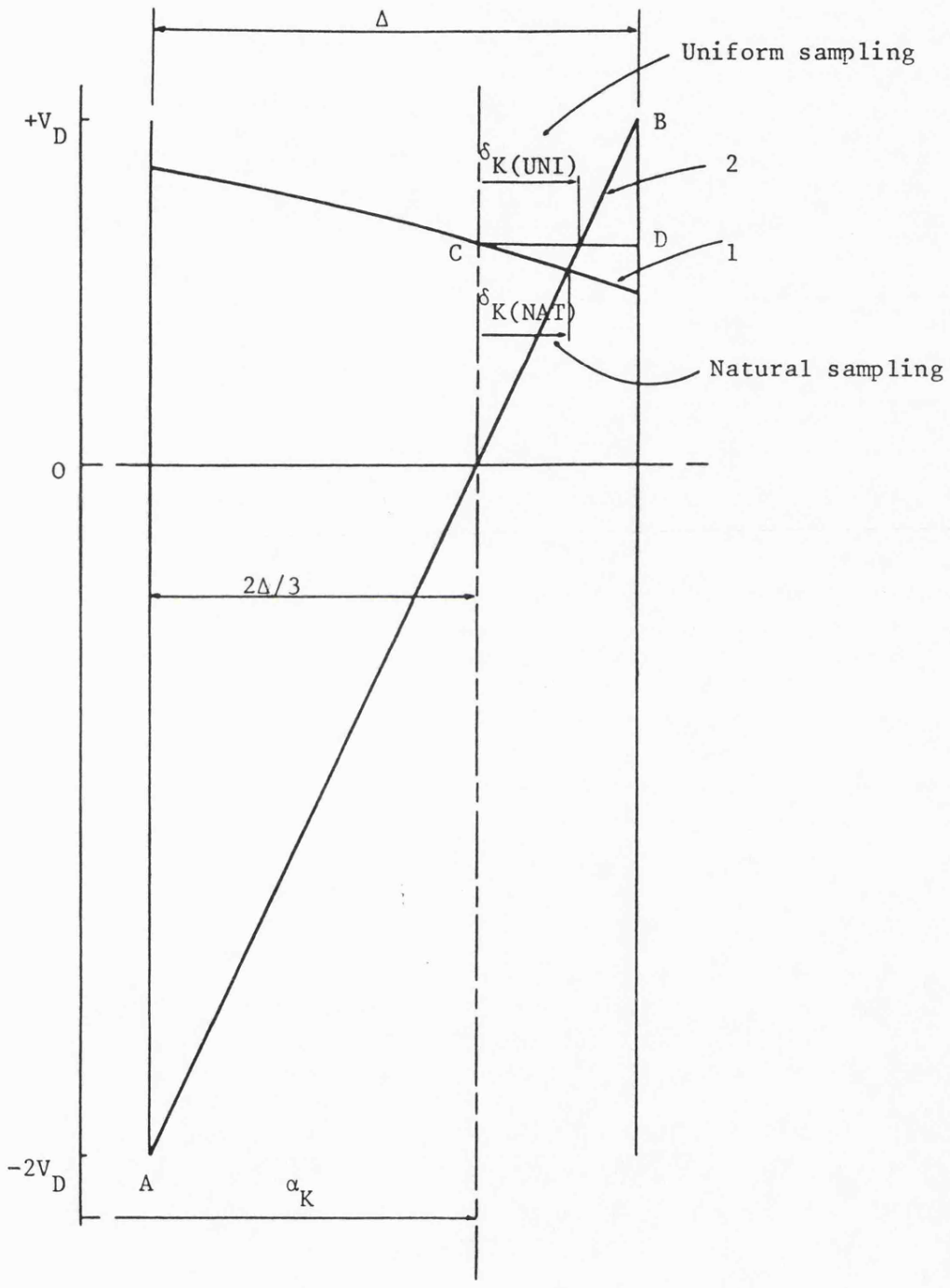

Fig. 3.15 General Pulse for Lagging Edge Modulation - Methods of Natural and Uniform Sampling

1) Cosinusoidal modulating signal
2) Ramp function

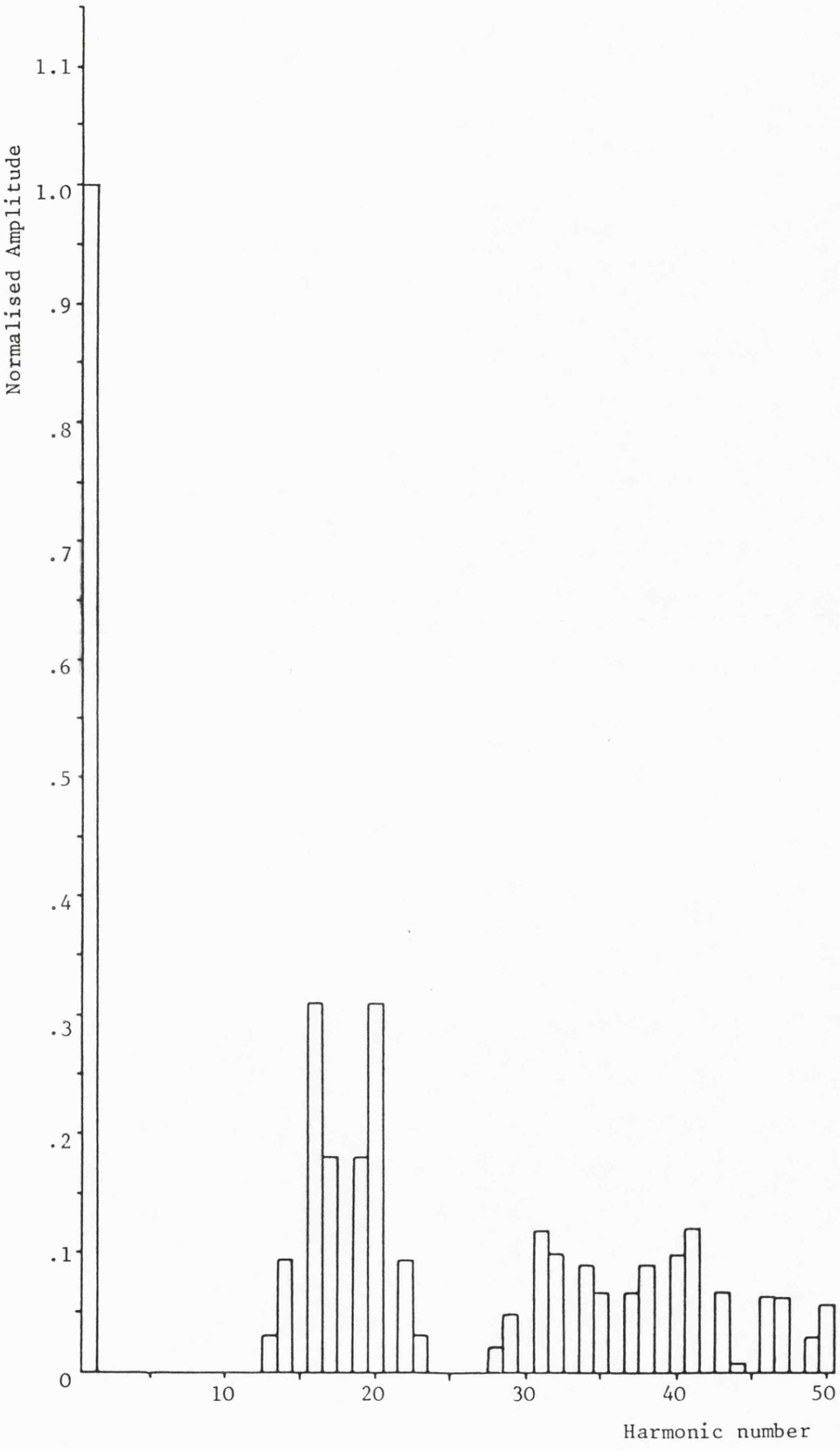

Fig. 3.16 Harmonic Spectrum Single Edge Modulation, Natural Sampling - Bridge Inverter

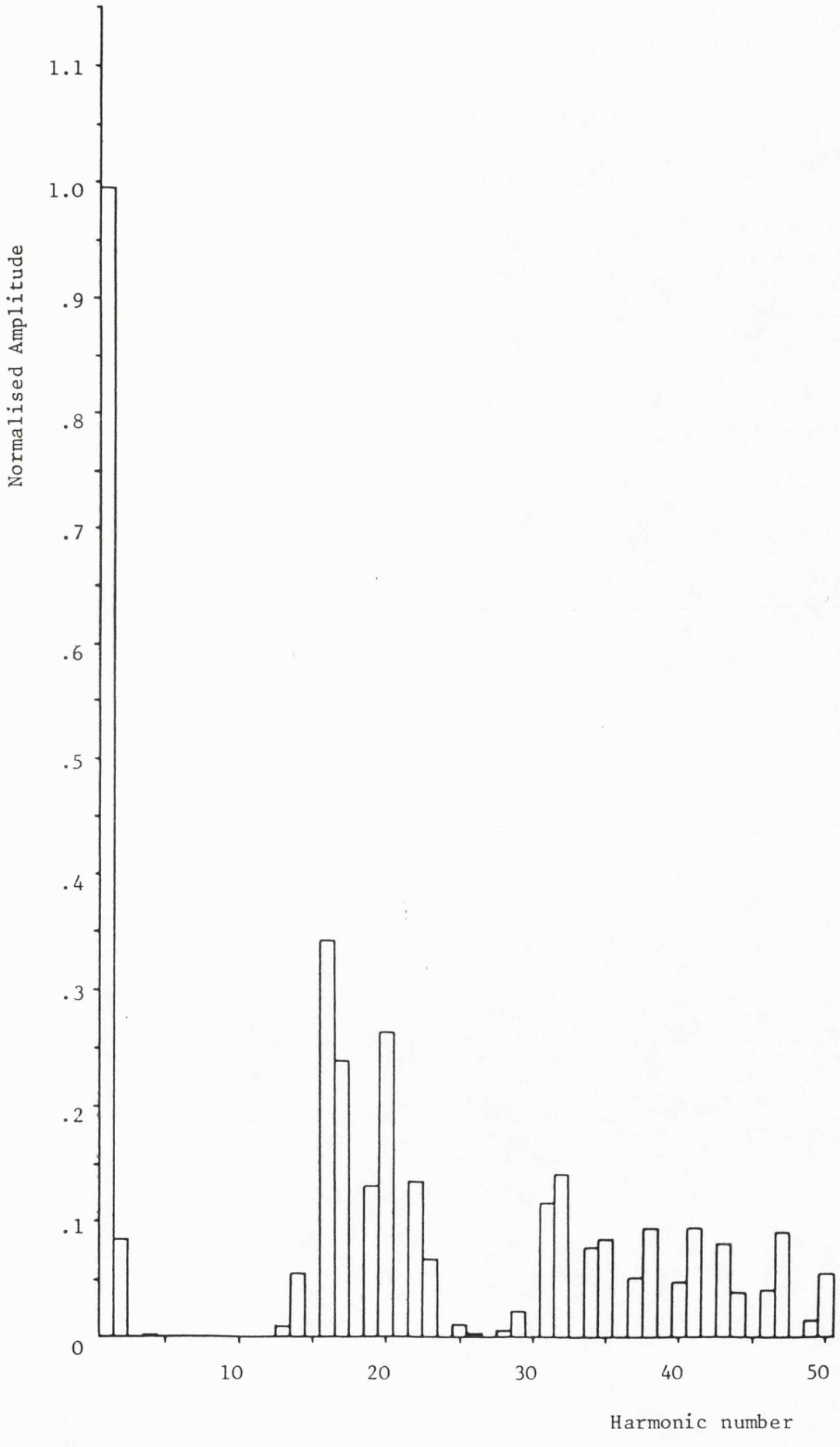

Fig. 3.17 Harmonic Spectrum, Single Edge Modulation, Uniform Sampling - Bridge Inverter

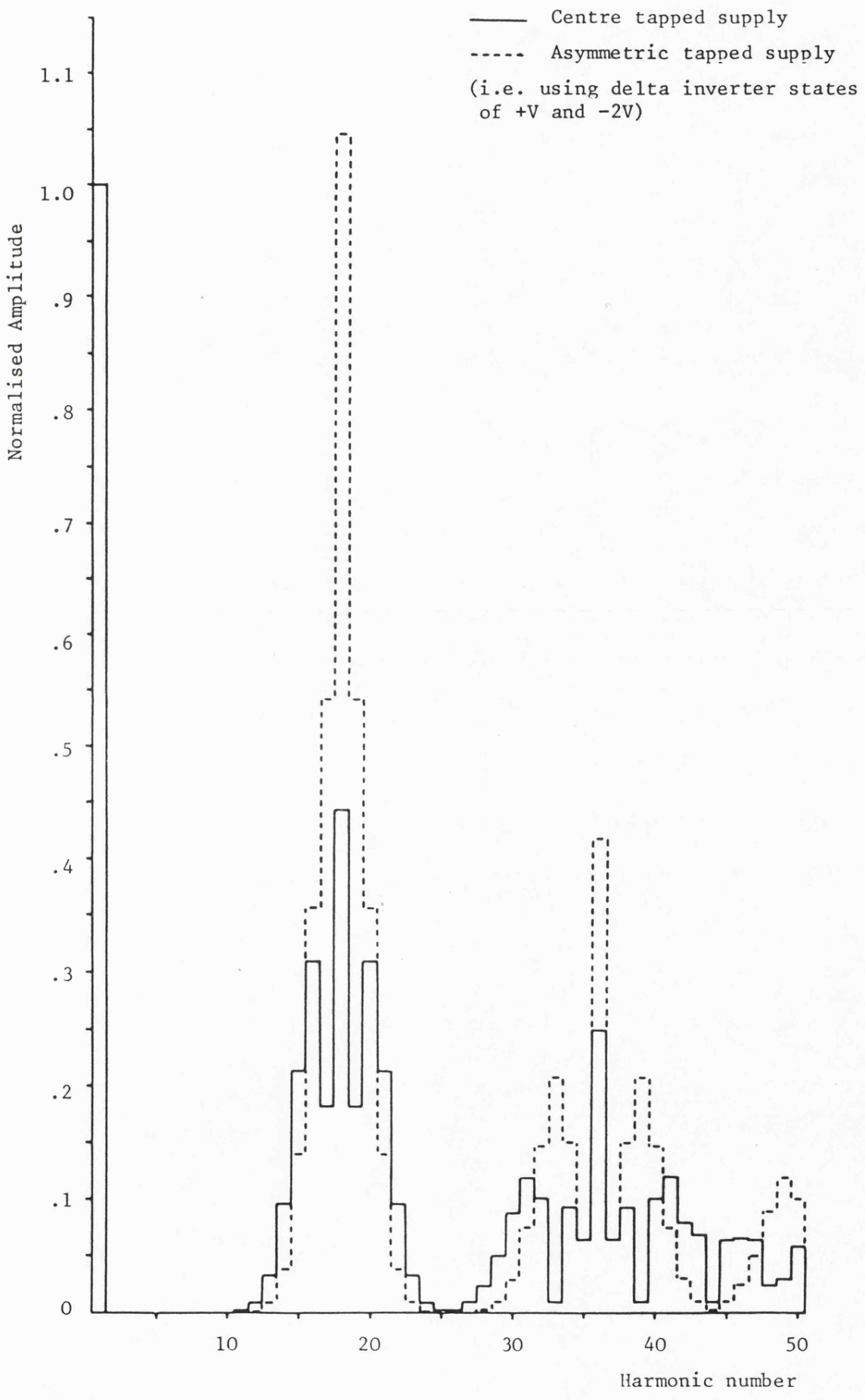

Fig. 3.18 Pseudo Phase Voltage Spectra With the Bridge Inverter - Single Edge Modulation, Natural Sampling

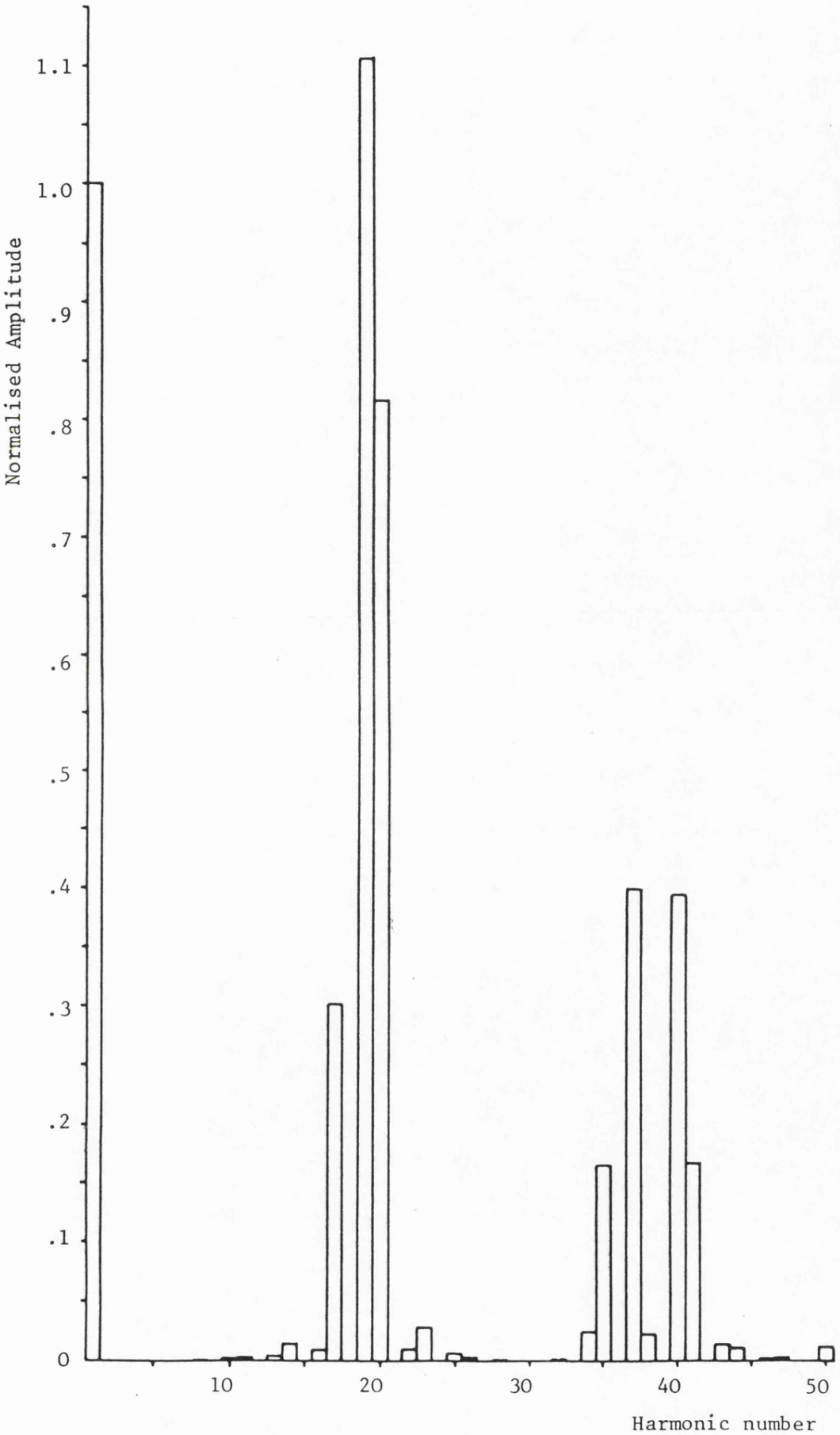

Fig. 3.19 Harmonic Spectrum Single Edge Modulation, Natural Sampling - Delta Inverter

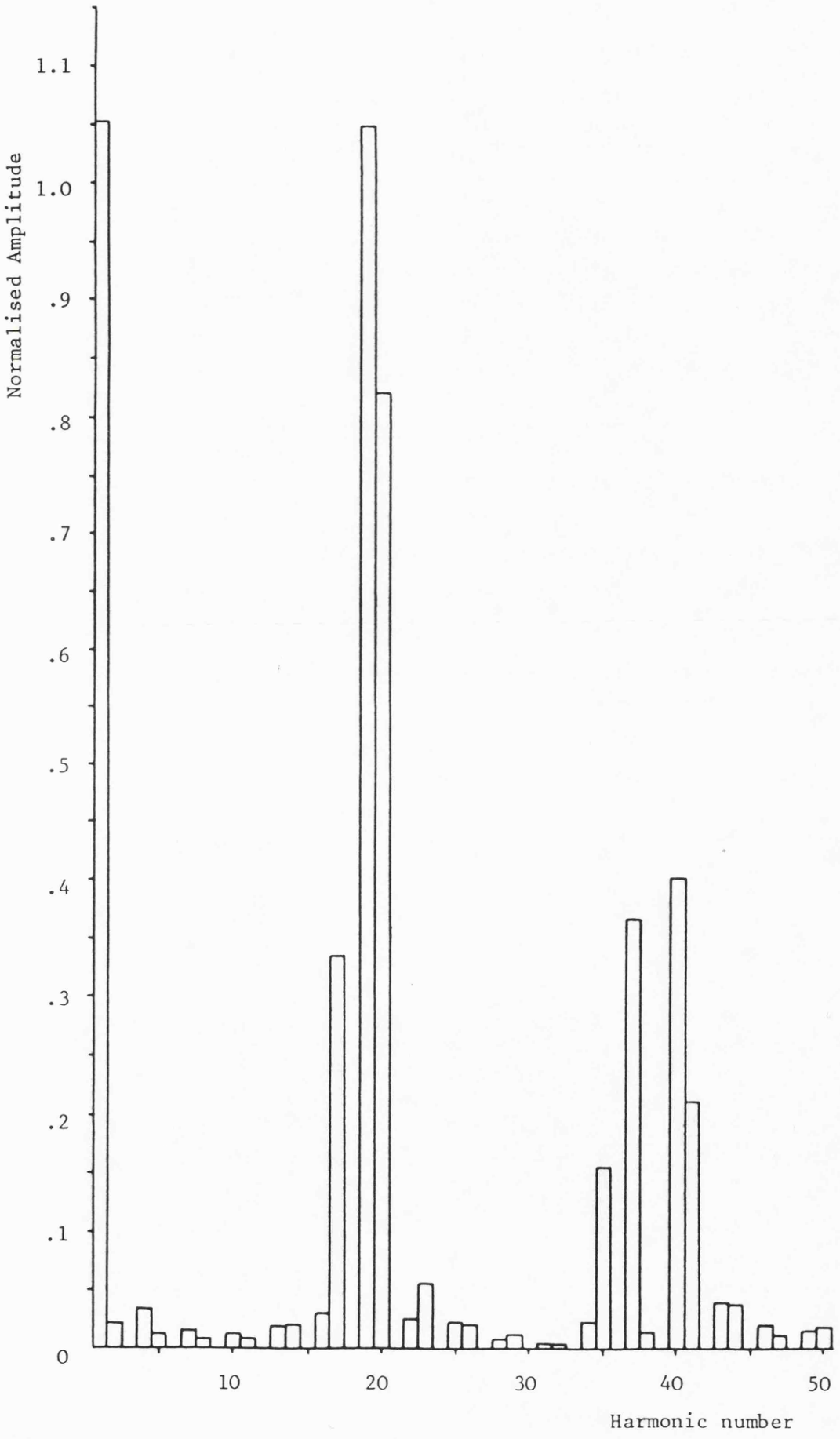

Fig. 3.20 Harmonic Spectrum, Single Edge Modulation, Uniform Sampling - Delta Inverter

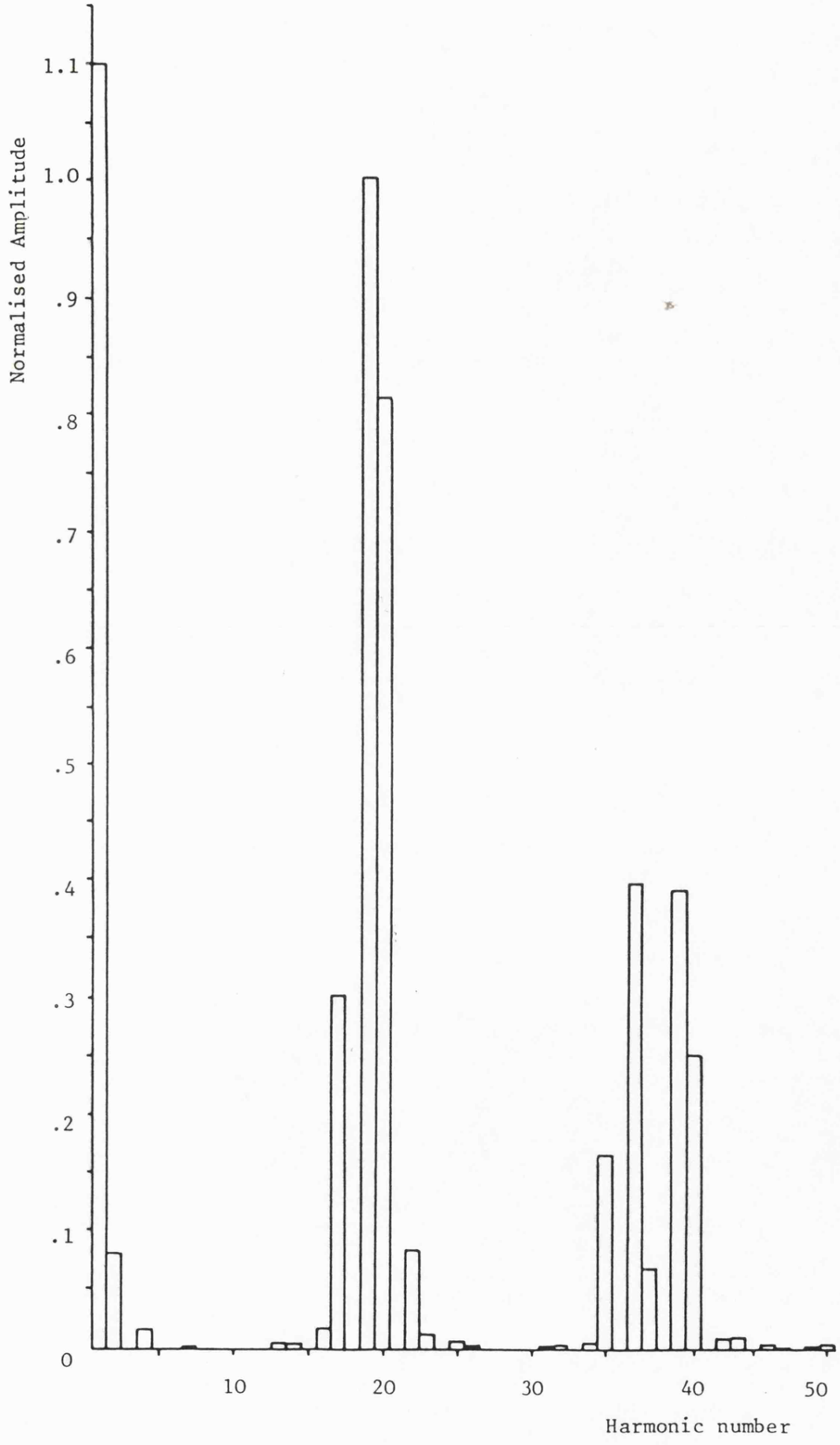

Fig. 3.21 Harmonic Spectrum, Single Edge Modulation, Linear Piecewise Technique - Delta Inverter

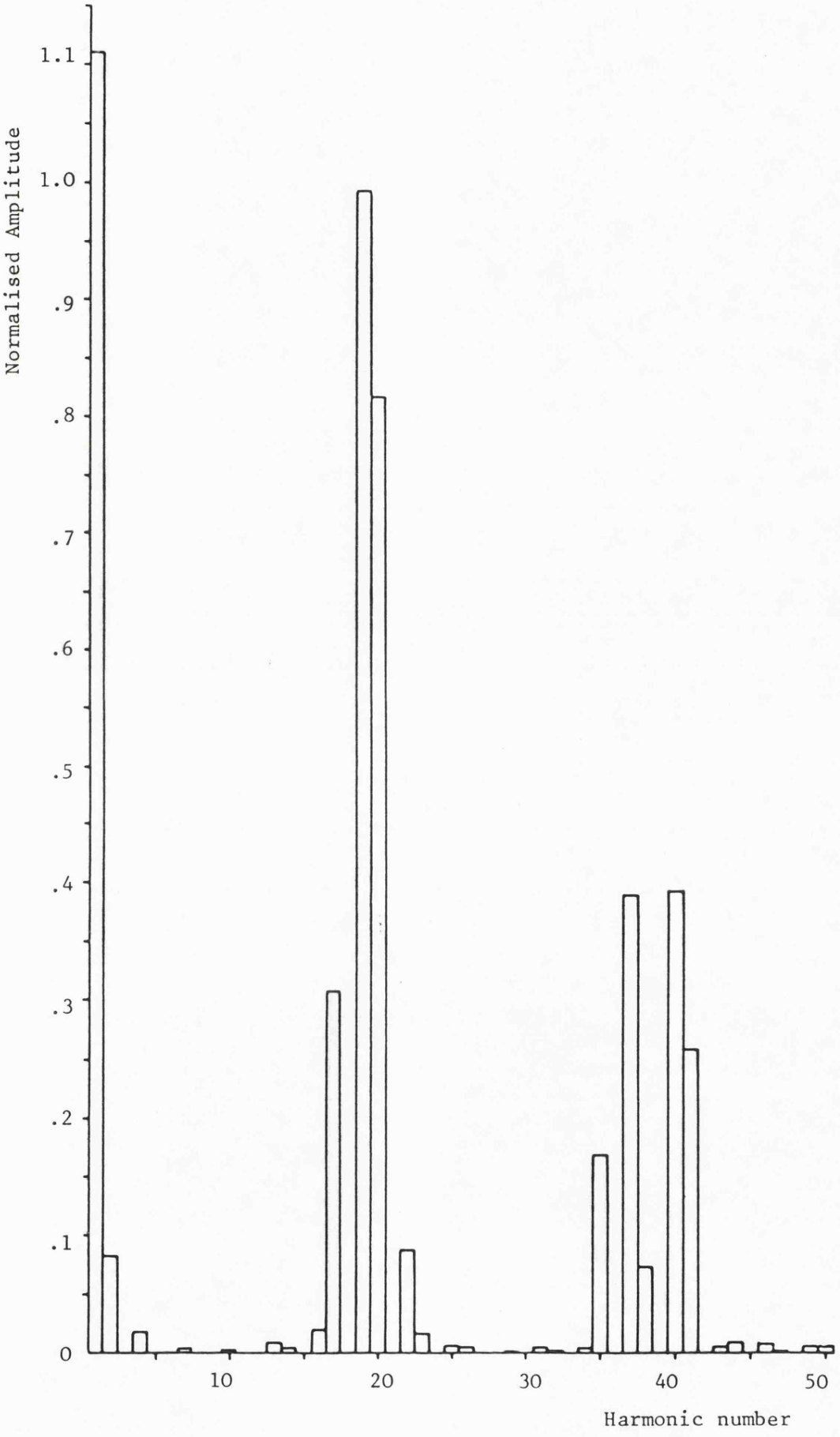

Fig. 3.22 Harmonic Spectrum Single Edge Modulation, Equal Area Technique - Delta Inverter

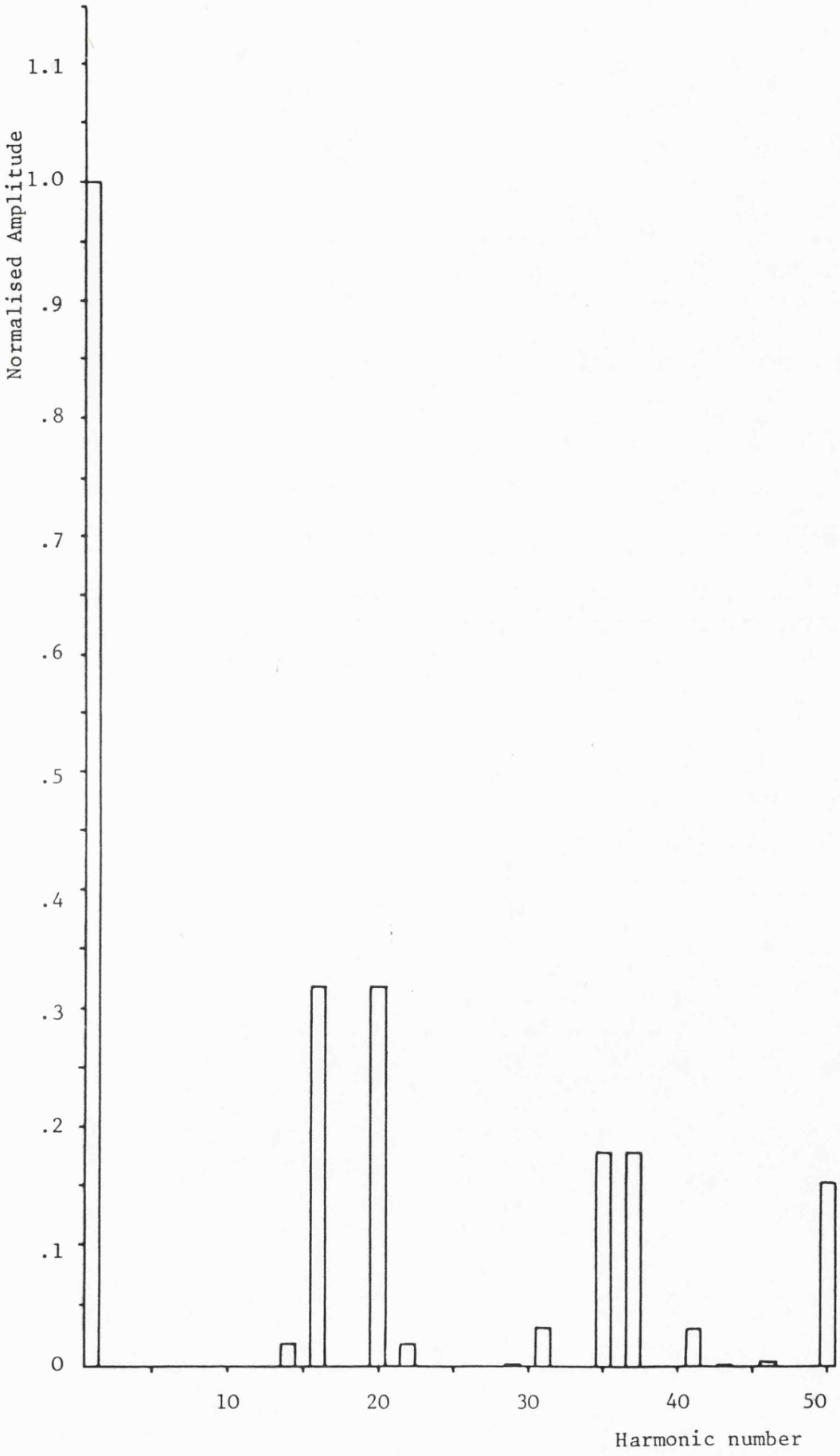

Fig. 3.23 Harmonic Spectrum Double Edge Modulation, Natural Sampling - Bridge Inverter

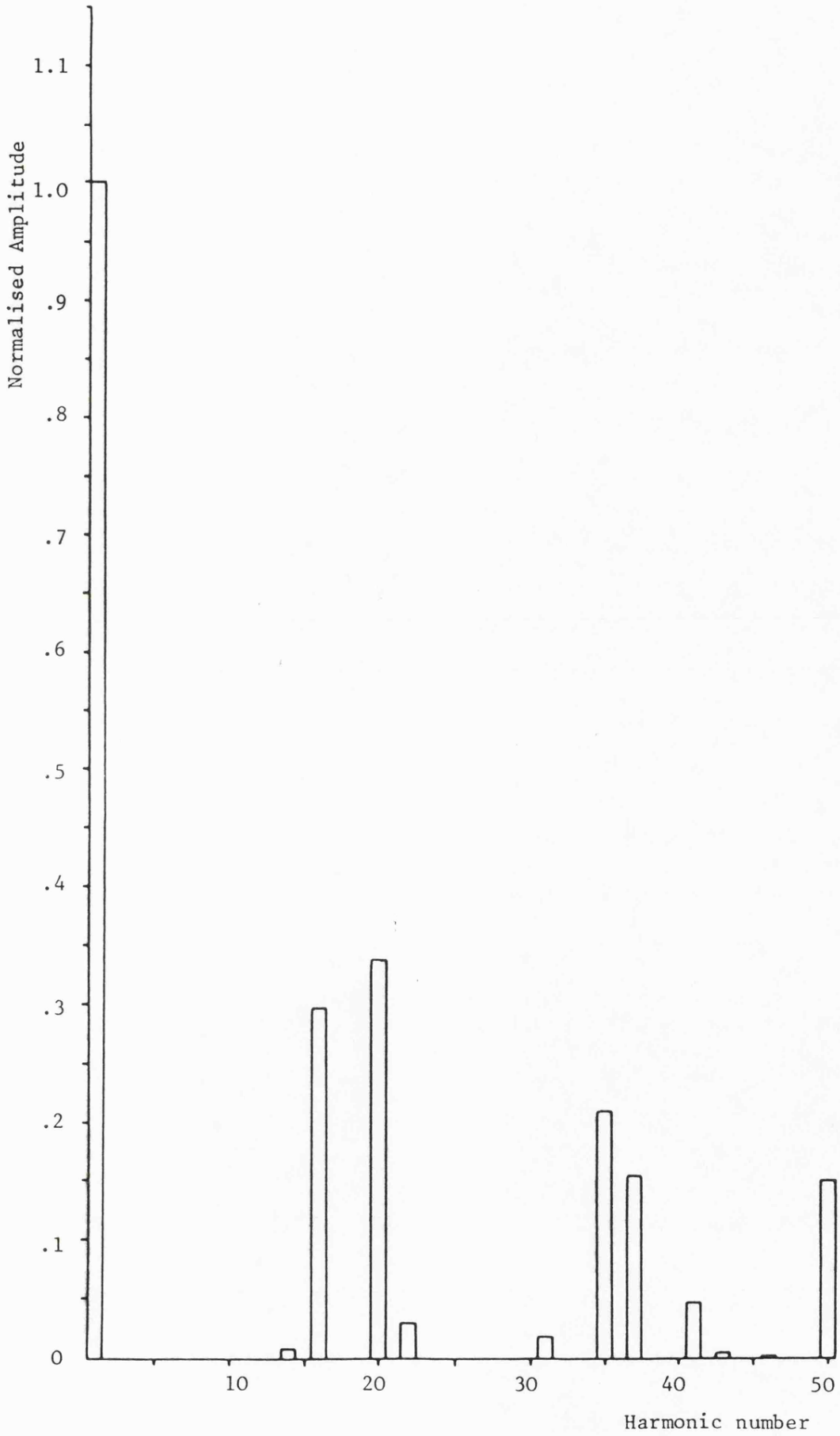

Fig. 3.24 Harmonic Spectrum Double Edge Modulation, Uniform Sampling - Bridge Inverter

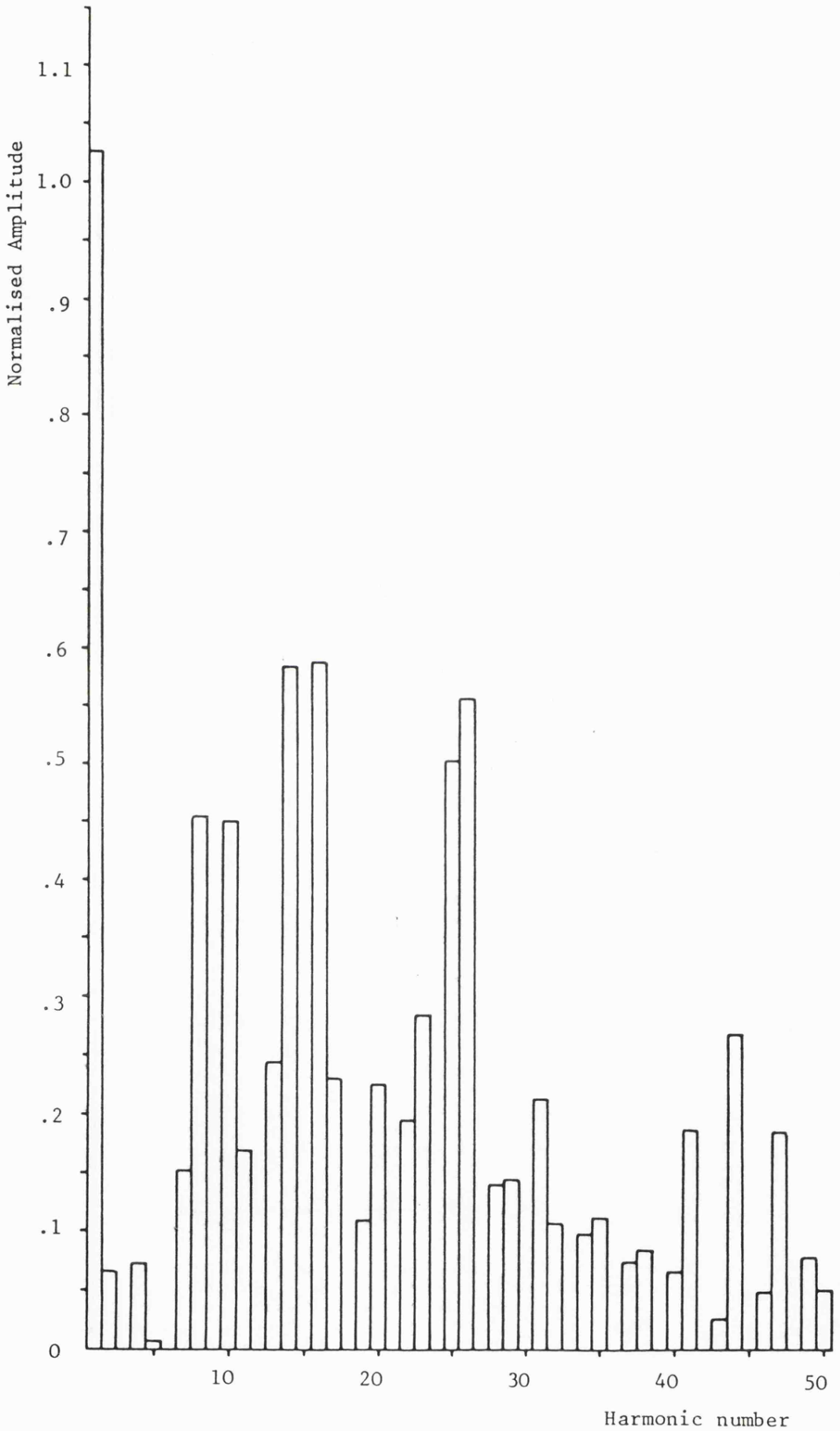

Fig. 3.25 Harmonic Spectrum Double Edge Modulation, Natural Sampling - Delta Inverter

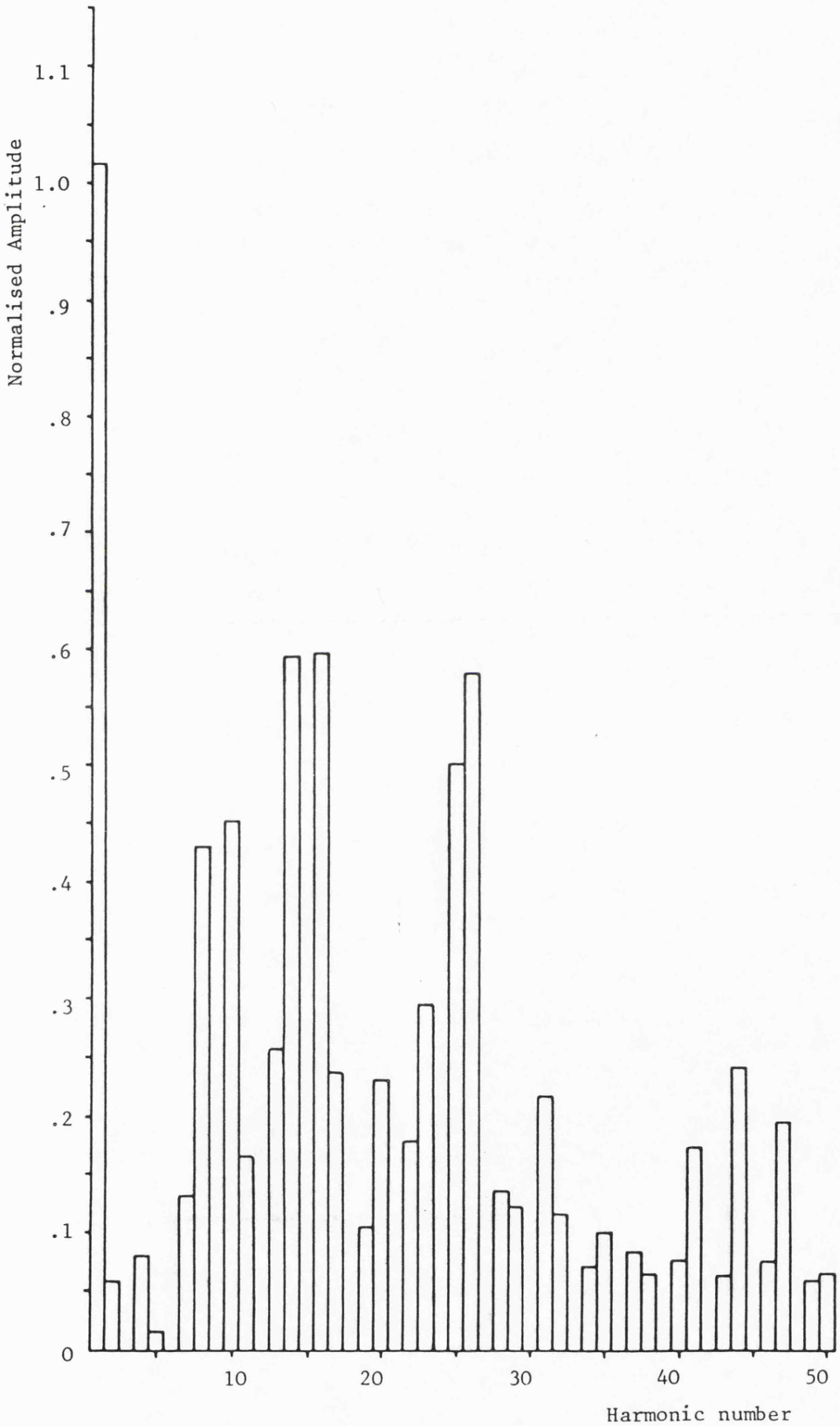

Fig. 3.26 Harmonic Spectrum Double Edge Modulation, Uniform Sampling - Delta Inverter

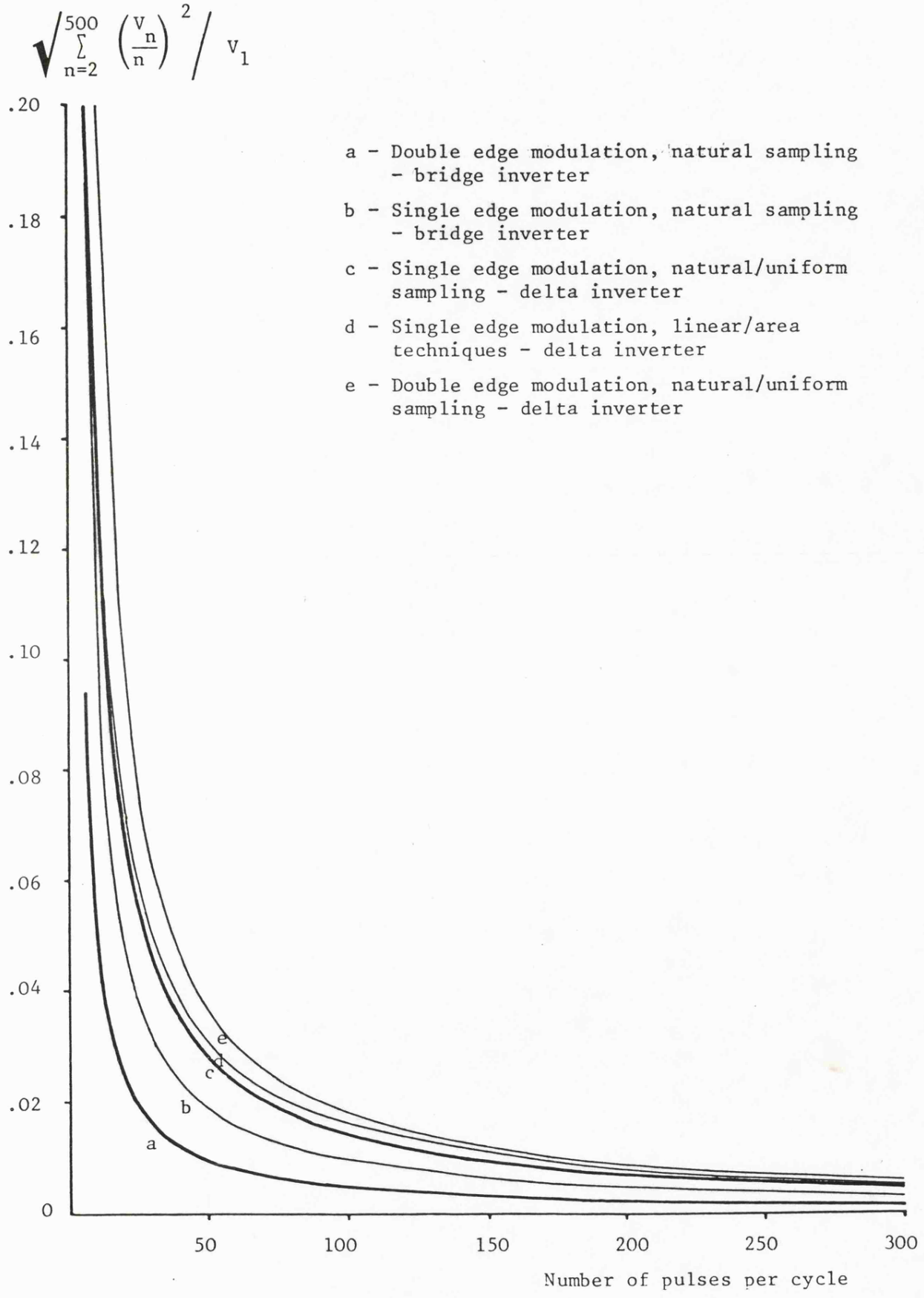

Fig. 3.27 Comparison of bridge and delta inverter modulation techniques.

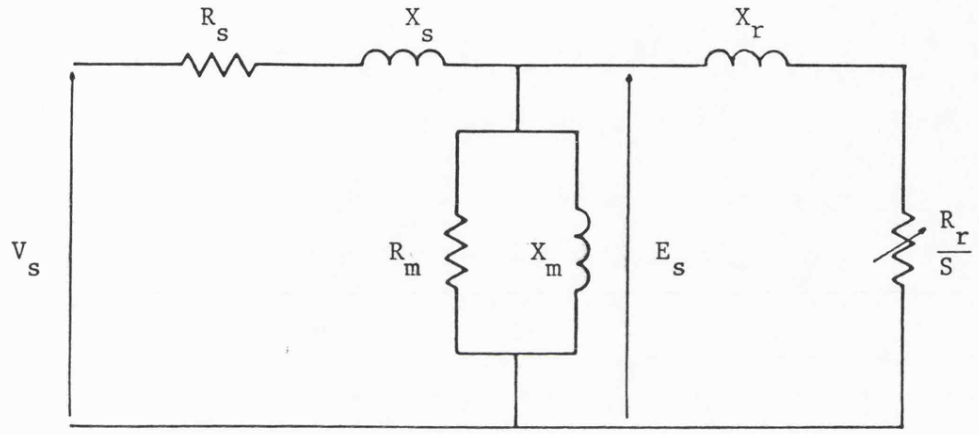

Fig. 4.1 Single-Phase Equivalent Circuit of Induction Motor - Referring Rotor Quantities to Stator

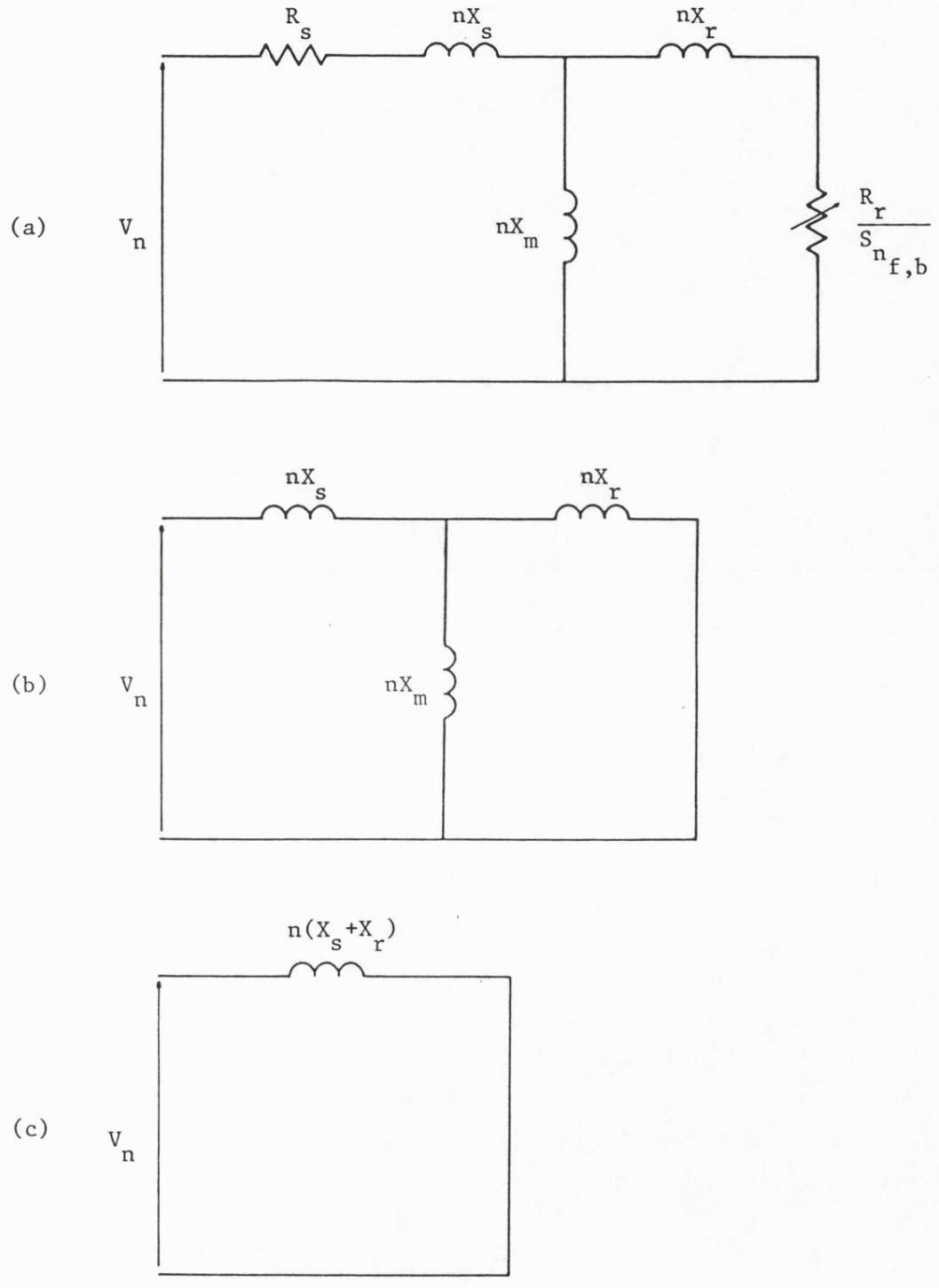

Fig. 4.2 Single-Phase Equivalent Circuits for the n^{th} Harmonic

a) Full circuit
b) Neglecting resistances
c) Neglecting magnetising branch

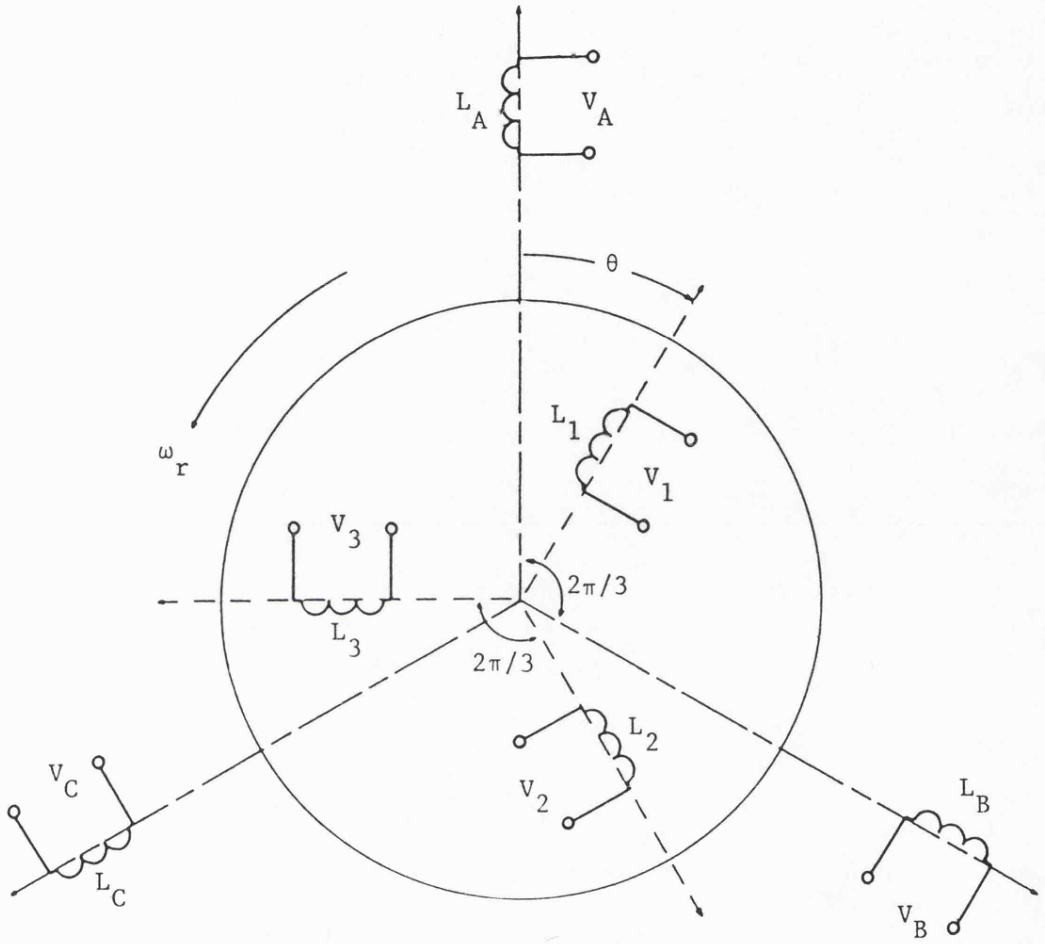

Fig. 4.3 Three-Phase Equivalent Circuit of Induction Motor

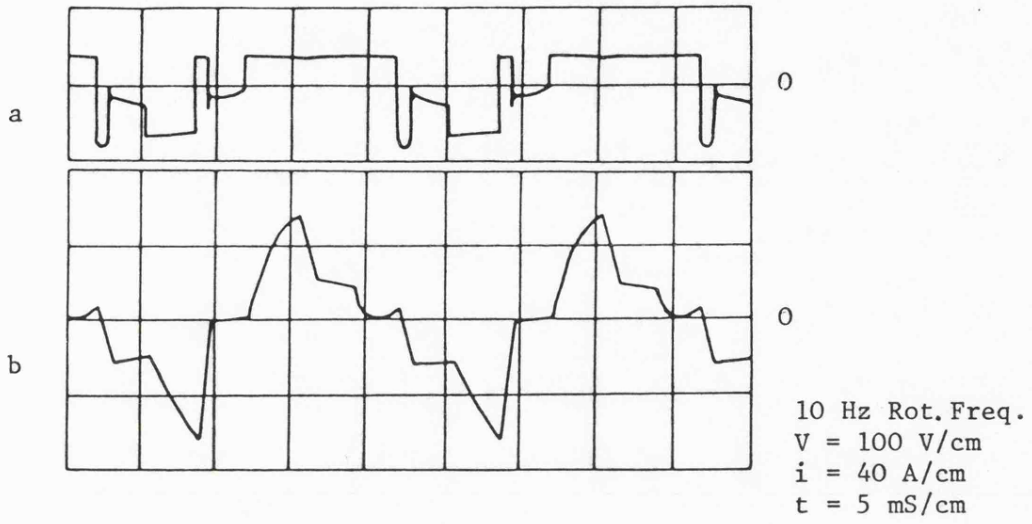

Fig. 4.4 Delta Inverter with Motor Load, 180° Unmodulated Conduction

a) Line voltage
b) Load current

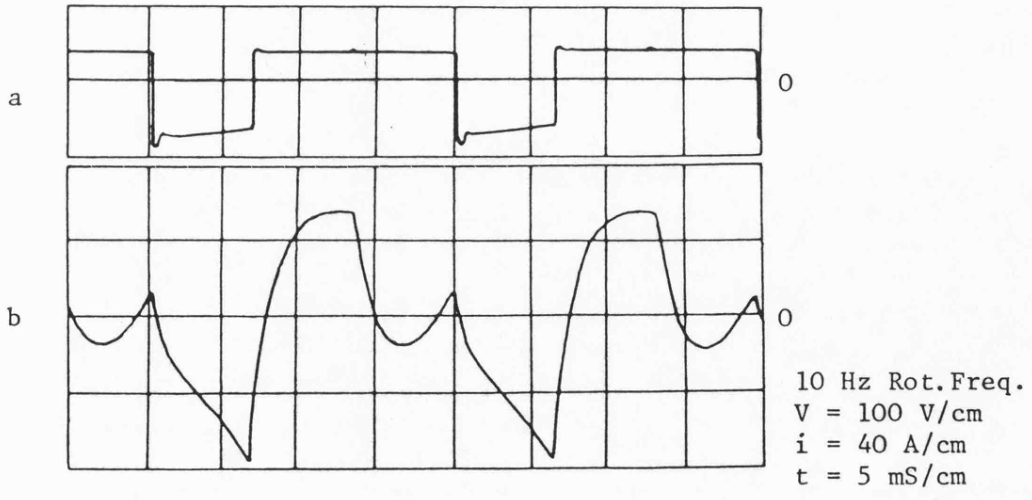

Fig. 4.5 Delta Inverter with Motor Load, 240° Unmodulated Conduction

a) Line voltage
b) Load current

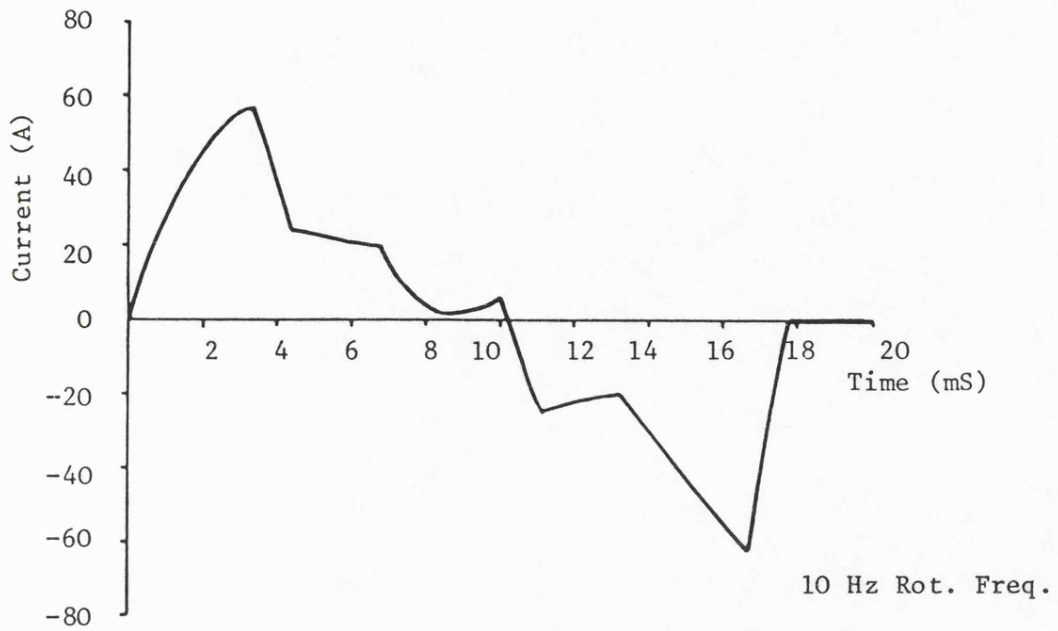

Fig. 4.6 Delta Inverter with Motor Load, 180° Conduction - Computed Load Current

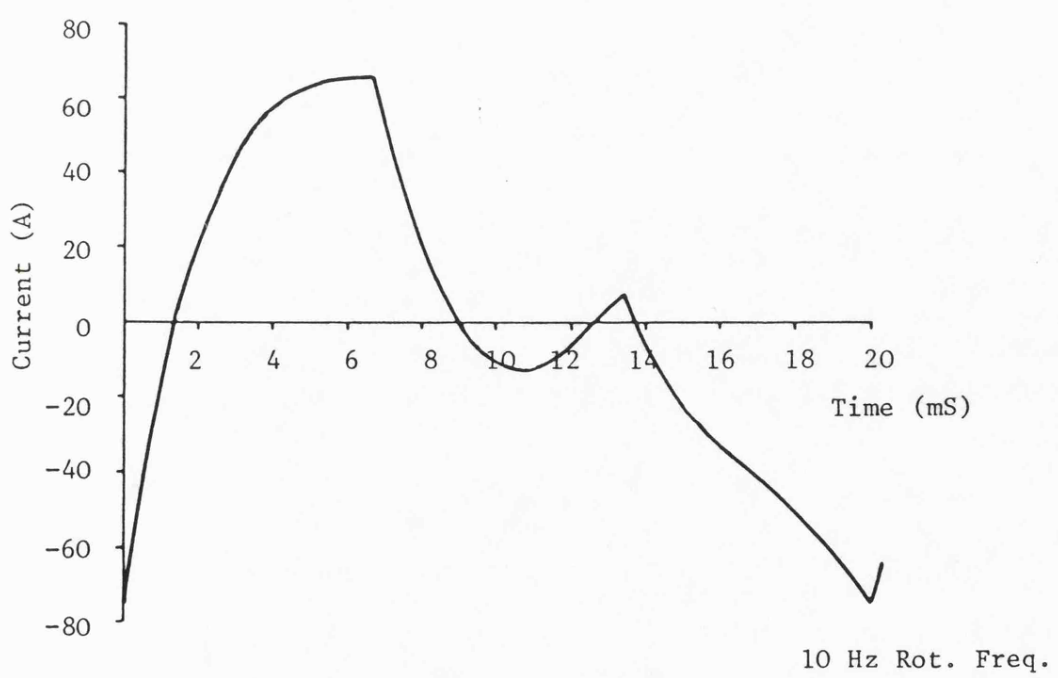

Fig. 4.7 Delta Inverter with Motor Load, 240° Conduction - Computed Load Current

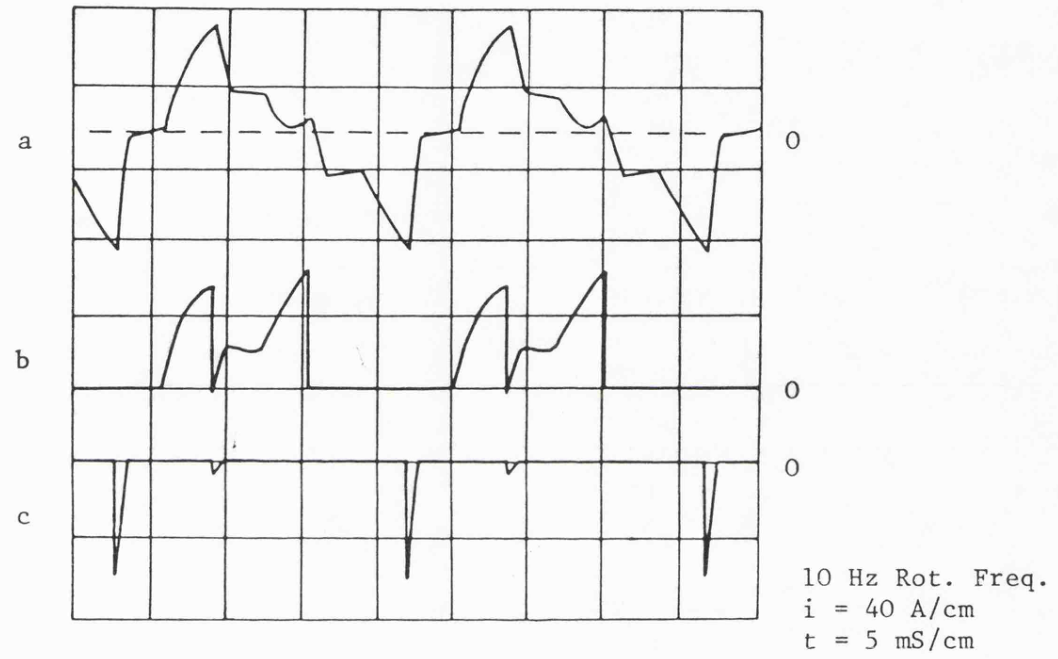

Fig. 4.8 Delta Inverter with Motor Load, 180° Conduction

a) Load current
b) Transistor current
c) Diode current

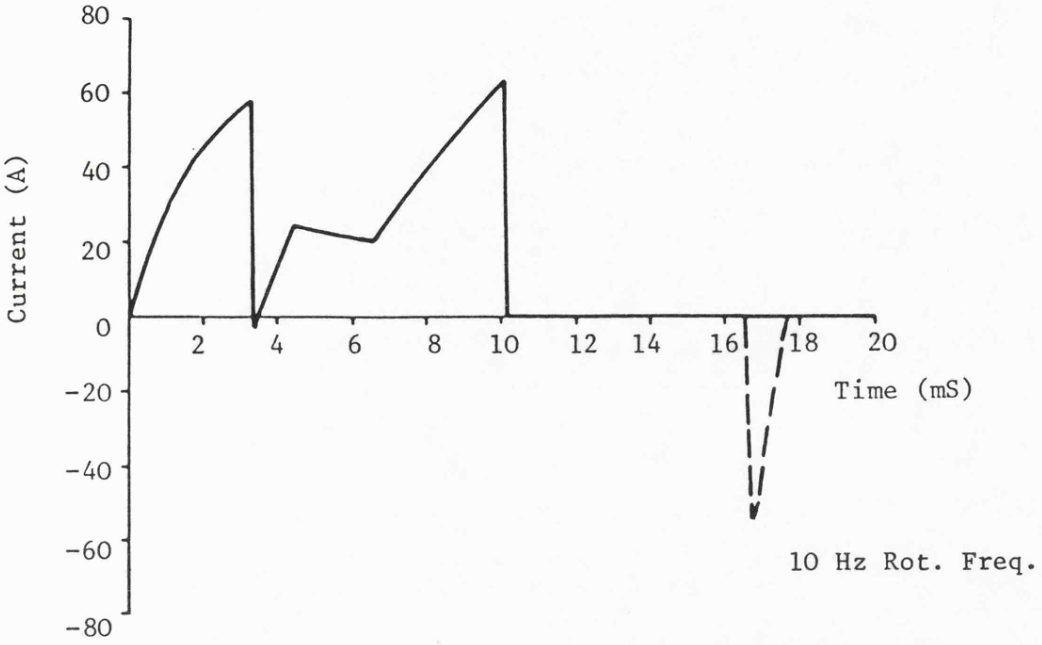

Fig. 4.9 Delta Inverter with Motor Load, 180° Conduction
-- Computed Results

——— Transistor current

– – – Diode current

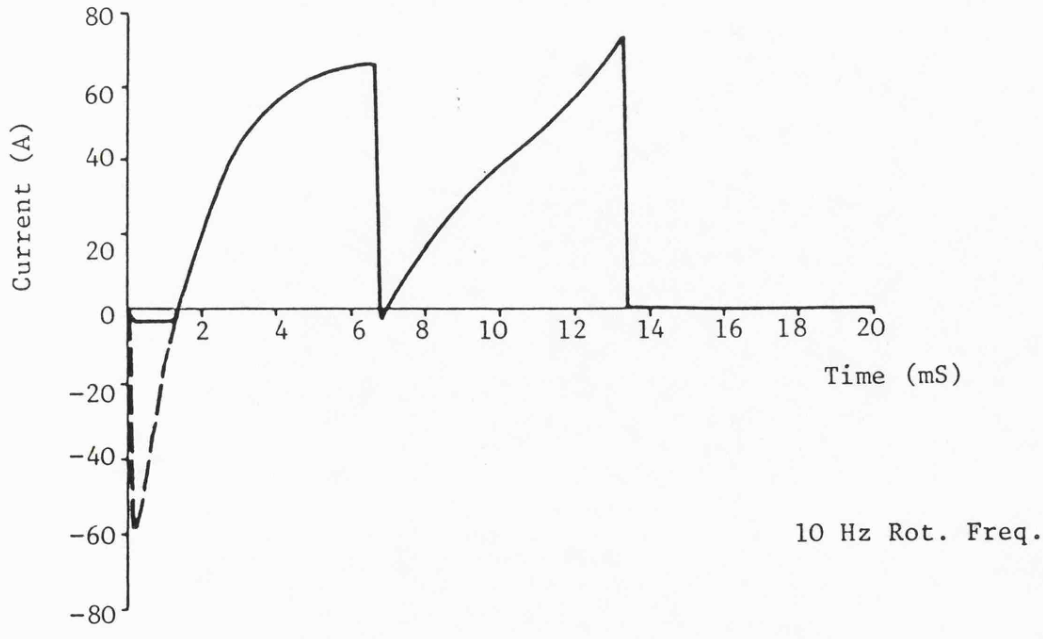

Fig. 4.10 Delta Inverter withMotor Load, 240° Conduction
- Computed Results

——— Transistor current

– – – Diode current

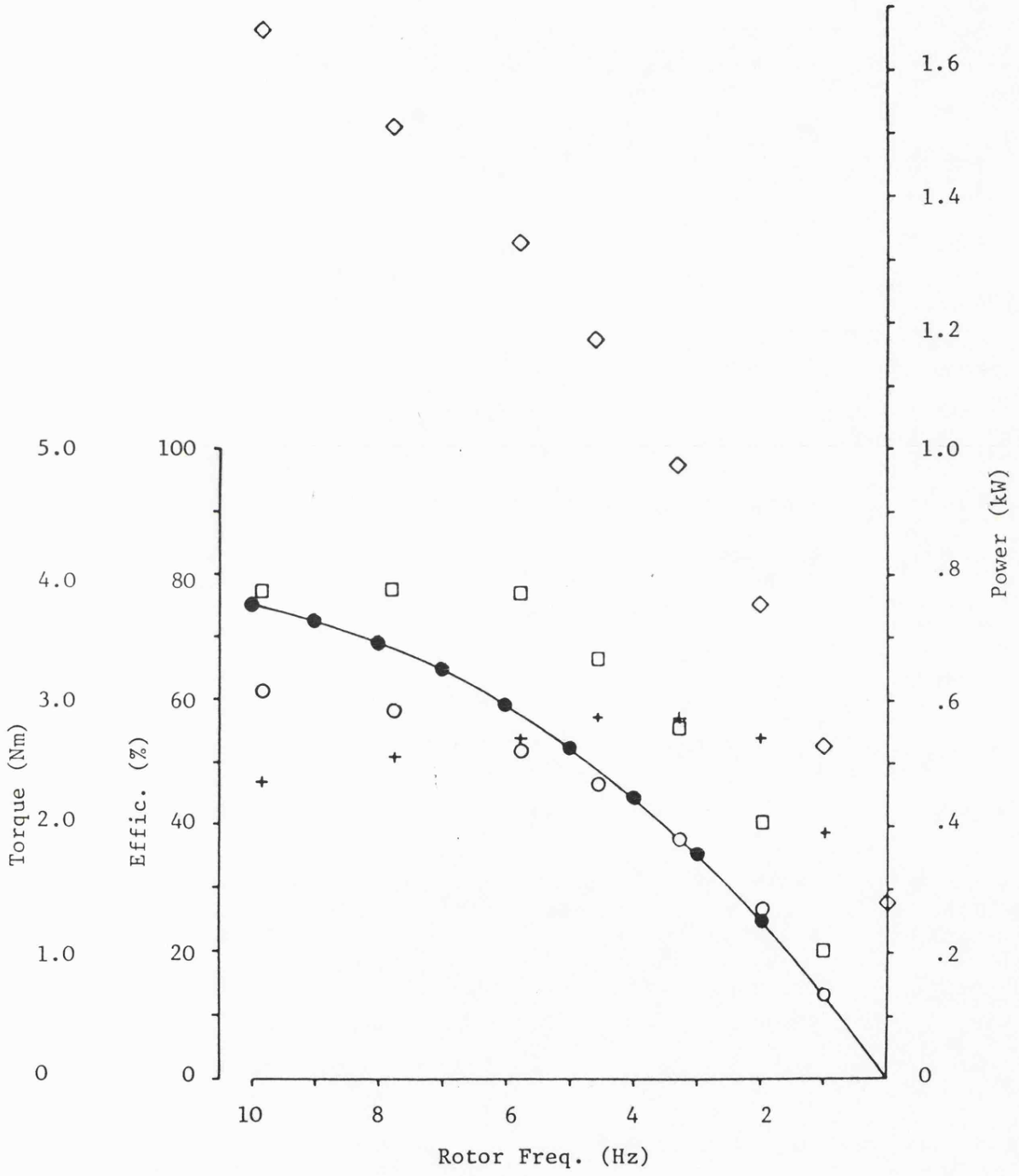

Fig. 4.11 Delta Inverter AC Drive System Performance, 180° Conduction

◇ i/p power (elec) □ o/p power (mech)

○ Actual torque ● Predicted torque

\+ Overall system efficiency

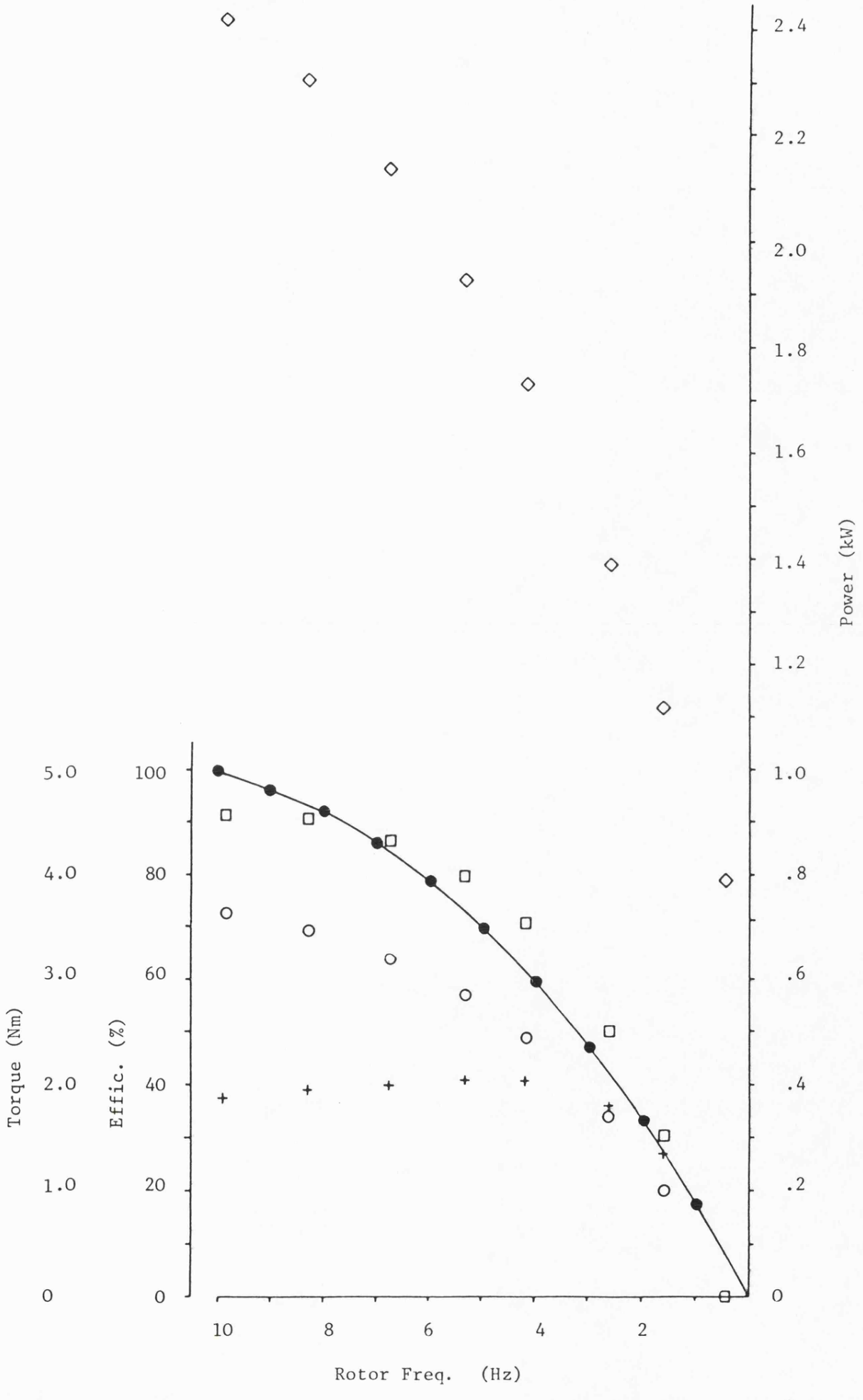

Fig. 4.12 Delta Inverter AC Drive System Performance, 240° Conduction
(Symbols key as Fig. 4.11)

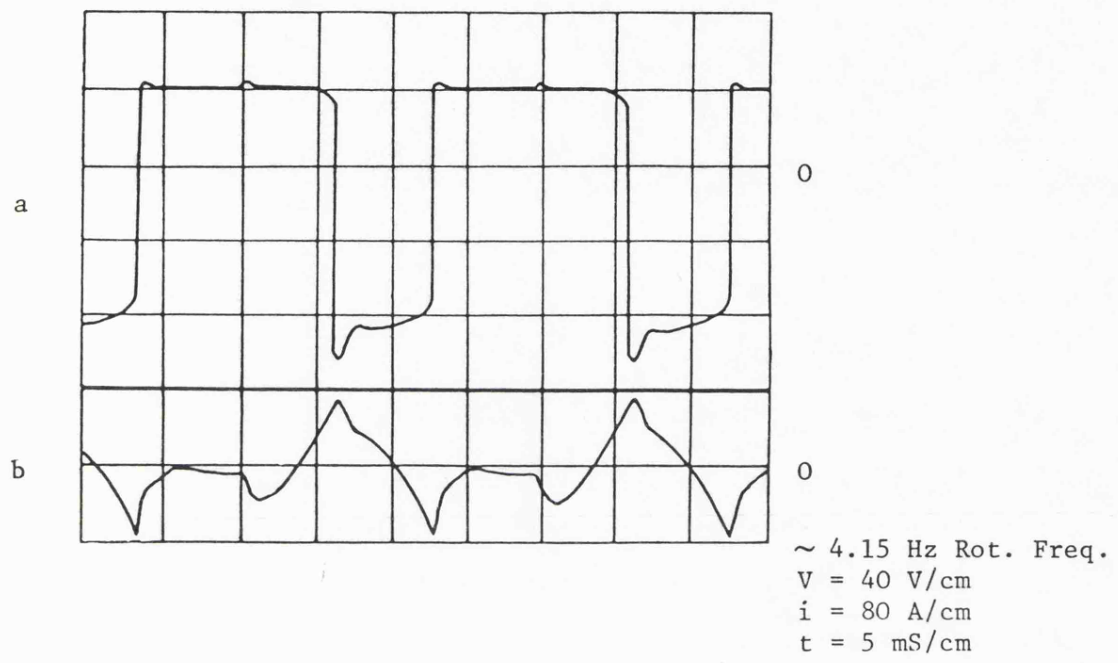

Fig. 4.13 Delta Inverter with Motor Load, 240° Conduction - Regeneration

a) Line voltage
b) Load Current

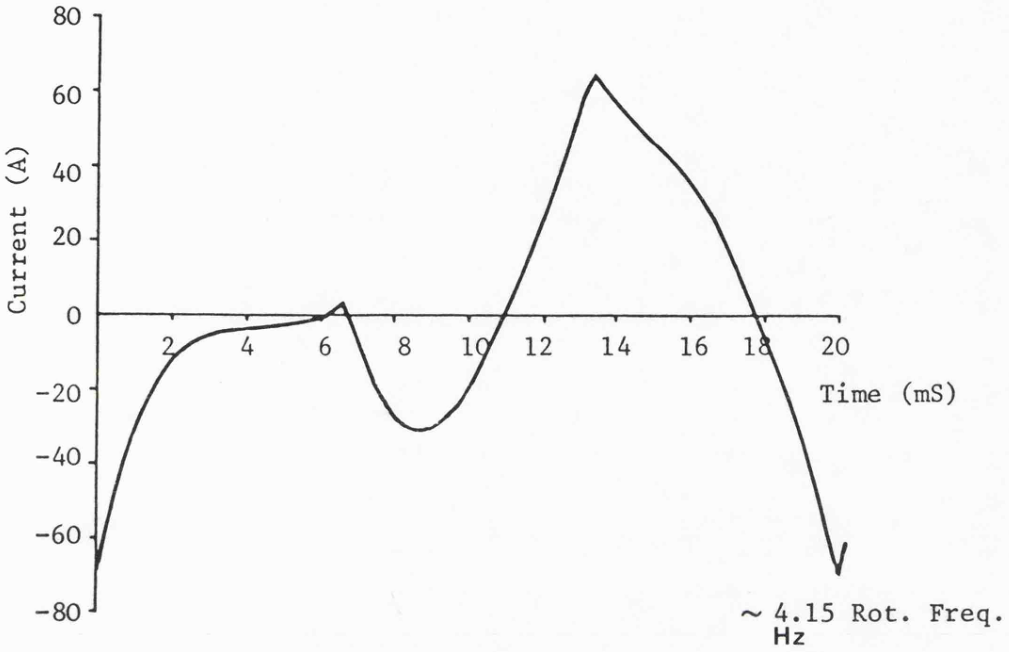

Fig. 4.14(a) Delta Inverter with Motor Load, 240° Conduction
- Regeneration
Computed results: Load current

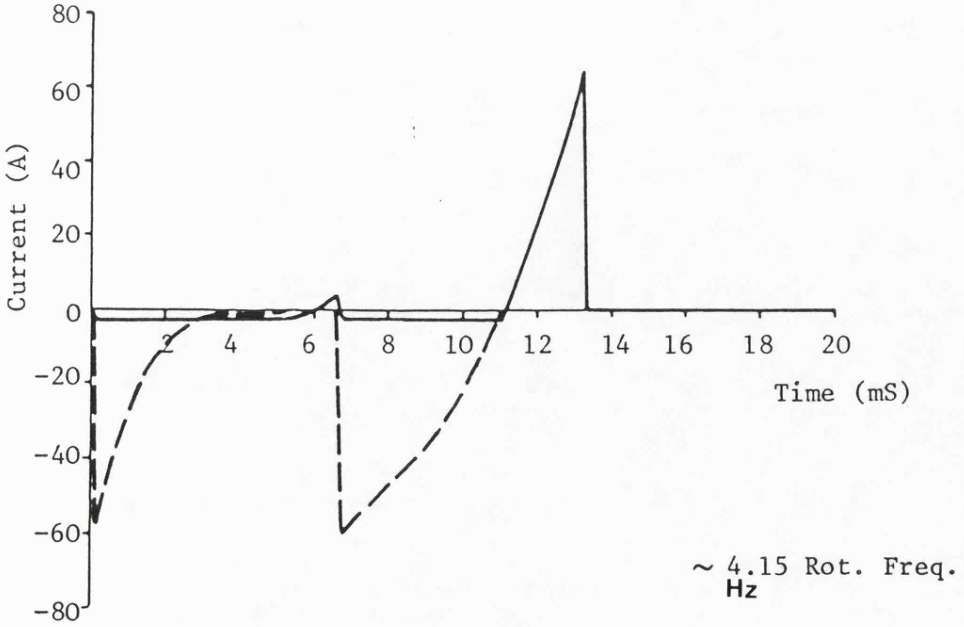

Fig. 4.14(b) Delta Inverter wih Motor Load, 240° Conduction
- Regeneration
Computed results:

——— Transistor current
– – – Diode current

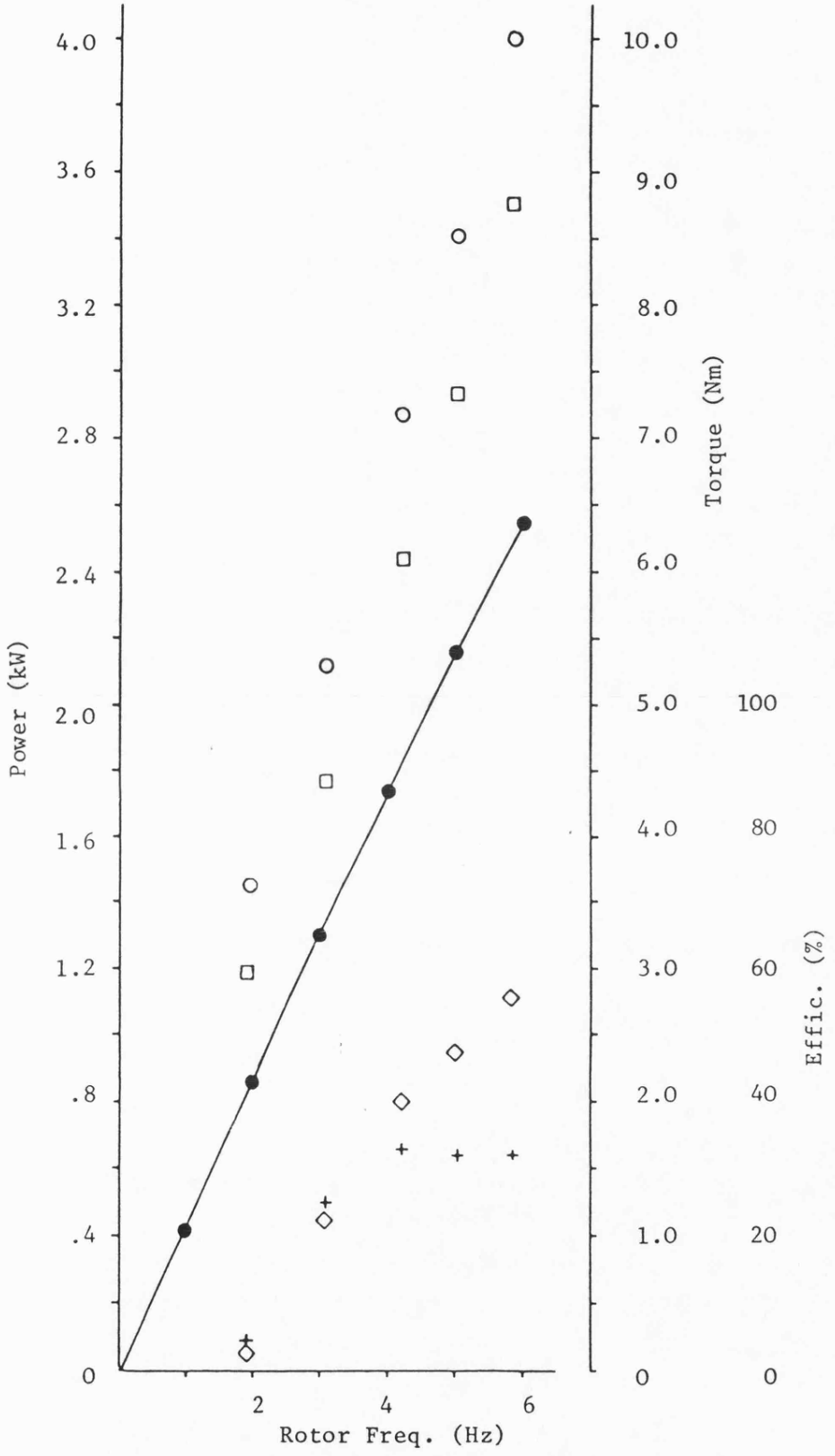

Fig. 4.15 Delta Invertor AC Drive System Performance, 240 Conduction - Regeneration

◇ o/p power (elec) □ i/p power (mech)
○ Actual torque ● Predicted torque
\+ Overall system efficiency

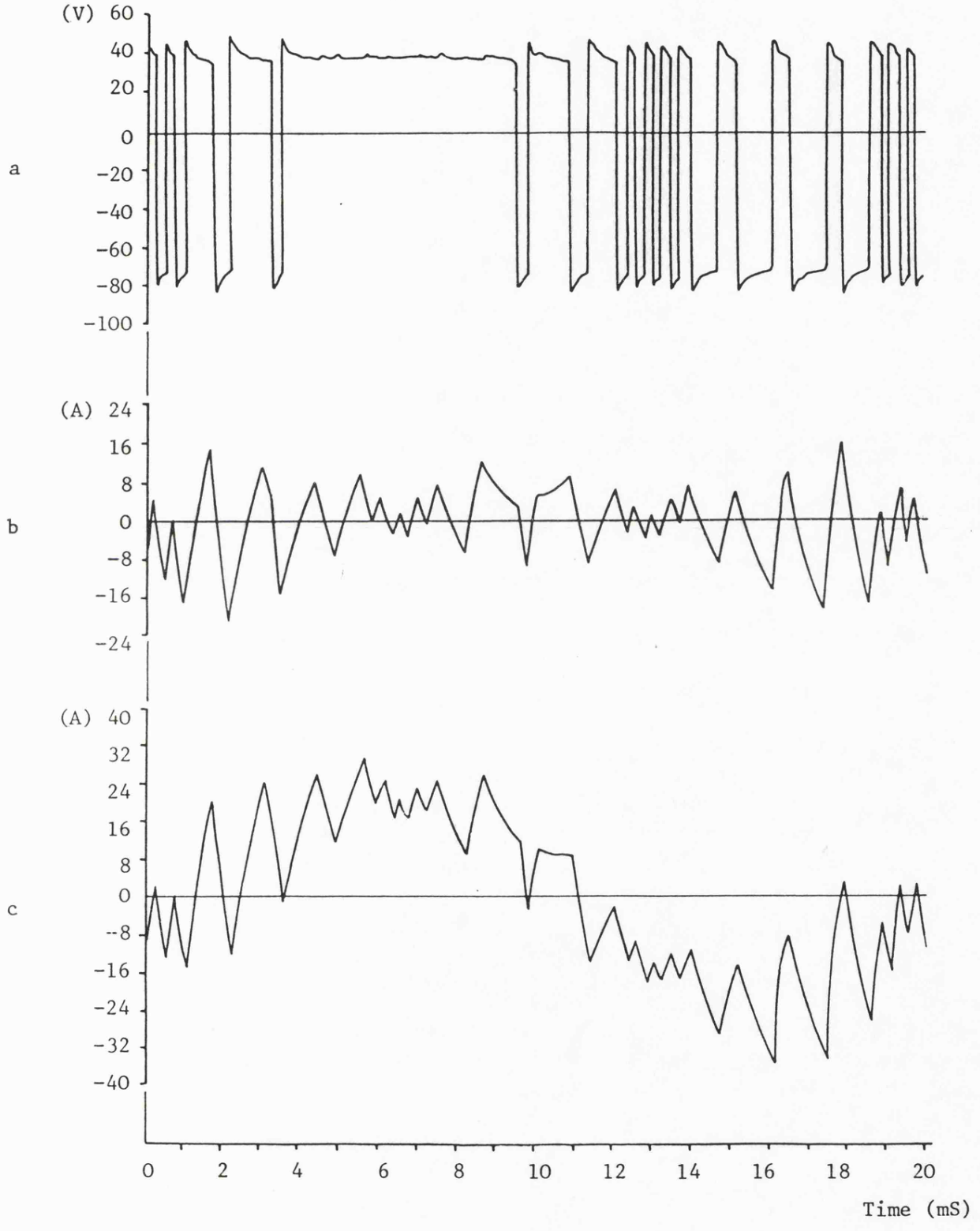

Fig. 4.16 Delta Inverter with Motor Load - SHR Waveforms

a) Line voltage
b) Load current at synchronous speed
c) Load current at 5 Hz rotor freq.

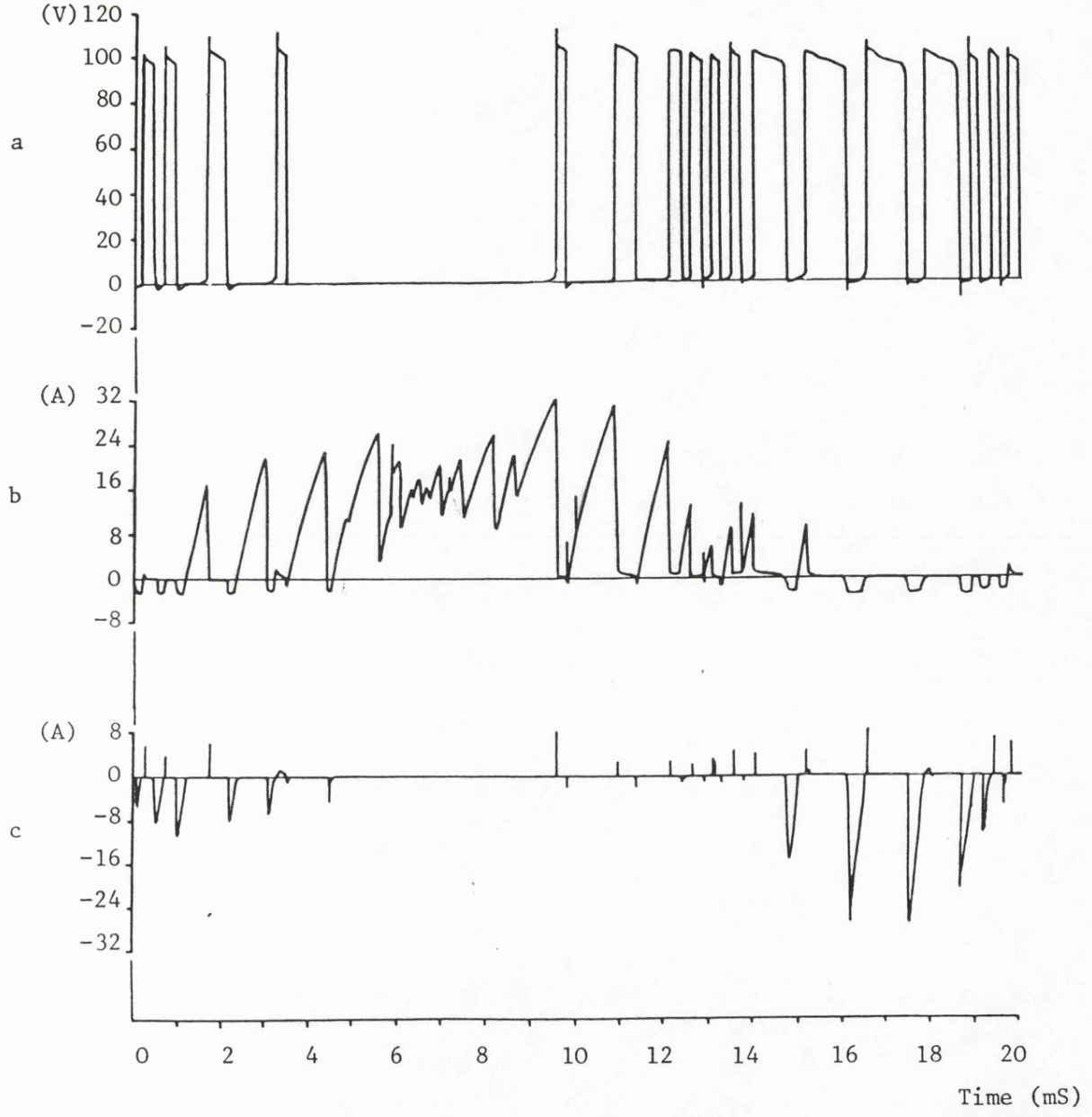

Fig. 4.17 Delta Inverter with Motor Load - SHR Waveforms (at 5 Hz rotor freq.)

a) Transistor voltage, V_{CE}

b) Transistor current, I_E

c) Diode current

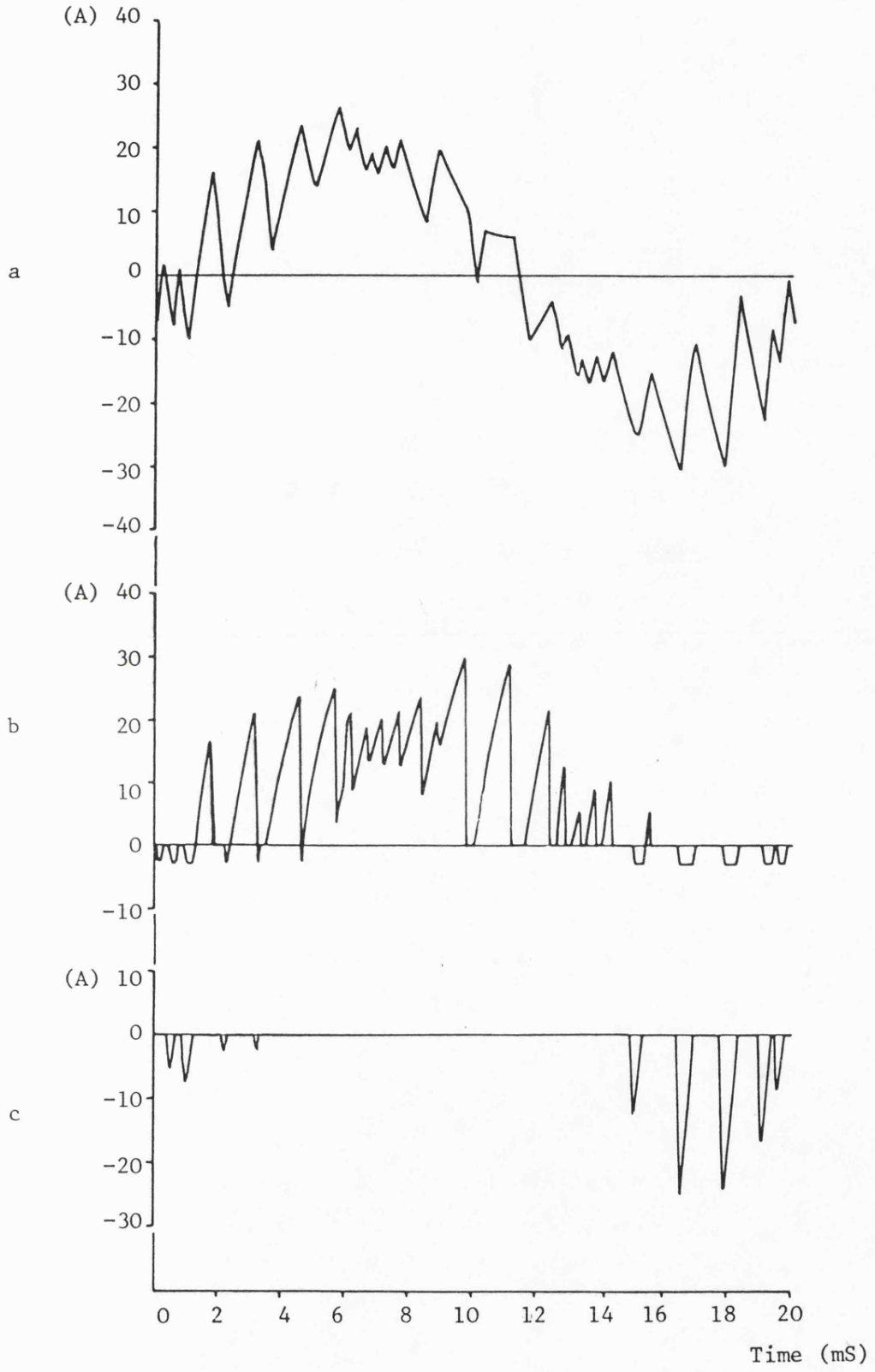

Fig. 4.18 Delta Inverter with Motor Load - SHR Waveforms (at 5 Hz Rotor Freq.)
Computed results:

a) Load current
b) Transistor current
c) Diode current

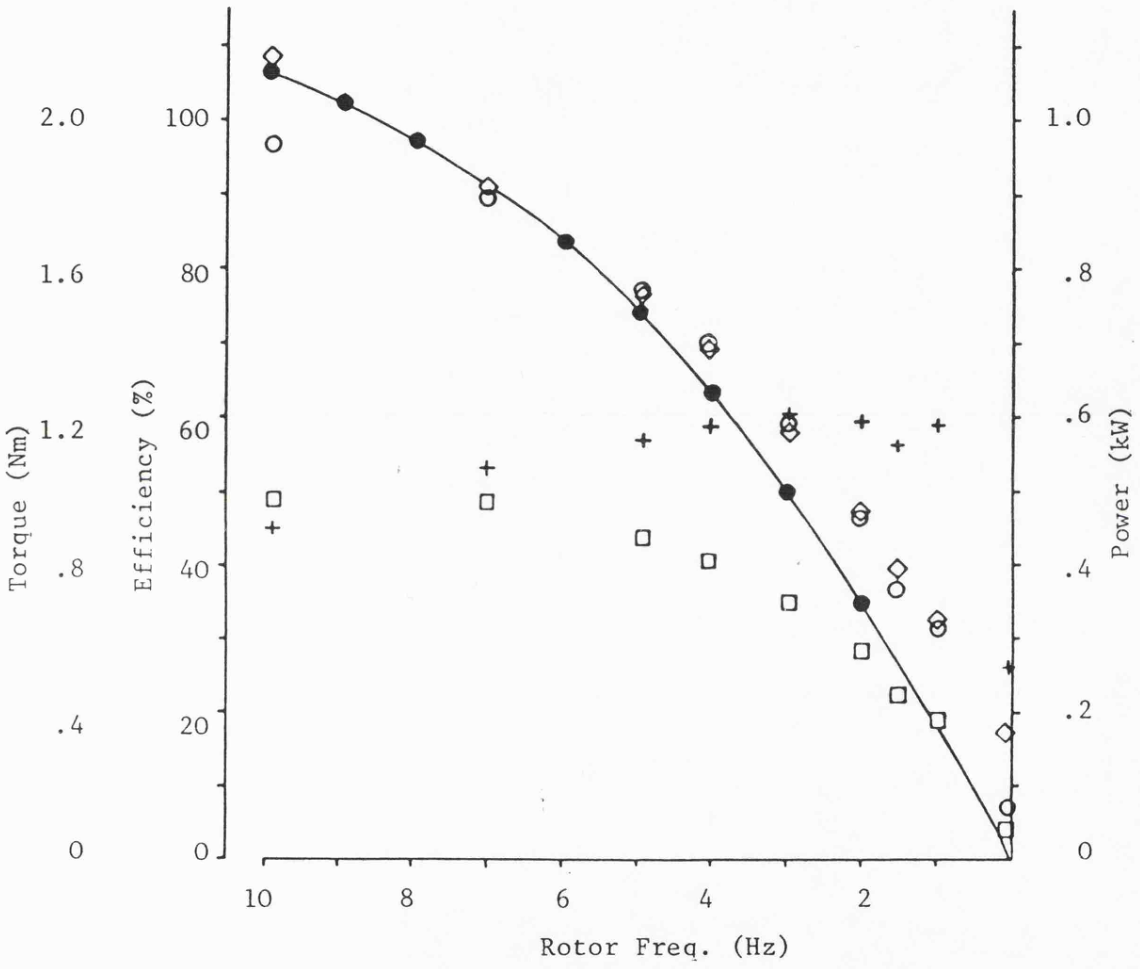

Fig. 4.19 Delta Inverter AC Drive System Performance, with SHR

◇ i/p power (elec) □ o/p power (mech)
○ Actual torque ● Predicted torque
\+ Overall system efficiency

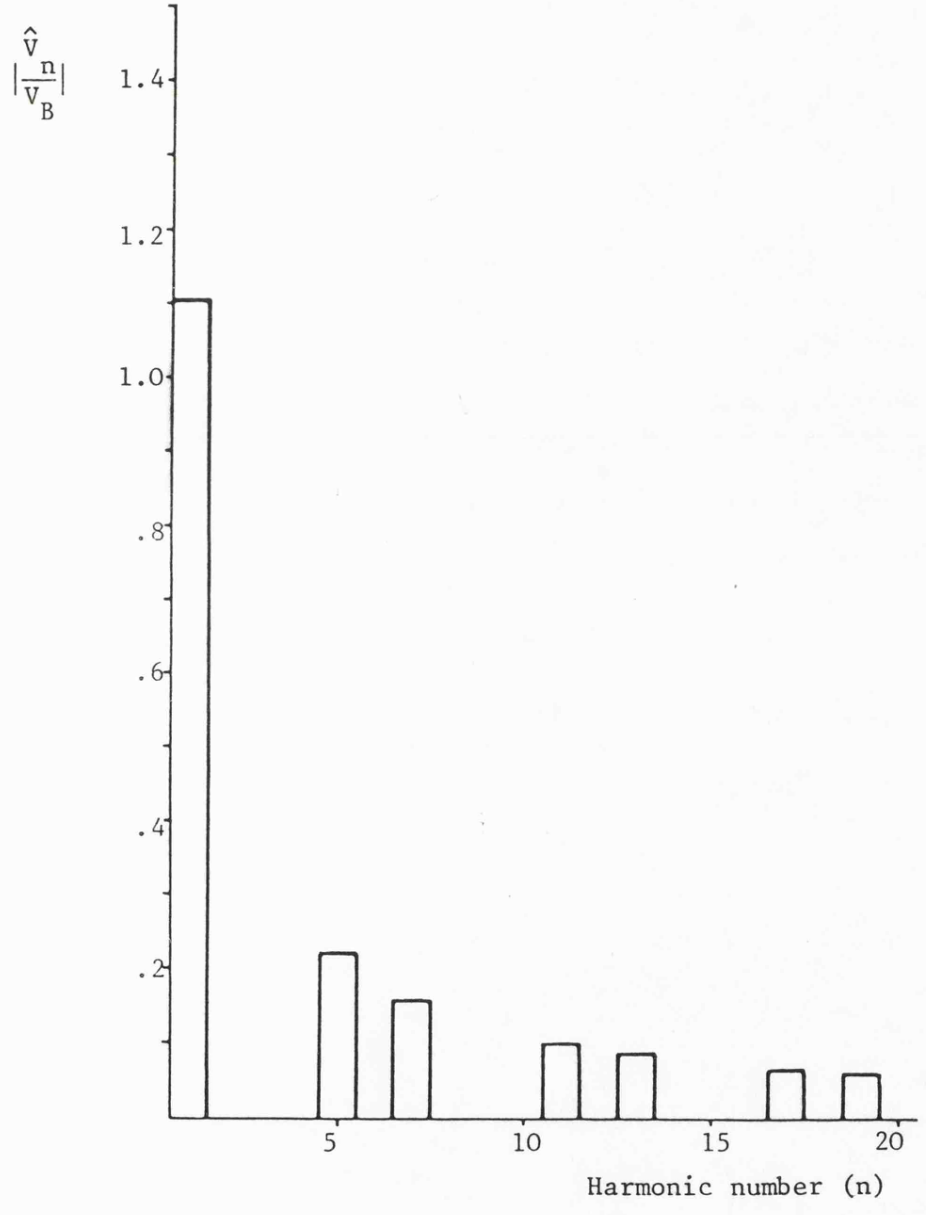

Fig. 4.20 Harmonic Spectrum for the Unmodulated Bridge Inverter Line Voltage

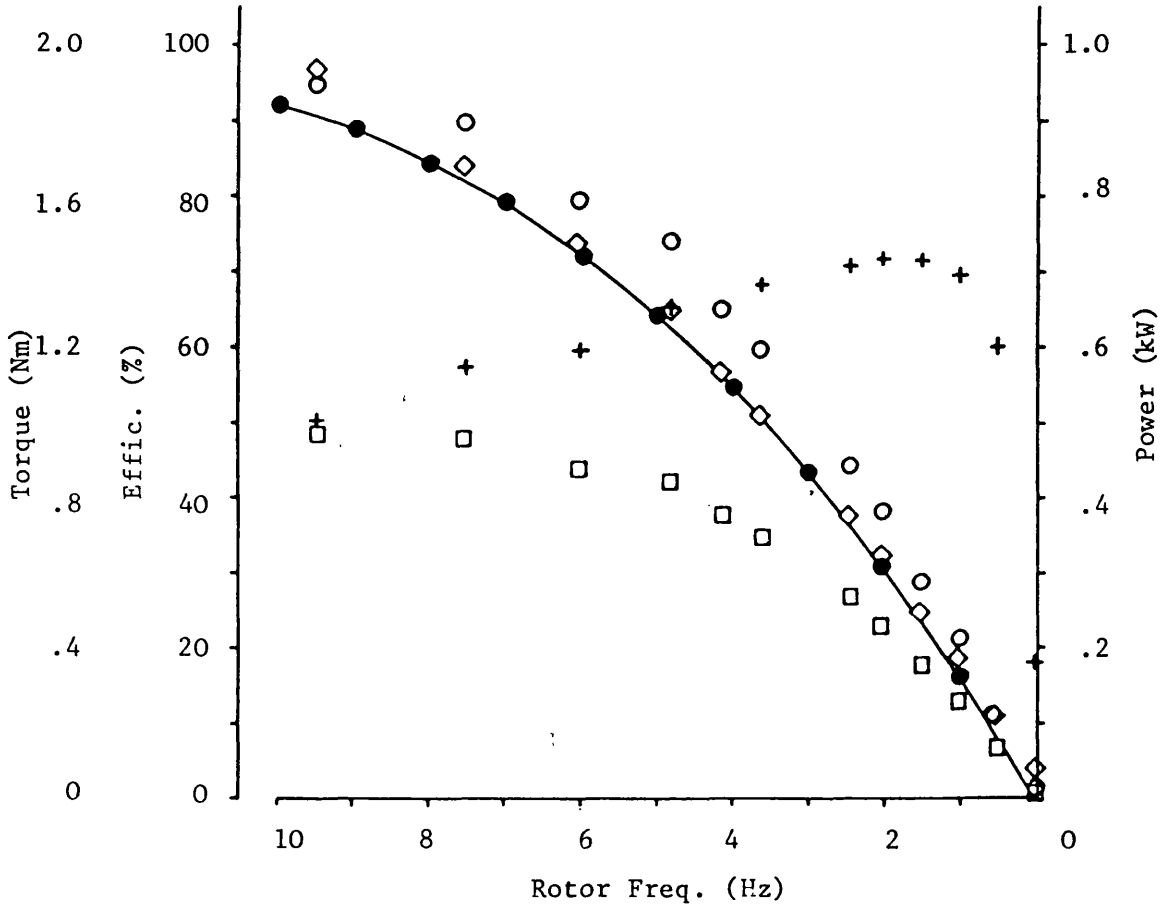

Fig. 4.21 Unmodulated Bridge Inverter AC Drive System Performance

◇ i/p power (elec) □ o/p power (mech)
○ Actual torque ● Predicted torque
\+ Overall system efficiency

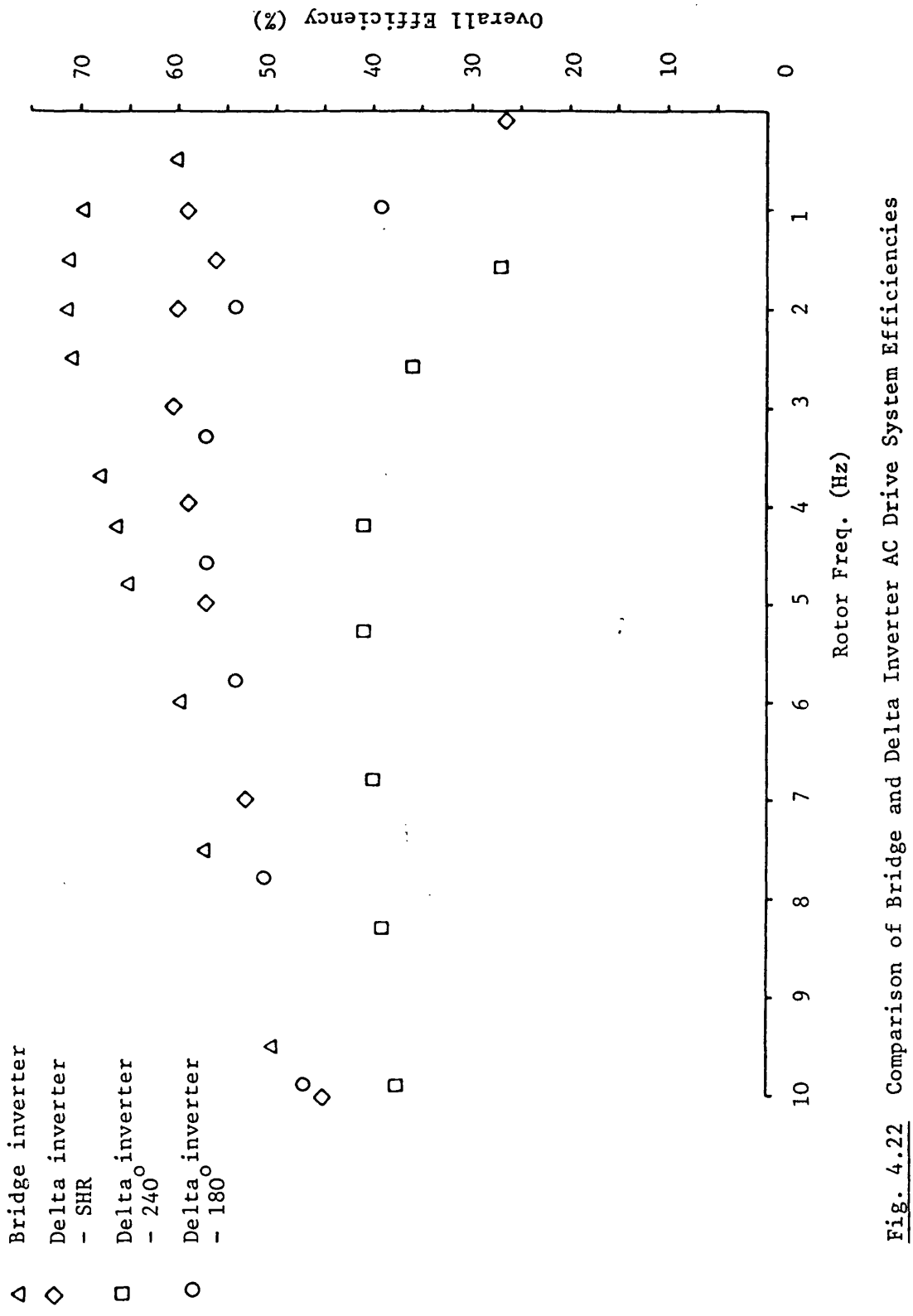

Fig. 4.22 Comparison of Bridge and Delta Inverter AC Drive System Efficiencies

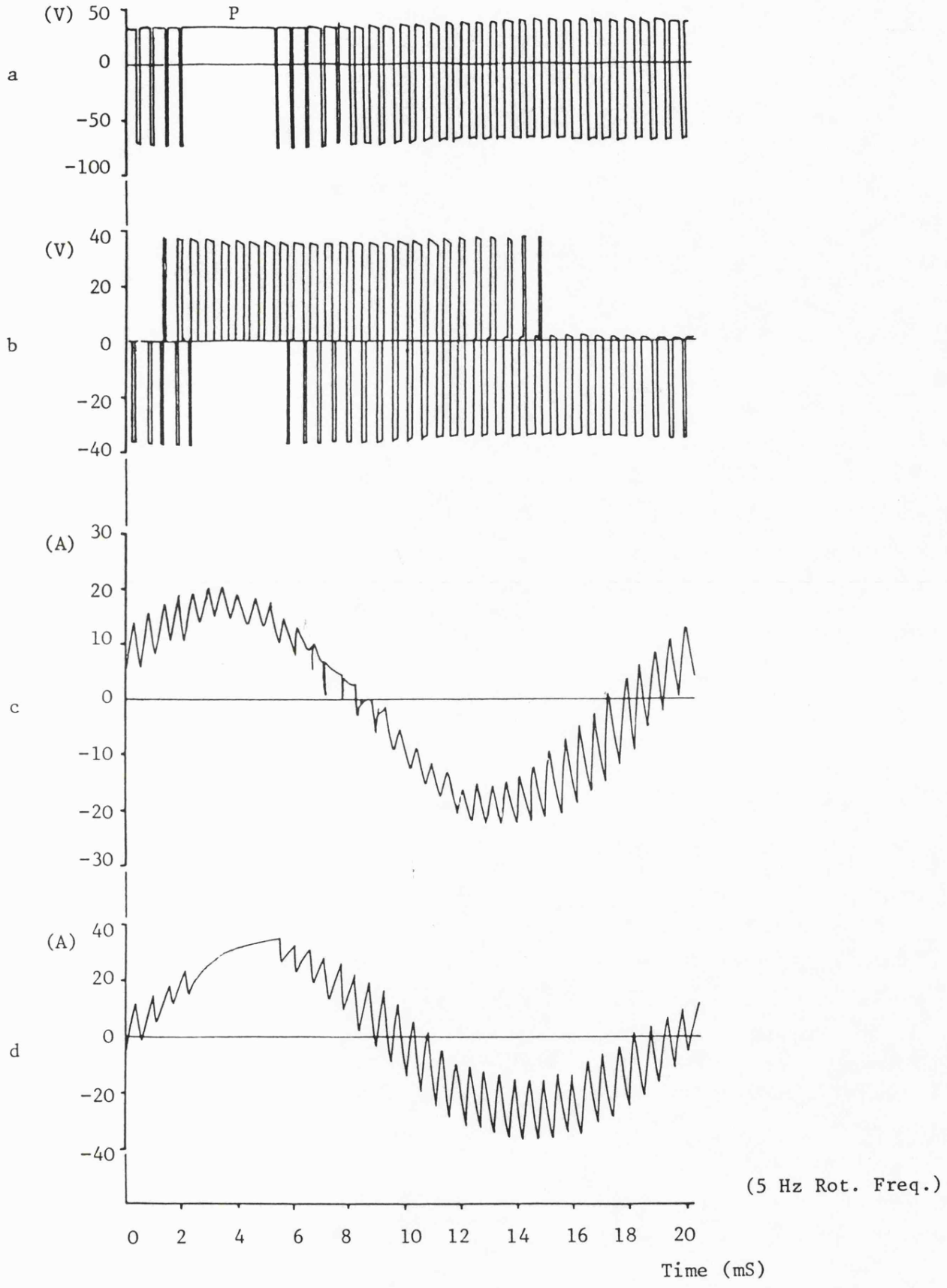

Fig. 4.23 Delta Inverter with Motor Load - Sinusoidal PWM

a) Line voltage
b) Phase voltage (star connected load)
c) Load current (star connected load)
d) Load current (delta connected load)

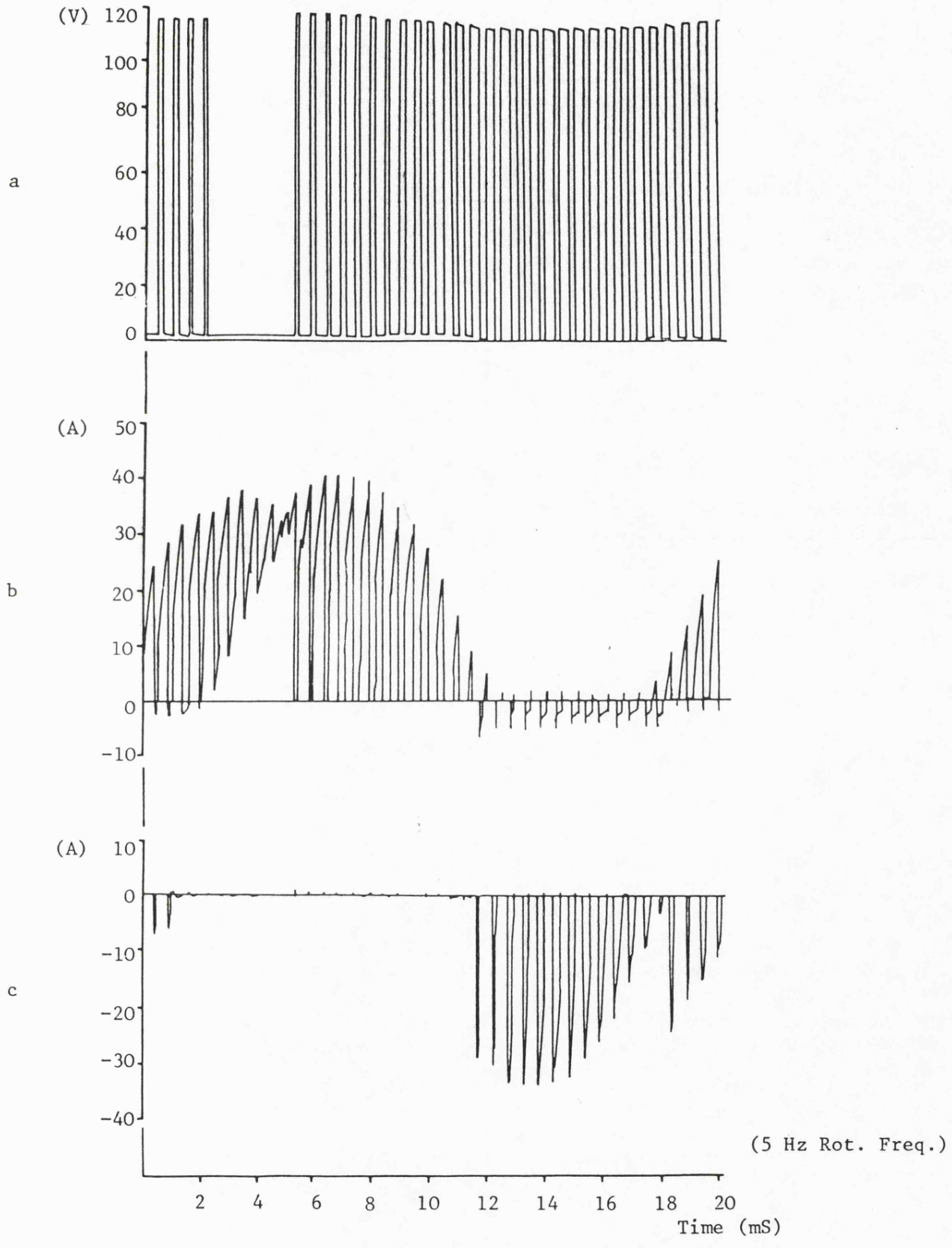

Fig. 4.24 Delta Inverter with Motor Load - Sinusoidal PWM

a) Transistor voltage V_{CE}
b) Transistor current I_E
c) Diode current

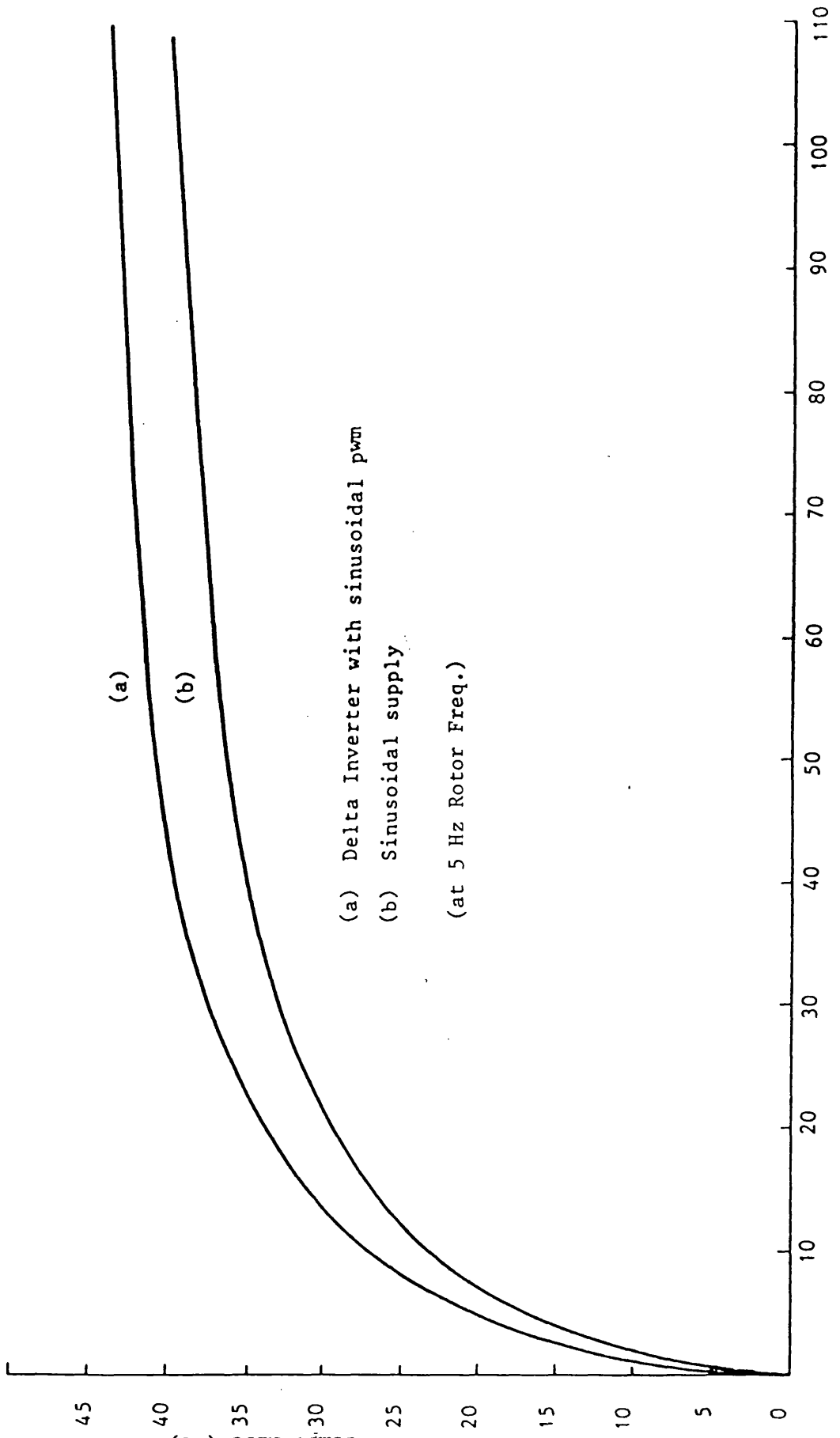

Fig. 4.25 Comparison of Motor System Performance using End-Winding Temperature Rise

a

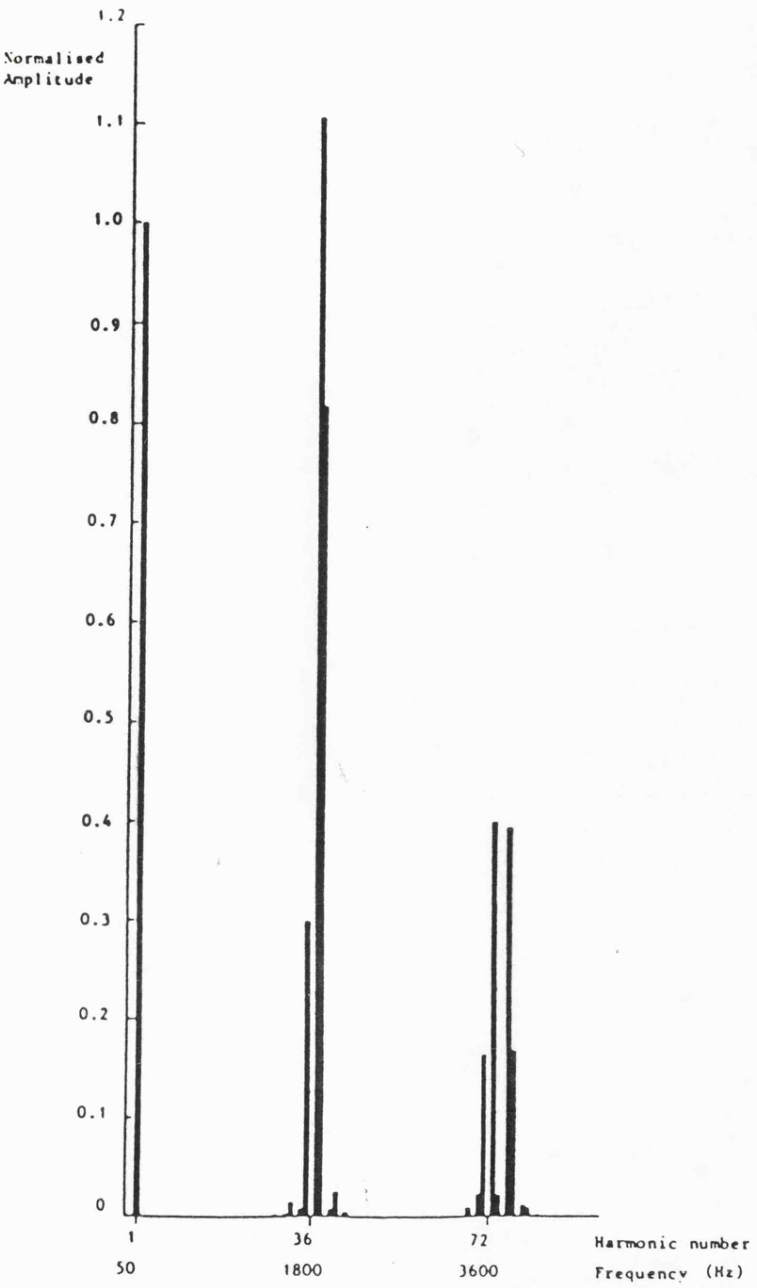

b

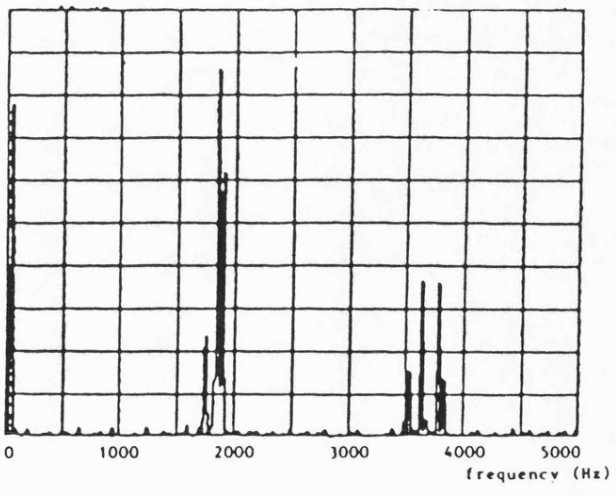

Fig. 4.26 Voltage Spectra for Delta Inverter - with Sinusoidal PWM (36 pulses/cycle)

a) Theoretical spectrum
b) Actual spectrum

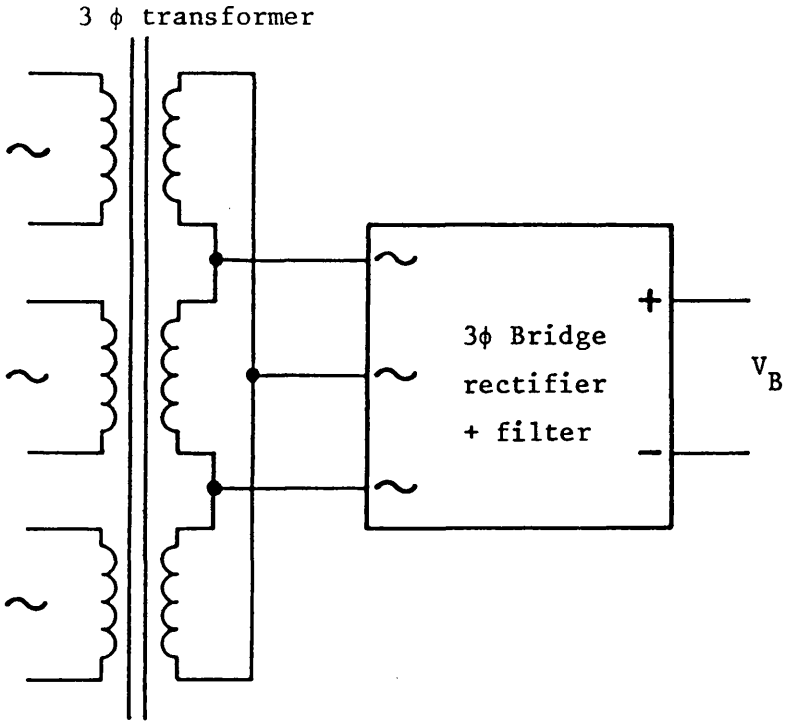

Fig. 4.27 Rectified Supply for Bridge Inverter

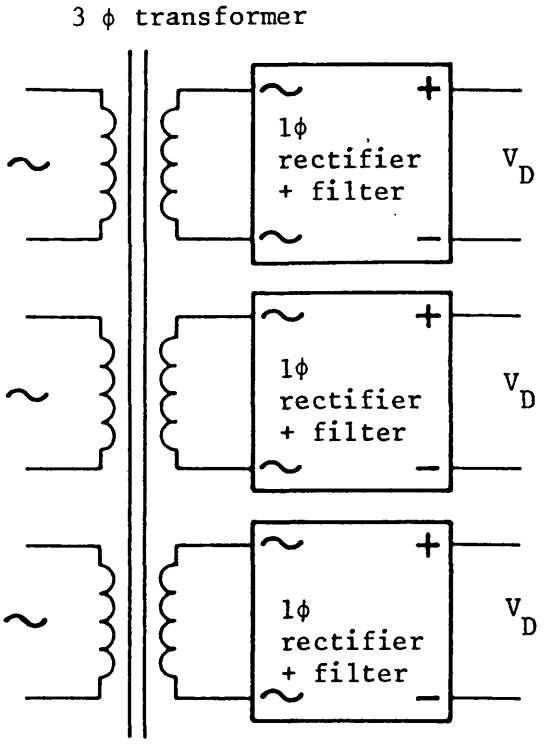

Fig. 4.28 Rectified Supply for Delta Inverter

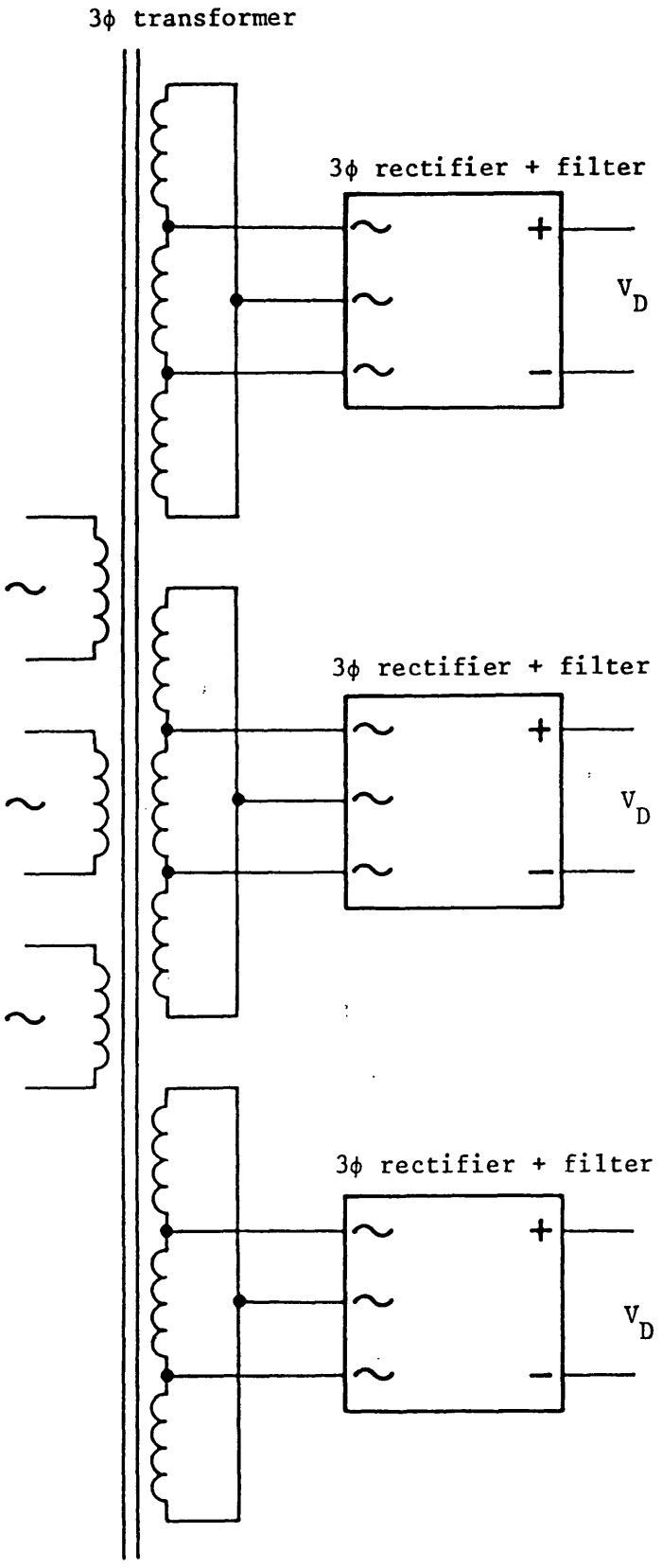

Fig. 4.29 Alternative Rectified Supply for Delta Inverter

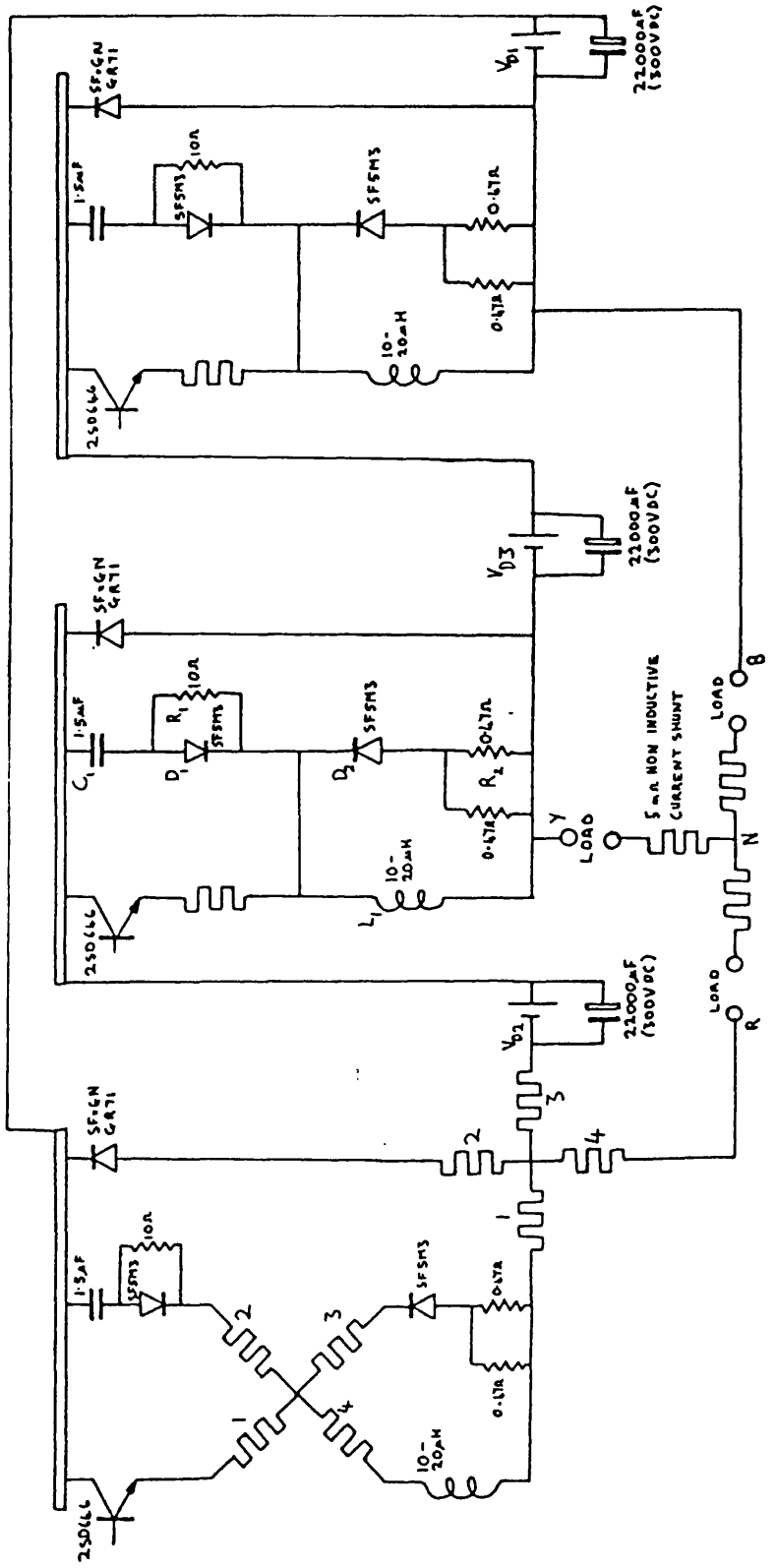

Fig. 4.30 Circuit Diagram of Delta Inverter Main Components (Star Load Connection)

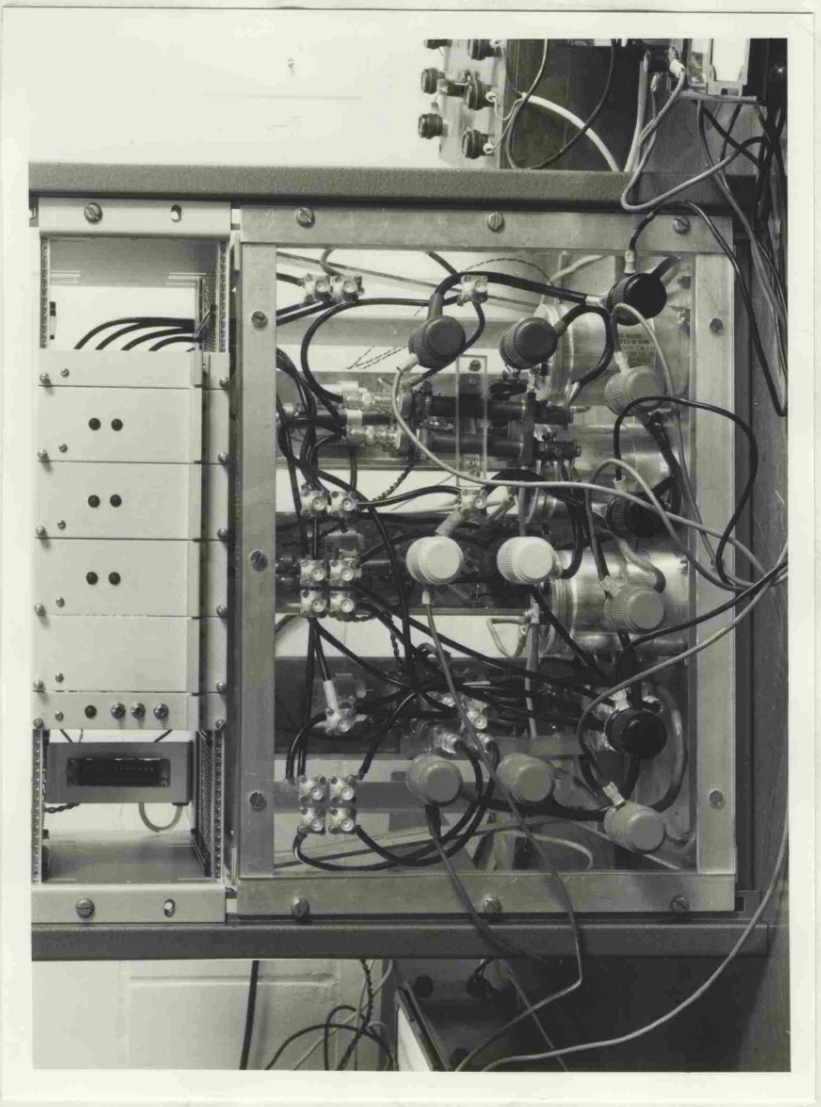

Fig. 4.31 Photograph of Prototype Delta Inverter

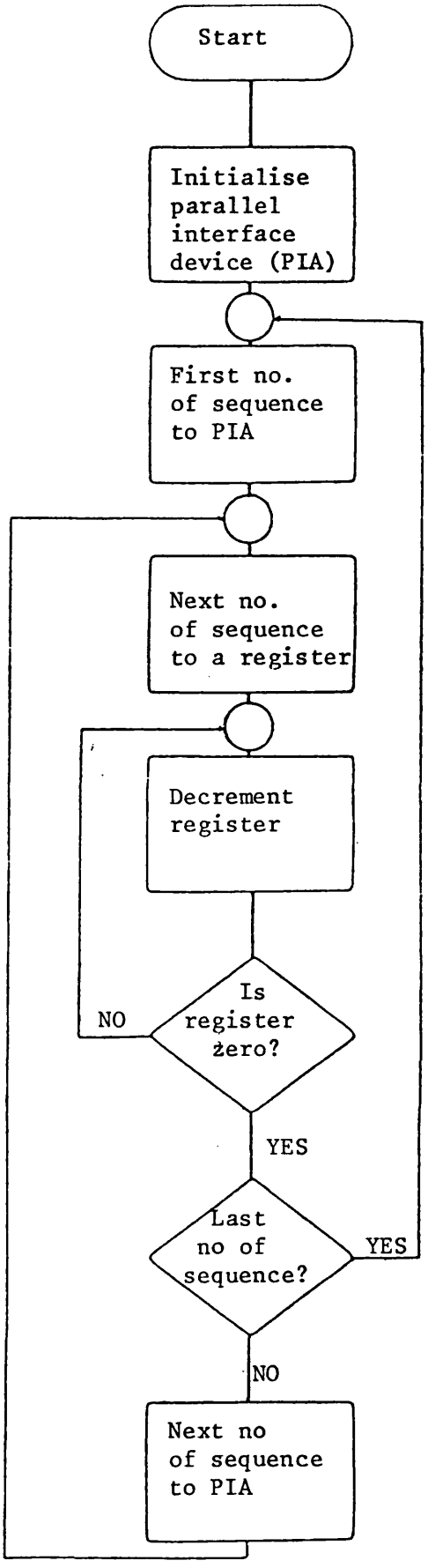

Fig. 4.32 Flowchart for Open Loop Microprocessor Control Scheme

a

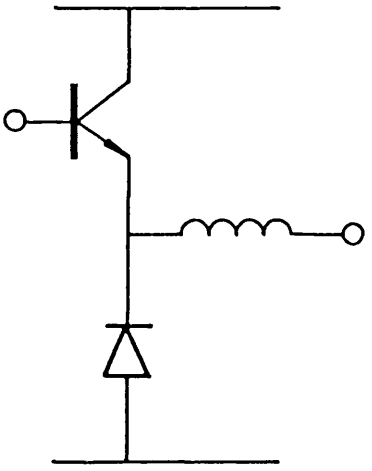

b

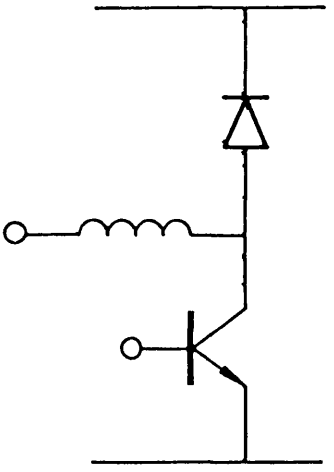

c

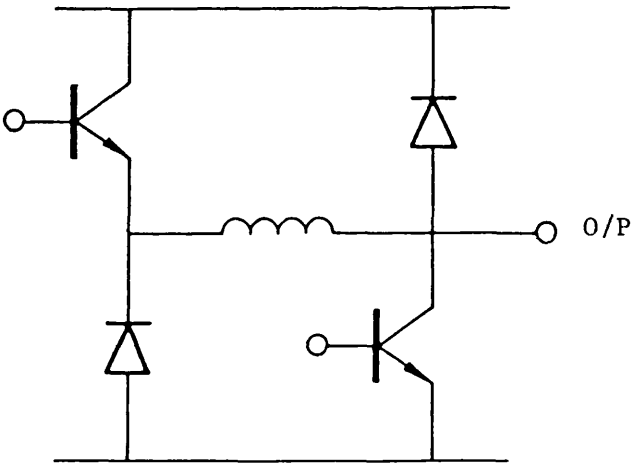

Fig. 4.33 Derivation of Fault Protection Circuit for Bridge Inverter

a) Step-down chopper
b) Step-up chopper
c) The modified inverter leg

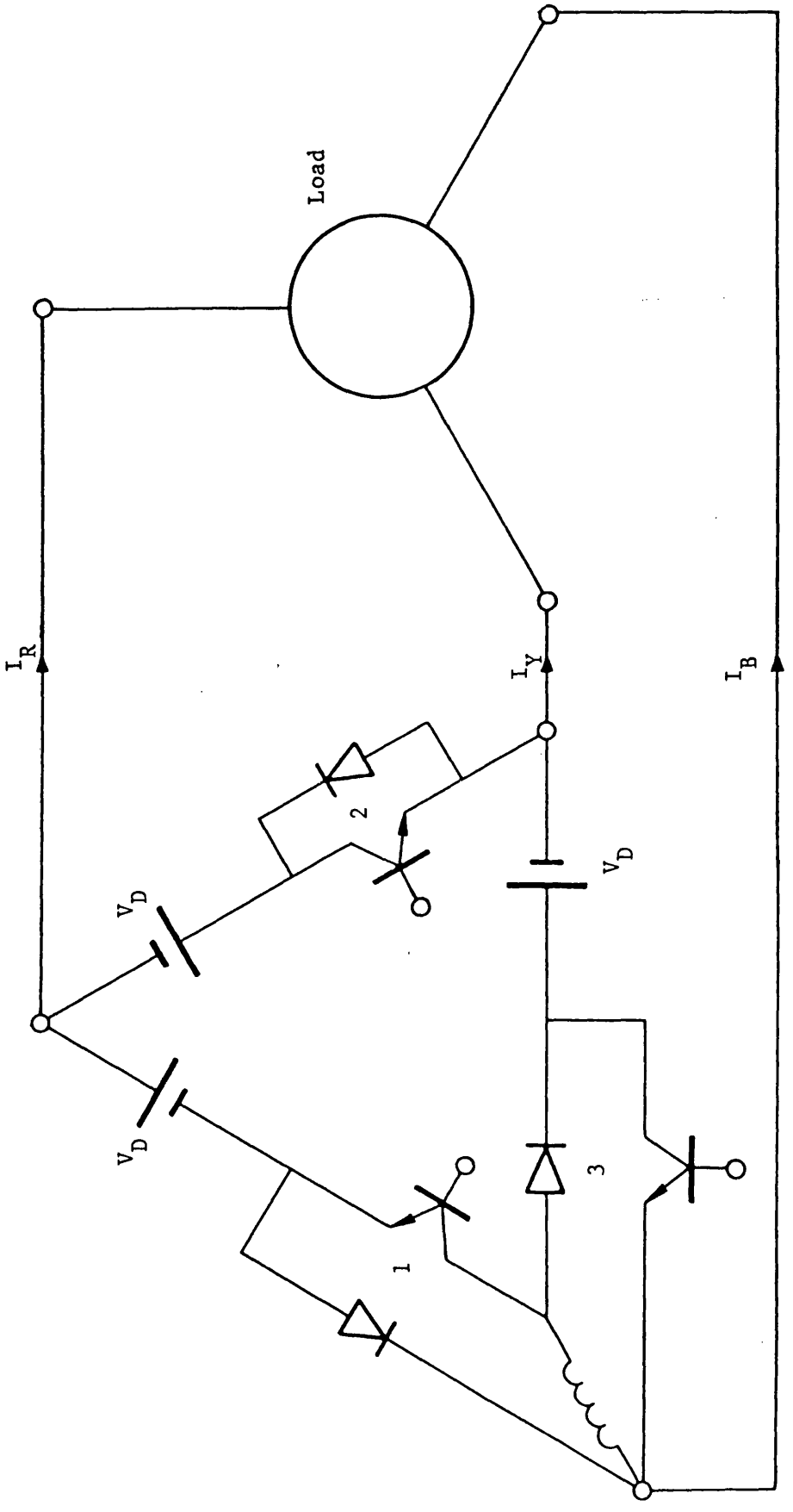

Fig. 4.34 Modified Delta Inverter with Fault Protection Choke

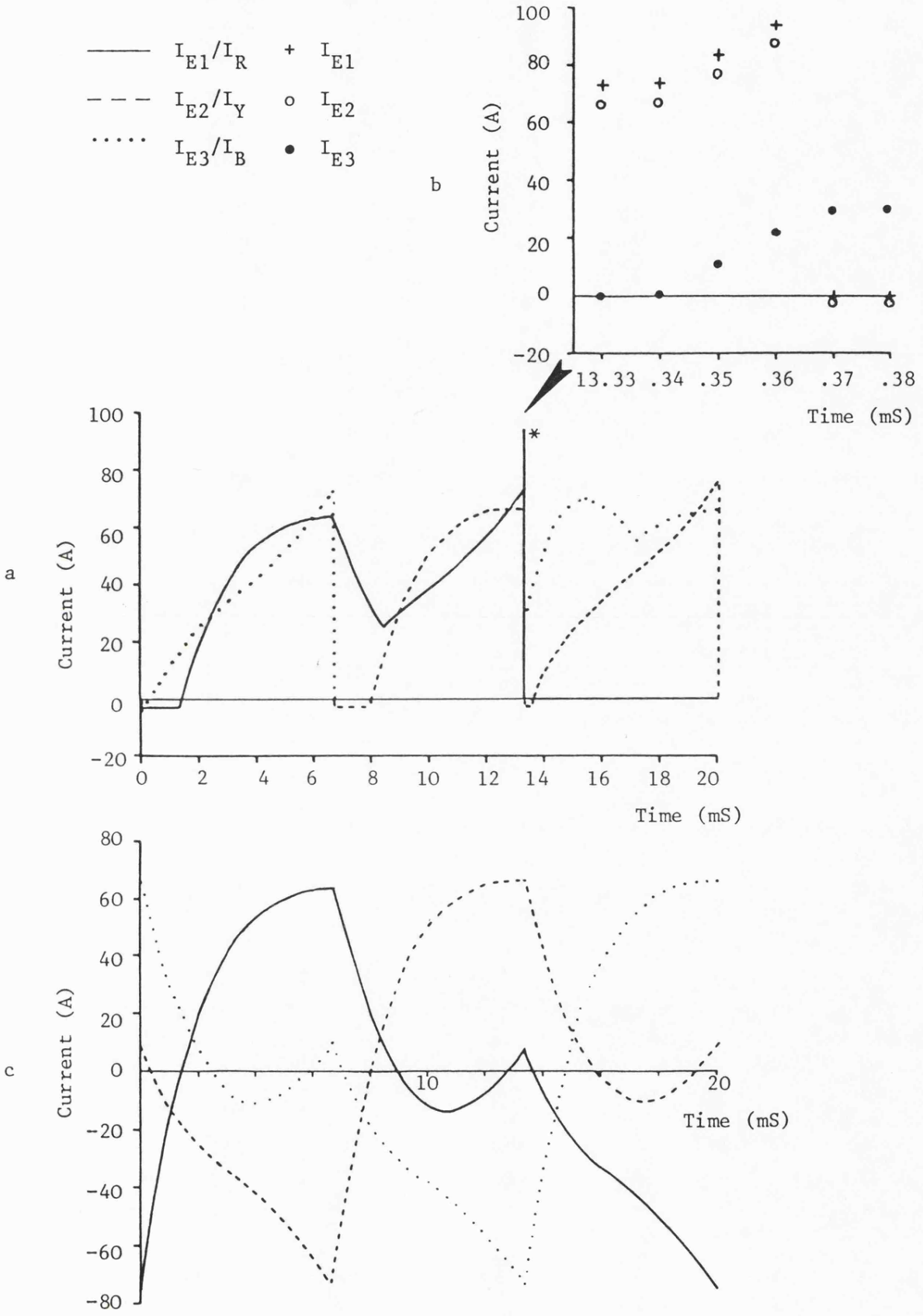

Fig. 4.35 Delta Inverter AC Drive System Subjected to a Fault (240^{o} conduction, 10 Hz Rotor Freq.). Computed results:

a) Transistor currents
b) Transistor currents over duration of fault
c) Load currents